MONASH University

Analysis of plasmid maintenance, incompatibility and conjugation in *Clostridium perfringens*

Thomas Dean Watts

BSc (Hons)

A thesis submitted for the degree of Doctor of Philosophy at

Monash University

Department of Microbiology

Monash Biomedicine Discovery Institute

2018

Copyright notice

Table of Contents

List of Tables

List of Figures

List of Abbreviations

2YT	2 x Yeast Tryptone
aa	Amino acid
ADP	Adenosine diphosphate
ATP	Adenosine triphosphate
AUC	Analytical Ultracentrifugation
BHI	Brain Heart Infusion
Bp	Base Pairs
CCR	Central Control Region
Chl	Saturated Potassium Chlorate
Cm	Chloramphenicol
CPE	*C. perfringens* enterotoxin
DIG	Digoxigenin
DNA	Deoxyribonucleic Acid
dNTP	Deoxyribonucleotide Triphosphate
dsDNA	Double stranded DNA
EBS	Exon Binding Site
Em	Erythromycin
FTG	Fluid Thioglycolate
HI	Heart Infusion
IBS	Intron Binding Site
IDT	Integrated DNA Technologies©
Kb	Kilobases
Mpf	Mating Pair Formation
mRNA	Messenger Ribonucleic Acid
NA	Nutrient Agar
Nal	Nalidixic Acid

NEB	New England Biolabs®
OD	Optical Density
ORF	Open Reading Frame
oriT	Origin of Transfer
oriV	Origin of Replication
PCR	Polymerase Chain Reaction
RAM	Retrotransposition-activated selectable marker
Rif	Rifampicin
RNA	Ribonucleic Acid
SD	Standard deviation
SEM	Standard Error of the Mean
Sm	Streptomycin
SPR	Surface Plasmon Resonance
ssDNA	Single Stranded Deoxyribonucleic Acid
T4SS	Type IV Secretion System
Tc	Tetracycline
Tcp	Transfer Clostridial Plasmid
Tm	Thiamphenicol
TPG	Tryptone, Peptone, Glucose
TPGY	Tryptone, Peptone, Glucose and Yeast
UV	Ultraviolet

Abstract

Clostridium perfringens is an important Gram-positive pathogen that causes a range of histotoxic and enteric infections in humans and domestic animals. These diseases are mediated by protein toxins, most of which are encoded by genes that are carried by two families of large virulence plasmids: the pCP13-family and the pCW3-family. Although these plasmids are important for virulence, questions remain about fundamental plasmid biology processes, such as conjugative transfer, plasmid replication and plasmid maintenance. Several of these processes were investigated in this thesis.

pCP13-like plasmids harbour important toxin genes, including genes that encode the novel binary clostridial enterotoxin, BEC. This family of plasmids was initially designated as non-conjugative, but recent studies have shown that an approximately 25 kb region of pCP13 has similarity to the Cst conjugation locus of the *Paeniclostridium sordellii* toxin plasmid pCS1-1 and a putative conjugation locus in the *Clostridium botulinum* toxin plasmid pCLL. To determine if pCP13 was conjugative, a genetically marked pCP13 derivative was constructed. This strain was used as a donor in a conjugation assay with a plasmid-free recipient strain of the same genetic background. The marked pCP13 derivative transferred by conjugation at a high frequency. The PcpB4 protein encoded within the conserved locus has similarity to the VirB4-family of conjugation proteins. A *pcpB4* mutant had a much lower transfer frequency than the wild-type and complementation *in trans* with the wild-type *pcpB4* gene restored transfer to wild-type levels. In conclusion, pCP13 was shown to be conjugative and the *pcpB4* gene was shown to be required for conjugative transfer.

Many *C. perfringens* strains carry multiple closely related toxin or antibiotic resistance plasmids of the pCW3 family, most of which encode a similar Rep protein. A key question is how are these closely related plasmids maintained within a single strain of *C. perfringens*? Phylogenetic analysis showed that there are at least ten different ParMRC partitioning families

(ParMRC$_{A-J}$) in *C. perfringens*. Plasmids with genes belonging to the same ParMRC family have not been observed in a single strain, with one minor exception. This result suggested that differences between these families represented the basis for plasmid incompatibility in *C. perfringens*. To validate this hypothesis, pairs of genetically marked plasmids with different combinations of *parMRC* genes were introduced into a single strain and the relative stability of each plasmid determined. The results demonstrated that plasmids with identical ParMRC homologues were incompatible and could not co-exist in the absence of external selection, whereas plasmids that had closely related, but different, ParMRC homologues could co-exist in the same cell under these conditions.

To understand the mechanism by which differences in these partitioning systems lead to plasmid compatibility, surface plasmon resonance was used to interrogate key recognition steps between the ParR and *parC* components. The results showed that ParR homologues from different ParMRC families bound efficiently to repeats in their cognate *parC* sequences, but did not interact with non-cognate *parC* sequences. These ParR homologues could bind to non-cognate *parC* sequences from the same family. In conclusion, these data provide evidence that the incompatibility of the conjugative toxin and resistance plasmids of *C. perfringens* is mediated primarily by their ParMRC-like partitioning systems.

Publications during enrolment

Published journal articles

Adams, V, Watts, TD, Bulach, DM, Lyras, D & Rood, JI (2015). Plasmid partitioning systems of conjugative plasmids from *Clostridium perfringens*. *Plasmid* **80**, 90-96. (Chapter 3)

Watts TD, Johanesen PA, Lyras D, Rood JI, Adams V (2017). Evidence that compatibility of closely related replicons in *Clostridium perfringens* depends on linkage to *parMRC*-like partitioning systems of different subfamilies. *Plasmid* **91,** 68-75. (Chapter 4)

Vidor CJ, Watts TD, Adams V, Bulach D, Couchman E, Rood JI, Fairweather NF, Awad M, Lyras D. (2018). *Clostridium sordellii* pathogenicity locus plasmid pCS1-1 encodes a novel clostridial conjugation locus. mBio 9: e01761-17. https://doi.org/10.1128/mBio.01761-17. (Appendix)

Submitted journal articles

Watts TD, Vidor CJ, Awad M, Lyras D, Rood JI, Adams V (2018 submitted). pCP13, a representative of a new family of conjugative toxin plasmids in *Clostridium perfringens*. (Chapter 2)

Watts TD, Traore DAK, Atkinson SA, Lao C, Caltabiano N, Rood JI, Adams V (2018 submitted). The specificity of ParR binding is related to compatibility of conjugative plasmids of *Clostridium perfringens*. (Chapter 5)

Book chapter

Revitt-Mills, S. A, Vidor, C. J., Watts, T. D., Lyras, D., Rood, J. I, & Adams, V. Virulence Plasmids of the Pathogenic Clostridia. Gram-Positive Pathogens, 3rd Edn, Microbiology Spectrum. (accepted 8-8-18).

Thesis including published works declaration

I hereby declare that this thesis contains no material which has been accepted for the award of any other degree or diploma at any university or equivalent institution and that, to the best of my knowledge and belief, this thesis contains no material previously published or written by another person, except where due reference is made in the text of the thesis.

This thesis includes two original papers published in peer reviewed journals and two submitted publications. The core theme of the thesis is Plasmid biology of *Clostridium perfringens*. The ideas, development and writing up of all the papers in the thesis were the principal responsibility of myself, the student, working within the Department of Microbiology under the supervision of Professor Julian Rood and Dr Vicki Adams.

The inclusion of co-authors reflects the fact that the work came from active collaboration between researchers and acknowledges input into team-based research.

In the case of Chapters 2, 4, 5 & appendix my contribution to the work involved the following:

Thesis Chapter	Publication Title	Status	Nature and % of student contribution	Co-author names nature and % of author's contribution	Co-authors Monash student (Y/N)
2	pCP13, a representative of a new family of conjugative toxin plasmids in *Clostridium perfringens*	Submitted	60%. Conducted all biological and molecular experiments, bioinformatics analysis, experimental design, data analysis and preparation of the manuscript. Including writing, constructing figures and editing.	1) Callum Vidor 10%, manuscript preparation, bioinformatics, experimental design. 2) Vicki Adams 10%, manuscript preparation, experimental design. 3) Dena Lyras 5%, manuscript preparation and experimental design. 4) Julian Rood 10%, manuscript preparation and experimental design 5) Milena Awad 5%, manuscript preparation and experimental design.	1) Y 2) N 3) N 4) N 5) N
4	Evidence that compatibility of closely related replicons in *Clostridium perfringens* depends on linkage to *parMRC*-like partitioning systems of different subfamilies	Published	75%. All biological experiments. Experimental design, data analysis and manuscript preparation.	1) Vicki Adams 10%, manuscript preparation and experimental design. 2) Julian Rood 10%, manuscript preparation and experimental design. 3) Priscilla Johanesen 2.5%, manuscript preparation and experimental design. 4) Dena Lyras 2.5%, manuscript preparation and experimental design.	1) N 2) N 3) N 4) N
5	The specificity of ParR binding is related to compatibility of conjugative plasmids of *Clostridium perfringens*	Submitted	60%. Experimental work including, expression vector construction, protein expression and purification, SPR and AUC data acquisition and bioinformatics analysis. Experimental design, data analysis, preparation of the manuscript.	1) Daouda Traore 7.5%, SPR data acquisition, experimental design and manuscript preparation. 2) Sarah Atkinson 7.5%, AUC data acquisition and analysis, experimental design and manuscript preparation. 3) Carmen Lao 2.5%, constructing a subset of ParR expression vectors. 4) Natalie Caltabiano 2.5%, expression/purification of initial ParR proteins.	1) N 2) N 3) N 4) N 5) N 6) N

				5) Julian Rood 10%, experimental design and manuscript preparation. 6) Vicki Adams 10%, experimental design and manuscript preparation.	
Appendix 1	*Clostridium sordellii* Pathogenicity Locus plasmid pCS1-1 encodes a novel clostridial conjugation locus	Published	7.5%. Bioinformatic analysis, experiemtnal design, data analysis and manuscript preparation.	1) Callum Vidor 60%, of biological and molecular experiments, bioinformatic analysis, experimental design, manuscript preparation. 2) Dieter Bulach 2.5, Bioinformatics 3) Ed Couchman 2.5%, initial identification and provision of *P. sordellii* sequences associated with conjugation loci. 4) Neil Fairweather 2.5%, experimental design and manuscript preparation. 5) Vicki Adams 2.5%, experimental design and manuscript preparation. 6) Julian Rood 2.5%, experimental design and manuscript preparation. 7) Milena Awad 10%, experimental design and manuscript preparation. 8) Dena Lyras 10%, experimental design and manuscript preparation.	1) Y 2) N 3) N 4) N 5) N 6) N 7) N 8) N

I have renumbered sections of submitted or published papers in order to generate a consistent presentation within the thesis.

Student signature: 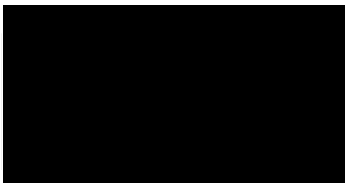 **Date:** 8-1-19

The undersigned hereby certify that the above declaration correctly reflects the nature and extent of the student's and co-authors' contributions to this work. In instances where I am not the responsible author I have consulted with the responsible author to agree on the respective contributions of the authors.

Main Supervisor signature:  **Date:** 8-1-19

Acknowledgements

The path trod in pursuit of a PhD can be a lonely path indeed. There are many days spent alone in the laboratory or chained to a desktop writing in isolation. It is easy to forget that the many setbacks encountered along the road are normal, and do not constitute deep and inherent flaws of character. In reality, a PhD is a collaborative effort. Without the proper support, encouragement and guidance I would have faltered at countless points along the road. I have been both lucky and privileged to have more support than I know what to do with! The time comes to finally thank all those whom have propped me up and encouraged me throughout this academic expedition.

First and foremost, I would like to thank my two tremendous PhD supervisors, without whom, I would not be the scientist I am today. To Julian, I am incredibly grateful for the opportunity to conduct research in your laboratory and have learnt so much whilst under your tutelage. Your constant encouragement for me to think about the next experiment and the next question really challenged me and drove me forward. You also taught me the 'K.I.S.S principle': keep it simple stupid. This principle single-handedly transformed my science writing from the over descriptive, Tolkien-esque paragraphs I set out with, into the sleek and economic sentences that I use today (I'm sure they would get the nod from Hemmingway… well maybe not). It's ironic that this acknowledgements section is not at all reflective of the statements of the previous sentence. Oh well.

To Vicki, where do I begin? Thank you for your friendship, wisdom and sarcastic digs and jives! I began my research journey with you in honours as a blank slate, and over the years you've helped populate my mind with proper lab techniques and the ability to solve complex problems. I almost didn't come back for a PhD after honours, but you helped change my mind, and I'm glad you did. I couldn't ask for a better advisor and friend over the last couple of years. Sorry for driving you mad (or more mad).

xx

I've been lucky enough to receive several sources of funding over the course of my candidature. Thank you to the Australian government for providing me with a Research Training Program scholarship, the scholarship has allowed me to devote my time solely to conducting and sharing my research. Thank you to MicroMon for granting me travel scholarships, which enabled me to attend several scientific conferences.

I've collaborated with several incredible scientists during my candidature. Thank you to Daouda Traore, for teaching me the ins and outs of protein characterisation, with special thanks for teaching me how to develop surface plasmon resonance experiments. Thank you to Sarah Atkinson, whom taught me how to perform analytical ultracentrifugation and was patient with me during data analysis. Thank you to Dena Lyras and Priscilla Johanesen for discussions about each of my projects and my career. I'd also like to thank Dena for her mentorship throughout my candidature, as Chair of my academic panel your comments were always insightful and valuable - it was greatly appreciated. I'd also like to thank all the members of the Rood and Lyras laboratories, past and present, for welcoming me and making the Monash Microbiology Department a home away from home.

Finally, I need to thank my friends and family. I'd like to thank my fellow PhD champions Jacob Amy, Sam Munn, Sarah Revitt-Mills, Tom Stent, Ben Vezina and Callum Vidor for their undying support throughout my PhD. We have all bonded over our shared plasmid-inflicted woes and you have all been great friends. Thanks to each of you for making coming to work a lot easier. I'd particularly like to thank Tom and Jacob for all the banter and the 'brotherly' love they've provided over the years. I'd also like to say a special thanks to Sarah for being my coffee buddy for last two years or so. To Carina, my remaining honours buddy and fellow vegetarian, thanks for all the chats and support - your thesis comments will come through soon!

To my good old Deakin Hall family, Tim, Scott, Shakira, Katherine, Steve and Chloe, thank you for your patience and understanding. You've all been there for me at different times along the way. I feel that I may have fallen off the map a bit over the last couple of years, and when I've resurfaced all I've had to talk about was my PhD. I promise I'll be more interesting to talk to in the future. Thanks especially to Tim and Scott for sticking it out with me in the Prince Street Manor all these years.

To Carmen, thank you for being there for me over the past couple of years. You're my partner in crime. There have been ups and downs, and round-abouts, but it's been a pretty smooth ride thanks to you, and I'm lucky to have you in my life.

To my family, particularly Mum, Dad, Liam and Sam, thank you for being so supportive over the years, and understanding why I've been at university far too long. As much as I hate to admit it, my brothers are both wonderful human beings and I'm so proud of them and grateful to have two wonderful friends that I can cajole into helping me when I need it (they have to do it, we are related). To my wonderfully kooky and creative Mum, thank you for everything. Your love, understanding and interest in what I'm doing have been what has kept me going. You have always been a source of inspiration, the stories you told me when I was young of going to university always prompted me to strive for the same heights. I'm sorry I've been rather absent in recent years. Finally, I'd like to thank my best friend, my Dad, whom I miss with all my heart. Thank you for giving me my 'doctor's name', just in case I wanted to become one. Now I'm here, and you're late to the party, but I'll forgive you and I'd like to thank you all the same.

Chapter 1

Introduction

Plasmid biology and *Clostridium perfringens*

Plasmids are non-essential, autonomously replicating, extrachromosomal elements that are often implicated in the spread of virulence and antibiotic resistance determinants through bacterial populations (1). The importance of plasmids first became apparent in the early 1950s and 1960s, when it was discovered that the emerging threat of antibiotic resistance was due, in part, to the possession of plasmids that carried antibiotic resistance determinants (2,3). These plasmids, termed Resistance (R) plasmids, were first seen in strains of *E. coli* and *Shigella spp*. (3). Since then it has become evident that plasmids are ubiquitous in nature and can be found in many bacterial genera, where they often carry essential virulence and antimicrobial resistance genes. Many members of the genus *Clostridium* rely upon plasmids for virulence, antimicrobial resistance and metabolic functions, including *Clostridium perfringens,* which houses an abundance of virulence and resistance plasmids (4). All plasmids must replicate and most encode the mechanisms to stabilise their inheritance in a bacterial population. This chapter will discuss the processes that are integral to prokaryotic plasmid replication, maintenance and transfer, and compare the most intensively researched paradigm plasmids to our current understanding of plasmid biology in *C. perfringens*.

Clostridium perfringens: disease, toxins and typing

Clostridium perfringens is a Gram-positive, rod-shaped, anaerobe that is found ubiquitously in the environment due to its ability to produce heat-resistant endospores (4,5). In addition, *C. perfringens* is often found as a commensal organism within the gastrointestinal tract of both humans and animals; it also has the capacity to act as a primary pathogen, causing an array of diseases. These diseases range from enterotoxaemia and enteritis in humans and animals, to more debilitating wound-associated infections in humans, the classic example being alpha-toxin-mediated clostridial myonecrosis or gas gangrene (5-7). Disease can be attributed to the ability of *C. perfringens* to produce an arsenal of at least 20 distinct extracellular toxins and enzymes (8-12). These toxins are so intimately involved in the determination of disease that

they remain the basis for typing *C. perfringens* isolates. The toxinotype (A-G) of each isolate is determined by its ability to produce the six major typing toxins (α, β, ε, ι, CPE and NetB toxins) (5,8,13) (Table 1.1).

Mechanistically *C. perfringens* toxins fall into one of four categories, membrane damaging enzymes, pore-forming toxins, toxins that act on intracellular targets and hydrolytic enzymes (14,15). The importance of several of these toxins in relation to their role in the production of disease has been established through the satisfaction of Koch's molecular postulates (4,6,9). Although these toxins represent one of the most important aspects of *C. perfringens* biology, they are not the focus of this review and will be discussed only briefly in the context of their genetic location and arrangement. Therefore, the mechanism of action, disease outcomes and genetic localisation of these toxins has been summarised in Table 1.2.

Table 1.1: Toxin typing of *C. perfringens* isolates

Type	Major toxin/s produced					
	α	**β**	**ε**	**ι**	**CPE**	**NetB**
A	+	-	-	-	-	-
B	+	+	+	-	-	-
C	+	+	-	-	±	-
D	+	-	+	-	±	-
E	+	-	-	+	±	-
F	+	-	-	-	+	-
G	+	-	-	-	-	+

This table was adapted from (Rood et al., 2018) and shows the subset of the six typing toxins produced by each *C. perfringens* toxinotype:
+ indicates that the toxin is produced by this type,
- indicates that the toxin is not produced by this type,
± indicates that toxin may or may not be produced by this type.

The majority of *C. perfringens* toxins, including five of the six typing toxins (β-toxin, ε-toxin, ι-toxin, CPE and NetB) and many of the non-typing toxins, are encoded by genes located on plasmids that have either been shown to be conjugative or are highly likely to be conjugative (4) (Table 1.1). The presence of these plasmids has significant implications for the dissemination of virulence and antimicrobial resistance determinants throughout *C. perfringens* populations. It has been postulated that during infection a virulent *C. perfringens* isolate could act as a plasmid donor in the gastrointestinal tract, transferring a toxin plasmid to a commensal *C. perfringens* isolate, thus negating the need for a virulent bacterium to colonise to cause disease (4,16-19).

Importantly, the knowledge that many of the toxin genes are associated with mobile genetic elements calls into question the practicality of the current system used to type *C. perfringens* isolates, especially in the face of what seems to be a relatively fluid genetic system (4,16). With our current understanding, it can be envisaged that all strains are fundamentally type A isolates (producing alpha-toxin), which have received plasmids encoding other typing toxins through a horizontal gene transfer event, leading to alteration of the genotype and therefore the toxinotype of a particular isolate (4,16,20). This hypothesis has been supported in a study where a type D donor strain CN1020 was used to convert a type A recipient strain, JIR325, to a type D genotype through the movement of an epsilon-toxin plasmid *via* conjugation (16). The newly derived transconjugants were found to express active epsilon-toxin, which was cytotoxic to MDCK (Madin-Darby Canine Kidney Epithelial) cells and lethal to mice upon intravenous injection, thus demonstrating that type A strains can be converted both genotypically and phenotypically to different toxinotypes, through the acquisition of a conjugative plasmid (16,21).

Table 1.2 Toxins and extracellular enzymes of *C. perfringens* and associated diseases

Toxin/enzyme	Gene	Type/Activity	Associated disease	Location
Alpha toxin	*plc/cpa*	Phospholipase C and sphingomyelinase	Clostridial myonecrosis	Chromosome
Beta-toxin	*cpb*	Pore-forming toxin	Necrotising enteritis in humans (pigbel) and animals	Plasmid
Epsilon-toxin	*etx*	Pore-forming toxin	Enterotoxemia in sheep and goats	Plasmid
Iota-toxin	*iap*, *ibp*	Binary toxin, actin-specific ADP ribosyltransferase	Enteritis in sheep and cattle, enterotoxaemia in rabbits	Plasmid
Perfringolysin O	*pfoA*	Pore-forming toxin, cholesterol dependent cytolysin	Clostridial myonecrosis in combination with alpha-toxin	Chromosome
CPE	*cpe*	Pore-forming toxin	Food poisoning and non-foodborne gastrointestinal infection in humans	Chromosome or Plasmid
BEC	*becA, becB*	Actin-specific ADP-ribosyltransferase	CPE negative food poisoning in humans	Plasmid
Cpb2	*cpb2*	Pore-forming toxin	No confirmed disease association	Plasmid
TpeL	*tpeL*	Ras-specific monoglucosyltransferase	No confirmed disease association	Plasmid
Delta-toxin	*cpd*	Pore-forming toxin	No confirmed disease association	Plasmid
Mu-toxin	*nagH*	Hyaluronidase	No confirmed disease association	Chromosome
NetB	*netB*	Pore-forming toxin	Avian necrotic enteritis	Plasmid
NetE	*netE*	Putative pore-forming toxin	No confirmed disease association	Plasmid

NetF	*netF*	Pore-forming toxin	Haemorrhagic gastroenteritis in dogs and necrotic enteritis in foals	Plasmid
NetG	*netG*	Putative pore-forming toxin	No confirmed disease association	Plasmid
NanI	*nanI*	Sialidase	Accessory role in cell adherence	Chromosome
NanJ	*nanJ*	Sialidase	No confirmed disease association	Chromosome
Urease	*ureABC*	Urease	No confirmed disease association	Plasmid
Kappa-toxin	*colA*	Collagenase	No confirmed disease association	Chromosome
Lambda-toxin	*lam*	Protease	No confirmed disease association	Plasmid
α-clostripain	*ccp*	Cysteine protease	No confirmed disease association	Chromosome

Table adapted from (14).

pCW3-like plasmids

Plasmid associated antimicrobial resistance determinants

C. perfringens cells frequently harbour plasmids that carry antimicrobial resistance determinants, the most common of which are those that confer resistance to tetracycline. A suite of tetracycline resistance plasmids has been isolated from a variety of sources including human clinical samples, porcine faeces and the small intestine of birds with necrotic enteritis (18,22-25). All tetracycline resistance plasmids isolated to date are either identical to or closely related to the paradigm resistance plasmid, pCW3 (26,27). pCW3 has been thoroughly characterized using detailed restriction enzyme and hybridisation analysis as well as nucleotide sequencing (17,28). Strains carrying pCW3 transfer tetracycline resistance at a high frequency by a conjugation-like mechanism and the transconjugants retain the ability to transfer tetracycline resistance (22,29).

pCW3 is 47 kb in size and encodes a 4.4 kb tetracycline resistance operon (27,30). DNA hybridisation studies with known tetracycline resistance determinants revealed that pCW3 carried a tetracycline resistance determinant that was novel to *C. perfringens,* which was designated *tet*(P) (30). The *tet*(P) operon consists of the two genes *tetA*(P) and *tetB*(P), which overlap by 17 bp (31). The *tetA*(P) gene encodes a 420 amino acid transmembrane protein that actively effluxes tetracycline from the cell. The *tetB*(P) gene encodes a 652 amino acid TetM-like ribosomal protection protein. Transcriptional analysis of these genes showed that they were expressed from the P3 promoter, which is located 523 bp upstream of the *tetA*(P) gene (32). Southern hybridisation and PCR analysis has also demonstrated that tetracycline resistance is widespread in *C. perfringens*. A panel of 81 tetracycline resistant *C. perfringens* strains carried the *tetA*(P) gene and 93% of isolates carried a second tetracycline resistance determinant, either *tetB*(P) or *tet(M)*-like genes (33).

C. perfringens strains that harbour plasmids encoding erythromycin, bacitracin, lincomycin or chloramphenicol resistance determinants have also been identified (24,34,35). Sebald and Brefort (1975) first described a strain of *C perfringens* that carried two plasmids pIP401 and pIP402. The 54 kb conjugative plasmid pIP401 confers resistance to both tetracycline and chloramphenicol through its *tet*(P) operon and the chloramphenicol resistance determinant *catP* (24), whereas the 63 kb plasmid pIP402 is non-conjugative and carries genes that confer erythromycin and clindamycin resistance (18,24,26,36,37). It was noted in studies by both Brefort *et al*., (1977) and Abraham *et al*., (1985) that pIP401 is unstable upon conjugative transfer and undergoes a precise deletion event of 6.3 kb, which corresponds to the loss of chloramphenicol resistance and results in the formation of a plasmid almost identical to pCW3 (18,26,36).

This deletion corresponds with the excision of the mobilisable transposon Tn*4451* from pIP401 (36). Alignment of the sequence adjacent to the Tn*4451* insertion site in pIP401 with the sequence of pCW3 demonstrated that the transposon integrated into and disrupted the end of the *cna* gene (17). Sequencing of the 6.3 kb region comprising the transposon showed the presence of six genes named *tnpX*, *tnpV*, *catP*, *tnpY*, *tnpZ* and *tnpW* (38). *tnpX* encodes a large serine recombinase and is the only component of Tn*4451* that is required for excision and transposition (38-40). Excision from a high-copy number vector and subsequent transposition and integration of Tn*4451* has been demonstrated in *E. coli*, however, transposition has not been demonstrated in *C. perfringens* (36,41). Another important component of Tn*4451* is the *tnpZ* gene, which encodes a protein with similarity to Mob/Pre family relaxase proteins (38,42). TnpZ and its recognition of an upstream *oriT* site has been shown to be essential for mobilisation of Tn*4451* in the presence of the *E. coli* RP4 conjugation machinery (42).

Plasmids that confer resistance to lincomycin and bacitracin have also been found in *C. perfringens*. Similar to the *catP* gene of pIP401, these resistance determinants have been

shown to be associated with transposable elements (34,35). The lincomycin resistance plasmid pJIR2774 is similar to pCW3, sharing genes involved in replication and conjugative transfer, whilst lacking the *tet(P)* operon (17,34). Sequence analysis of the lincomycin resistance gene *lnuP* found that it had similarity to the *lnuC* gene of *Streptococcus agalacticae,* which encodes a lincosamide nucleotidyltransferase (34). Further sequence and functional analysis showed that *lnuP* is associated with an IS*1595*-family transposable element with a similar genetic arrangement to tIS*Sag10* element found in *S. agalacticae*; the *lnuP* transposable element was therefore designated tIS*Cpe8* (34).

A bacitracin resistant avian necrotic enteritis isolate was found to carry three large conjugative plasmids, including an 89.7 kb plasmid, pJIR4150, carrying the bacitracin resistance genes *bcrRABD* (35). Other studies have reported chromosomally encoded bacitracin resistance in *C. perfringens* (43). Mutagenesis of the *bcrRABD* operon showed that *bcrA* and *bcrB* are the only genes required to confer bacitracin resistance. Next generation sequence analysis of pJIR4150 revealed that the bacitracin resistance genes have 85% identity to bacitracin resistance genes from *Enterococcus faecalis* and are associated with a Tn*916*-like integrative conjugative element (ICE) called ICE*Cp1* (35). Similar to the other resistance plasmids discussed above, pJIR4150 also has 35 kb of sequence similarity with pCW3, including those genes involved in conjugative transfer and replication (35).

Sequenced pCW3-like plasmids

Complete sequencing of the archetype tetracycline resistance plasmid pCW3 led to the discovery of regions required for conjugative transfer and plasmid replication (17). Many of the large *C. perfringens* toxin plasmids have been sequenced (17,25,35,44-47) (Figure 1.1) and strains often harbour more than one highly similar plasmid making the sequences hard to resolve (4,25).

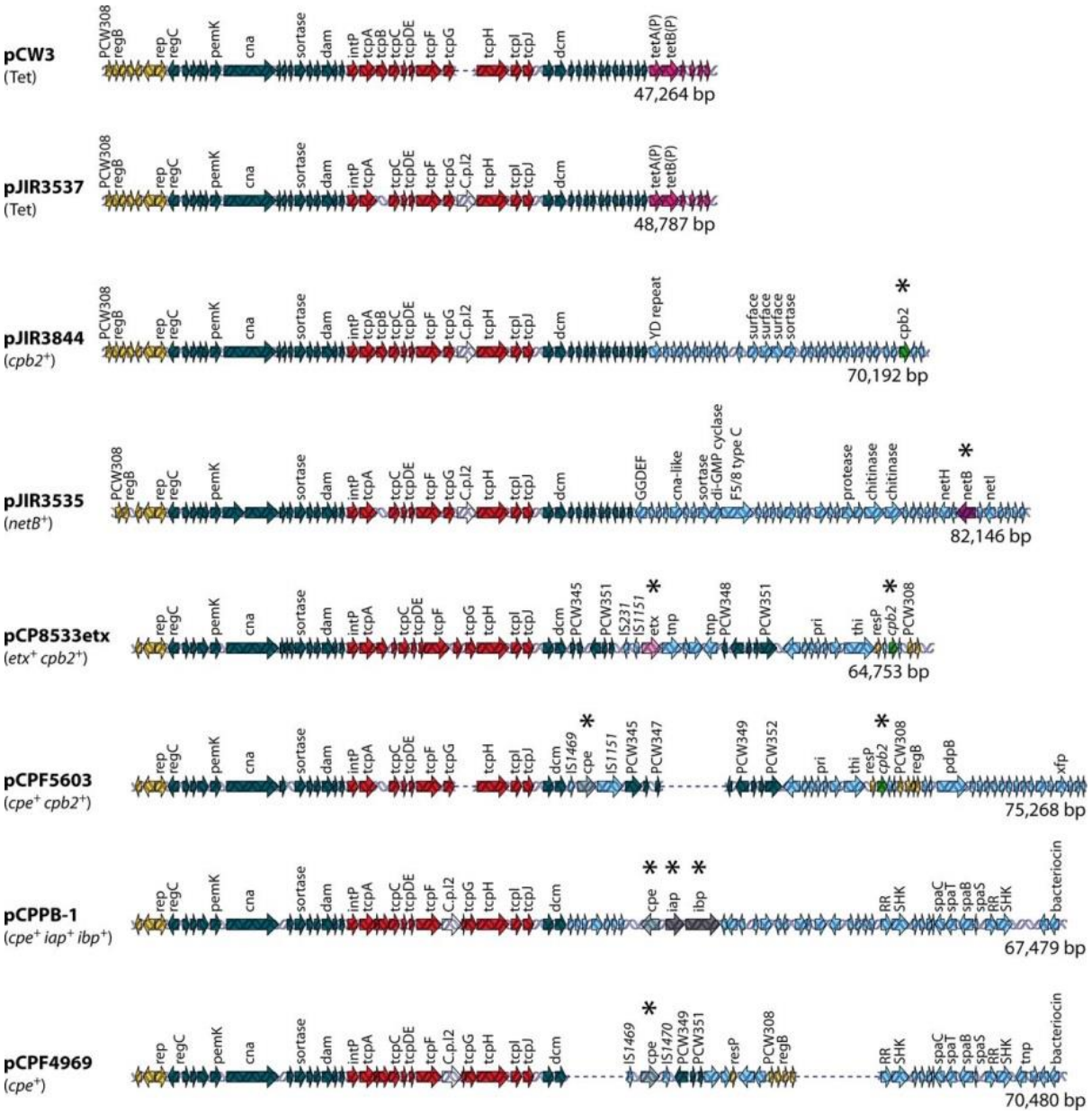

Figure 1.1. Sequence alignment of eight sequenced large conjugative plasmids in *C. perfringens*: Shown are the sequences of pCW3, pJIR3537, pJIR3844, pJIR3535, pCP8533etx, pCPF5603, pCPPB-1 and pCPF4969. Each arrow denotes an ORF. Red arrows are the conserved Tcp loci, involved in conjugative transfer, yellow arrows show the central control region, dark blue arrows denote other regions of similarity shared between these plasmids. Purple arrows denote tetracycline resistance genes, green arrows show the *cpb2* toxin encoding gene, dark purple arrows indicate the *netB* gene (pJIR3535), pink arrows represent the *etx* gene, grey arrows represent the *cpe* gene, dark grey arrows represent the *iap* and *ibp* genes, light blue arrows denote areas that are unique to the plasmid. *Indicates a toxin gene. This figure was reproduced from (4)

The sequences of these plasmids were found to be very similar, each plasmid shared ~35 kb of homology in a conserved backbone region. As more plasmids were sequenced it became clear that all known conjugative plasmids in *C. perfringens* are related to the archetypal tetracycline resistance plasmid, pCW3.

pCW3-like toxin plasmid diversity

Although pCW3-like plasmids share a conserved backbone, pulsed-field gel electrophoresis and Southern blotting with plasmid and toxin gene specific probes has revealed that *C. perfringens* strains show significant variability in their pCW3-like toxin plasmid composition (4,48-50). This variability includes plasmid size (~47-135 kb), number of plasmids present per isolate and also toxin gene composition of these plasmids.

For example, type D isolates can carry one of more plasmids that vary in size and toxin gene content (45,48,51). Simple type D isolates carry a single *etx*-carrying plasmid. However, this epsilon-toxin plasmid can vary in size from 48 kb to 75 kb (48,50). By contrast complex type D isolates carry the *etx*, *cpe* and *cpb2* genes on plasmids that range in size from ~48 kb to ~110 kb (45,52). These toxins can be carried by one large plasmid with all three toxin genes or up to three plasmids that each carry a single toxin gene in isolation (52).

However, the plasmids of type B isolates exhibit much less heterogeneity when compared with plasmids from other *C. perfringens* types. Type B strains by definition must carry plasmid-borne *etx* and *cpb* genes, but may also carry plasmids encoding other putative virulence genes such as *tpeL*, *lam, ureC* and *cpb2* (50). Most type B isolates have a well conserved battery of plasmids, including variants of pCP8533etx, which is ~65 kb and encodes both *etx* and *cpb2* (45,50). Type B isolates may also carry a well conserved ~90 kb *cpb*-encoding plasmid and more rarely a ~65 kb *cpb* plasmid, both of which are distinct from the *etx* plasmid (50). Finally,

most type B isolates also contain a ~80 kb toxin plasmid, which carries the lambda toxin (*lam*) and urease (*ureABC*) genes (53,54).

The reduced plasmid heterogeneity in these strains could reflect restrictions imposed upon type B isolates by plasmid incompatibility exhibited between different toxin plasmids (see 'plasmid incompatibility' pg 52). That is, only the ~90 kb, and albeit less commonly, the ~65 kb *cpb* plasmids may be able to coexist with the ~65 kb *etx* plasmid found in most type B isolates (50). Other *cpb* plasmids, such as those commonly found in type C strains, may be excluded from type D isolates on the grounds they are incompatible with the 65 kb *etx* plasmid. The restrictions imposed by this potential plasmid incompatibility and the knowledge that only certain plasmid combinations can exist in a type B isolate, may explain why these strains seem to be far less common in nature (50).

Toxin genes associated with insertion sequences

The propensity for near identical toxin genes to be found in a variety of different genetic contexts can most likely be attributed to the close association of many of these genes with insertion sequences (44,52,53,55). The *cpe*, *etx*, *cpb*, *tpeL* and *iap/ibp* genes have been shown to be associated with different IS elements and have been found to be carried by different pCW3-like plasmids (44,45,48-51,56-59). Outward firing primers have been used to detect circular intermediates containing these toxin genes, suggesting that these IS elements may be able to transpose these adjacent genes, however, there is no direct evidence of transposition (51).

pCW3-like toxin plasmid evolution

The large regions of similar sequence that is conserved between these large conjugative plasmids suggests that they may have evolved from the same common progenitor plasmid. It has been postulated that a non-conjugative progenitor plasmid may have undergone an

insertion event that saw the integration of a Tn*916*-like conjugative transposon, which has since lost its ability to excise (17). Transposons associated with toxin genes may have inserted in these progenitor plasmids close to the *dcm* region, leading to the formation of plasmids that are similar to those that are currently observed in *C. perfringens* isolates (4,17,48-51,60). In addition, the similarity between multiple plasmids within the same strain suggests that recombination events may also have played a role in shaping new plasmid configurations, adding to the already diverse collection of plasmids observed in different strains of *C. perfringens*. The association of key virulence factors and resistance determinants with conjugative plasmids and putative transposons illustrates the importance of studying the mechanisms that underpin the replication, maintenance and propagation of these mobile genetic elements.

pCP13-like plasmids

Most studies have focused on the pCW3-like toxin and antimicrobial resistance plasmids of *C. perfringens*, however, another class of toxin plasmid is beginning to garner more interest in the field (61). Whole genome sequencing of the *C. perfringens* type A isolate, strain 13, revealed the presence of a 54 kb plasmid called pCP13 (62). pCP13 has a lower % G+C content than the strain 13 chromosome and encodes 63 putative ORFs, many of which encode proteins of unknown function. Several ORFs could be assigned a predicted function, including ORFs encoding a consensus beta2-toxin, collagen binding protein (Cna), conjugation protein homologues and also plasmid partitioning homologues, ParA and ParB (62). Although this plasmid has been sequenced, it remains relatively uncharacterised in comparison to the pCW3-like plasmids and initial sequencing of pCP13 did not show any similarity between pCP13 and the conjugation locus of pCW3. However, it was noted that pCP13 has several ORFs with similarity to conjugation machinery components (17,62,63). Although pCP13-like plasmids have conventionally been thought to be non-conjugative, there is no adequate

evidence to support or disprove this statement and as yet conjugative transfer of these plasmids remains an unexplored avenue of investigation in *C. perfringens*.

Recently, two plasmids, pCP-TS1 and pCP-OS1, were isolated from two *cpe* negative *C. perfringens* food poisoning isolates from two separate outbreaks in Japan (10). Sequencing of these plasmids led to the identification of a novel clostridial binary toxin, designated BEC (or CPILE) (10,64). BEC is comprised of two components, BECa and BECb, which show ~45% similarity to iota toxin components (10). The BECb component is responsible for most of the enterotoxic effects, however, its activity is enhanced by the BECa component, which has been shown to have ADP-ribosylating activity on actin *in vitro* (10). The BEC plasmids have substantial sequence similarity with pCP13 and thus represent an addition to the new family of pCP13-like plasmids (Figure 1.2). A genomic sequencing survey of a disparate collection of *C. perfringens* isolates may reveal more pCP13-like plasmids.

The most recent addition to the pCP13-like family is the bacteriocin-encoding plasmid pBCNF5603, a plasmid found to coexist with a pCW3-like CPE plasmid in the type A isolate F5603 (61) (Figure 1.2). Bacteriocins are antibacterial factors produced by bacteria to inhibit the growth of similar bacterial strains (65). Plasmid-encoded bacteriocins may also play an important role in killing plasmid-free segregants in the population (66). *C. perfringens* has been demonstrated to produce a number of bacteriocins (61,67-69), some of which have been implicated in strain competition in the GI tract of broiler chickens (61,70,71).

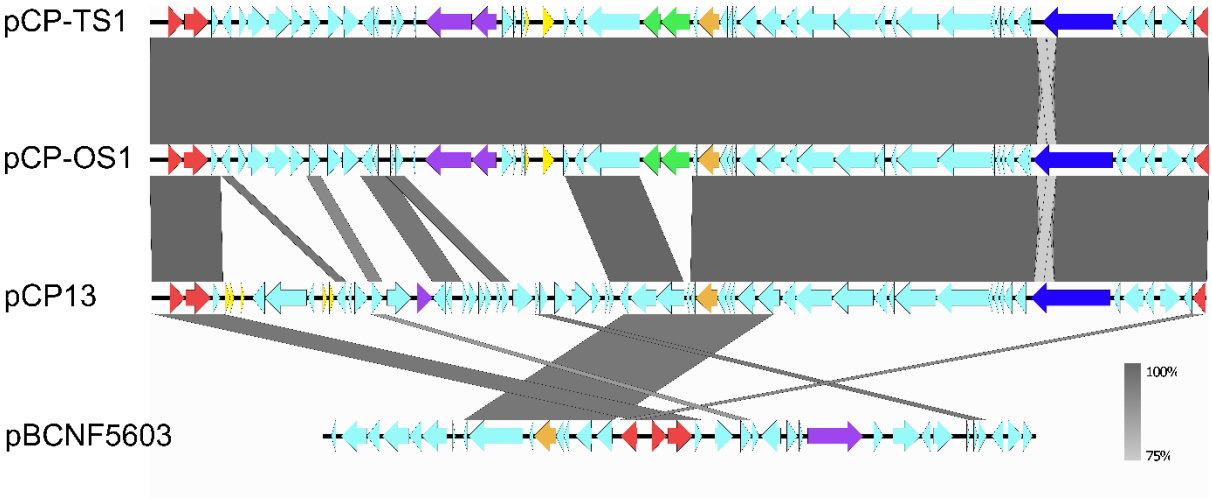

Figure 1.2. Comparison of pCP13-like plasmids in *C. perfringens*: The sequences of pCP-TS1, pCP-OS1, pCP13 and pBCNF5603 were compared using EasyFig (72), the percentage nt identity is indicated by the scale bar in the bottom right. ORFs are represented as arrows and ORFs of interest are coloured as follows: red arrows are plasmid replication and maintenance genes, purple arrows are toxin genes, dark blue arrows are putative collagen adhesins, orange arrows are putative relaxases, green arrows are restriction modification systems yellow arrows are transposase genes.

pBCNF5603 was recently sequenced and found to have a range of ORFs that have a high level of similarity with those of pCP13 and the bacteriocin plasmid pIP404, suggesting that it may have arisen from a recombination event between these two *C. perfringens* plasmids (61). Sequencing of this plasmid has provided insight into the replication functions of pCP13-like plasmids by allowing two potential replication regions to be identified (61). The first replication region has homology to the *rep* and *cop* genes of the small bacteriocin plasmid pIP404, whereas the second region displayed similarity to the *pcp63parAparB* gene cluster of pCP13 (Figure 1.2, red arrows). A 5.5 kb pBCNF5603 gene region (*pbcn16parAparBpbcn19*) was shown to support replication of a recombinant plasmid in *C. perfringens*, whereas the replication region with similarity to pIP404 (*pbcn29* and *pbcn30*) did not (61). Further deletion derivatives of the *pbcn16* to *pbcn19* recombinant plasmid resulted in the isolation of a replicating plasmid containing only the *pbcn16* gene, the intergenic region and part of the divergently transcribed *parA* gene, suggesting that an undisrupted *pbcn16* ORF is required for the replication of pBCNF5603. *pbcn16* has similarity to *pcp63* from pCP13, as well as genes from several other *C. perfringens* plasmids including the BEC plasmids pCP-TS1 and pCP-OS1 (10,61,62). The similarity between these ORFs indicates that these genes may also be involved in initiating plasmid replication in their respective plasmids (10,61,62).

The intergenic region between the putative *rep* (*pbcn16*) and *parA* genes was also analysed. This region was found to be AT-rich, with a series of inverted repeats likely to be potential iterons and to be important for replication initiation (61) These recently identified plasmid replication proteins may represent a novel replication protein family in *C. perfringens*, however, the mechanism by which these proteins initiate replication requires further characterisation. As yet the processes governing replication initiation and replication regulatory control in *C. perfringens* are yet to be explored in great mechanistic detail (61).

Non-conjugative *C. perfringens* plasmids

Although most virulence and antimicrobial determinants that are integral for *C. perfringens* pathogenicity are localised to pCW3-like and pCP13-like plasmids, there also are a number of less characterised, non-conjugative plasmids that either encode bacteriocins or remain cryptic. Research regarding these plasmids has been neglected due to a focus on the toxin plasmids (9,10,12).

The bacteriocin plasmid pIP404

Bacteriocin plasmids have been isolated from a variety of *C. perfringens* strains (5,61,73-76), but only a small number of these plasmids have been sequenced and characterised (61,76,77). The best characterised example of these plasmids is the 10.2 kb plasmid pIP404, which encodes the genes required for the production of the BCN5 bacteriocin (77,78). Though non-conjugative, pIP404 is able to be mobilised by conjugative resistance plasmids present in *C. perfringens* and potentially in its native strain by the cryptic plasmid pIP405 (18). pIP404 carriers 10 ORFs, including genes required for UV-induced bacteriocin production and immunity, *bcn, uviA* and *uviB,* as well as several genes involved in replication initiation, multimer resolution and copy number control, namely *rep, res* and *cop* (77-79).

The minimal replication region of pIP404 was characterised using restriction analysis and cloning, where it was shown that *rep* and its downstream repeat region were required for replication in *Bacillus subtilus* (80). Although the *rep* gene product does not have similarity to any other known replication proteins it does possess a putative helix-turn-helix motif suggestive of DNA-binding potential. The downstream repeat region consists of a dispersed tandem array of two families of direct repeats and is similar to the origin of replication found in other plasmids (5,80,81). No evidence of a single stranded replication intermediate was discovered for pIP404, which suggests that this plasmid replicates by a theta rather than a rolling circle replication mechanism.

Replication or copy number control is often multifactorial, consisting of multiple layers of regulation (81,82). pIP404 seems to rely upon three different copy number control mechanisms. The *cop* gene is not required for replication, however, recombinant vectors that encode the minimal *rep* region, but lack the *cop* gene, have a five-fold higher copy number indicating that this gene plays a role in copy number control (80). In addition, a 150 nucleotide RNA molecule that is complementary to the 3' 130 bp of the *rep* gene was also recognised during the characterisation of the replication region. This RNA species, denoted RNA1, may play a role in antisense regulation of replication by sequestering the pIP404 *rep* mRNA. Further studies to validate this hypothesis are required (80). Some plasmids have a tendency to form multimers, which can result in copy number imbalances and the unstable inheritance of these plasmids at cell division (83). To ensure their faithful inheritance and maintenance of a stable copy number these plasmids often encode a site-specific recombinase to resolve multimeric forms of the plasmid, thus freeing plasmid monomers to ensure equal segregation at cell division (83). pIP404 encodes a gene, *res*, which shows similarity to the invertases *hin, pin, cin* and *gin* of *E. coli, Samonella* Typhimurium and the bacteriophage Mu (79). It has been suggested that this gene may play a role in stabilising plasmid copy number and therefore ensuring stable inheritance (79).

Plasmid replication

All plasmids must replicate and maintain a stable copy number relative to the host chromosome in order to be faithfully inherited by daughter cells at cell division. Plasmids generally replicate *via* one of three mechanisms, theta, strand displacement or rolling circle replication (reviewed in (84-87). Theta replication requires the presence of an origin of replication (*oriV*) on which a replication initiator acts to prepare the plasmid DNA for replication (84,87,88). Unlike theta replication, plasmids that replicate via the strand displacement mechanism do not require host encoded factors such as DnaA, DnaB/C or DnaG (85). These plasmids encode their own replication initiator (RepC), helicase (RepA) and primase (RepB)

and as such possess a much broader host range than plasmids that rely upon the host-encoded replication machinery (85). Rolling circle replication (RCR) generally involves recognition and nicking of a double strand origin (*dso*) by an initiator (86).

The initiation of plasmid replication must also be tightly controlled, especially for large plasmids that impose a significant metabolic burden on the host cell (87,88). Plasmids that replicate too infrequently will be lost upon cell division, whereas plasmids that replicate too often will exaggerate the metabolic burden they confer upon the cell, leading to destabilisation of both the plasmid and the host (88). The ability to replicate autonomously from the chromosome and therefore adjust the rate of replication initiation to account for copy number abnormalities is critical for the maintenance of large plasmids (88,89).

Replication of pCW3

Sequencing of pCW3 identified a gene cluster containing potential plasmid maintenance and regulation functions, although initial attempts to annotate the pCW3 sequence did not successfully identify a gene with significant similarity to any known replication genes (17). Restriction enzyme analysis and cloning were used to determine the region of pCW3 that was required to support plasmid replication in *C. perfringens*. This analysis showed that replication was supported by a 4 kb region that included four genes, *pcw310-pcw314* (Figure 1.3). An intergenic region was also identified, between *pcw313* and *pcw314*; this region had five inverted repeats and a series of 17-bp direct repeats. Random transposon mutagenesis and mapping in *E. coli* was used to construct several insertions in the *pcw310-pcw314* gene region. Vectors with insertions in the *pcw314,* gene or at position 13047 bp within the upstream intergenic region, could no longer support replication in *C. perfringens*, indicating that *pcw314* is a unique replication protein, now designated as the Rep protein, that most probably acts on an upstream target site encompassing position 13047 in pCW3 (17).

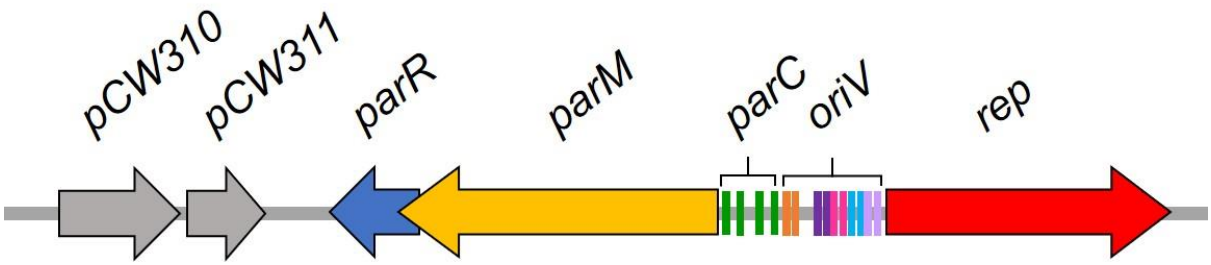

Figure 1.3. Replication region of pCW3: The minimal replication region of pCW3 is shown. The red arrow is *rep* or *pcw314*, the *oriV* site is shown upstream of the *rep* gene, IR1 (orange), IR2 (purple), IR3 (pink), IR4 (blue) and IR5 (lavender) are indicated by the coloured boxes. The *parC* site (green) direct repeats are shown upstream of *parM,* represented by the yellow arrow, *parR* is represented as a blue arrow, *pCW310* and *pCW311* are hypothetical proteins indicated by the grey arrows.

There are still many questions yet to answer regarding how this plasmid replicates in *C. perfringens*. How does the unique Rep protein act to initiate replication in *C. perfringens*? How is replication initiation and therefore copy number controlled in these plasmids? What is the minimal replicon of pCW3-like plasmids? Further experiments are required to determine the answers to these fundamental questions.

Conjugative transfer mechanisms

Conjugation involves the direct transfer of genetic material from one bacterium to another *via* cellular contact. Conjugation was first described in 1946 by Lederberg and Tatum as bacterial sex (90,91), since then our understanding of the mechanisms governing transfer have improved considerably. The mechanism by which plasmids undergo conjugation has primarily been studied in Gram-negative organisms and generally involves three major components (92): (i) the relaxosome, which is involved in initial DNA processing and nicking of the origin of transfer (*oriT*), (ii) the coupling protein, which facilitates interaction of the nucleoprotein complex comprised of the relaxase enzyme and ssDNA with (iii) the type 4 secretion system (T4SS) transfer apparatus, which facilitates mating pair formation (mpf) between the donor and the recipient cell, thus ensuring effective plasmid transfer. The systems that have been most well characterised are that of the *Agrobacterium tumefaciens* Ti plasmid and the *E. coli* plasmids F, pKM101, RP4 and R388. The *A. tumefaciens* nomenclature (*virD1-virD4*, v*irB1-virB11*) is the accepted standard for discussing conjugation systems (92,93).

The relaxosome

The genes that encode the components of both the relaxosome and the T4SS are usually organised into several operons. The *A. tumefaciens* VirB/D T4SS is arranged into two operons: an operon that has 11 genes (*virB1-virB11*), which encode the components of the T4SS and a second operon that has four genes (*virD1-virD4*) that encode components of the relaxosome and the coupling protein (VirD4) (94). Formation of the relaxosome and

processing of the DNA substrate is the first step in plasmid transfer. The relaxosome consists of several components including the relaxase and a series of accessory proteins that bind to *oriT* (95-97). Relaxases have been classified into six groups (98). They are generally large proteins with an N-terminal relaxase domain and a C-terminal helicase domain (97,99-101). The relaxase has phosphodiesterase activity that allows it to recognise, nick and covalently bind to *oriT* in both a site and strand-specific manner (96,97). The result of this interaction is a covalent 5'- phosphotyrosine linkage between the *nic* site within *oriT* and the reactive tyrosine of the relaxase (96). Interaction of the nucleoprotein intermediate with the coupling protein then facilitates transfer of the ssDNA through the transferosome or mpf complex (92,94).

The coupling protein

VirD4-like coupling proteins are responsible for linking the relaxosome nucleoprotein complex to the T4SS transfer machinery. Coupling proteins generally possess an N-terminal transmembrane domain that is important for protein stability and interaction with other components of the T4SS channel such as the VirB10-like proteins, and a large C-terminal cytoplasmic domain, which generally has nucleotide binding domains (94,102-106). Functional analysis of the R388 coupling protein TrwB has shown that it is a DNA-dependent ATPase and that this activity can be controlled by interaction with relaxosome accessory proteins such as TrwA (107-109). The structure of several coupling proteins have been solved (110-112) and analysis has shown that they generally form a hexameric ring-like arrangement with a 20 Å wide channel and an 8 Å diameter pore at the cytoplasmic side, large enough to allow ssDNA to pass through (110-113).

The T4SS transfer complex

T4SSs have a variety of functions in nature, they may deliver protein effectors or toxins to host cells, be involved in the uptake or secretion of DNA or facilitate plasmid DNA transfer between

bacterial cells (92,94). The T4SS utilised in Gram-negative conjugation spans both the inner and outer membranes. The complex itself has several key components including ATPases, which provide energy for translocation and pilus biogenesis, structural components that form the membrane spanning transfer channel and protein components that make up the conjugation pilus (94).

In addition to the coupling protein, the T4SS have two other ATPases that provide energy for pilus biogenesis and DNA translocation, namely, VirB4 and VirB11. VirB4 is the most well conserved T4SS component and is found in all conjugation systems. It is important for pilus biogenesis and DNA translocation (92,114-116) and is localised to the inner membrane where it interacts with several other T4SS components including the channel proteins VirB3, VirB6, VirB7 and VirB8 (92,116). VirB4 has an N-terminal domain and a more conserved C-terminal ATPase domain containing nucleotide binding Walker A and B motifs, as well as two other conserved motifs called motif C and motif D (117). Monomeric and higher oligomeric structures (dimeric, hexameric) have been suggested for VirB4 (118-120). Studies using electron microscopy have led to the elucidation of the structural organisation of the R388 VirB4 homologue TrwK, which was found to exist in a hexameric ring-like configuration (120). The VirB11 protein belongs to the traffic ATPase family and is localised to the cytoplasmic membrane (121). It interacts with both VirB4 and VirD4 (122) and is thought to be important for both pilus biogenesis and DNA translocation (92). Structural studies using both X-ray crystallography and electron microscopy have revealed that it also exists in a hexameric form (123,124).

The translocation channel is the structure through which the DNA is transferred to the recipient cell. The channel is made up of the T4SS components VirB3, VirB6, VirB7, VirB8, VirB9 and VirB10 (92,94). Cryo-electron microscopy was recently used to deduce the structure of the core complex (CC) of the *E. coli* plasmid pKM101 transferosome to a resolution of 15 Å (125,126). This complex can be split into inner and outer layers. The inner layer is comprised

of the VirB3, VirB6 and VirB8 proteins (92,94,126). VirB3 is a transmembrane protein that is the least characterised component of the T4SS (127). VirB6 is an essential hydrophobic protein localised to the inner membrane, it has five transmembrane domains with an N-terminal periplasmic domain and a C-terminal cytoplasmic domain (94). VirB8 is important for the recruitment of other T4SS components for pore assembly. VirB8 has a cytosolic domain, a transmembrane helix and a periplasmic domain and interacts with VirB1, VirB4, VirB5, VirB6, VirB9, VirB10 and VirB11 suggesting that it plays an important part in complex assembly (94).

The outer layer is comprised of VirB7, VirB9 and VirB10 (94,128). VirB7 is a small membrane protein that acts to direct the assembly and insertion of the channel into the outer membrane (125). VirB9 proteins are found in the periplasm and interact with both VirB7 and VirB10 (94). VirB10 spans both the inner and outer membrane and with VirB7 and VirB9 forms the central portion of the T4SS channel (128). Although not part of the central structure, VirB1 also plays a role in preparing the membrane for complex assembly. VirB1 is a lytic transglycosylase that has muramidase activity and is involved in digestion of peptidoglycan to allow complex assembly and pilus biogenesis (94).

The T4SS pilus

The conjugation pilus is an extracellular tubular structure that is involved in making contact with, and transferring DNA to, the recipient cell (92). The pilus is generally made up of two components, a major pilin subunit, VirB2 and a minor pilin subunit VirB5 (129,130). The VirB2 homologue from *A. tumefaciens* is a cyclic peptide that makes up most of the pilus structure (131). VirB5 adorns the tip of the pilus and likely plays a role in host cell recognition or adhesion (132).

Gram-positive conjugation

In the 1970s and early 1980s plasmids from several Gram-positive genera were shown to move between strains *via* a conjugation-like mechanism (18,22). Conjugative plasmids have now been identified in many Gram-positive genera including *Bacillus*, *Streptococcus*, *Staphylococcus*, *Enterococcus* and *Clostridium* (4,133). Gram-positive organisms rely upon a reduced or minimised T4SS, likely due to the difference in cell wall structure between Gram-positive and Gram-negative organisms (133). Gram-positive organisms lack an outer membrane and therefore do not require many of the outer membrane components of the Gram-negative T4SS, including a pilus component, which has not been identified in any Gram-positive conjugation system. Gram-positive conjugation is not as well characterised as Gram-negative conjugation, however, the principles and mechanism remain the same. Therefore, the processes and machinery that control conjugation bear some similarity (4,133).

Conjugative transfer of the broad host range plasmid pIP501

pIP501 is a 30.2 kb conjugative plasmid that encodes the genes required for both erythromycin and chloramphenicol resistance. It was first isolated from *Streptococcus agalacticae* in the 1970s (134), but has since been found to have a broad host range (135). The pIP501 conjugation system represents one of the most well characterised Gram-positive transfer mechanisms. The transfer or *tra* locus of pIP501 is organised into an operon consisting of 15 *tra* genes (*traA*-*traO*), which is preceded by an *oriT* site (136-139) (Figure 1.4).

Similar to Gram-negative conjugation mechanisms, pIP501 must be processed by a relaxase, TraA, at its *oriT* site before being recruited to the T4SS by a coupling protein (137,140,141). Additionally, the *tra* operon promoter overlaps partially with *oriT* and is repressed upon TraA binding, thus TraA autoregulates the *tra* operon (138). The transfer region of pIP501 also encodes several ATPases, including a VirB4 homologue called TraE, and a VirD4 homologue,

TraJ. TraJ is predicted to be the pIP501 coupling protein. This hypothesis is supported by data showing that it interacts with the pIP501 relaxase, TraA (139).

Unlike Gram-negative organisms, Gram-positive bacteria must contend with a thick layer of peptidoglycan in order to undergo conjugative transfer. Therefore, pIP501 encodes a peptidoglycan hydrolase called TraG that is essential for plasmid transfer (142). TraG has several predicted catalytic domains, including a C-terminal cysteine-histidine dependent aminohydrolase and a transmembrane anchor followed closely by a lytic transglycosylase. The catalytic activity of these domains has been demonstrated by TraG-mediated cleavage of peptidoglycan from *E. faecalis* and *E. coli* (142). TraG is therefore important for the formation of the transfer channel.

The transfer channel or T4SS in Gram-positive organisms is much simpler, but only two components, TraM and TraL, have been studied in detail in pIP501. Determination of the structure of the C-terminal surface exposed region of TraM revealed that it is a VirB8 homologue with some similarity to TcpC from *C. perfringens* (133). Based on this structural similarity it is predicted to form part of the transfer channel scaffold (133). TraL is a VirB6 homologue and is predicted to act as a scaffold protein that is important in the structure of the inner membrane channel (139). pIP501 also encodes a putative surface adhesin, TraO, a protein that is predicted to facilitate contact with the recipient cell prior to conjugation (133).

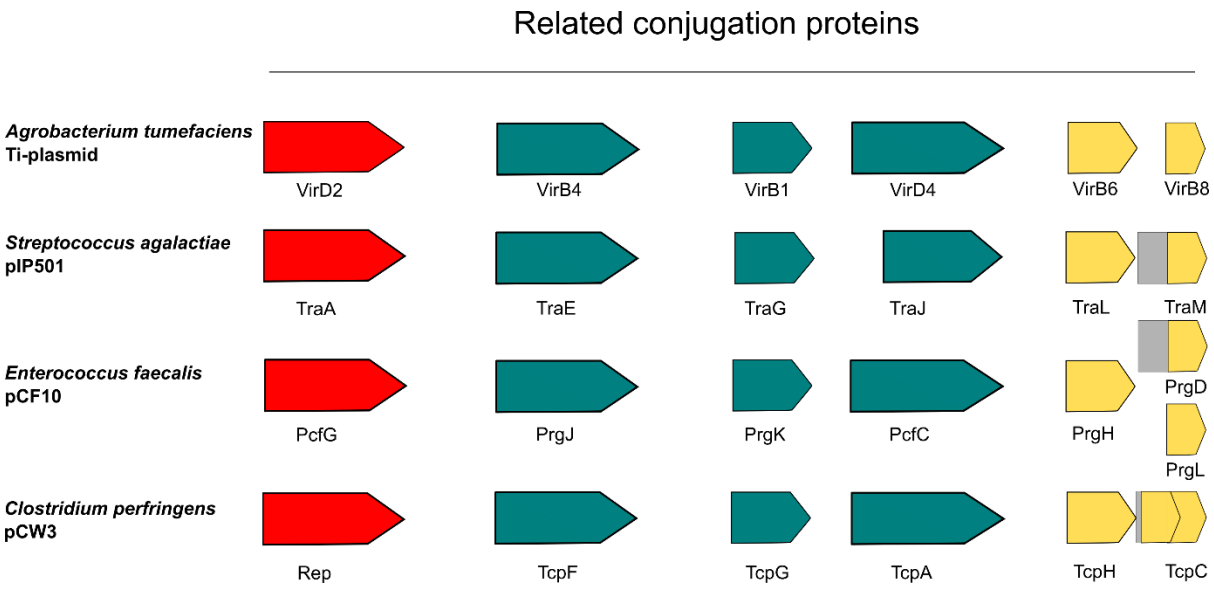

Figure 1.4. Related Gram-positive conjugation proteins compared to *A. tumefaciens* Ti-homologues: Red genes are putative relaxases, blue genes are conjugation homologues, yellow genes are conjugation scaffold genes, grey regions are extended domains. Adapted from (133). pTi is the *Agrobacterium tumefaciens* virulence plasmid, pIP501 is a broad host range Gram-positive plasmid that carries chloramphenicol and erythromycin resistance determinants, pCF10 is the enterococcus sex pheromone plasmid, pCW3 is a *C. perfringens* plasmid that carries tetracycline resistance determinants Tet(P).

The pCW3 Tcp locus and conjugative transfer

The conjugative potential of pCW3-like plasmids from *C. perfringens* was first shown in the 1970s where it was demonstrated that the transfer of tetracycline resistance could be attributed to the acquisition of large plasmids (18,22). The ability of these plasmids to transfer between *C. perfringens* strains was retained after treatment with DNase, but abolished when cell to cell contact was disrupted by a physical barrier such as a Millipore filter, indicating that plasmid transfer was mediated by conjugation rather than transformation or transduction (18). Many of the large pCW3-like plasmids of *C. perfringens* have been shown to be conjugative, including the resistance plasmids pCW3, pIP404 and pJIR4150, as well as plasmids carrying the toxin genes *etx*, *cpe*, *cpb2* and *netB* (16,17,25,35,44-47)

All conjugative *C. perfringens* plasmids examined to date carry the Tcp locus, although not all pCW3-like plasmids have been demonstrated to be conjugative experimentally, Southern hybridisation of pulse field gels has been used to show that many more toxin plasmids also encode Tcp loci and are therefore highly likely to be conjugative (44,52,53,55). The finding that many of these toxin plasmids carry a Tcp locus suggests that this mechanism of conjugation is highly conserved in *C. perfringens* (4,143).

The pCW3 Tcp (transfer of clostridial plasmid) locus consists of 12 genes (designated *tcpM and tcpK* and *tcpA-tcpJ*), five of which encode putative proteins that show limited similarity to proteins from the conjugative transposon Tn*916* (17). The role of each *tcp* gene in conjugative transfer of pCW3 has been assessed by mutagenesis, complementation and protein interaction studies (4,17,63,144,145).

Until recently, no relaxase homologue or *oriT* site had been identified for pCW3. Recent work has revealed that TcpM (formerly IntP), a putative tyrosine recombinase, acts as an atypical relaxase enzyme and is essential for efficient pCW3 conjugation (146). TcpM activity is ablated

by substitution of tyrosine 259, suggesting that this residue is responsible for nicking of the *oriT* site (146). The *oriT* site was identified using mobilisation studies, which showed that vectors containing the 391 bp region upstream of *tcpM* could be mobilised (146). Gel mobility shift assays with TcpM and a variety of *oriT* deletion derivatives, demonstrated that *oriT* was located within a 150 bp site within this intergenic region (146).

The *in vitro* DNA nicking activity of TcpM is not site-specific, suggesting that *oriT* nicking requires an additional recognition factor (147). The gene directly upstream of the *oriT* site, *tcpK*, is required for efficient conjugative transfer of pCW3 (147) and TcpK was shown to form an unusual wHTH dimer in solution, which is able to bind with specificity to 9-bp repeats within the *oriT* site (147). The role TcpK plays in conjugation remains unclear, however, it is likely to have an accessory role in the formation of the relaxosome. Future studies will focus on dissecting the relaxosome further by determining whether there are any other accessory proteins present in the complex, whether other *tcp* components are able to interact with TcpM to facilitate transfer and whether TcpM is transferred to the recipient cell along with its bound plasmid DNA cargo.

After initial processing of *oriT,* the relaxosome must interact with the rest of the transfer apparatus; this interaction is facilitated by the coupling protein. The putative pCW3 coupling protein, TcpA, possesses two N-terminal transmembrane domains and a cytoplasmic domain that possess an FtsK/SpoIIIE-like domain. Within this FtsK-like domain there are three motifs that are essential for the function of TcpA, Walker A and B ATP-binding domains, and an FtsK RAAG motif. Site directed mutagenesis of any one of these motifs led to abrogation of plasmid transfer (63). To perform its function as a coupling protein and to ensure that plasmid DNA is transferred effectively TcpA must interact with other components of the transfer apparatus. Bacterial two hybrid analysis and chemical cross-linking showed that TcpA interacts with itself to form homooligomers as well as with TcpC, TcpG and TcpH (148). Mutation of either the Walker B domain or N-terminal transmembrane domains of TcpA abolished self-interaction.

Loss of the transmembrane domains also resulted in abrogation of the TcpA-TcpG and TcpA-TcpH interactions. TcpA-TcpC interaction was dependent on the C-terminal 61 amino acids of TcpA, as deletion of these residues resulted in abolition of interactions between these proteins (148).

The T4SS conjugation apparatus generally has two hexameric ATPases: the coupling protein and a second ATPase to provide energy for plasmid transfer (92,94). TcpF has a conserved ATPase domain and shows similarity to ORF16 of Tn*916*, it most likely provides energy to the conjugation apparatus for plasmid transfer (17). The *tcpF* gene is essential for transfer (17). and studies employing immunofluorescence microscopy indicated that TcpF is located at the poles of the donor cell, in close association with TcpH, suggesting that the transfer complex assembles or accumulates at the cell poles of the donor cell (149).

TcpC has 24% amino acid similarity to ORF13 of Tn*916* and although *tcpC* is not essential for plasmid transfer, mutation of *tcpC* results in a significant decrease in transfer efficiency (17,150). TcpC has an N-terminal transmembrane domain that is important for protein function, localises to the cell membrane and interacts with itself and other Tcp-encoded proteins, including TcpA, TcpG and TcpH (148-150). To further characterise the basis for these interactions the crystal structure of soluble C-terminal domain of TcpC was determined to 1.8Å. The structure revealed that TcpC forms a trimer and is structurally similar to the VirB8 scaffold protein of the *A. tumefaciens* T4SS (150). Therefore, TcpC is predicted to be a scaffold protein that is important for stability and formation of the *C. perfringens* transfer apparatus (4,150).

TcpH is an integral transmembrane protein with eight putative N-terminal transmembrane domains, a VirB6-like domain and two predicted C-terminal coiled-coil domains. The N-terminal transmembrane domains of TcpH show low level amino acid sequence similarity to ORF15 from the conjugative transposon Tn*916*. *tcpH* is essential for conjugation as Δ*tcpH*

mutants are unable to undergo transfer (17). Functional analysis of TcpH using site-directed mutagenesis and deletion studies showed that the N terminal 581 amino acids, the last four transmembrane domains, which have similarity to VirB6-like protein family, and the transmembrane motif $_{242}$VQAAA$_{246}$ were all essential for its function (149). Bacterial two hybrid experiments also showed that TcpH was capable of interacting with itself, TcpA and TcpC, and that the N-terminal domain was critical for these interactions (149). Cell fractionation, Western blotting and immunofluorescence microscopy showed that TcpH was present in the membrane fraction and was localised specifically to the cell poles along with TcpF, TcpD and TcpE (145,148,149). Based on the current evidence, including its similarity to VirB6-like proteins, TcpH is predicted to be an integral membrane protein that, along with TcpC, forms the major structural component of the transfer apparatus channel (149).

TcpD and TcpE are conserved hypothetical proteins that are encoded within the Tcp locus; they are relatively small proteins of 115 amino acids and 122 amino acids, respectively. Both TcpD and TcpE possess predicted transmembrane domains, which is the only clue to their putative function. TcpD shows no significant similarity to any known proteins, whereas TcpE has 27% amino acid sequence similarity to ORF17 of Tn*916*, the function of which is unknown. Despite their unknown function, mutagenesis and subsequent complementation has shown that TcpD and TcpE are essential for conjugative transfer (145). Cell fractionation and immunofluorescence has shown that both TcpD and TcpE are localised to the cell membrane, specifically to the cell poles, like TcpF and TcpH (145,149). *tcpJ* is another hypothetical protein found within the Tcp locus, however unlike *tcpD* and *tcpE,* mutation of *tcpJ* results in wild-type levels of transfer, indicating that it is not required for conjugation (145).

Gram-positive organisms must be able to produce a localised pore or channel in the peptidoglycan layer to allow for the assembly of the transfer apparatus. Therefore, they often encode a conjugation-specific peptidoglycan hydrolase, and *C. perfringens* is no exception. Within the *tcp* locus of pCW3 there are two genes, *tcpG* and *tcpI,* that encode products with

similarity to peptidoglycan hydrolases (17,144). Mutation of *tcpG* and *tcpI* showed that *tcpG* was required for efficient conjugative transfer, but not *tcpI* (144). TcpG has a putative signal peptide and is a 334 amino acid protein that shares low level similarity to ORF14 of Tn*916*. TcpG has two catalytic domains including an N-terminal catalytic muramidase-like FlgJ domain and a C-terminal NlpC/P60 endopeptidase domain, both of which are functionally important since alteration of these domains leads to lower transfer efficiency (144). The peptidoglycan hydrolase activity of TcpG has also been demonstrated using *in vitro* peptidoglycan hydrolysis assays (144).

Most of the *tcp* locus components have been investigated individually and a great deal is known about the function of each component in isolation, allowing a model of the pCW3 plasmid conjugation apparatus to be proposed (Figure 1.5). Future experiments will aim to put the individual functions of these proteins into context, by studying them as part of the full transfer apparatus or as a series of sub-complexes. Isolation and imaging of the transfer apparatus as a whole or imaging of mating pair formation between donor and recipient cells will provide valuable insight into the mechanisms that govern plasmid transfer in this novel conjugation system.

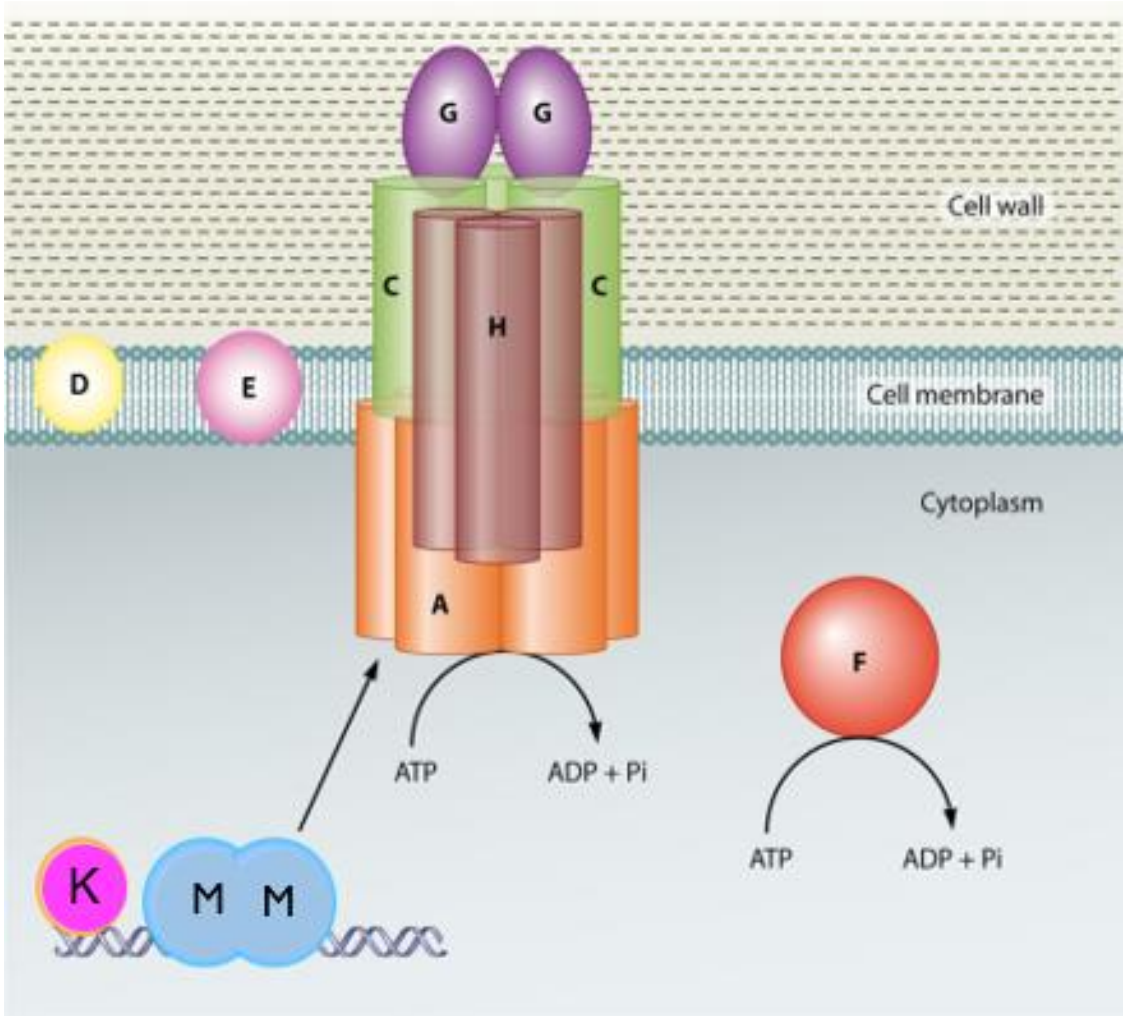

Figure 1.5. Model of the pCW3 conjugative transfer machinery: TcpA is the coupling protein and is represented as an orange hexamer, TcpF is an ATPase shown as a red circle, TcpC makes up part of the channel and is shown in green, TcpH is brown and also makes up part of the channel, TcpG is a peptidoglycan hydrolase and is shown in purple at the complex/peptidoglycan interface, TcpD (yellow) and TcpE (light pink) are integral membrane proteins, the blue spheres coupled to the DNA represent TcpM, TcpK is represented as a bright pink sphere bound to the *oriT*. Adapted from (4).

Plasmid maintenance mechanisms

Large plasmids typically exist at lower copy number to reduce the metabolic burden that they impose upon a host cell (83). Low or unit-copy number plasmids are inherently susceptible to loss at cell division and as a consequence must encode both active and passive maintenance systems to ensure they are faithfully inherited (66). In contrast, high-copy number plasmids are thought to rarely require stabilisation systems as they exist in excess and therefore rely on random distribution to daughter cells at cell division (66,89,151). In 1963, Jacob and Brenner proposed a plasmid replicon model (152), after which there were suggestions that the stable inheritance of plasmids would be dependent on the attachment to specific structural sites within the growing bacterial cell prior to cell division (153).

This model provided a simple explanation for the mechanism of plasmid segregation and stable inheritance. Since then our understanding of plasmid inheritance and the systems that are responsible for this phenomenon has progressed. The three major mechanisms utilised by low-copy number plasmids to ensure they are effectively maintained in a bacterial population are: post-segregational killing systems or toxin-antitoxin systems, multimer resolution systems and plasmid partitioning systems (154-157).

Toxin-antitoxin systems and post-segregational killing

Toxin-antitoxin systems also known as post-segregation killing systems are employed by low-copy number plasmids as an auxiliary method of stabilising vertical plasmid inheritance if true partition functions fail (83). These systems generally encode two components, a stable toxin, which acts to disrupt cell growth and is always a protein, and a labile antitoxin, which counteracts the effects of the toxin and can either be a protein or a small regulatory RNA species (158). The differential stability of the toxin and antitoxin components is important for stabilisation of the plasmid. Plasmid-containing cells function normally as the toxin component is inhibited by the constitutive expression of the labile antitoxin (158,159). Upon curing of a toxin-antitoxin system-encoding plasmid, the labile antitoxin component is degraded rapidly

by cellular proteases or RNases, thus activating the toxic component, which decreases cell viability and leads to removal of plasmid-free cells from the bacterial population (158,159). Several studies propose alternative functions for plasmid-encoded toxin-antitoxin modules. These systems have been suggested to provide an advantage to plasmids after horizontal gene transfer events, whereby toxin-antitoxin encoding plasmids can exclude and therefore outcompete non-toxin-antitoxin encoding plasmids (160,161).

Multimer resolution

Plasmids occasionally recombine after replication to form multimers. Plasmid copy number control mechanisms sense the number of *oriV* sites present within a cell. As a consequence plasmid multimers will be recognised as two separate origins rather than one multi-origin molecule, resulting in a reduction in the number of segregating plasmid units, which subsequently leads to defects in segregation and unequal inheritance of plasmids at cell division (66,162). To ensure that these multimers are resolved to produce monomers, thereby ensuring an adequate number of plasmid copies for segregation, plasmids frequently encode their own multimer resolution systems (83,162). Resolution systems mediate multimer separation *via* controlled DNA breakage, strand exchange and re-joining of specific plasmid sequences; these reactions are mediated by plasmid-encoded enzymes called site-specific recombinases. Site-specific recombinases can be split into one of two families based upon whether the residue that makes a covalent attachment to the DNA in the reaction intermediate is a serine or a tyrosine (163).

Serine recombinases or resolvases act by binding each strand of the DNA at the recombination site (one monomer per strand), leading to cooperative breakage of all four strands and the formation of a covalent 5' phosphoserine attachment between the DNA and its adjacent monomer (reviewed in (163)). An example of a plasmid that relies upon site

specific recombination mediated by serine recombinase is the *E. coli* plasmid RP4, which utilises the protein ParA to resolve multimers (164).

The mechanism of tyrosine recombinase-mediated recombination is more complex (reviewed in (163)). In contrast to serine recombinases, tyrosine recombinases break two of the four DNA strands at the recombination site leading to the exchange of only half the DNA strands with the subsequent formation of a Holliday junction. Once the Holliday junction is formed the recombinases facilitate second strand breakage and exchange leading to resolution of the Holliday junction and formation of the new recombinant species. Examples of plasmid encoded tyrosine recombinases that are thought to be important for stabilisation include the ResD recombinase of the F plasmid and the Cre recombinase of the bacteriophage P1 (165,166).

Plasmid partitioning systems

Partitioning or *par* loci are defined by their ability to stabilise the inheritance of low-copy number plasmids separate from plasmid replication or other copy control mechanisms (167). Plasmid partitioning systems mediate the correct segregation of low-copy number plasmids to daughter cells at cell division, thus ensuring that plasmids are inherited stably throughout a bacterial population. These simple tripartite systems are entirely plasmid encoded and typically rely on the action of two *trans*-acting proteins and a *cis*-acting centromere site (168-170). The *trans*-acting proteins include an NTPase that utilises NTP-binding and hydrolysis to provide force for plasmid segregation and a DNA-binding protein that acts as an adaptor, which links the NTPase to the plasmid by binding to the centromere site (Figure 1.6) (170).

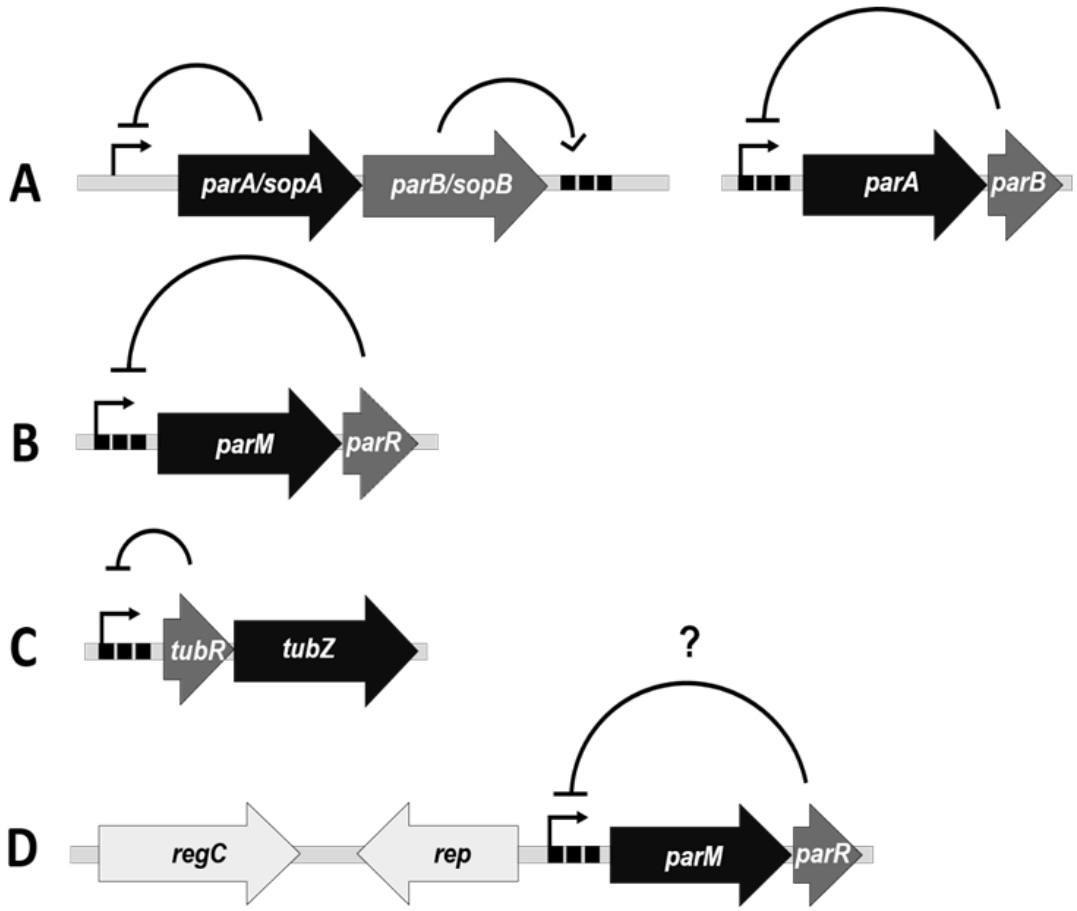

Figure 1.6. Genetic structure of plasmid encoded partitioning systems: A: The arrangement of the type Ia and Ib *parABS* locus. *parA* encodes a Walker A cytoskeletal P loop ATPase, *parB* encodes a DNA-binding protein and *parS* is the centromeric DNA. Type Ib *parABS* locus, the centromere *parS* is located in the promoter region **B:** *parMRC* operon, *parM* encodes the actin-like ATPase, *parR* encodes a DNA-binding protein and *parC* is the centromere which consists of a series of DNA repeats and also contains the *parMR* promotor thus allowing autoregulation. **C:**The genetic arrangement of the *par* locus which encodes the prokaryotic tubulin homolog partitioning system. The arrangement of this locus is somewhat different to the other loci as the order of genes is reversed. *tubR* is first in the operon and encodes a putative DNA- binding protein, this is followed by another gene called *tubZ* which encodes a tubulin homologue GTPase. **D:** Genetic structure of ParMRC systems from pCW3-like plasmids, where ParR binding to *parC* potentially autoregulates the ParMR operon. Figure reproduced from (171).

There are three types of partitioning systems in bacteria, each is categorised by the type of NTPase it encodes (170). Type I partitioning systems encode a variant Walker A ATPase, Type II systems encode an actin-like ATPase, while Type III partitioning systems encode a tubulin-like GTPase. A fourth partitioning type has also been described for the staphylococcal plasmid pSK41, which relies upon a single partition protein for segregation (172). Although the components and the mechanisms by which they achieve plasmid segregation are different in each of these plasmid partitioning systems, the basic mechanism is conserved. In each system a nucleoprotein complex consisting of a plasmid-located centromere site and bound centromere binding proteins are linked to a plasmid-encoded ATPase to effectively position sister plasmids on either side of the septum at cell division to ensure stable inheritance of the plasmid (170,173).

Type I partitioning systems

Type I partitioning systems were first identified in the early 1980s and are the most common partitioning system, often implicated in the maintenance of both plasmids and bacterial chromosomes (170,174-177). Type I partitioning systems are characterised by the possession of a Walker A type ATPase known as ParA (178). The type I systems can be further divided into two sub-types: Ia, which have large ParA proteins that possess an N-terminal helix-turn-helix DNA binding domain, or Ib, which have small ParA proteins without this domain (169,170).

Both type I systems consist of three components, ParA (SopA), a DNA binding adaptor protein, ParB (SopB), and the centromere site, *parS* (*sopC)* (169,170,174-176). Type Ia and type Ib systems also differ in the position of the centromere site. Type Ia partitioning systems are only encoded by plasmids, with the partitioning loci of the *E. coli* prophage P1 representing the most comprehensively studied type Ia system (170,173).

ParB/*parS* nucleoprotein complex

The first step in *parABS* mediated partition is the formation of the partition complex or segrosome. The P1 partition complex is comprised of ParB and integration host factor (IHF) bound specifically to different regions of the *parS* centromere (179-181). P1-ParB is a centromere binding protein that exists as a dimer in solution and interacts specifically with the *parS* centromere site (181,182).

The P1 centromere consists of an IHF binding site flanked by two regions important for ParB binding called the A and B boxes (181,183,184). The A-box is made up of four copies of a heptamer sequence, whereas the B box consists of two copies of a hexameric site (173). Binding of the central region by IHF results in the bending of the *parS* site, which in turn brings the A- and B-boxes into close proximity allowing ParB dimers to bind and effectively bridge each position (181,183,185,186). Structural analysis of a truncated P1-ParB derivative (C terminal 142-333 amino acids) has revealed that interaction with the A-box relies on a central HTH motif. B-box interaction requires C-terminal dimer domains (187). These two domains are connected *via* a flexible linker that allows bridging of multiple binding sites or *parS*-containing DNA molecules (187,188).

The initial partition complex consisting of IHF bound *parS* and a single ParB dimer acts as a nucleation point for the addition of subsequent ParB dimers, which are loaded and spread non-specifically either side (~500 bp) of *parS,* resulting in the formation of higher-order nucleoprotein structures (189,190). ParB spreading has been suggested to involve one-dimensional filamentation of ParB in complex with DNA (189,191). However, a model suggesting that DNA looping and bridging leads to DNA condensation and is required for ParB spreading has been proposed (192).

ParA plasmid positioning- Cytoskeletal filaments or an ATPase gradient?

parABS-mediated plasmid partitioning is a positioning reaction that relies upon correctly localising plasmids to discrete foci located on either side of the division plane in the bacterial cell. Therefore, the next step in *parABS* plasmid partitioning involves positioning of the ParB/*parS* nucleoprotein complex by the ParA ATPase (170,173). Plasmid localisation can be visualised *in vivo* using a GFP-*lac* repressor fusion and a plasmid tagged with an array of lac operator sites (193). Utilising this method, P1 and F plasmid derivatives that carry *parABS* loci have been shown to localise to discrete foci at both mid- and quarter-cell positions in a ParA dependent manner (193-195).

ParA has weak ATPase activity *in vitro* that is stimulated upon binding ParB (196). ParA exhibits site-specific DNA binding activity in its ADP-bound form, where it binds the *par* promoter and autoregulates the *parAB* operon; this repression is further stimulated by interaction with ParB (197). P1-ParA also exhibits ATP-dependent non-specific DNA-binding activity, which allows ParA to associate with the nucleoid (198). The switch between specific and non-specific DNA binding activity is therefore dependent on the nucleotide bound state of ParA (199). Both ATPase activity and non-specific DNA binding are important for correct plasmid localisation and partitioning, since mutation of the domains involved in ATP hydrolysis and DNA binding leads to the abrogation of partitioning (200-204).

Unlike ParB and *parS*-containing plasmids, which form discrete foci *in vivo*, ParA-GFP fusions have been shown to form dynamic patterns that oscillate over the bacterial nucleoid (204,205). Two alternative models have been proposed to explain these observations (198,204). Dynamic patterning of ParA was initially interpreted as the formation of DNA-associated cytoskeletal ParA filaments (204,206,207). It was proposed that equipositioning of sister plasmids is facilitated by ParA filaments that pull plasmids apart *via* filament depolymerisation (204). Although ParA filaments have been observed *in vitro*, they have only been detected when ParA proteins have been expressed in concentrations much higher than is

physiologically pertinent, and their relevance in the partition reaction *in vivo* therefore remains unclear (198).

More recently, support has been growing for a diffusion-ratchet mechanism, whereby ParB-bound plasmids 'surf' across a ParA ATPase gradient that is maintained by a non-specific DNA-binding interaction between ParA and the nucleoid (198,208-210). This model presents two distinct species of ParA, DNA-binding ParA (ParA-ATP) and non-DNA-binding ParA (ParA-ADP). Many molecules of ParA-ATP bind non-specifically to the nucleoid, which acts as a scaffold or matrix for the partition reaction. Upon interaction with the ParB/*parS* partition complex, ParA ATPase activity is activated. Once ParA has hydrolysed its ATP it dissociates from the nucleoid leaving a ParA depletion zone (lower ParA concentration); slow regeneration of the DNA-binding form of ParA leads to diffusion throughout the cell and loss of positional memory of the site of dissociation (198). The ParB-bound plasmid subsequently migrates to a region of the nucleoid with a higher ParA concentration and the reaction cycle continues (Figure 1.7) (198). Further evidence in support of this model of partition came from the reconstitution of F-plasmid partition *in vitro* using a DNA-carpeted flow-cell as an artificial nucleoid and magnetic beads coated in partition complexes as a surface cargo (209-211). Finally, a third hypothesis has been proposed that suggests a 'Nucleation and Caging' mechanism to explain type I mediated partition (211a,211b).

Type II partitioning systems

Type II or ParMRC partitioning systems encode three components: (i) ParM, a filament-forming actin-like ATPase, (ii) ParR, a DNA binding adaptor protein that binds (iii) *parC*, a centromeric site situated immediately upstream of *parM* (170,212-216). In contrast to type I systems, *parMRC* systems mediate plasmid segregation *via* a pushing mechanism, which has been studied in the *E. coli* plasmid R1 and the *S. aureus* plasmid pSK41 (170,212,217,218).

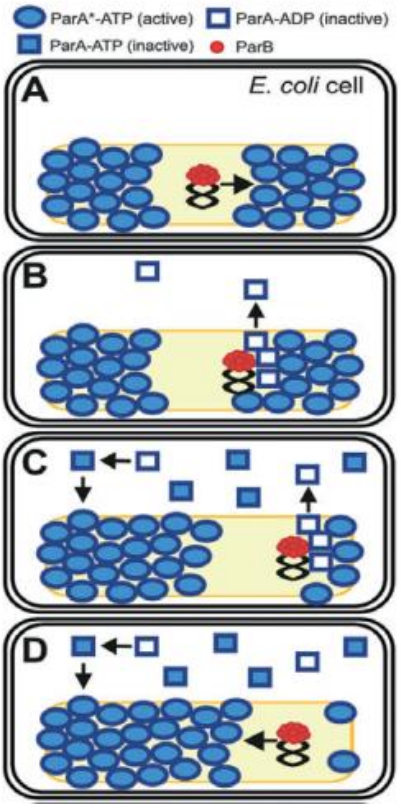

Figure 1.7. Diffusion ratchet model of type Ia mediated plasmid partition: A) This model presents two distinct species of ParA, DNA binding ParA (ParA-ATP) shown as the blue circle and non-DNA-binding ParA (ParA-ADP) shown as an open blue square. Many molecules of ParA-ATP bind non-specifically to the nucleoid, which acts as a scaffold or matrix for the partition reaction. **B)** and **C)** Upon interaction with the ParB/*parS* partition complex, ParA ATPase activity is activated. Once ParA has hydrolysed its ATP it dissociates from the nucleoid leaving a ParA depletion zone (lower ParA concentration), **D)** slow regeneration of the DNA-binding form of ParA leads to diffusion throughout the cell and loss of positional memory of the site of dissociation. The ParB bound plasmid subsequently migrates to a region of the nucleoid with a higher ParA concentration and the reaction cycle continues. Reproduced from (198).

parMRC-mediated partition relies upon the formation of two components: a series of dynamic cytomotive filaments comprised of ParM and a ParR/*parC* nucleoprotein complex known as the segrosome or partition complex (188,213,215,218,219). In this process sister plasmids are linked to the ends of two antiparallel ParM filaments *via* the ParR/*parC* nucleoprotein complex. ParM filaments polymerise and act to push each sister plasmid to opposite cell poles, thereby ensuring that each daughter cell inherits a plasmid copy at cell division. Both the ParM filaments and the ParR/*parC* nucleoprotein complex are essential for correct partition.

ParM filament structure

ParM shares a common ATP-binding motif with members of the diverse actin/Hsp70 ATPase superfamily, including the prokaryotic actin-like protein MreB (220). Structural analysis of the R1-derived ParM monomer confirmed this prediction (215). The conserved region of this superfamily consists of five conserved sequence motifs, which translate structurally into two sets of subdomains (Ia, Ib, IIa and IIb) that flank a nucleotide-binding cleft (220). A recent bioinformatics survey using this conserved ATPase motif to interrogate the NCBI database predicted the existence of over 35 distinct families of actin-like proteins (ALPs) in prokaryotes ($ParM_C$ from pCW3 is from the ALP19 family) (221). The possession of the conserved motif correlates to the ability to bind nucleotides, in addition, all ALPs characterised to date have the ability of to form actin-like filaments (213,215,218,221,222). ParM ATPase activity has also been validated *in vitro*, and disruption of this activity leads to partition defects *in vivo* (214). Aside from this common ATP binding domain, the sequence conservation between ParM and other actin-family proteins is low (216,221).

Many members of the actin/Hsp70 superfamily can form cytoskeletal filaments, however, the structure and dynamics of these filaments can vary greatly. In the presence of ATP and specific cofactors, actin forms right-handed helical filaments made up of two proto-filaments whereas MreB forms straight filaments made up of two antiparallel protofilaments (222,223). Similar to actin and MreB, ParM self-assembles into cytomotive filaments in an ATP-

dependent manner (213,215). These filaments were first visualised *in vivo* using ParM-specific monoclonal antibodies, which showed the formation of filamentous structures along the longitudinal axis of the cell (215). Structural analysis of both ParM monomers and filaments using a combination of electron microscopy (EM), Cryo-EM, X-ray crystallography and total internal reflection microscopy has provided insight into the filament formation process (213,215,224,225).

Initial structural analysis using electron microscopy and X-ray crystallography predicted that ParM, like actin, would form right-handed helical filaments comprised of two proto-filaments (213). However, further structural analysis revealed that R1 ParM filaments possess different monomer interfaces and polymerisation dynamics to actin (213,226). Specifically, ParM forms left-handed two-start helical filaments in the presence of ATP (213,215,224,225,227). Upon nucleotide binding, the two conserved actin/Hsp70 domains of the ParM monomer move towards one another by 25°, adopting a closed confirmation (213). A similar conformational change has also been suggested to be involved in the conversion of G-actin to F-actin (228). The closed conformation has been reported for binding of both the non-hydrolysable ATP homologue AMP-PNP and ADP, however, ParM filaments form in the presence of ATP not ADP (213,215,224,225). Resolution of the structure of AMP-PNP bound ParM interacting with the C-terminal 17 amino acids of ParR displayed two further domain shifts, leading to the flattening of ParM monomers at the inter-protofilament interface (225). The ParR bound ParM-AMPPNP structures fit closely into the 8.5 Å cryo-EM reconstruction of the R1-ParM filament, suggesting that filament conformation of ParM is similar to this monomeric state (224,225). Conversion of ParM to its filament conformation is important to make stable inter-protofilament interactions (225). Interruption of these contacts by substitution of interface residues to alanine leads to the abolition of polymerisation, thus illustrating the importance of these interactions in ParM function. Additionally, these inter-protofilament contacts cannot be made if ParM monomers are in an ADP-bound or open conformation, providing structural evidence that ATP is required for filament formation (215,224,226,229). The helical repeat or crossover distance

of the protofilaments within each ParM filament is 300 Å (12 subunits per turn), which is close to the 360 Å repeat (13 subunits per turn) of actin filaments (213). The longitudinal monomer repeat unit is 49 Å, which is similar to the 51 Å and 55 Å monomer repeat units, for MreB and actin respectively (213).

Studies utilising fluorescence microscopy have shown that GFP-fused ParM co-localises with *parMRC* plasmids *in vivo*, both at mid-cell and cell-pole positions (230). Direct interrogation of this interaction using surface plasmon resonance and yeast two hybrid analysis showed that ParM can interact with ParR/*parC* complexes in an ATP-dependent manner (214,215,229). The ParR/*parC* complex co-localises with the tip of growing ParM filaments and has been reported to bind both ends of a single filament (215,229). However, ParM filaments are helical and are therefore polar, suggesting that the ParR/*parC* complex must recognise and bind to two different filament interfaces (224). The ParR/*parC* complex binds *via* the C-terminal domain of ParR, which inserts into the hydrophobic pocket between ParM subdomains Ia and IIa (224,225). The position at which ParR interacts with ParM is at the polymerisation interface between ParM monomers, therefore the only place at which ParR can bind is at the barbed end of the polar ParM filament (224,229). ParM filaments have been observed to form bundles in *E. coli* cells under wild-type expression conditions (231,232). The structure of ParM filaments (12 monomers per turn) is amenable to filament packing or bundling (224). ParM filament bundles have been shown to contain both parallel and antiparallel filaments *in vitro* and more recently doublets have been observed *in vivo* (224,233-235). The formation of bipolar spindles addresses the issue of filament polarity and allows two interacting ParM filaments to bind ParR/*parC* complexes at their respective barbed end and partition them to either cell pole (224,235).

The minimal segregating unit is therefore made up of an antiparallel ParM doublet and two ParR/*parC* bound plasmids (224,233,235). Therefore, plasmid replication and partition does

not need to be synchronised for each plasmid copy in the cell. Each plasmid encodes its own spindle and can therefore mediate its own partitioning (224).

Electron microscopy has shown that ParM derived from the *E. coli* plasmid pB171 forms dynamic ParM filaments with similar structural and kinetic properties to R1-ParM, although they are distantly related (41% identity to R1 ParM) (221,236). By contrast, the structure of the *S. aureus* pSK41 ParM homologue is distinct from R1-ParM or pB171-ParM (218). pSK41-ParM is only 18% similar to R1-ParM and as a consequence its monomer and filament structure is markedly different (218,221). Despite originating from a bacterial source, the pSK41-ParM monomer structure shares more similarity with the archaeal ALP Ta0583 than ParM or MreB (218,237,238). Instead of left-handed double helical filaments of R1-ParM, pSK41-ParM forms single helical filaments with 10 subunits per 4 helical turns and a helical repeat of ~250 Å, which readily form bundles (218).

ParM filament dynamics

R1-ParM filaments exhibit dynamic instability similar to that of eukaryotic microtubules, where filaments undergo rounds of rapid polymerisation and depolymerisation, allowing them to efficiently 'search' the cell space for ParR-bound plasmids to segregate (216,239-241) (Figure 1.8). Polymerisation of ParM filaments is ATP-dependent, whereas depolymerisation of filaments is coupled to ATP hydrolysis and is therefore dependent on ParM ATPase activity (226). Disruption of ATPase activity by substitution of a conserved aspartate (170) or glutamate (148) residue to alanine in the ATP binding pocket of ParM results in the formation of long stable filaments, which do not support the partition of plasmids *in vivo,* suggesting that correct filament dynamics is important for the partition reaction (214,226).

ParM filaments are protected from rapid disassembly by an ATP-bound monomer cap, whereas filaments with an ADP-bound cap rapidly depolymerise by catastrophic disassembly (226) (Figure 1.8).

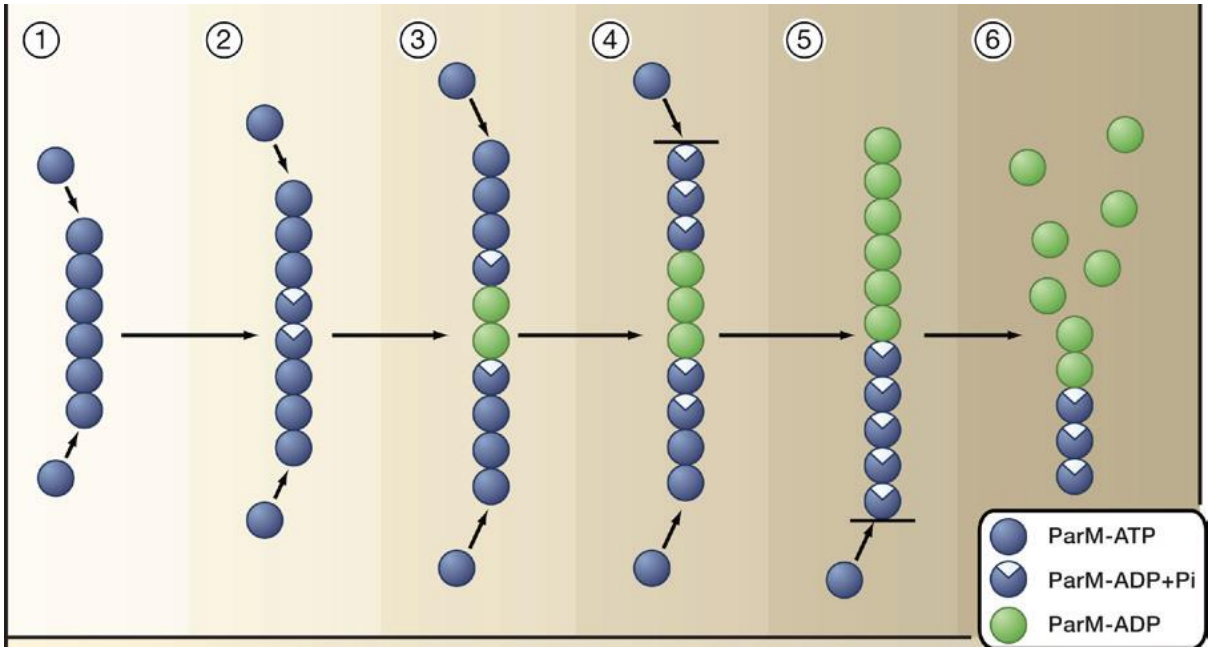

Figure 1.8. ParM filament dynamics: A model of ParM filament dynamics, ParM-ATP monomers are shown as blue circles, ParM-ADP monomers are shown as green circles and ParM-ADP-Pi monomers are shown as blue circles with an indent (these monomers have undergone ATP hydrolysis). **1)** ATP bound ParM monomers are able to form a nucleus and then polymerize bidirectionally **2)** The ATPase action of the ParM monomers leads to the hydrolysis of bound ATP over time **3)** Eventually this leads to ADP bound monomers being present in the filament, however, the filament remains stable as long as it retains its ATP bound ParM cap **4)** Once the ATP bound ParM cap hydrolyses its ATP to ADP, ParM monomers can no longer be added to the filament **5)** once the ParM monomer cap has fully hydrolysed its ATP the filament becomes destabilized **6)** Following destabilization the filament rapidly depolymerizes. This process is very similar to the dynamic instability model that is used to describe the dynamics of microtubules in eukaryotes.(170,216,242). Figure reproduced from (170)

The kinetic differences between ParM and actin (higher nucleation and ADP-bound monomer dissociation rates) ensure that ParM can form filaments in the absence of cellular cofactors such as formin or the Arp2/3 complex (216). Reconstitution of the *parMRC* system *in vitro* has shown that the process of ParM polymerisation and ParR/*parC* capture only requires these three plasmid-encoded components and no other cellular factors (240). Dynamic instability exhibited by ParM filaments is quelled upon interaction with the ParR-*parC* segrosome complex, which stabilises ParM polymerisation by facilitating the addition of further ParM-ATP monomers and protects against catastrophic disassembly (240). ParR-bound plasmids are positioned at the ends of interacting ParM filaments where new NTP-bound monomers are added at the filament/segrosome interface *via* insertional polymerisation (219,224,229). ParR-bound sister plasmids that have been 'captured' by interacting bundles of anti-parallel ParM filaments can be segregated to either cell pole (216,224,227,240).

The ParR/*parC* segrosome complex

ParR is a DNA-binding protein, which generally exists as a dimer in solution (214,229). The ParR dimer has an N-terminal ribbon-helix-helix dimer (RHH_2) domain similar to the Arc/MetJ family of transcriptional repressors; this motif is essential for DNA binding and plasmid partitioning (188,219). The *cis*-acting *parC* centromere in R1 is intrinsically curved and comprises two sets of five 11 bp direct repeats that flank the -10 and -35 boxes of the *parMR* promoter (243,244). Binding of the *parC* centromere by ParR also leads to autoregulation of the *parMR* operon (243). All ten *parC* repeats are required for *parMRC*-mediated plasmid stabilisation and effective repression (243,245). ParR has also been implicated in the pairing of *parC*-containing replicons *in vitro*, suggesting that it may be a central step in positioning sister plasmids prior to the partition reaction (246). ParR also interacts with ParM filaments *via* its C-terminal domain and acts to link the centromeric site, and therefore the plasmid, to growing ParM filaments (214,229,240).

The structure of the ParR/*parC* complex has been elucidated for both pSK41 and pB171 (188,219). Although there are apparent structural differences between the ParM filaments of these plasmids the ParR/*parC* complex seems to be structurally conserved, suggesting that the mechanism of filament recognition and capture may be similar. Electron microscopy of both pB171-ParR and pSK41-ParR in complex with linear DNA showed the formation of higher order ring-like structures (188,219). Analysis of the crystal structure of both pB171-ParR and the N-terminal domain of pSK41-ParR supported the structural data gathered from electron microscopy, showing that both ParR homologues bind their respective repeats as a dimer-of-dimers and have the capacity to form multimeric super-helical or solenoid-like nucleoprotein complexes (188,219). In both cases, the N-terminal DNA binding portion of the ParR dimers face outwards to form a super-helical scaffold for the *parC* DNA to wrap around. The C-terminal region of the ParR dimers faces inwards towards the centre of the helix (188,219). The diameter of the central region is 18 nm in the pSK41 segrosome, large enough to interact with the end of a ParM filament (~6 nm) (188).

A model for *parMRC*-mediated plasmid partition has been devised by consolidating the above information (Figure 1.9). First, dynamically unstable ParM filaments rapidly polymerise and depolymerise, searching the cellular space for ParR/*parC* nucleoprotein complexes to bind (170,216,226,240). Once bound to a ParR/*parC* complex at one end, ParM filament polymerisation is stabilised, allowing it to interact with a second, oppositely oriented, ParR/*parC* bound filament (224,226). Interacting ParM filaments produce a simple bipolar spindle that continues to polymerise *via* insertional polymerisation at each segrosome/filament interface, therefore generating the force required to actively segregate each sister plasmid to either cell pole (216,224,225,233-235).

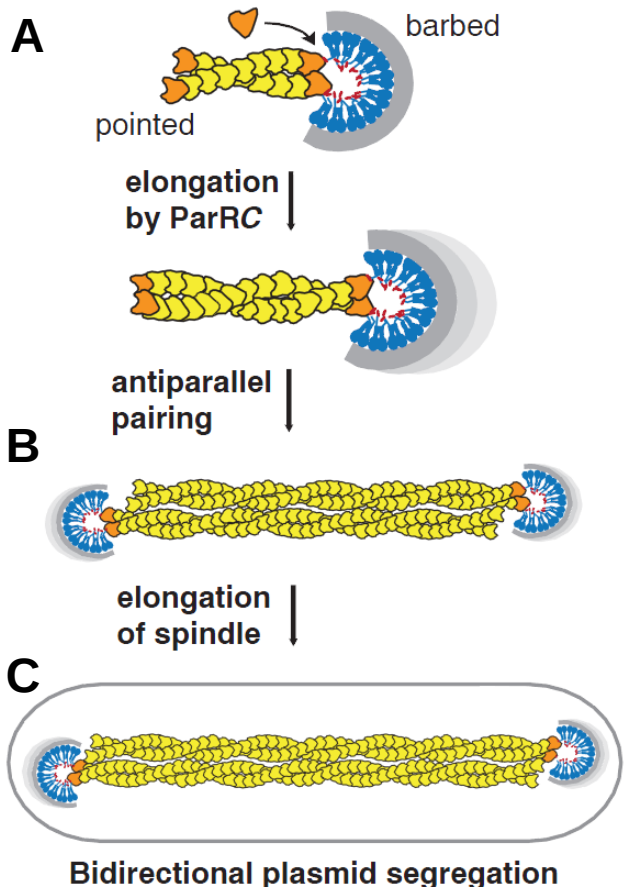

Figure 1.9. ParM filament capping by ParR-*parC* complex: ParM double filaments are represented in yellow (the ATP bound cap is orange), ParR molecules are represented as a blue oligomeric ring bound to *parC*, which is shown in grey on the outside of the ParR complex. **A)** The current model suggests that the ParR-*parC* nucleoprotein complex forms an oligomeric ring like structure that can 'clamp' one end of a ParM double filament (247), this interaction in turn stabilizes the polymerization of the ParM filaments. **B)** Because the ParM filaments are polar and each end of the filament is in a different orientation, it has been suggested that ParM can only bind to one end of a double stranded ParM filament. It is now thought that several double stranded ParM filaments can interact to form an antiparallel pair, this pairing would eliminate the need for the ParR-*parC* complex to accommodate its binding to opposing structures **C)** The ParM filament pair can then stably elongate in either direction and actively segregate the plasmids to either pole of the bacterium. Adapted from (224)

Type III partitioning systems

Type III, or *tubZRC*-mediated, partitioning relies upon the formation of cytoskeletal filaments similar to those of *parMRC* partitioning systems (170). Type III systems utilise a tubulin-like GTPase (248) and have been described in several *Bacillus* spp. virulence plasmids and a clostridial bacteriophage (249,250). The best characterised *tubZRC* system is that of the *Bacillus thuringiensis* plasmid pBtoxis, where it has been shown to be essential for plasmid partitioning (248). The pBtoxis partition system is comprised of two *trans*-acting proteins, TubZ a GTPase that shares a common fold with eukaryotic tubulin and the cell division protein FtsZ, and TubR a DNA-binding protein that interacts with high affinity to an upstream centromere region consisting of seven repeat sequences (217,248,249,251,252). Similar to ParR, the DNA adaptor protein of the *parMRC* system, binding of the *tubC* centromere by TubR leads to autoregulation of the *tubRZ* operon (248,251). TubR exists as a dimer in solution, the structure of which has been solved (252). Dimerization of TubR leads to formation of a winged-helix-turn-helix (wHTH) DNA-binding motif, which allows TubR to interact with its respective binding site.

TubZ plays a role analogous to ParM, as it has the ability to polymerise to form cytomotive filaments (248,253,254). Unlike ParM, *in vitro* studies of TubZ have shown that it forms right-handed filaments that are comprised of either two or four proto-filaments depending on the nucleotide state of the monomers within the filament (254-256). Despite being distantly related to tubulin (~15%), TubZ filaments generate the force required for plasmid partitioning through a GTP-dependent treadmilling mechanism similar to eukaryotic actin, where filaments are kinetically polar and polymerise at one end whilst depolymerising at the other (248,257,258). The C-terminal domain of TubZ is important for GTP-dependent interaction with TubR*C* complexes (252). Similar to the ParR/*parC* complex of *parMRC* systems, the TubR*C* complex acts to establish a link between the force generated by the treadmilling of TubZ filaments and the partition of sister plasmids (258,259). The structure of the TubR*C* complex has been

solved for both *B. thuringiensis* and *Bacillus megaterium* (259). Both of these structures showed the formation of higher order DNA-protein filament structures, not dissimilar to the ParR*C* complex of pSK41 and R1 (188,219,259). In contrast to the *parMRC* systems of R1 and pSK1, reconstitution of the *tubZRC* system *in vitro* showed that TubR*C* complexes track the minus end of TubZ filaments rather than capture the growing end (258). Treadmilling TubZ filaments therefore work to partition plasmids by pulling TubR*C* nucleoprotein complexes to the cell poles prior to cell division (258).

pSK1 partition system

In addition to the three partitioning types already discussed, there is a unique partitioning system encoded by the 28.4 kb *S. aureus* multi-resistance plasmid pSK1 (172,260). This system is comprised of a single partitioning protein, Par, encoded upstream and divergently transcribed from *rep* in pSK1 (260). The presence of the Par protein increases the segregational stability of mini-replicons (172,260). The Par protein is predicted to contain an N-terminal HTH motif and a C-terminal coiled-coiled domain and the 204 bp region upstream of *par* exhibits centromere-mediated incompatibility, suggesting that it is a *cis*-acting centromere site for the Par protein (172,260). However, the mechanism of action of this partitioning system still remains unclear (172). A second partitioning system that also uses a single protein to confer stability exists on the plasmid incW plasmid R388. The R388 plasmid uses a protein called StbA to ensure plasmids are maintained at cell division (260a).

Plasmid incompatibility

When two plasmids are unable to coexist in the same cell without the presence of external selection or if introduction of one plasmid leads to the destabilisation of the other's inheritance, then the plasmids are incompatible (89,261,262). Plasmid incompatibility occurs most commonly when two plasmids have the same replication, replication control or maintenance

determinants, which ultimately leads to substantial copy number variance and the inability to correct copy number fluctuations (Figure 1.10).

Plasmids are chosen at random for replication throughout the cell cycle, meaning that in each cell cycle some plasmid copies are chosen for replication, whereas others are not (263). The consequence of random selection when two plasmids with the same replication machinery are present in a single cell is plasmid incompatibility. If two plasmids share the same origin of replication they will both be recognised by the replication initiator as the same replicon, despite other differences in the plasmids. If plasmids are chosen at random for replication, copy number variance will consequently arise (Figure 1.10). Shared replication mechanisms also lead to the inability of each plasmid to correct copy number fluctuations in daughter cells, ultimately leading to dilution of the plasmid in the population after each generation (89) (Figure 1.10). If initiation control mechanisms are shared by each plasmid, both plasmids are acted upon by that mechanism so that neither replicates enough to remain stable in the population.

The *cis*-acting centromere sites encoded by plasmid partition loci also exhibit incompatibility (264-267). Partition-mediated incompatibility can be described using several models. Prior to partition, sister replicons are often observed to pair. Pairing is mediated by the centromere-binding protein, either ParB for type I or ParR for type II partitioning systems (246,268,269). If two plasmids possess the same partition loci they may be randomly selected from a pool and paired prior to partition. If a mismatched pair consisting of heterologous plasmids is formed, these two plasmids will be unequally segregated at cell division, leading to plasmid instability and therefore incompatibility (89,264,270).

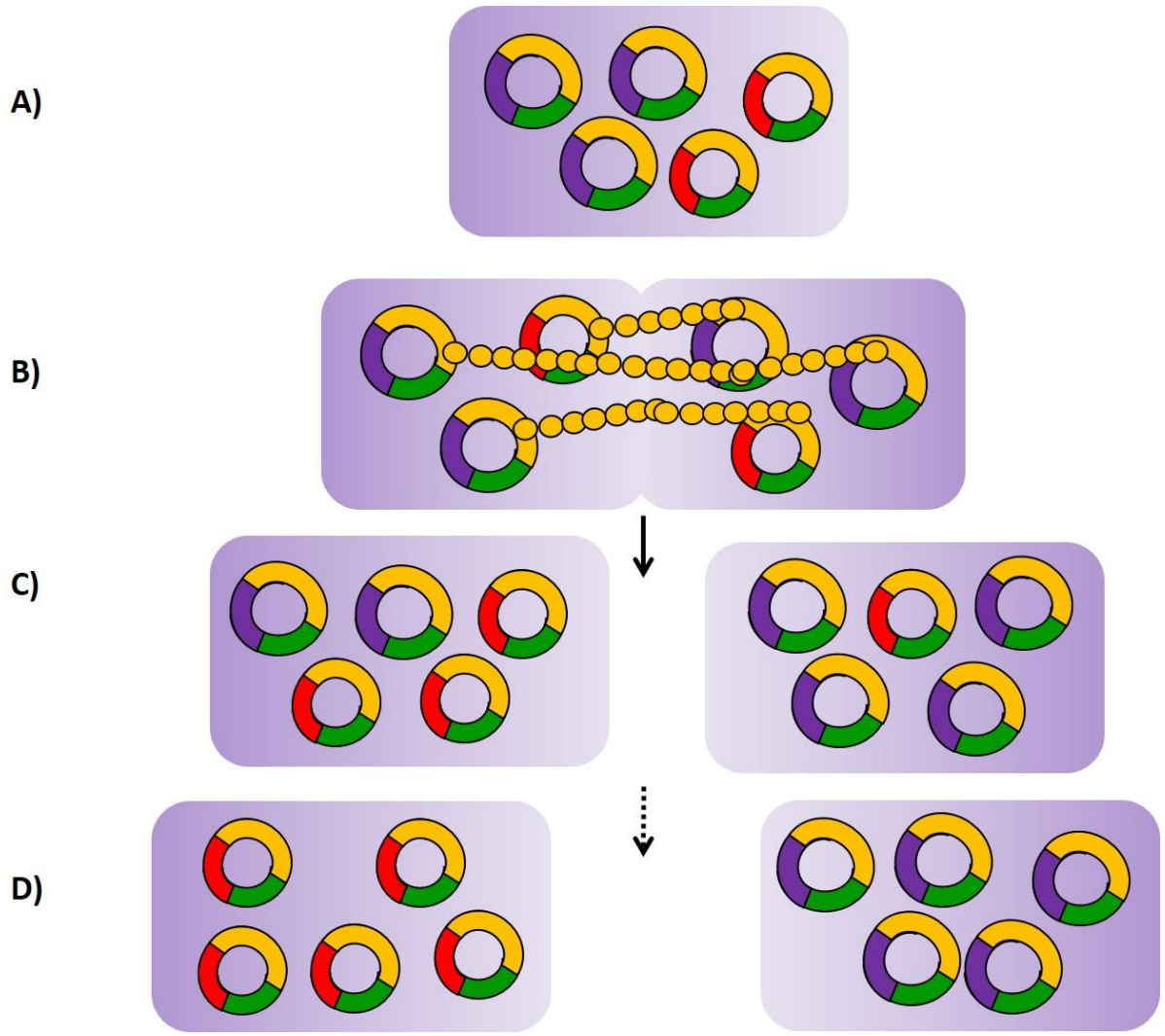

Figure 1.10. Diagrammatic representation of plasmid incompatibility mediated by a shared replication and partition machinery. The replication region is shown in green and is shared by all plasmids, the partitioning region is shown in yellow and is shared by all plasmids, purple and red regions signify unique sections of the plasmid**. A)** Two different plasmids that share replication and maintenance functions, each with a copy number of five. The similar replication proteins are unable to distinguish between the two plasmids, leading to an overall total copy number of five for both plasmids combined. **B)** When coupled with similar partitioning systems, plasmids are improperly segregated due to the inability to distinguish each plasmid as different, ultimately leading to pairing of heterologous plasmids and unequal partition into daughter cells. **C)** In the daughter cell the replication machinery is unable to adjust for copy number imbalances, which leads to another round of unequal replication back to an overall copy number of five. **D)** After rounds of unequal replication and partitioning, cells containing only one plasmid type will arise.

Mismatched pairing of heterologous replicons is conceptually simple and can clearly be envisioned to be the cause of incompatibility for those plasmids that encode *parMRC*-like partition loci. For *parABS*-encoding plasmids, however, the mechanism is less clear. Ebersbach *et al.,* (2005) showed, using fluorescence tagging of incompatible *parABS*-encoding plasmids, that mixed pairing does not contribute to type I partition mediated incompatibility (264,265). Normally, *parABS*-encoding plasmids form discrete foci at mid and quarter cell positions. Rather than random pairing, random positioning of pure plasmid clusters was observed, where incompatible plasmid clusters competed for the mid-cell position (264,265). Plasmid clusters that were initially excluded from the mid-cell were unable to segregate correctly, leading to a higher chance of loss at cell division (264,265).

Although plasmids that encode similar partitioning systems can be incompatible, some plasmids have evolved to ensure that they are maintained within the same isolate. The pathogenic *B. cenopacia* strain J2315 maintains three chromosomes and a large, low-copy number plasmid (271). The type I ParABS partitioning systems of these replicons are closely related. However, the partition centromeres (*parS*) have coevolved to become distinct so that each replicon is partitioned independently (271-274). Likewise, *Rhizobium leguminosarum bv. trifolii* RepB (ParB homologue) discriminates between similar *parS* centromeres to independently segregate and maintain a chromosome in addition to four plasmids (275). Subtle differences in partitioning system machinery appear to be important for the maintenance of multipartite genomes.

Plasmid incompatibility in *C. perfringens*

Although plasmids carry essential virulence and antimicrobial resistance genes in *C. perfringens* many of the processes that are fundamental to plasmid biology have not been well characterised, including plasmid incompatibly (4). *C. perfringens* strains often house more than one very similar plasmid (4,25,48-51) and other workers have noticed that some

combinations of toxin plasmids seem to be more common than others, where some combinations appear to be unable to exist naturally (49,50). Furthermore, many of the large plasmids found in *C. perfringens* share highly similar or identical replication initiator proteins and origins of replication to that of the paradigm conjugative plasmid pCW3 (17,171). For example, the Australian avian necrotic enteritis strain EHE-NE18 carries three large pCW3-like plasmids, pJIR3535, pJIR3537 and pJIR3844. pJIR3535 is an 82kb plasmid that carries the *netB* gene, pJIR3537 is a 49 kb tetracycline resistance plasmid that is almost identical to pCW3 (48 kb) and pJIR3844 is a 70 kb plasmid that carries the beta2 toxin gene. Comparative bioinformatic analysis of the replication region of each plasmid showed that they are all highly similar despite being maintained stably within the same strain (25,171).

Two genes that were adjacent to, but divergently transcribed from the *rep* gene were identified in the central control region of these pCW3-like plasmids. These genes encode a putative ParM and ParR homologue, with a potential centromere site immediately preceding the *parM* gene (17,25,47,171). Closer inspection of the sequence of the three plasmids in EHE-NE18 showed that they each carried a different ParM allele (25). Expanding the survey to all available *C. perfringens* plasmid sequences showed that these putative *parMRC*-like partitioning systems fall into at least 10 distinct phylogenetic groups and that strains of *C. perfringens* do not carry plasmids that encode the same partitioning group (171,221). A representative *parMRC* system from the type E *C. perfringens* isolate, JGS1987, has been shown to stabilise an unstable mini-replicon in *E. coli* (276). Together these findings suggest that differences in ParMRC families found on these plasmids may be the basis for plasmid incompatibility in *C. perfringens* (25,47,171).

Hypotheses, aims and objectives

This study focusses on two major aspects of *C. perfringens* plasmid biology: (i) conjugative transfer of pCP13 plasmids and (ii) the basis of pCW3-like plasmid incompatibility. Based on

their similarity to the conjugative *P. sordellii* plasmid pCS1-1, it is proposed that the pCP13-like family of plasmids in *C. perfringens* is conjugative. It is also hypothesised that the putative ParMRC plasmid partitioning systems are responsible for the determination of plasmid incompatibility in *C. perfringens*. To examine the ability of pCP13 to transfer *via* conjugation the sequence of similar plasmids in *C. perfringens* and other clostridia was analysed and a putative conjugation locus identified and genes within that locus subsequently mutated. The mutations were characterised using conjugation assays, in addition to complementation and cross-complementation studies with homologous genes from *P. sordellii* (Chapter 5). To investigate the incompatibility hypothesis the aim was to conduct bioinformatics analysis of all available *C. perfringens* plasmid sequences (Chapter 2), introduce different combinations of ParMRC family plasmids into the same isolate and determine their ability to coexist (Chapter 3), and characterise the ability of ParMRC components to undergo inter- and intra-family interactions (Chapter 4). The results of these studies showed that pCP13 is conjugative, pCW3-like plasmid incompatibility correlates with ParMRC family designation and, incompatibility is driven by interactons between ParR and *parC* components.

References

1. Frost, L.S., Leplae, R., Summers, A.O. and Toussaint, A. (2005) Mobile genetic elements: the agents of open source evolution. *Nat. Rev. Microbiol.*, **3**, 722-732.
2. Mitsuhashi, S. (1971) The problems of drug-resistant pathogenic bacteria. Epidemiology and genetics of R factors. *Ann. N. Y. Acad. Sci.*, **182**, 141-152.
3. Mitsuhashi, S. (1969) The R Factors. *The Journal of Infectious Diseases*, **119**, 89-100.
4. Li, J., Adams, V., Bannam, T.L., Miyamoto, K., Garcia, J.P., Uzal, F.A., Rood, J.I. and McClane, B.A. (2013) Toxin plasmids of *Clostridium perfringens*. *MMBR* **77**, 208-233.
5. Rood, J.I. and Cole, S.T. (1991) Molecular genetics and pathogenesis of *Clostridium perfringens*. *Microbiological Reviews*, **55**, 621-648.

6. Awad, M.M., Bryant, A.E., Stevens, D.L. and Rood, J.I. (1995) Virulence studies on chromosomal alpha-toxin and theta-toxin mutants constructed by allelic exchange provide genetic evidence for the essential role of alpha-toxin in *Clostridium perfringens*-mediated gas gangrene. *Mol. Microbiol.*, **15**, 191-202.

7. Songer, J.G. (1996) Clostridial enteric diseases of domestic animals. *Clin. Microbiol. Rev.*, **9**, 216-234.

8. McDonel, J.L. (1980) *Clostridium perfringens* toxins (type A, B, C, D, E). *Pharmacol. Ther.*, **10**, 617-655.

9. Keyburn, A.L., Boyce, J.D., Vaz, P., Bannam, T.L., Ford, M.E., Parker, D., Di Rubbo, A., Rood, J.I. and Moore, R.J. (2008) NetB, a new toxin that is associated with avian necrotic enteritis caused by *Clostridium perfringens*. *PLOS Path.*, **4**, e26.

10. Yonogi, S., Matsuda, S., Kawai, T., Yoda, T., Harada, T., Kumeda, Y., Gotoh, K., Hiyoshi, H., Nakamura, S., Kodama, T. *et al.* (2014) BEC, a novel enterotoxin of *Clostridium perfringens* found in human clinical isolates from acute gastroenteritis outbreaks. *Infect. Immun.*, **82**, 2390-2399.

11. Uzal, F.A., Freedman, J.C., Shrestha, A., Theoret, J.R., Garcia, J., Awad, M.M., Adams, V., Moore, R.J., Rood, J.I. and McClane, B.A. (2014) Towards an understanding of the role of *Clostridium perfringens* toxins in human and animal disease. *Future Microbiology*, **9**, 361-377.

12. Gohari, M.I., Parreira, V.R., Nowell, V.J., Nicholson, V.M., Oliphant, K. and Prescott, J.F. (2015) A novel pore-forming toxin in type A *Clostridium perfringens* is associated with both fatal canine hemorrhagic gastroenteritis and fatal foal necrotizing enterocolitis. *PLOS One*, **10**, e0122684.

13. Rood, J.I., Adams, V., Lacey, J., Lyras, D., McClane, B.A., Melville, S.B., Moore, R.J., Popoff, M.R., Sarker, M.R., Songer, J.G. *et al.* (2018) Expansion of the *Clostridium perfringens* toxin-based typing scheme. *Anaerobe*.

14. Revitt-Mills, S.A., Rood, R.I. and V., A. (2015) *Clostridium perfringens* extracellular toxins and enzymes: 20 and counting. *Microbiology Australia*, **36**, 114-117.

15. Petit, L., Gibert, M. and Popoff, M.R. (1999) *Clostridium perfringens*: toxinotype and genotype. *Trends Microbiol.*, **7**, 104-110.

16. Hughes, M.L., Poon, R., Adams, V., Sayeed, S., Saputo, J., Uzal, F.A., McClane, B.A. and Rood, J.I. (2007) Epsilon-toxin plasmids of *Clostridium perfringens* type D are conjugative. *J. Bacteriol.*, **189**, 7531-7538.

17. Bannam, T.L., Teng, W.L., Bulach, D., Lyras, D. and Rood, J.I. (2006) Functional identification of conjugation and replication regions of the tetracycline resistance plasmid pCW3 from *Clostridium perfringens*. *J Bacteriol* **188**, 4942-4951.

18. Brefort, G., Magot, M., Ionesco, H. and Sebald, M. (1977) Characterization and transferability of *Clostridium perfringens* plasmids. *Plasmid*, **1**, 52-66.

19. Lacey, J.A., Keyburn, A.L., Ford, M.E., Portela, R.W., Johanesen, P.A., Lyras, D. and Moore, R.J. (2017) Conjugation-mediated horizontal gene transfer of *Clostridium perfringens* plasmids in the chicken gastrointestinal tract results in the formation of new virulent strains. *Appl. Environ. Microbiol.*

20. Hassan, K.A., Elbourne, L.D., Tetu, S.G., Melville, S.B., Rood, J.I. and Paulsen, I.T. (2015) Genomic analyses of *Clostridium perfringens* isolates from five toxinotypes. *Res. Microbiol.*, **166**, 255-263.

21. Garcia, J.P., Adams, V., Beingesser, J., Hughes, M.L., Poon, R., Lyras, D., Hill, A., McClane, B.A., Rood, J.I. and Uzal, F.A. (2013) Epsilon toxin is essential for the virulence of *Clostridium perfringens* type D infection in sheep, goats, and mice. *Infect. Immun.*, **81**, 2405-2414.

22. Rood, J.I., Scott, V.N. and Duncan, C.L. (1978) Identification of a transferable tetracycline resistance plasmid (pCW3) from *Clostridium perfringens*. *Plasmid*, **1**, 563-570.

23. Rood, J.I. (1983) Transferable tetracycline resistance in *Clostridium perfringens* strains of porcine origin. *Canadian Journal of Microbiology*, **29**, 1241-1246.

24. Sebald, M. and Brefort, M.G. (1975) Transfer of the tetracycline-chloramphenicol plasmid in *Clostridium perfringens*. *Comptes rendus hebdomadaires des seances de l'Academie des sciences. Serie D: Sciences Naturelles*, **281**, 317-319.

25. Bannam, T.L., Yan, X.X., Harrison, P.F., Seemann, T., Keyburn, A.L., Stubenrauch, C., Weeramantri, L.H., Cheung, J.K., McClane, B.A., Boyce, J.D. *et al.* (2011) Necrotic enteritis-derived *Clostridium perfringens* strain with three closely related independently conjugative toxin and antibiotic resistance plasmids. *MBio*, **2**, e00190-00111.

26. Abraham, L.J. and Rood, J.I. (1985) Molecular analysis of transferable tetracycline resistance plasmids from *Clostridium perfringens*. *J. Bacteriol.*, **161**, 636-640.

27. Abraham, L.J. and Rood, J.I. (1985) Cloning and analysis of the *Clostridium perfringens* tetracycline resistance plasmid, pCW3. *Plasmid*, **13**, 155-162.

28. Abraham, L.J. and Rood, J.I. (1985) Cloning and analysis of the *Clostridium perfringens* tetracycline resistance plasmid, pCW3. *Plasmid*, **13**, 155-162.

29. Abraham, L.J., Wales, A.J. and Rood, J.I. (1985) Worldwide distribution of the conjugative *Clostridium perfringens* tetracycline resistance plasmid, pCW3. *Plasmid*, **14**, 37-46.

30. Sloan, J., McMurry, L.M., Lyras, D., Levy, S.B. and Rood, J.I. (1994) The *Clostridium perfringens* Tet P determinant comprises two overlapping genes: *tetA*(P), which mediates active tetracycline efflux, and *tetB*(P), which is related to the ribosomal protection family of tetracycline-resistance determinants. *Mol. Microbiol.*, **11**, 403-415.

31. Sloan, J., McMurry, L.M., Lyras, D., Levy, S.B. and Rood, J.I. (1994) The *Clostridium perfringens* TetP determinant comprises two overlapping genes:*tetA*(P) which mediates active tetracycline efflux and *tetB*(P) which is related to the ribosomal protection family of tetracycline resistance determinants. *Mol. Microbiol*, **11**, 403-415.

32. Johanesen, P.A., Lyras, D., Bannam, T.L. and Rood, J.I. (2001) Transcriptional analysis of the tet(P) operon from *Clostridium perfringens*. *J. Bacteriol.*, **183**, 7110-7119.

33. Lyras, D. and Rood, J.I. (1996) Genetic organization and distribution of tetracycline resistance determinants in *Clostridium perfringens*. *Antimicrob. Agents Chemother.*, **40**, 2500-2504.

34. Lyras, D., Adams, V., Ballard, S.A., Teng, W.L., Howarth, P.M., Crellin, P.K., Bannam, T.L., Songer, J.G. and Rood, J.I. (2009) tISCpe8, an IS1595-family lincomycin resistance element located on a conjugative plasmid in *Clostridium perfringens*. *J. Bacteriol.*, **191**, 6345-6351.

35. Han, X., Du, X.D., Southey, L., Bulach, D.M., Seemann, T., Yan, X.X., Bannam, T.L. and Rood, J.I. (2015) Functional analysis of a bacitracin resistance determinant located on ICE*Cp1*, a novel Tn*916*-like element from a conjugative plasmid in *Clostridium perfringens*. *Antimicrob. Agents Chemother.*, **59**, 6855-6865.

36. Abraham, L.J. and Rood, J.I. (1987) Identification of Tn4451 and Tn4452, chloramphenicol resistance transposons from *Clostridium perfringens*. *J. Bacteriol.*, **169**, 1579-1584.

37. Rood, J.I., Jefferson, S., Bannam, T.L., Wilkie, J.M., Mullany, P. and Wren, B.W. (1989) Hybridization analysis of three chloramphenicol resistance determinants from *Clostridium perfringens* and *Clostridium difficile*. *Antimicrob. Agents Chemother.*, **33**, 1569-1574.

38. Bannam, T.L., Crellin, P.K. and Rood, J.I. (1995) Molecular genetics of the chloramphenicol-resistance transposon Tn4451 from *Clostridium perfringens*: the TnpX site-specific recombinase excises a circular transposon molecule. *Mol. Microbiol.*, **16**, 535-551.

39. Crellin, P.K. and Rood, J.I. (1997) The resolvase/invertase domain of the site-specific recombinase TnpX is functional and recognizes a target sequence that resembles the junction of the circular form of the *Clostridium perfringens* transposon Tn4451. *J. Bacteriol.*, **179**, 5148-5156.

40. Lyras, D., Adams, V., Lucet, I. and Rood, J.I. (2004) The large resolvase TnpX is the only transposon-encoded protein required for transposition of the Tn*4451*/*3* family of integrative mobilizable elements. *Mol. Microbiol.*, **51**, 1787-1800.

41. Abraham, L.J. and Rood, J.I. (1988) The *Clostridium perfringens* chloramphenicol resistance transposon Tn4451 excises precisely in *Escherichia coli*. *Plasmid*, **19**, 164-168.

42. Crellin, P.K. and Rood, J.I. (1998) Tn4451 from *Clostridium perfringens* is a mobilizable transposon that encodes the functional Mob protein, TnpZ. *Mol. Microbiol.*, **27**, 631-642.

43. Charlebois, A., Jalbert, L.A., Harel, J., Masson, L. and Archambault, M. (2012) Characterization of genes encoding for acquired bacitracin resistance in *Clostridium perfringens*. *PLOS One*, **7**, e44449.

44. Miyamoto, K., Fisher, D.J., Li, J., Sayeed, S., Akimoto, S. and McClane, B.A. (2006) Complete sequencing and diversity analysis of the enterotoxin-encoding plasmids in *Clostridium perfringens* type A non-food-borne human gastrointestinal disease isolates. *J. Bacteriol.*, **188**, 1585-1598.

45. Miyamoto, K., Li, J., Sayeed, S., Akimoto, S. and McClane, B.A. (2008) Sequencing and diversity analyses reveal extensive similarities between some epsilon-toxin-encoding plasmids and the pCPF5603 *Clostridium perfringens* enterotoxin plasmid. *J. Bacteriol.*, **190**, 7178-7188.

46. Miyamoto, K., Yumine, N., Mimura, K., Nagahama, M., Li, J., McClane, B.A. and Akimoto, S. (2011) Identification of novel *Clostridium perfringens* type E strains that carry an iota toxin plasmid with a functional enterotoxin gene. *PLOS One*, **6**, e20376.

47. Parreira, V.R., Costa, M., Eikmeyer, F., Blom, J. and Prescott, J.F. (2012) Sequence of two plasmids from *Clostridium perfringens* chicken necrotic enteritis isolates and comparison with *C. perfringens* conjugative plasmids. *PLOS One*, **7**, e49753.

48. Sayeed, S., Li, J. and McClane, B.A. (2007) Virulence plasmid diversity in *Clostridium perfringens* type D isolates. *Infect. Immun.*, **75**, 2391-2398.

49. Gurjar, A., Li, J. and McClane, B.A. (2010) Characterization of toxin plasmids in *Clostridium perfringens* type C isolates. *Infect. Immun.*, **78**, 4860-4869.

50. Sayeed, S., Li, J. and McClane, B.A. (2010) Characterization of virulence plasmid diversity among *Clostridium perfringens* type B isolates. *Infect. Immun.*, **78**, 495-504.

51. Li, J., Miyamoto, K. and McClane, B.A. (2007) Comparison of virulence plasmids among *Clostridium perfringens* type E isolates. *Infect. Immun.*, **75**, 1811-1819.

52. Sayeed, S., Li, J. and McClane, B.A. (2007) Virulence plasmid diversity In *Clostridium perfringens* type D isolates. *Infect. Immun*, **75**, 2391-2398.

53. Sayeed, S., Li, J. and McClane, B.A. (2010) Characterization of virulence plasmid diversity among *Clostridium perfringens* type B isolates. *Infect. Immun*, **78**, 495-504.

54. Dupuy, B., Daube, G., Popoff, M.R. and Cole, S.T. (1997) *Clostridium perfringens* urease genes are plasmid borne. *Infect. Immun*, **65**, 2313-2320.

55. Gurjar, A., Li, J. and McClane, B.A. (2010) Characterization of toxin plasmids in *Clostridium perfringens* type C isolates. *Infect. Immun*, **2010/09/09**.

56. Li, J., Miyamoto, K., Sayeed, S. and McClane, B.A. (2010) Organization of the *cpe* locus in CPE-positive *Clostridium perfringens* type C and D isolates. *PLOS One*, **5**, e10932.

57. Brynestad, S., Synstad, B. and Granum, P.E. (1997) The *Clostridium perfringens* enterotoxin gene is on a transposable element in type A human food poisoning strains. *Microbiology*, **143 (Pt 7)**, 2109-2115.

58. Brynestad, S. and Granum, P.E. (1999) Evidence that Tn*5565,* which includes the enterotoxin gene in *Clostridium perfringens*, can have a circular form which may be a transposition intermediate. *FEMS Microbiol. Lett.*, **170**, 281-286.

59. Miyamoto, K., Chakrabarti, G., Morino, Y. and McClane, B.A. (2002) Organization of the plasmid *cpe* Locus in *Clostridium perfringens* type A isolates. *Infect. Immun.*, **70**, 4261-4272.

60. Billington, S.J., Wieckowski, E.U., Sarkar, M.R., Bueschel, D., Songer, J.G. and McClane, B.A. (1998) *Clostridium perfringens* type E animal enteritis isolates with highly conserved, silent enterotoxin gene sequences. *Infect. Immun*, **66**, 4531-4536.

61. Miyamoto, K., Seike, S., Takagishi, T., Okui, K., Oda, M., Takehara, M. and Nagahama, M. (2015) Identification of the replication region in pBCNF5603, a bacteriocin-encoding plasmid, in the enterotoxigenic *Clostridium perfringens* strain F5603. *BMC Microbiol.*, **15**, 118.

62. Shimizu, T., Ohtani, K., Hirakawa, H., Ohshima, K., Yamashita, A., Shiba, T., Ogasawara, N., Hattori, M., Kuhara, S. and Hayashi, H. (2002) Complete genome sequence of *Clostridium perfringens*, an anaerobic flesh-eater. *Proc Natl Acad Sci U S A*, **99**, 996-1001.

63. Parsons, J.A., Bannam, T.L., Devenish, R.J. and Rood, J.I. (2007) TcpA, an FtsK/SpoIIIE homolog, is essential for transfer of the conjugative plasmid pCW3 in *Clostridium perfringens*. *J. Bacteriol.*, **189**, 7782-7790.

64. Irikura, D., Monma, C., Suzuki, Y., Nakama, A., Kai, A., Fukui-Miyazaki, A., Horiguchi, Y., Yoshinari, T., Sugita-Konishi, Y. and Kamata, Y. (2015) Identification and characterization of a new enterotoxin produced by *Clostridium perfringens* isolated from food poisoning outbreaks. *PLOS One*, **10**, e0138183.

65. Riley, M.A. and Wertz, J.E. (2002) Bacteriocins: evolution, ecology, and application. *Annu. Rev. Microbiol.*, **56**, 117-137.

66. Summers, D.K. (1991) The kinetics of plasmid loss. *Trends Biotechnol.*, **9**, 273-278.

67. Mahony, D.E. and Butler, M.E. (1971) Bacteriocins of Clostridium perfringens. 1. Isolation and preliminary studies. *Can J Microbiol*, **17**, 1-6.

68. Mahony, D.E. and Li, A. (1978) Comparative study of ten bacteriocins of *Clostridium perfringens*. *Antimicrob Agents Chemother*, **14**, 886-892.

69. Li, A.W., Verpoorte, J.A., Lewis, R.G. and Mahony, D.E. (1982) Characterization of bacteriocin 28 produced by *Clostridium perfringens. Can J Microbiol*, **28**, 860-873.

70. Tagg, J.R., Dajani, A.S. and Wannamaker, L.W. (1976) Bacteriocins of Gram-positive bacteria. *Bacteriological Reviews*, **40**, 722-756.

71. Barbara, A.J., Trinh, H.T., Glock, R.D. and Glenn Songer, J. (2008) Necrotic enteritis-producing strains of *Clostridium perfringens* displace non-necrotic enteritis strains from the gut of chicks. *Vet. Microbiol.*, **126**, 377-382.

72. Sullivan, M.J., Petty, N.K. and Beatson, S.A. (2011) Easyfig: a genome comparison visualizer. *Bioinformatics*, **27**, 1009-1010.

73. Ionesco, H., Bieth, G., Dauguet, C. and Bouanchaud, D. (1976) Identification of two plasmids isolated from a bacteriocinogenic strain of *Clostridium perfringens*. *Annales de microbiologie*, **127b**, 283-294.

74. Ionesco, H. and Bouanchaud, D.H. (1973) Bacteriocin production linked to the presence of a plasmid, in *Clostridium perfringens*, type A. *Comptes rendus hebdomadaires des seances de l'Academie des sciences. Serie D: Sciences Naturelles*, **276**, 2855-2857.

75. Mihelc, V.A., Duncan, C.L. and Chambliss, G.H. (1978) Characterization of a bacteriocinogenic plasmid in C*lostridium perfringens* CW55. *Antimicrob Agents Chemother* **14**, 771-779.

76. Myers, G.S., Rasko, D.A., Cheung, J.K., Ravel, J., Seshadri, R., DeBoy, R.T., Ren, Q., Varga, J., Awad, M.M., Brinkac, L.M. *et al.* (2006) Skewed genomic variability in strains of the toxigenic bacterial pathogen, *Clostridium perfringens*. *Genome Res.*, **16**, 1031-1040.

77. Garnier, T. and Cole, S.T. (1988) Complete nucleotide sequence and genetic organization of the bacteriocinogenic plasmid, pIP404, from *Clostridium perfringens*. *Plasmid*, **19**, 134-150.

78. Garnier, T. and Cole, S.T. (1986) Characterization of a bacteriocinogenic plasmid from *Clostridium perfringens* and molecular genetic analysis of the bacteriocin-encoding gene. *J. Bacteriol.*, **168**, 1189-1196.

79. Garnier, T., Saurin, W. and Cole, S.T. (1987) Molecular characterization of the resolvase gene, *res*, carried by a multicopy plasmid from *Clostridium perfringens*: common evolutionary origin for prokaryotic site-specific recombinases. *Mol. Microbiol.*, **1**, 371-376.

80. Garnier, T. and Cole, S.T. (1988) Identification and molecular genetic analysis of replication functions of the bacteriocinogenic plasmid pIP404 from *Clostridium perfringens*. *Plasmid*, **19**, 151-160.

81. Scott, J.R. (1984) Regulation of plasmid replication. *Microbiological reviews*, **48**, 1-23.

82. Brantl, S. (2014) Plasmid replication control by antisense RNAs. *Microbiology Spectrum*, **2**, Plas-0001-2013.

83. Ebersbach, G. and Gerdes, K. (2005) Plasmid segregation mechanisms. *Annu. Rev. Genet.*, **39**, 453-479.

84. del Solar, G., Giraldo, R., Ruiz-Echevarria, M.J., Espinosa, M. and Diaz-Orejas, R. (1998) Replication and control of circular bacterial plasmids. *Microbiol. Mol. Biol. Rev.*, **62**, 434-464.

85. Lilly, J. and Camps, M. (2015), *Plasmids: Biology and Impact in Biotechnology and Discovery*. American Society of Microbiology.

86. Ruiz-Masó, J.A., Machón, C., Bordanaba-Ruiseco, L., Espinosa, M., Coll, M. and del Solar, G. (2015), *Plasmids: Biology and Impact in Biotechnology and Discovery*. American Society of Microbiology.

87. Konieczny, I., Bury, K., Wawrzycka, A. and Wegrzyn, K. (2015), *Plasmids: Biology and Impact in Biotechnology and Discovery*. American Society of Microbiology.

88. Chattoraj, D.K. (2000) Control of plasmid DNA replication by iterons: no longer paradoxical. *Mol. Microbiol.*, **37**, 467-476.

89. Novick, R.P. (1987) Plasmid incompatibility. *Microbiological Reviews*, **51**, 381-395.

90. Lederberg, J. and Tatum, E.L. (1953) Sex in Bacteria: Genetic Studies, 1945-1952. *Science*, **118**, 169-175.

91. Lederberg, J. and Tatum, E.L. (1946) Gene recombination in *Escherichia coli*. *Nature*, **158**, 558.

92. Ilangovan, A., Connery, S. and Waksman, G. (2015) Structural biology of the Gram-negative bacterial conjugation systems. *Trends Microbiol.*, **23**, 301-310.

93. Schroder, G. and Lanka, E. (2005) The mating pair formation system of conjugative plasmids-A versatile secretion machinery for transfer of proteins and DNA. *Plasmid*, **54**, 1-25.

94. Chandran Darbari, V. and Waksman, G. (2015) Structural Biology of Bacterial Type IV Secretion Systems. *Annu. Rev. Biochem.*, **84**, 603-629.

95. Furste, J.P., Pansegrau, W., Ziegelin, G., Kroger, M. and Lanka, E. (1989) Conjugative transfer of promiscuous IncP plasmids: interaction of plasmid-encoded products with the transfer origin. *Proc Natl Acad Sci U S A*, **86**, 1771-1775.

96. Byrd, D.R. and Matson, S.W. (1997) Nicking by transesterification: the reaction catalysed by a relaxase. *Mol. Microbiol.*, **25**, 1011-1022.

97. de la Cruz, F., Frost, L.S., Meyer, R.J. and Zechner, E.L. (2010) Conjugative DNA metabolism in Gram-negative bacteria. *FEMS Microbiol. Rev.*, **34**, 18-40.

98. Garcillan-Barcia, M.P., Francia, M.V. and de la Cruz, F. (2009) The diversity of conjugative relaxases and its application in plasmid classification. *FEMS Microbiol. Rev.*, **33**, 657-687.

99. Llosa, M., Grandoso, G., Hernando, M.A. and de la Cruz, F. (1996) Functional domains in protein TrwC of plasmid R388: dissected DNA strand transferase and DNA helicase activities reconstitute protein function. *J. Mol. Biol.*, **264**, 56-67.

100. Llosa, M., Grandoso, G. and de la Cruz, F. (1995) Nicking activity of TrwC directed against the origin of transfer of the IncW plasmid R388. *J. Mol. Biol.*, **246**, 54-62.

101. Llosa, M., Bolland, S., Grandoso, G. and de la Cruz, F. (1994) Conjugation-independent, site-specific recombination at the *oriT* of the IncW plasmid R388 mediated by TrwC. *J. Bacteriol.*, **176**, 3210-3217.

102. de Paz, H.D., Larrea, D., Zunzunegui, S., Dehio, C., de la Cruz, F. and Llosa, M. (2010) Functional dissection of the conjugative coupling protein TrwB. *J. Bacteriol.*, **192**, 2655-2669.

103. Hormaeche, I., Iloro, I., Arrondo, J.L., Goni, F.M., de la Cruz, F. and Alkorta, I. (2004) Role of the transmembrane domain in the stability of TrwB, an integral protein involved in bacterial conjugation. *J. Biol. Chem.*, **279**, 10955-10961.

104. Segura, R.L., Aguila-Arcos, S., Ugarte-Uribe, B., Vecino, A.J., de la Cruz, F., Goni, F.M. and Alkorta, I. (2013) The transmembrane domain of the T4SS coupling protein TrwB and its role in protein-protein interactions. *Biochim. Biophys. Acta*, **1828**, 2015-2025.

105. de Paz, H.D., Sangari, F.J., Bolland, S., Garcia-Lobo, J.M., Dehio, C., de la Cruz, F. and Llosa, M. (2005) Functional interactions between type IV secretion systems involved in DNA transfer and virulence. *Microbiology*, **151**, 3505-3516.

106. Llosa, M., Zunzunegui, S. and de la Cruz, F. (2003) Conjugative coupling proteins interact with cognate and heterologous VirB10-like proteins while exhibiting specificity for cognate relaxosomes. *Proc Natl Acad Sci U S A*, **100**, 10465-10470.

107. Tato, I., Matilla, I., Arechaga, I., Zunzunegui, S., de la Cruz, F. and Cabezon, E. (2007) The ATPase activity of the DNA transporter TrwB is modulated by protein TrwA: implications for a common assembly mechanism of DNA translocating motors. *J. Biol. Chem.*, **282**, 25569-25576.

108. Moncalian, G., Cabezon, E., Alkorta, I., Valle, M., Moro, F., Valpuesta, J.M., Goni, F.M. and de La Cruz, F. (1999) Characterization of ATP and DNA binding activities of TrwB, the coupling protein essential in plasmid R388 conjugation. *J. Biol. Chem.*, **274**, 36117-36124.

109. Tato, I., Zunzunegui, S., de la Cruz, F. and Cabezon, E. (2005) TrwB, the coupling protein involved in DNA transport during bacterial conjugation, is a DNA-dependent ATPase. *Proc Natl Acad Sci U S A*, **102**, 8156-8161.

110. Gomis-Ruth, F.X., Moncalian, G., de la Cruz, F. and Coll, M. (2002) Conjugative plasmid protein TrwB, an integral membrane type IV secretion system coupling protein. Detailed structural features and mapping of the active site cleft. *J. Biol. Chem.*, **277**, 7556-7566.

111. Gomis-Ruth, F.X. and Coll, M. (2001) Structure of TrwB, a gatekeeper in bacterial conjugation. *The International Journal of Biochemistry & Cell Biology*, **33**, 839-843.

112. Gomis-Ruth, F.X. and Coll, M. (2001) Solving a 300 kDa multimeric protein by low-resolution MAD phasing and averaging/phase extension. *Acta crystallographica. Section D, Biological Crystallography*, **57**, 800-805.

113. Hormaeche, I., Alkorta, I., Moro, F., Valpuesta, J.M., Goni, F.M. and De La Cruz, F. (2002) Purification and properties of TrwB, a hexameric, ATP-binding integral membrane protein essential for R388 plasmid conjugation. *J. Biol. Chem.*, **277**, 46456-46462.

114. Shirasu, K., Koukolikova-Nicola, Z., Hohn, B. and Kado, C.I. (1994) An inner-membrane-associated virulence protein essential for T-DNA transfer from *Agrobacterium tumefaciens* to plants exhibits ATPase activity and similarities to conjugative transfer genes. *Mol. Microbiol.*, **11**, 581-588.

115. Fullner, K.J., Lara, J.C. and Nester, E.W. (1996) Pilus assembly by Agrobacterium T-DNA transfer genes. *Science*, **273**, 1107-1109.

116. Dang, T.A. and Christie, P.J. (1997) The VirB4 ATPase of *Agrobacterium tumefaciens* is a cytoplasmic membrane protein exposed at the periplasmic surface. *J. Bacteriol.*, **179**, 453-462.

117. Rabel, C., Grahn, A.M., Lurz, R. and Lanka, E. (2003) The VirB4 family of proposed traffic nucleoside triphosphatases: common motifs in plasmid RP4 TrbE are essential for conjugation and phage adsorption. *J. Bacteriol.*, **185**, 1045-1058.

118. Dang, T.A., Zhou, X.R., Graf, B. and Christie, P.J. (1999) Dimerization of the *Agrobacterium tumefaciens* VirB4 ATPase and the effect of ATP-binding cassette

mutations on the assembly and function of the T-DNA transporter. *Mol. Microbiol.*, **32**, 1239-1253.

119. Arechaga, I., Pena, A., Zunzunegui, S., del Carmen Fernandez-Alonso, M., Rivas, G. and de la Cruz, F. (2008) ATPase activity and oligomeric state of TrwK, the VirB4 homologue of the plasmid R388 type IV secretion system. *J. Bacteriol.*, **190**, 5472-5479.

120. Pena, A., Matilla, I., Martin-Benito, J., Valpuesta, J.M., Carrascosa, J.L., de la Cruz, F., Cabezon, E. and Arechaga, I. (2012) The hexameric structure of a conjugative VirB4 protein ATPase provides new insights for a functional and phylogenetic relationship with DNA translocases. *J. Biol. Chem.*, **287**, 39925-39932.

121. Rashkova, S., Spudich, G.M. and Christie, P.J. (1997) Characterization of membrane and protein interaction determinants of the *Agrobacterium tumefaciens* VirB11 ATPase. *J. Bacteriol.*, **179**, 583-591.

122. Ripoll-Rozada, J., Zunzunegui, S., de la Cruz, F., Arechaga, I. and Cabezon, E. (2013) Functional interactions of VirB11 traffic ATPases with VirB4 and VirD4 molecular motors in type IV secretion systems. *J. Bacteriol.*, **195**, 4195-4201.

123. Krause, S., Pansegrau, W., Lurz, R., de la Cruz, F. and Lanka, E. (2000) Enzymology of type IV macromolecule secretion systems: the conjugative transfer regions of plasmids RP4 and R388 and the cag pathogenicity island of *Helicobacter pylori* encode structurally and functionally related nucleoside triphosphate hydrolases. *J. Bacteriol.*, **182**, 2761-2770.

124. Yeo, H.-J., Savvides, S.N., Herr, A.B., Lanka, E. and Waksman, G. Crystal structure of the hexameric traffic ATPase of the *Helicobacter pylori* Type IV Secretion System. *Mol. Cell*, **6**, 1461-1472.

125. Fronzes, R., Schafer, E., Wang, L., Saibil, H.R., Orlova, E.V. and Waksman, G. (2009) Structure of a type IV secretion system core complex. *Science*, **323**, 266-268.

126. Rivera-Calzada, A., Fronzes, R., Savva, C.G., Chandran, V., Lian, P.W., Laeremans, T., Pardon, E., Steyaert, J., Remaut, H., Waksman, G. *et al.* (2013) Structure of a

bacterial type IV secretion core complex at subnanometre resolution. *EMBO J.*, **32**, 1195-1204.

127. Mossey, P., Hudacek, A. and Das, A. (2010) *Agrobacterium tumefaciens* type IV secretion protein VirB3 is an inner membrane protein and requires VirB4, VirB7, and VirB8 for stabilization. *J. Bacteriol.*, **192**, 2830-2838.

128. Chandran, V., Fronzes, R., Duquerroy, S., Cronin, N., Navaza, J. and Waksman, G. (2009) Structure of the outer membrane complex of a type IV secretion system. *Nature*, **462**, 1011-1015.

129. Lai, E.M. and Kado, C.I. (1998) Processed VirB2 is the major subunit of the promiscuous pilus of *Agrobacterium tumefaciens*. *J. Bacteriol.*, **180**, 2711-2717.

130. Schmidt-Eisenlohr, H., Domke, N., Angerer, C., Wanner, G., Zambryski, P.C. and Baron, C. (1999) Vir proteins stabilize VirB5 and mediate its association with the T pilus of *Agrobacterium tumefaciens*. *J. Bacteriol.*, **181**, 7485-7492.

131. Lai, E.M. and Kado, C.I. (2002) The *Agrobacterium tumefaciens* T pilus composed of cyclic T pilin is highly resilient to extreme environments. *FEMS Microbiol. Lett.*, **210**, 111-114.

132. Aly, K.A. and Baron, C. (2007) The VirB5 protein localizes to the T-pilus tips in *Agrobacterium tumefaciens*. *Microbiology*, **153**, 3766-3775.

133. Goessweiner-Mohr, N., Arends, K., Keller, W. and Grohmann, E. (2013) Conjugative type IV secretion systems in Gram-positive bacteria. *Plasmid*, **70**, 289-302.

134. Horodniceanu, T., Bougueleret, L., El-Solh, N., Bouanchaud, D.H. and Chabbert, Y.A. (1979) Conjugative R plasmids in *Streptococcus agalactiae* (group B). *Plasmid*, **2**, 197-206.

135. Kurenbach, B., Bohn, C., Prabhu, J., Abudukerim, M., Szewzyk, U. and Grohmann, E. (2003) Intergeneric transfer of the *Enterococcus faecalis* plasmid pIP501 to *Escherichia coli* and *Streptomyces lividans* and sequence analysis of its *tra* region. *Plasmid*, **50**, 86-93.

136. Wang, A. and Macrina, F.L. (1995) Characterization of six linked open reading frames necessary for pIP501-mediated conjugation. *Plasmid*, **34**, 206-210.

137. Kurenbach, B., Grothe, D., Farias, M.E., Szewzyk, U. and Grohmann, E. (2002) The tra region of the conjugative plasmid pIP501 is organized in an operon with the first gene encoding the relaxase. *J. Bacteriol.*, **184**, 1801-1805.

138. Kurenbach, B., Kopec, J., Magdefrau, M., Andreas, K., Keller, W., Bohn, C., Abajy, M.Y. and Grohmann, E. (2006) The TraA relaxase autoregulates the putative type IV secretion-like system encoded by the broad-host-range *Streptococcus agalactiae* plasmid pIP501. *Microbiology*, **152**, 637-645.

139. Abajy, M.Y., Kopec, J., Schiwon, K., Burzynski, M., Doring, M., Bohn, C. and Grohmann, E. (2007) A type IV-secretion-like system is required for conjugative DNA transport of broad-host-range plasmid pIP501 in Gram-positive bacteria. *J. Bacteriol.*, **189**, 2487-2496.

140. Wang, A. and Macrina, F.L. (1995) Streptococcal plasmid pIP501 has a functional *oriT* site. *J. Bacteriol.*, **177**, 4199-4206.

141. Kopec, J., Bergmann, A., Fritz, G., Grohmann, E. and Keller, W. (2005) TraA and its N-terminal relaxase domain of the Gram-positive plasmid pIP501 show specific *oriT* binding and behave as dimers in solution. *Biochem. J.*, **387**, 401-409.

142. Arends, K., Celik, E.K., Probst, I., Goessweiner-Mohr, N., Fercher, C., Grumet, L., Soellue, C., Abajy, M.Y., Sakinc, T., Broszat, M. *et al.* (2013) TraG encoded by the pIP501 type IV secretion system is a two-domain peptidoglycan-degrading enzyme essential for conjugative transfer. *J. Bacteriol.*, **195**, 4436-4444.

143. Freedman, J.C., Theoret, J.R., Wisniewski, J.A., Uzal, F.A., Rood, J.I. and McClane, B.A. (2014) *Clostridium perfringens* type A-E toxin plasmids. *Res. Microbiol.*, **166**, 264-279.

144. Bantwal, R., Bannam, T.L., Porter, C.J., Quinsey, N.S., Lyras, D., Adams, V. and Rood, J.I. (2012) The peptidoglycan hydrolase TcpG is required for efficient conjugative transfer of pCW3 in *Clostridium perfringens*. *Plasmid*, **67**, 139-147.

145. Wisniewski, J.A., Teng, W.L., Bannam, T.L. and Rood, J.I. (2015) Two novel membrane proteins TcpD and TcpE are essential for conjugative transfer of pCW3 in *Clostridium perfringens*. *J. Bacteriol.*

146. Wisniewski, J.A., Traore, D.A., Bannam, T.L., Lyras, D., Whisstock, J.C. and Rood, J.I. (2016) TcpM: a novel relaxase that mediates transfer of large conjugative plasmids from *Clostridium perfringens*. *Mol. Microbiol.*, **99**, 884-896.

147. Traore, D.A.K., Wisniewski, J.A., Flanigan, S.F., Conroy, P.J., Panjikar, S., Mok, Y.F., Lao, C., Griffin, M.D.W., Adams, V., Rood, J.I. *et al.* (2018) Crystal structure of TcpK in complex with *oriT* DNA of the antibiotic resistance plasmid pCW3. *Nature Communications*, **9**, 3732.

148. Steen, J.A., Bannam, T.L., Teng, W.L., Devenish, R.J. and Rood, J.I. (2009) The putative coupling protein TcpA interacts with other pCW3-encoded proteins to form an essential part of the conjugation complex. *J. Bacteriol.*, **191**, 2926-2933.

149. Teng, W.L., Bannam, T.L., Parsons, J.A. and Rood, J.I. (2008) Functional characterization and localization of the TcpH conjugation protein from *Clostridium perfringens*. *J. Bacteriol.*, **190**, 5075-5086.

150. Porter, C.J., Bantwal, R., Bannam, T.L., Rosado, C.J., Pearce, M.C., Adams, V., Lyras, D., Whisstock, J.C. and Rood, J.I. (2012) The conjugation protein TcpC from *Clostridium perfringens* is structurally related to the type IV secretion system protein VirB8 from Gram-negative bacteria. *Mol. Microbiol.*, **83**, 275-288.

151. Reyes-Lamothe, R., Tran, T., Meas, D., Lee, L., Li, A.M., Sherratt, D.J. and Tolmasky, M.E. (2014) High-copy bacterial plasmids diffuse in the nucleoid-free space, replicate stochastically and are randomly partitioned at cell division. *Nucleic Acids Res.*, **42**, 1042-1051.

152. Jacob, F. and Brenner, S. (1963) On the regulation of DNA synthesis in bacteria: the hypothesis of the replicon. *Comptes Rendus Hebdomadaires des Seances de l'Academie des Sciences*, **256**, 298-300.

153. Novick, R.P. (1969) Extrachromosomal inheritance in bacteria. *Bacteriological Reviews*, **33**, 210-263.

154. Gerdes, K., Rasmussen, P.B. and Molin, S. (1986) Unique type of plasmid maintenance function: postsegregational killing of plasmid-free cells. *Proc Natl Acad Sci U S A*, **83**, 3116-3120.

155. Gerdes, K., Bech, F.W., Jorgensen, S.T., Lobner-Olesen, A., Rasmussen, P.B., Atlung, T., Boe, L., Karlstrom, O., Molin, S. and von Meyenburg, K. (1986) Mechanism of postsegregational killing by the hok gene product of the *parB* system of plasmid R1 and its homology with the relF gene product of the *E. coli relB* operon. *EMBO J.*, **5**, 2023-2029.

156. Unterholzner, S.J., Poppenberger, B. and Rozhon, W. (2013) Toxin-antitoxin systems: Biology, identification, and application. *Mobile Genetic Elements*, **3**, e26219.

157. Sengupta, M. and Austin, S. (2011) Prevalence and significance of plasmid maintenance functions in the virulence plasmids of pathogenic bacteria. *Infect. Immun.*, **79**, 2502-2509.

158. Gerdes, K. and Wagner, E.G. (2007) RNA antitoxins. *Curr. Opin. Microbiol.*, **10**, 117-124.

159. Hernández-Arriaga, A.M., Chan, W.T., Espinosa, M. and Díaz-Orejas, R. (2015), *Plasmids: Biology and Impact in Biotechnology and Discovery*. American Society of Microbiology.

160. Cooper, T.F., Paixao, T. and Heinemann, J.A. (2010) Within-host competition selects for plasmid-encoded toxin-antitoxin systems. *Proceedings. Biological sciences / The Royal Society*, **277**, 3149-3155.

161. Cooper, T.F. and Heinemann, J.A. (2000) Postsegregational killing does not increase plasmid stability but acts to mediate the exclusion of competing plasmids. *Proc Natl Acad Sci U S A*, **97**, 12643-12648.

162. Austin, S., Ziese, M. and Sternberg, N. (1981) A novel role for site-specific recombination in maintenance of bacterial replicons. *Cell*, **25**, 729-736.

163. Grindley, N.D.F., Whiteson, K.L. and Rice, P.A. (2006) Mechanisms of site-specific recombination. *Annu. Rev. Biochem.*, **75**, 567-605.

164. Eberl, L., Kristensen, C.S., Givskov, M., Grohmann, E., Gerlitz, M. and Schwab, H. (1994) Analysis of the multimer resolution system encoded by the *parCBA* operon of broad-host-range plasmid RP4. *Mol. Microbiol.*, **12**, 131-141.

165. Bouet, J.Y., Bouvier, M. and Lane, D. (2006) Concerted action of plasmid maintenance functions: partition complexes create a requirement for dimer resolution. *Mol. Microbiol.*, **62**, 1447-1459.

166. Hamilton, D.L. and Abremski, K. (1984) Site-specific recombination by the bacteriophage P1 lox-Cre system. Cre-mediated synapsis of two lox sites. *J. Mol. Biol.*, **178**, 481-486.

167. Phillips, G. and Funnell, B.E. (2004) *Plasmid Biology*. ASM Press.

168. Moller-Jensen, J., Jensen, R.B. and Gerdes, K. (2000) Plasmid and chromosome segregation in prokaryotes. *Trends Microbiol.*, **8**, 313-320.

169. Gerdes, K., Moller-Jensen, J. and Bugge Jensen, R. (2000) Plasmid and chromosome partitioning: surprises from phylogeny. *Mol. Microbiol.*, **37**, 455-466.

170. Gerdes, K., Howard, M. and Szardenings, F. (2010) Pushing and pulling in prokaryotic DNA segregation. *Cell*, **141**, 927-942.

171. Adams, V., Watts, T.D., Bulach, D.M., Lyras, D. and Rood, J.I. (2015) Plasmid partitioning systems of conjugative plasmids from *Clostridium perfringens*. *Plasmid*, **80**, 90-96.

172. Simpson, A.E., Skurray, R.A. and Firth, N. (2003) A single gene on the staphylococcal multiresistance plasmid pSK1 encodes a novel partitioning system. *J. Bacteriol.*, **185**, 2143-2152.

173. Baxter, J.C. and Funnell, B.E. (2015), *Plasmids: Biology and Impact in Biotechnology and Discovery*. American Society of Microbiology.

174. Austin, S. and Abeles, A. (1983) Partition of unit-copy miniplasmids to daughter cells. I. P1 and F miniplasmids contain discrete, interchangeable sequences sufficient to promote equipartition. *J. Mol. Biol.*, **169**, 353-372.

175. Austin, S. and Abeles, A. (1983) Partition of unit-copy miniplasmids to daughter cells. II. The partition region of miniplasmid P1 encodes an essential protein and a centromere-like site at which it acts. *J. Mol. Biol.*, **169**, 373-387.

176. Ogura, T. and Hiraga, S. (1983) Partition mechanism of F plasmid: two plasmid gene-encoded products and a cis-acting region are involved in partition. *Cell*, **32**, 351-360.

177. Abeles, A.L., Friedman, S.A. and Austin, S.J. (1985) Partition of unit-copy miniplasmids to daughter cells. III. The DNA sequence and functional organization of the P1 partition region. *J. Mol. Biol.*, **185**, 261-272.

178. Koonin, E.V. (1993) A superfamily of ATPases with diverse functions containing either classical or deviant ATP-binding motif. *J. Mol. Biol.*, **229**, 1165-1174.

179. Funnell, B.E. (1988) Mini-P1 plasmid partitioning: excess ParB protein destabilizes plasmids containing the centromere *parS*. *J. Bacteriol.*, **170**, 954-960.

180. Funnell, B.E. (1988) Participation of *Escherichia coli* integration host factor in the P1 plasmid partition system. *Proc Natl Acad Sci U S A*, **85**, 6657-6661.

181. Funnell, B.E. (1991) The P1 plasmid partition complex at *parS*. The influence of *Escherichia coli* integration host factor and of substrate topology. *J. Biol. Chem.*, **266**, 14328-14337.

182. Davis, M.A. and Austin, S.J. (1988) Recognition of the P1 plasmid centromere analog involves binding of the ParB protein and is modified by a specific host factor. *EMBO J.*, **7**, 1881-1888.

183. Funnell, B.E. and Gagnier, L. (1993) The P1 plasmid partition complex at *parS*. II. Analysis of ParB protein binding activity and specificity. *J. Biol. Chem.*, **268**, 3616-3624.

184. Funnell, B.E. and Gagnier, L. (1994) P1 plasmid partition: binding of P1 ParB protein and *Escherichia coli* integration host factor to altered *parS* sites. *Biochimie*, **76**, 924-932.

185. Bouet, J.-Y., Surtees, J.A. and Funnell, B.E. (2000) Stoichiometry of P1 Plasmid Partition Complexes. *J. Biol. Chem.*, **275**, 8213-8219.

186. Surtees, J.A. and Funnell, B.E. (2001) The DNA binding domains of P1 ParB and the architecture of the P1 plasmid partition complex. *J. Biol. Chem.*, **276**, 12385-12394.

187. Schumacher, M.A. and Funnell, B.E. (2005) Structures of ParB bound to DNA reveal mechanism of partition complex formation. *Nature*, **438**, 516-519.

188. Schumacher, M.A., Glover, T.C., Brzoska, A.J., Jensen, S.O., Dunham, T.D., Skurray, R.A. and Firth, N. (2007) Segrosome structure revealed by a complex of ParR with centromere DNA. *Nature*, **450**, 1268-1271.

189. Rodionov, O., Lobocka, M. and Yarmolinsky, M. (1999) Silencing of genes flanking the P1 plasmid centromere. *Science*, **283**, 546-549.

190. Rodionov, O. and Yarmolinsky, M. (2004) Plasmid partitioning and the spreading of P1 partition protein ParB. *Mol. Microbiol.*, **52**, 1215-1223.

191. Bingle, L.E., Macartney, D.P., Fantozzi, A., Manzoor, S.E. and Thomas, C.M. (2005) Flexibility in repression and cooperativity by KorB of broad host range IncP-1 plasmid RK2. *J. Mol. Biol.*, **349**, 302-316.

192. Graham, T.G., Wang, X., Song, D., Etson, C.M., van Oijen, A.M., Rudner, D.Z. and Loparo, J.J. (2014) ParB spreading requires DNA bridging. *Genes Dev.*, **28**, 1228-1238.

193. Gordon, G.S., Sitnikov, D., Webb, C.D., Teleman, A., Straight, A., Losick, R., Murray, A.W. and Wright, A. (1997) Chromosome and low copy plasmid segregation in *E. coli*: visual evidence for distinct mechanisms. *Cell*, **90**, 1113-1121.

194. Niki, H. and Hiraga, S. (1997) Subcellular distribution of actively partitioning F plasmid during the cell division cycle in *E. coli*. *Cell*, **90**, 951-957.

195. Erdmann, N., Petroff, T. and Funnell, B.E. (1999) Intracellular localization of P1 ParB protein depends on ParA and *parS*. *Proc Natl Acad Sci U S A*, **96**, 14905-14910.

196. Davis, M.A., Martin, K.A. and Austin, S.J. (1992) Biochemical activities of the *parA* partition protein of the P1 plasmid. *Mol. Microbiol.*, **6**, 1141-1147.

197. Friedman, S.A. and Austin, S.J. (1988) The P1 plasmid-partition system synthesizes two essential proteins from an autoregulated operon. *Plasmid*, **19**, 103-112.

198. Vecchiarelli, A.G., Han, Y.W., Tan, X., Mizuuchi, M., Ghirlando, R., Biertumpfel, C., Funnell, B.E. and Mizuuchi, K. (2010) ATP control of dynamic P1 ParA-DNA interactions: a key role for the nucleoid in plasmid partition. *Mol. Microbiol.*, **78**, 78-91.

199. Bouet, J.Y. and Funnell, B.E. (1999) P1 ParA interacts with the P1 partition complex at *parS* and an ATP-ADP switch controls ParA activities. *EMBO J.*, **18**, 1415-1424.

200. Davis, M.A., Radnedge, L., Martin, K.A., Hayes, F., Youngren, B. and Austin, S.J. (1996) The P1 ParA protein and its ATPase activity play a direct role in the segregation of plasmid copies to daughter cells. *Mol. Microbiol.*, **21**, 1029-1036.

201. Fung, E., Bouet, J.Y. and Funnell, B.E. (2001) Probing the ATP-binding site of P1 ParA: partition and repression have different requirements for ATP binding and hydrolysis. *EMBO J.*, **20**, 4901-4911.

202. Castaing, J.P., Bouet, J.Y. and Lane, D. (2008) F plasmid partition depends on interaction of SopA with non-specific DNA. *Mol. Microbiol.*, **70**, 1000-1011.

203. Hester, C.M. and Lutkenhaus, J. (2007) Soj (ParA) DNA binding is mediated by conserved arginines and is essential for plasmid segregation. *Proc Natl Acad Sci U S A*, **104**, 20326-20331.

204. Ringgaard, S., van Zon, J., Howard, M. and Gerdes, K. (2009) Movement and equipositioning of plasmids by ParA filament disassembly. *Proc Natl Acad Sci U S A*, **106**, 19369-19374.

205. Ebersbach, G. and Gerdes, K. (2004) Bacterial mitosis: partitioning protein ParA oscillates in spiral-shaped structures and positions plasmids at mid-cell. *Mol. Microbiol.*, **52**, 385-398.

206. Hatano, T., Yamaichi, Y. and Niki, H. (2007) Oscillating focus of SopA associated with filamentous structure guides partitioning of F plasmid. *Mol. Microbiol.*, **64**, 1198-1213.

207. Lim, G.E., Derman, A.I. and Pogliano, J. (2005) Bacterial DNA segregation by dynamic SopA polymers. *Proc Natl Acad Sci U S A*, **102**, 17658-17663.

208. Vecchiarelli, A.G., Mizuuchi, K. and Funnell, B.E. (2012) Surfing biological surfaces: exploiting the nucleoid for partition and transport in bacteria. *Mol. Microbiol.*, **86**, 513-523.

209. Vecchiarelli, A.G., Hwang, L.C. and Mizuuchi, K. (2013) Cell-free study of F plasmid partition provides evidence for cargo transport by a diffusion-ratchet mechanism. *Proc Natl Acad Sci U S A*, **110**, E1390-1397.

210. Vecchiarelli, A.G., Neuman, K.C. and Mizuuchi, K. (2014) A propagating ATPase gradient drives transport of surface-confined cellular cargo. *Proc Natl Acad Sci U S A*, **111**, 4880-4885.

211. Hwang, L.C., Vecchiarelli, A.G., Han, Y.-W., Mizuuchi, M., Harada, Y., Funnell, B.E. and Mizuuchi, K. (2013) ParA-mediated plasmid partition driven by protein pattern self-organization. *EMBO J.*, **32**, 1238-1249.

211a. Sanchez, A., Cattoni D.I., Walter, J.C., Rech, J., Parmeggiani, A., Nollmann, M., Bouet, J.Y. (2015) Stochastic Self-Assembly of ParB Proteins Builds the Bacterial DNA Segregation Apparatus. *Cell Systems* 1(2):163-73. doi: 10.1016/j.cels.2015.07.013

211b. Debaugny, R. E., Sanchez, A., Rech, J., Labourdette, D., Dorignac, J., Geniet, F., Palmeri, J., Parmeggiani, A., Boudsocq, F., Anton Leberre, V., Walter, J. C., Bouet, J. Y. (2018) A conserved mechanism drives partition complex assembly on bacterial chromosomes and plasmids. *Molecular systems biology*, *14*(11), e8516. oi:10.15252/msb.20188516

212. Gerdes, K. and Molin, S. (1986) Partitioning of plasmid R1. Structural and functional analysis of the *parA* locus. *J. Mol. Biol.*, **190**, 269-279.

213. van den Ent, F., Moller-Jensen, J., Amos, L.A., Gerdes, K. and Lowe, J. (2002) F-actin-like filaments formed by plasmid segregation protein ParM. *EMBO J.*, **21**, 6935-6943.

214. Jensen, R.B. and Gerdes, K. (1997) Partitioning of plasmid R1. The ParM protein exhibits ATPase activity and interacts with the centromere-like ParR-*parC* complex. *J. Mol. Biol.*, **269**, 505-513.

215. Moller-Jensen, J., Jensen, R.B., Lowe, J. and Gerdes, K. (2002) Prokaryotic DNA segregation by an actin-like filament. *EMBO J.*, **21**, 3119-3127.

216. Salje, J., Gayathri, P. and Lowe, J. (2010) The ParMRC system: molecular mechanisms of plasmid segregation by actin-like filaments. *Nat. Rev. Microbiol.*, **8**, 683-692.

217. Gerdes, K., Larsen, J.E. and Molin, S. (1985) Stable inheritance of plasmid R1 requires two different loci. *J. Bacteriol.*, **161**, 292-298.

218. Popp, D., Xu, W., Narita, A., Brzoska, A.J., Skurray, R.A., Firth, N., Ghoshdastider, U., Maeda, Y., Robinson, R.C. and Schumacher, M.A. (2010) Structure and filament dynamics of the pSK41 actin-like ParM protein: implications for plasmid DNA segregation. *J. Biol. Chem.*, **285**, 10130-10140.

219. Moller-Jensen, J., Ringgaard, S., Mercogliano, C.P., Gerdes, K. and Lowe, J. (2007) Structural analysis of the ParR/*parC* plasmid partition complex. *EMBO J.*, **26**, 4413-4422.

220. Bork, P., Sander, C. and Valencia, A. (1992) An ATPase domain common to prokaryotic cell cycle proteins, sugar kinases, actin, and hsp70 heat shock proteins. *Proc Natl Acad Sci U S A*, **89**, 7290-7294.

221. Derman, A.I., Becker, E.C., Truong, B.D., Fujioka, A., Tucey, T.M., Erb, M.L., Patterson, P.C. and Pogliano, J. (2009) Phylogenetic analysis identifies many uncharacterized actin-like proteins (Alps) in bacteria: regulated polymerization, dynamic instability and treadmilling in Alp7A. *Mol. Microbiol.*, **73**, 534-552.

222. van den Ent, F., Izore, T., Bharat, T.A., Johnson, C.M. and Lowe, J. (2014) Bacterial actin MreB forms antiparallel double filaments. *eLife*, **3**, e02634.

223. Depue, R.H., Jr. and Rice, R.V. (1965) F-actin is a right-handed helix. *J. Mol. Biol.*, **12**, 302-303.

224. Gayathri, P., Fujii, T., Moller-Jensen, J., van den Ent, F., Namba, K. and Lowe, J. (2012) A bipolar spindle of antiparallel ParM filaments drives bacterial plasmid segregation. *Science*, **338**, 1334-1337.

225. Gayathri, P., Fujii, T., Namba, K. and Lowe, J. (2013) Structure of the ParM filament at 8.5A resolution. *Journal of Structural Biology*, **184**, 33-42.

226. Garner, E.C., Campbell, C.S. and Mullins, R.D. (2004) Dynamic instability in a DNA-segregating prokaryotic actin homolog. *Science*, **306**, 1021-1025.

227. Orlova, A., Garner, E.C., Galkin, V.E., Heuser, J., Mullins, R.D. and Egelman, E.H. (2007) The structure of bacterial ParM filaments. *Nat. Struct. Mol. Biol.*, **14**, 921-926.

228. Galkin, V.E., VanLoock, M.S., Orlova, A. and Egelman, E.H. (2002) A new internal mode in F-actin helps explain the remarkable evolutionary conservation of actin's sequence and structure. *Curr. Biol.*, **12**, 570-575.

229. Moller-Jensen, J., Borch, J., Dam, M., Jensen, R.B., Roepstorff, P. and Gerdes, K. (2003) Bacterial mitosis: ParM of plasmid R1 moves plasmid DNA by an actin-like insertional polymerization mechanism. *Mol. Cell*, **12**, 1477-1487.

230. Jensen, R.B. and Gerdes, K. (1999) Mechanism of DNA segregation in prokaryotes: ParM partitioning protein of plasmid R1 co-localizes with its replicon during the cell cycle. *EMBO J.*, **18**, 4076-4084.

231. Campbell, C.S. and Mullins, R.D. (2007) In vivo visualization of type II plasmid segregation: bacterial actin filaments pushing plasmids. *J. Cell Biol.*, **179**, 1059-1066.

232. Salje, J., Zuber, B. and Lowe, J. (2009) Electron cryomicroscopy of *E. coli* reveals filament bundles involved in plasmid DNA segregation. *Science*, **323**, 509-512.

233. Popp, D., Yamamoto, A., Iwasa, M., Narita, A., Maeda, K. and Maeda, Y. (2007) Concerning the dynamic instability of actin homolog ParM. *Biochem. Biophys. Res. Commun.*, **353**, 109-114.

234. Popp, D., Narita, A., Iwasa, M., Maeda, Y. and Robinson, R.C. (2010) Molecular mechanism of bundle formation by the bacterial actin ParM. *Biochem. Biophys. Res. Commun.*, **391**, 1598-1603.

235. Bharat, T.A., Murshudov, G.N., Sachse, C. and Lowe, J. (2015) Structures of actin-like ParM filaments show architecture of plasmid-segregating spindles. *Nature*, **523**, 106-110.

236. Rivera, C.R., Kollman, J.M., Polka, J.K., Agard, D.A. and Mullins, R.D. (2011) Architecture and assembly of a divergent member of the ParM family of bacterial actin-like proteins. *J. Biol. Chem.*, **286**, 14282-14290.

237. Roeben, A., Kofler, C., Nagy, I., Nickell, S., Hartl, F.U. and Bracher, A. (2006) Crystal structure of an archaeal actin homolog. *J. Mol. Biol.*, **358**, 145-156.

238. Hara, F., Yamashiro, K., Nemoto, N., Ohta, Y., Yokobori, S., Yasunaga, T., Hisanaga, S. and Yamagishi, A. (2007) An actin homolog of the archaeon *Thermoplasma acidophilum* that retains the ancient characteristics of eukaryotic actin. *J. Bacteriol.*, **189**, 2039-2045.

239. Holy, T.E. and Leibler, S. (1994) Dynamic instability of microtubules as an efficient way to search in space. *Proc Natl Acad Sci U S A*, **91**, 5682-5685.

240. Garner, E.C., Campbell, C.S., Weibel, D.B. and Mullins, R.D. (2007) Reconstitution of DNA segregation driven by assembly of a prokaryotic actin homolog. *Science*, **315**, 1270-1274.

241. Popp, D., Narita, A., Oda, T., Fujisawa, T., Matsuo, H., Nitanai, Y., Iwasa, M., Maeda, K., Onishi, H. and Maeda, Y. (2008) Molecular structure of the ParM polymer and the mechanism leading to its nucleotide-driven dynamic instability. *EMBO J.*, **27**, 570-579.

242. Garner, E.C., Campbell, C.S. and Mullins, R.D. (2004) Dynamic instability in a DNA-segregating prokaryotic actin homolog. *Science*, **306**, 1021-1025.

243. Jensen, R.B., Dam, M. and Gerdes, K. (1994) Partitioning of plasmid R1. The *parA* operon is autoregulated by ParR and its transcription is highly stimulated by a downstream activating element. *J. Mol. Biol.*, **236**, 1299-1309.

244. Hoischen, C., Bolshoy, A., Gerdes, K. and Diekmann, S. (2004) Centromere *parC* of plasmid R1 is curved. *Nucleic Acids Res.*, **32**, 5907-5915.

245. Breuner, A., Jensen, R.B., Dam, M., Pedersen, S. and Gerdes, K. (1996) The centromere-like *parC* locus of plasmid R1. *Mol. Microbiol.*, **20**, 581-592.

246. Jensen, R.B., Lurz, R. and Gerdes, K. (1998) Mechanism of DNA segregation in prokaryotes: replicon pairing by *parC* of plasmid R1. *Proc Natl Acad Sci U S A*, **95**, 8550-8555.

247. Salje, J. and Lowe, J. (2008) Bacterial actin: architecture of the ParMRC plasmid DNA partitioning complex. *EMBO J.*, **27**, 2230-2238.

248. Larsen, R.A., Cusumano, C., Fujioka, A., Lim-Fong, G., Patterson, P. and Pogliano, J. (2007) Treadmilling of a prokaryotic tubulin-like protein, TubZ, required for plasmid stability in *Bacillus thuringiensis*. *Genes Dev.*, **21**, 1340-1352.

249. Barilla, D. (2010) One-way ticket to the cell pole: plasmid transport by the prokaryotic tubulin homolog TubZ. *Proc Natl Acad Sci U S A*, **107**, 12061-12062.

250. Oliva, M.A., Martin-Galiano, A.J., Sakaguchi, Y. and Andreu, J.M. (2012) Tubulin homolog TubZ in a phage-encoded partition system. *Proc Natl Acad Sci U S A*, **109**, 7711-7716.

251. Tang, M., Bideshi, D.K., Park, H.W. and Federici, B.A. (2007) Iteron-binding ORF157 and FtsZ-like ORF156 proteins encoded by pBtoxis play a role in its replication in *Bacillus thuringiensis* subsp. *israelensis*. *J. Bacteriol.*, **189**, 8053-8058.

252. Ni, L., Xu, W., Kumaraswami, M. and Schumacher, M.A. (2010) Plasmid protein TubR uses a distinct mode of HTH-DNA binding and recruits the prokaryotic tubulin homolog TubZ to effect DNA partition. *Proc Natl Acad Sci U S A*, **107**, 11763-11768.

253. Chen, Y. and Erickson, H.P. (2008) *in vitro* assembly studies of FtsZ/tubulin-like proteins (TubZ) from Bacillus plasmids: evidence for a capping mechanism. *J. Biol. Chem.*, **283**, 8102-8109.

254. Aylett, C.H., Wang, Q., Michie, K.A., Amos, L.A. and Lowe, J. (2010) Filament structure of bacterial tubulin homologue TubZ. *Proc Natl Acad Sci U S A*, **107**, 19766-19771.

255. Montabana, E.A. and Agard, D.A. (2014) Bacterial tubulin TubZ-Bt transitions between a two-stranded intermediate and a four-stranded filament upon GTP hydrolysis. *Proc Natl Acad Sci U S A*, **111**, 3407-3412.

256. Zehr, E.A., Kraemer, J.A., Erb, M.L., Coker, J.K., Montabana, E.A., Pogliano, J. and Agard, D.A. (2014) The structure and assembly mechanism of a novel three-stranded tubulin filament that centers phage DNA. *Structure*, **22**, 539-548.

257. Wegner, A. and Isenberg, G. (1983) 12-fold difference between the critical monomer concentrations of the two ends of actin filaments in physiological salt conditions. *Proc Natl Acad Sci U S A*, **80**, 4922-4925.

258. Fink, G. and Lowe, J. (2015) Reconstitution of a prokaryotic minus end-tracking system using TubRC centromeric complexes and tubulin-like protein TubZ filaments. *Proc Natl Acad Sci U S A*, **112**, E1845-1850.

259. Aylett, C.H. and Lowe, J. (2012) Superstructure of the centromeric complex of TubZRC plasmid partitioning systems. *Proc Natl Acad Sci U S A*, **109**, 16522-16527.

260. Firth, N., Apisiridej, S., Berg, T., O'Rourke, B.A., Curnock, S., Dyke, K.G. and Skurray, R.A. (2000) Replication of staphylococcal multiresistance plasmids. *J. Bacteriol.*, **182**, 2170-2178.

260a. Guynet C, Cuevas A, Moncalián G, de la Cruz F (2011) The *stb* Operon Balances the Requirements for Vegetative Stability and Conjugative Transfer of Plasmid R388. *PLOS Genetics* **7**(5): e1002073. https://doi.org/10.1371/journal.pgen.1002073

261. Novick, R.P. and Hoppensteadt, F.C. (1978) On plasmid incompatibility. *Plasmid*, **1**, 421-434.

262. Novick, R.P., Clowes, R.C., Cohen, S.N., Curtiss, R., 3rd, Datta, N. and Falkow, S. (1976) Uniform nomenclature for bacterial plasmids: a proposal. *Bacteriological Reviews*, **40**, 168-189.

263. Gustafsson, P. and Nordstrom, K. (1975) Random replication of the stringent plasmid R1 in *Escherichia coli* K-12. *J. Bacteriol.*, **123**, 443-448.

264. Ebersbach, G., Sherratt, D.J. and Gerdes, K. (2005) Partition-associated incompatibility caused by random assortment of pure plasmid clusters. *Mol. Microbiol.*, **56**, 1430-1440.

265. Bouet, J.Y., Nordstrom, K. and Lane, D. (2007) Plasmid partition and incompatibility--the focus shifts. *Mol. Microbiol.*, **65**, 1405-1414.

266. Bouet, J.Y., Rech, J., Egloff, S., Biek, D.P. and Lane, D. (2005) Probing plasmid partition with centromere-based incompatibility. *Mol. Microbiol.*, **55**, 511-525.

267. Ebersbach, G. and Gerdes, K. (2001) The double par locus of virulence factor pB171: DNA segregation is correlated with oscillation of ParA. *Proc Natl Acad Sci U S A*, **98**, 15078-15083.

268. Edgar, R., Chattoraj, D.K. and Yarmolinsky, M. (2001) Pairing of P1 plasmid partition sites by ParB. *Mol. Microbiol.*, **42**, 1363-1370.

269. Funnell, B.E. (2005) Partition-mediated plasmid pairing. *Plasmid*, **53**, 119-125.

270. Austin, S. and Nordstrom, K. (1990) Partition-mediated incompatibility of bacterial plasmids. *Cell*, **60**, 351-354.

271. Dubarry, N., Pasta, F. and Lane, D. (2006) ParABS systems of the four replicons of *Burkholderia cenocepacia*: new chromosome centromeres confer partition specificity. *J. Bacteriol.*, **188**, 1489-1496.

272. Du, W.L., Dubarry, N., Passot, F.M., Kamgoue, A., Murray, H., Lane, D. and Pasta, F. (2016) Orderly replication and segregation of the four replicons of *Burkholderia cenocepacia* J2315. *PLOS Genet.*, **12**, e1006172.

273. Passot, F.M., Calderon, V., Fichant, G., Lane, D. and Pasta, F. (2012) Centromere binding and evolution of chromosomal partition systems in the Burkholderiales. *J. Bacteriol.*, **194**, 3426-3436.

274. Pillet, F., Passot, F.M., Pasta, F., Anton Leberre, V. and Bouet, J.Y. (2017) Analysis of ParB-centromere interactions by multiplex SPR imaging reveals specific patterns for binding ParB in six centromeres of Burkholderiales chromosomes and plasmids. *PLOS One*, **12**, e0177056.

275. Koper, P., Zebracki, K., Marczak, M., Skorupska, A. and Mazur, A. (2016) RepB proteins of the multipartite *Rhizobium leguminosarum* bv. *trifolii* genome discriminate between centromere-like *parS* sequences for plasmid segregational stability. *Mol. Microbiol.*, **102**, 446-466.

276. Chen, S., Larsson, M., Robinson, R.C. and Chen, S.L. (2017) Direct and convenient measurement of plasmid stability in lab and clinical isolates of *E. coli*. *Scientific Reports*, **7**, 4788.

Chapter 2

pCP13, a representative of a new family of conjugative toxin plasmids in *Clostridium perfringens*

pCP13, a representative of a new family of conjugative toxin plasmids in *Clostridium perfringens*

Thomas D. Watts, Callum J. Vidor, Milena M. Awad, Dena Lyras, Julian I. Rood* and Vicki Adams*#

Infection and Immunity Program, Monash Biomedicine Discovery Institute and Department of Microbiology, Monash University, Victoria 3800, Australia

*Joint senior authors

#Corresponding author: Vicki Adams, Department of Microbiology, Monash University, Victoria, 3800, Australia.

Tel: [redacted]

Email: [redacted]

Keywords: Conjugation, *Clostridium perfringens*, pCP13, plasmid, VirB4, BEC toxin

Abstract

Conjugative transfer is a major contributor to the dissemination of antibiotic resistance and virulence genes in the human and animal pathogen, *Clostridium perfringens*. The *C. perfringens* plasmid pCW3 is the archetype of an extensive family of highly related conjugative toxin and antibiotic resistance plasmids found in this bacterium. These plasmids were thought to constitute the only conjugative plasmid family in *C. perfringens*. Recently, another series of *C. perfringens* plasmids, the pCP13-like family, have been shown to harbour important toxin genes, including genes that encode the novel binary clostridial enterotoxin, BEC. Based on early bioinformatics analysis this plasmid family was thought to be non-conjugative. Here we demonstrate that pCP13 is in fact conjugative, transfers at high frequency and that the newly defined Pcp conjugation locus encodes putative homologues of a type 4 secretion system (T4SS), one of which, PcpB4, was shown to be essential for transfer. The T4SS of pCP13 also appears to be evolutionarily related to conjugative toxin plasmids from other clostridia-like species, including *Paeniclostridium* (formerly *Clostridium*) *sordellii*, *Clostridioides* (formerly *Clostridium*) *difficile* and *Clostridium botulinum.* In conclusion, we have shown that the novel Pcp conjugation locus that is present on pCP13, and the related BEC toxin plasmids, is functional in *C. perfringens*. Therefore, it is clear that there are two distinct families of conjugative plasmids in *C. perfringens*: the pCW3 family and the pCP13 family. This study has significant implications for our understanding of the movement of toxin genes both within *C. perfringens,* but also potentially to other pathogenic clostridia.

Introduction

Clostridium perfringens is a Gram-positive pathogen that causes a variety of diseases in both humans and animals, including clostridial myonecrosis in humans and economically important avian necrotic enteritis in broiler chickens (1-3). Disease is mediated by the production of extracellular enzymes and toxins, many of which are encoded on large conjugative plasmids (4). The plasmids of *C. perfringens* can be categorised into three broad families based on the type of replication initiator that they encode: the pCW3, pCP13 and pIP404 families (4-7). Most studies have focused on the pCW3-like family of conjugative plasmids as they encode the majority of the clinically relevant *C. perfringens* toxins and antimicrobial resistance determinants (4,8). These plasmids each share approximately 35 kb of sequence similarity in a conserved backbone region (7,9,10). This conserved region includes the plasmid replication and maintenance region, as well as the (Tcp) conjugation locus (7,9-11).

The Tcp locus is composed of 12 genes (*tcpK*, *tcpM* and *tcpA* to *tcpJ*) and an origin of transfer (*oriT)* (11,12). Functional studies have shown that most of the proteins encoded within the Tcp locus are essential for the efficient conjugative transfer of pCW3. These proteins include several structural proteins (TcpH and TcpC) (7,13), a putative ATPase (TcpF) (7), the coupling protein (TcpA) (14,15), a peptidoglycan hydrolase (TcpG) (16), integral membrane proteins (TcpD and TcpE) (17) and the relaxosome components TcpM (a novel relaxase) and TcpK (a relaxosome accessory factor) (11,12,18).

The pCP13-like family is a distinct group of plasmids that also are found in *C. perfringens*. pCP13 was first isolated and sequenced from *C. perfringens* strain 13 (6). Initial annotation of this 54 kb plasmid showed that it carried *cpb2*, a gene encoding the beta2 toxin, but did not reveal any genes with homology to known conjugation loci ((6). Therefore, the pCP13-like plasmid family has been largely ignored since few of these plasmids appeared to encode clinically relevant virulence and antimicrobial resistance determinants. However, more

recently several food poisoning outbreaks in Japan resulted in the isolation of two enterotoxin (CPE) negative strains of *C. perfringens* that encoded a novel binary enterotoxin called BEC (or CPILE) (19,20). The BEC toxin is encoded by two genes, *becA* and *becB*, which were associated with the pCP13-like toxin plasmids pCP-TS1 and pCP-OS1 (19).

Initial bioinformatic analysis of pCP13 did not reveal any genes with similarity to known replication and conjugation genes (6). However, the replication initiator of the pCP13-like bacteriocin-encoding plasmid pBCNF5603 has since been identified and shown to have similarity to ORF63 from pCP13 (21). In addition, we recently showed that pCP13 has low-level nucleotide sequence similarity to the conjugative toxin plasmids pCS1-1 and pCLL from the Gram-positive pathogens *Paeniclostridium* (previously *Clostridium*) *sordellii* and *Clostridium botulinum*, respectively (22,23). Comparison to the most well characterised of these plasmids, pCS1-1, showed that there is a 17 kb region that is conserved in pCP13 and pCS1-1. This region corresponds to the pCS1-1 *P. sordellii* (Cst) conjugation locus (23). Several genes within this locus encode proteins with conserved domains that are similar to the archetypal *Agrobacterium tumefaciens* Vir conjugation proteins (23). In addition, mutation of either *cstB4* (encoding a VirB4 homologue) or *cstD4* (encoding a VirD4 homologue) abolished conjugative transfer of pCS1-1 (23).

Based on the pCS1-1 results we postulated that pCP13 also was conjugative. In this study we have used comparative bioinformatics and mutagenesis studies to show that pCP13 is conjugative and is a representative of a novel family of conjugative plasmids in *C. perfringens* that is also related to plasmids from two other members of the clostridia.

Materials and methods

Plasmids, bacterial strains, and culture conditions. All *C. perfringens, Escherichia coli* and *P. sordellii* strains and plasmids used in this study are listed in Table 2.1.

C. perfringens strains were cultured in preboiled fluid thioglycolate medium (FTG) (Oxoid), heart infusion (Diffco) (HI) broth or, tryptone-peptone-glucose (TPG) broth (24) and incubated at 37°C. When solid media were required, *C. perfringens* was grown on nutrient agar (NA) (25) or HI agar supplemented with glucose (0.375 % w/v). Where appropriate, NA was supplemented with 50 µg/ml of erythromycin (Em), 20 µg/ml of chloramphenicol (Cm), 2 mg/ml streptomycin (Sm), 1% potassium chlorate (Chl) or 50 ng/ml anhydrous tetracycline (AnTc). All agar cultures were incubated overnight at 37°C in an anaerobic jar (Oxoid) containing 10% (v/v) CO_2, 10% (v/v) H_2 and 80% (v/v) N_2. *P. sordellii* isolates were grown in HIS broth or on HIS agar (23) at 37°C in an anaerobic chamber (Coy Laboratory Products, Inc.) in an atmosphere of 10% H_2, 10% CO_2, and 80% N_2. Where appropriate, medium used to culture *P. sordellii* was supplemented with antibiotics at the following concentrations: Em 10 µg/ml, Tc; 10 µg/ml, Tm, 10 µg/ml, Sm, 200 µg/ml, Rifampicin (Rif); 20 µg/ml, AnTc, 20 ng/ml, and D-cycloserine (DCy); 250 µg/ml. *E. coli* isolates were grown in 2 × yeast extract, tryptone (2YT) broth or agar (1.5 % bacteriological agar, Difco) and incubated at 37°C under aerobic conditions with shaking overnight. Where appropriate, *E. coli* growth media were supplemented with Cm at 30 µg/ml.

Table 2.1 Bacterial strains and plasmids

Strain	Description	Reference/origin
C. perfringens		
JIR325	13 (pCP13) Rif^R Nal^R, spontaneous mutant	(26)
JIR13192	JIR325(pJIR4823) pCP13*parBΩermB* TargeTron mutant $Rif^RNal^REm^R$	This study
JIR13211	JIR325$(pCP13)^-$ JIR325 cured of pCP13	This study
JIR13270	JIR325(pJIR4537) pCP13*cpb2ΩermB* TargeTron mutant $Rif^RNal^REm^R$	This study
JIR13467	JIR13211 $Rif^RNal^RSm^RChl^R$, spontaneous mutant	This study
JIR13470	JIR325(pJIR4821) pCP13*pcpB4ΩermB* TargeTron mutant	This study
JIR13670	JIR13470(pRPF185)	This study
JIR13671	JIR13470(pDLL213)	This study
JIR13672	JIR13470(pDLL212)	This study
JIR13677	JIR13211(pJIR750)	This study
P. sordellii		
DLL5002	ATCC9714(pDLL230), Erm^R	(27)
DLL5153	ATCC9714 cured of pCS1-1, Sm^R, Rif^R	(23)
DLL5188	ATCC9714(pCS1-1*cstB4ΩermB*)	(23)

DLL5232	DLL5188(pDLL212)	(23)
DLL5234	DLL5188(pDLL213)	(C. Vidor, M. Awad, D. Lyras, unpublished)
Plasmids	**Description**	**Reference**
pCP13	54 kb plasmid (Genbank accession number: AP003515.1)	(6)
pCS1-1	*C. sordellii* ATCC9714 pCS1 plasmid, *tcsL*$^{+}$*tcsH*$^{-}$ (Genbank accession number: LN679999.1)	(28)
pDLL212	pRPF185 with *cstB4* cloned into *Sac*I/*Xho*I sites	(23)
pDLL213	pRPF185 with *pcpB4* cloned into *Sac*I/*Xho*I sites	This study
pDLL230	pCS1-1*tcsL*Ω*ermB*	(27)
pDLL252	pCS1-1*cstB4*Ω*ermB*	(23)
pJIR3566	pMTL9361 derivative with *Bsr*GI and *Hin*dIII sites removed from *rep*, contains RP4 and Tn*916 oriT* sites and *lacZα* within *Hin*dIII/*Bsr*GI sites of retargeting region for blue white screening, Cm^{R}	(29)
pJIR4821	pCP13*pcpB6*Ω*ermB* TargeTron mutant	This study
pJIR4822	pCP13*pcpB4*Ω*ermB* TargeTron mutant	This study
pJIR4823	pCP13*parB*Ω*ermB* TargTron mutant	This study

pJIR4832	pJIR3566 TargeTron vector retargeted to nucleotide position 1728 of *pcpB4*.	This study
pJIR4537	pCP13*cpb2*Ω*ermB* TargeTron mutant	This study
pRPF185	Clostridial tetracycline inducible expression vector, Cm^R	(30)

Em^R, erythromycin resistant, Tc^R, tetracycline resistant, Nal^R, nalidixic acid resistant, Rif^R, rifampicin resistant, Sm^R, streptomycin resistant Chl^R, potassium chlorate resistant, Cm^R, chloramphenicol resistant.

Molecular methods. *E. coli* plasmid DNA was extracted using an alkaline lysis kit (QIAgen) as per the manufacturer's instructions. *C. perfringens* genomic DNA (gDNA) was isolated after overnight growth in pre-boiled FTG broth, as previously described (31). PCR confirmation of mutants was conducted using *Taq* DNA polymerase (Roche), with a final concentration of 0.5 µM of each specific oligonucleotide primer. PCR conditions were as follows: denaturation (94°C for 30 seconds), annealing (50-55°C for 1 min) and extension (72 °C for 1 minute) for 35 cycles. All gDNA and PCR products were subjected to gel electrophoresis on either a 0.8% (w/v) or 1% (w/v) agarose gel for 40-50 minutes at 100 V, before being visualised with the Chemidoc XRS+ system (BioRad). Oligonucleotide primers are listed in Table S2.1. Plasmids were introduced into *C. perfringens* strains *via* electroporation as previously described (32). Southern hybridisation was conducted as follows: genomic DNA was digested with *Eco*RV, separated by gel electrophoresis, transferred to a nylon membrane (GE Healthcare), and probed with gene-specific (*pcpB4*, *parB*, *cpb2*), *ermB*, and *catP* (TargeTron vector backbone) PCR amplified Digoxigenin (DIG)-labelled probes. All DIG-labelled probes were prepared using a random labelling PCR method according to the manufacturer's instructions (Roche). All primers used to construct DIG-labelled probes are listed in Table S2.1. Hybridised probes

were detected using the CDP-star (Roche) detection system according to the manufacturer's instructions.

Pulsed-field gel electrophoresis (PFGE). Single colonies of the donor, recipient and transconjugants were subcultured from appropriate selective agar into BHI broth and grown to an OD_{600} of 1 before being centrifuged at 1575 × g for 5 minutes. Cell pellets were then washed in 10 ml of PIV buffer (10 mM Tris-HCl pH 7.6, 1M NaCl) before being centrifuged at 1575 × g for 5 minutes. Cell pellets were resuspended in 0.9 ml of PIV and mixed with 1 ml of 1.5% low melting temperature agarose (BioRad) before being aliquoted into pulse-field plug moulds. Once the plugs had set, they were treated in lysis buffer and proteinase K buffer, as previously described (33), before storage in 1×TE until use. PFGE was performed using a 1 % agarose gel (PFGE grade agarose, BioRad) using the CHEF-DR III pulse field gel electrophoresis system (BioRad) and 0.5 × Tris-borate-EDTA (TBE) buffer at 14 °C. The electrophoresis parameters were as follows: pulse 1-5s voltage, 6 V/cm, 4 hours. Low-range PFG markers (NEB) were included as size standards. Upon completion of electrophoresis, gels were post-stained using Gel Red (Biotium) and imaged using UV-light with the ChemiDoc XRS+ System (BioRad).

Bioinformatics analysis. Amino acid and nucleotide sequence alignments of pCS1-1 (Accession No.: LN679999.1), pCP13 (Accession No.: AP003515.1), pCP-OS1 (Accession No.: NC_023917.1), pCP-TS1 (Accession No.: NC_023918.1), pJFP55H (Accession No.: NZ_CP013043.1) and pBCNF5603 (Accession No.: NC_006872.1) were conducted using the CLUSTALΩ web tool (34). All genes within the Pcp conjugation locus were also analysed with BLAST and compared to the NCBI databases (35,36). Nucleotide (nt) and amino acid (aa) sequence alignment figures were constructed using EasyFig (37) and Blast Ring Image Generator (BRIG) (38).

TargeTron mutagenesis. The pCP13 genes *cpb2*, *pcpB4* and *parB* were insertionally inactivated using TargeTron mutagenesis (29,39). Insertion sites were identified using the Perutka Algorithm and Targetronics LLC web-based design tools (40). Appropriate group II intron insertion sites were chosen for each gene: *cpb2* (348/349 bp sense strand), *parB* (365/366 bp antisense), *pcpB4* (1728/1729 bp antisense). The TargeTron vector pJIR3566 was retargeted to each target site using splice overlap extension (SOE) PCR with retargeting oligonucleotides, as previously described (29). The 350 bp retargeted products were cloned into the *Hin*dIII/*Bsr*GI site of pJIR3566. Retargeted plasmids were introduced into the *C. perfringens* strain JIR325, which carries pCP13, *via* electroporation. Cm resistant transformants were subcultured twice onto NA containing Em and cross cultured onto NA containing Cm to detect loss of the TargeTron vector. Em^RCm^S mutants were screened for the correct TargeTron insertion using PCR and were confirmed by Southern hybridisation (data not shown).

pcpB4 complementation vector construction. The *pcpB4* and the *cstB4* mutants were complemented and cross-complemented *in trans* by introduction of appropriate complementation vectors. The *cstB4* complementation vector was constructed previously (23). In this study, *pcpB4* complementation vectors were constructed as described before (23,30,41). Briefly, the *pcpB4* gene was amplified using primers that included *Sac*I and *Bam*HI restriction endonuclease recognition sites, to produce a ~2 kb PCR product. This PCR product was cloned into the *Bam*HI/*Sac*I sites of pRPF185 (30) and the sequence confirmed, resulting in the construction of the complementation vector pDLL213. The *pcpB4* gene in this vector was under the control of an AnTc-inducible promoter (P_{tet}). The plasmids pDLL213, pDLL212 (*cstB4* complementation vector) and the pRPF185 vector control were introduced separately into the *pcpB4* and *cstB4* mutants using electroporation (32) or RP4-mediated conjugation from an *E. coli* donor containing pVS520, (27), respectively.

Construction of a plasmid-free recipient strain. A suitable recipient strain was constructed by insertionally inactivating the *parB* partitioning gene of pCP13 in the Rif^R Nal^R derivative of strain 13, JIR325, with an Em resistance determinant. The mutants were then passaged in non-selective broth twice a day for four days. On the final day the cultures were serially diluted and plated onto non-selective media and the resulting colonies were cultured onto media containing either Em or no selection. Em sensitive colonies were isolated and confirmed to be plasmid free using PCR for *parB* and *cpb2*, as well as *via* PFGE and Southern hybridisation with DIG-labelled *pcpB4* and *ermB* probes (Figure S2.1). This plasmid-free strain was designated JIR13211.

Conjugation assays. *C. perfringens* conjugative transfer assays were conducted as follows. Single colonies of each strain were subcultured into pre-boiled FTG broth (6 ml) and incubated for 6 hours at 37°C, to an optical density (OD_{600}) of approximately 1. A 100 µl sample of the donor was mixed with 400 µl of recipient and centrifuged at 17, 000 × g for 2 minutes and cell pellets were resuspended in 100 µl of BHI diluent (BHI (Oxoid) broth diluted 1:5 with dH_20) and spread onto BHI agar. Aliquots (100 µl) of the donor and recipient strains also were plated individually onto BHI agar as controls. These cultures were incubated for 20 hours at 37°C before the growth was resuspended in 3 ml of BHI diluent. These cells were diluted and plated onto NA supplemented with Em or Sm and Chl, or all three antimicrobials, before incubation under anaerobic conditions at 37 °C for 20 hours. The transfer frequency was calculated as the number of transconjugants per donor cell and all data were subjected to Mann-Whitney U statistical tests. The average limit of detection for *pcpB4* mutant transfer frequency was (4.27×10^{-10} transconjugants/donor cell). The limit of detection was calculated by determining the lowest theoretical transfer frequency for each independent mating and taking the average of these values.

Secondary matings were conducted in the same manner, but the diluted cells were plated onto NA supplemented with Em, or NA supplemented Em and Cm. Mutants, complemented mutants and cross-complemented mutants were mated with the same plasmid free Sm^RChl^R recipient, JIR13467, but AnTc (50 ng/ml) was added to the mating plates to induce expression of the wild-type and *P. sordellii* genes that were under the control of the AnTc-inducible promoter (P_{tet}). Donor, recipient and transconjugant plasmid profiles were confirmed using PFGE and Southern hybridisation.

Barrier matings were conducted as outlined above, however, a 0.45 µm filter was placed between the donor (plated on the agar) and the recipient (plated on the filter). After overnight incubation at 37°C under anaerobic conditions the bacteria on the recipient side (the side facing away from the agar) of the filter were isolated and transconjugants were selected as before. Transfer was also assessed in the presence of DNase I by supplementation of the BHI mating media with 1 mg/ml of DNase I (Sigma-Aldrich). Broth matings were conducted by inoculation of individual 20 ml BHI broth cultures with a single colony of either donor or recipient before incubation at 37°C overnight. These cultures were diluted 1:20 in fresh BHI and grown to an OD_{600} of 1. The donor and recipient cultures were mixed in a ratio of 1:4 in 20 ml of fresh BHI broth and grown for 3 hours at 37°C before being diluted and plated onto agar to select for transconjugants as outlined above. *P. sordellii* conjugative transfer assays were conducted as previously described (23).

Results

pCP13 has a putative conjugation locus that is conserved in other pCP13-like plasmids

pCP13 was thought to be non-conjugative as its initial annotation did not reveal the presence of any known conjugation homologues (6) and the transfer capacity of this plasmid had not been tested. However, we showed recently that the Cst conjugation locus from the *P. sordellii*

toxin plasmid pCS1-1 encodes proteins with low level aa sequence identity to several putative pCP13 gene products (23) (Figure 2.1a), which suggested that pCP13 may also have a conjugation locus. To examine this hypothesis, pCP13 was re-annotated using tBLASTx with a particular focus on genes that had similarity with *cst* genes (Table 2.2). The results showed that several predicted gene products had domains similar to those found in known conjugation proteins from the *Agrobacterium* and *Enterococcus* Vir and Tra conjugation systems (Figure 2.1b) (Table 2.2).

We designated this 27 kb locus as the pCP13 *Clostridium perfringens* (Pcp) transfer locus and designated each gene within this region as *pcpA* to *pcpT*, which is consistent with the original gene order and nomenclature (6). Predicted proteins with domains similar to existing conjugation proteins were designated using the *Agrobacterium tumefaciens* Ti plasmid nomenclature, as suggested for plasmid annotation nomenclature (42). For example, we have now designated the *pcp_51* gene product as PcpD4, based on its similarity to the CstD4 homologue from *P. sordellii* and conserved ATPase domains from other VirD4 homologues (23).

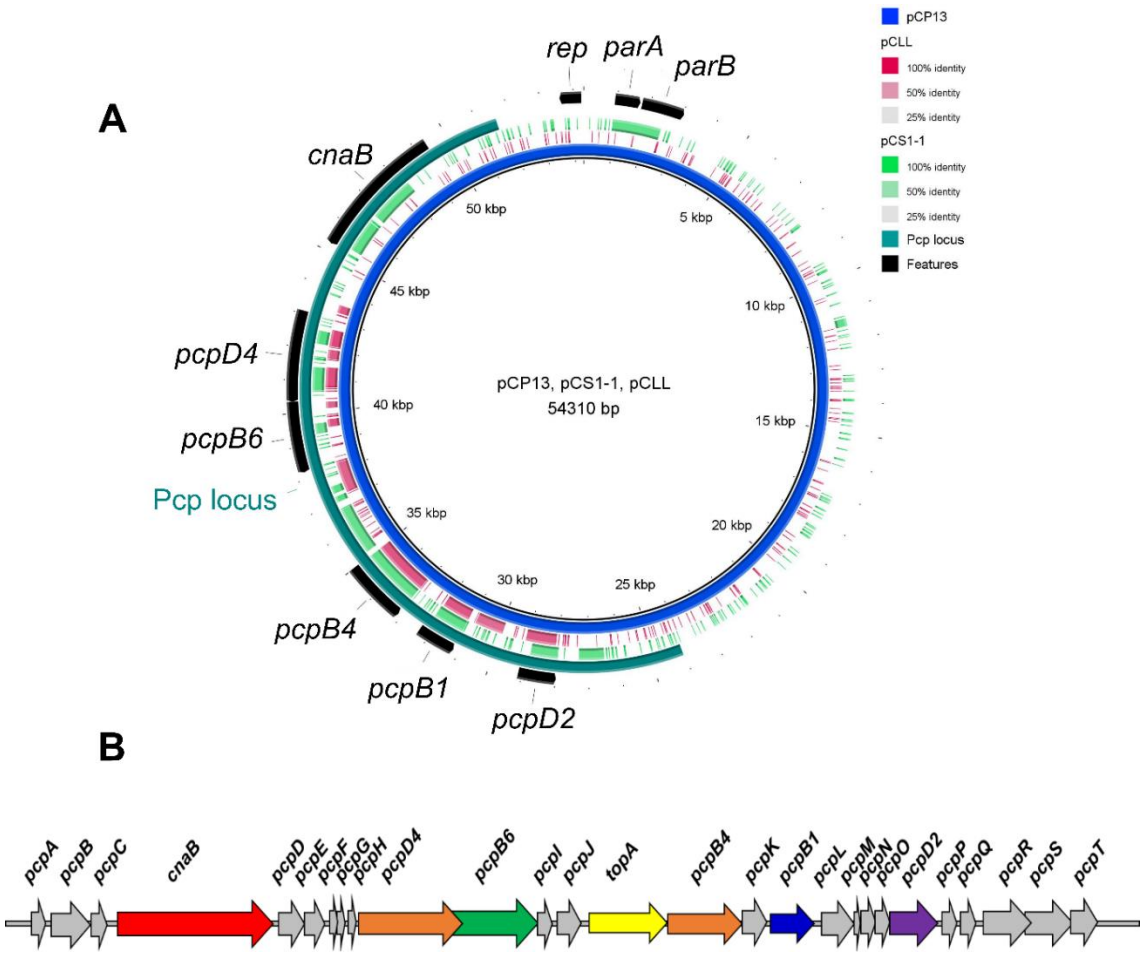

Figure 2.1. Comparative analysis of pCP13 plasmids. The sequences of pCP13 (blue), pCLL from *C. botulinum* (red) and pCS1-1 from *P. sordellii* (green) were analysed using BRIG (38). Solid colour reflects 100% nt identity, fainter colours indicate between 50% and 80% nt identity and grey features indicate less than 50% identity. The absence of a solid colour reflects a region lower than the similarity threshold of 25%. Conserved genes of interest including *rep*, *parA*, *parB* and putative conjugation homologues (*pcpB4*, *pcpB6*, *pcpD4*, *pcpB1*, *pcpD2* and *cnaB*) are marked on the outside of the rings in black. **B** Genetic organisation of the putative pCP13 conjugation locus. Coloured arrows indicate genes with potential roles in conjugation. Orange arrows indicate putative ATPase encoding genes (*virB4* and *virD4* homologues), red denotes *cna*, a potential collagen adhesion encoding gene, blue denotes a putative *tcpG* peptidoglycan hydrolase homologue, purple indicates a putative relaxase gene, green denotes a putative *virB6* homologue and yellow indicates the putative *topA* topoisomerase gene. Genes shown in grey are hypothetical.

Table 2.2. Reannotation of pCP13 ORFs

ORF (original)	Gene name	Nucleotide position (nt)	Size (bp) (orientation)	Annotation/Putative function
PCP01	*parA*	940…1692	753(+)	Type I partitioning system ATPase
PCP02	*parB*	1751…3031	1281(+)	Type I partitioning system centromere binding protein
PCP03	-	3147…3509	363(+)	Hypothetical
PCP04	-	3773…4024	252(+)	Putative transposase
PCP05	-	4040…4222	183(+)	Putative transposase
PCP06	-	4588…4746	159(+)	Putative transposase
PCP07	-	5169…5804	636(-)	Putative ABC transporter
PCP08	-	5804…7966	2163(-)	Putative bacteriocin immunity protein
PCP09	-	8043…8354	312(-)	Hypothetical
PCP10	-	8779…9012	234(+)	Putative transposase
PCP11	-	9127…9366	240(+)	Putative transposase
PCP12	-	9488…9973	486(-)	Hypothetical with SMC_N superfamily domain
PCP13	-	10102…10281	180(-)	Hypothetical
PCP14	-	10439…11113	675(-)	Hypothetical
PCP15	*resP*	11317…11886	570(+)	Serine Recombinase/resolvase (ResP)
PCP16	-	12101…13366	1266(+)	Hypothetical
PCP17	*cpb2*	13654…14451	798(+)	Consensus Cpb2 toxin
PCP18	-	14479…15123	645(-)	Hypothetical
PCP19	-	15135…15449	315(-)	PadR family transcriptional regulator
PCP20	-	16008…16232	225(+)	Hypothetical

PCP21	-	16323…16760	438(+)	RadC
PCP22	-	16820…17137	318(+)	Hypothetical
PCP23	-	17161…17484	324(+)	Hypothetical with NADH hydrogenase domain
PCP24	-	17739…17942	204(+)	Hypothetical
PCP25	-	18016…18405	390(+)	Hypothetical
PCP26	-	18575…19642	1068(+)	Hypothetical
PCP27	-	19722…19919	198(+)	HicA toxin (type II toxin-antitoxin system)
PCP28	-	19969…20385	417(+)	HicB antitoxin
PCP29	-	20737…21495	759(+)	Hypothetical
PCP30	-	21612…22625	1014(+)	Hypothetical
PCP31	-	22653…23123	471(+)	Hypothetical
PCP32	-	23328…23513	186(+)	Resolvase/invertase
PCP33	-	23553…23795	243(+)	Hypothetical
PCP34	*pcpT*	24051…24548	498(-)	Hypothetical
PCP35	*pcpS*	24604…25965	1362(-)	Hypothetical
PCP36	*pcpR*	25.943…27403	1461(-)	ImmA/IrrE family metallo-endopeptidase
PCP37	*pcpQ*	27506…27670	165(-)	Hypothetical
PCP38	*pcpP*	27747…27965	219(-)	Hypothetical
PCP39	*pcpD2*	27983…29116	1134(-)	Putative relaxase
PCP40	*pcpO*	29119…29526	408(-)	Hypothetical
PCP41	*pcpN*	29533…29799	267(-)	Hypothetical
PCP42	*pcpM*	29800…30003	204(-)	Hypothetical
PCP43	*pcpL*	30127…31041	915(-)	Hypothetical
PCP44	*pcpB1*	31168…32331	1164(-)	Putative peptidoglycan hydrolase

PCP45	*pcpK*	32417…33106	690(-)	Hypothetical
PCP46	*pcpB4*	33111…35009	1899(-)	VirB4-like ATPase
PCP47	*topA*	35027…37138	2112(-)	Topoisomerase III
PCP48	*pcpJ*	37182…37826	645(-)	Hypothetical
PCP49	*pcpI*	37937…38218	282(-)	Hypothetical
PCP50	*pcpB6*	38221…40350	2130(-)	VirB6-like
PCP51	*pcpD4*	40347…43088	2742(-)	VirD4-like coupling protein
PCP52	*pcpH*	43075…43287	213(-)	Hypothetical
PCP53	*pcpG*	43355…43591	237(-)	Hypothetical
PCP54	*pcpF*	43655…43849	195(-)	Hypothetical
PCP55	*pcpE*	43842…44300	459(-)	Spo0A-homologue
PCP56	*pcpD*	44413…45009	597(-)	Sortase
PCP57	*cnaB*	45255…49361	4107(-)	Collagen adhesion protein
PCP58	*pcpC*	49506…49856	351(-)	PemK toxin (type II toxin-antitoxin system)
PCP59	*pcpB*	49980…51053	1074(-)	Hypothetical
PCP60	*pcpA*	51099…51584	486(-)	Helix-turn-helix containing DNA-binding regulatory protein
PCP61	*regC*	51897…53000	1104(+)	LexA-like transcriptional regulator, similar to RegC from pCW3
PCP62	-	53114…53560	447(+)	Hypothetical
PCP63	*rep*	53589…183	651(-)	pCP13 replication protein (21)

(-) antisense, (+) sense

Several key putative conjugation proteins were identified in pCP13 (Figure 2.1B and Table S2.2) including a putative coupling protein (PcpD4), a putative conjugation-specific ATPase (PcpB4), a membrane binding protein with similarity to CstB6 (PcpB6), a putative peptidoglycan hydrolase with similarity to CstB1 and TcpG from pCW3 (PcpB1), a putative relaxase (PcpD2), a topoisomerase (TopA) and a Collagen binding protein (CnaB) (Table S2.2). The key homologues in this locus only had very low-level similarity (16-21% aa identity) with proteins encoded by the well-characterised Tcp locus from the pCW3-family plasmids, with the exception of TcpG and CnaB (48% and 69% aa identity, respectively), suggesting that the Pcp locus represents a distinct, and therefore novel, *C. perfringens* conjugation system (11,23).

Comparative analysis using BLAST ring image generator (BRIG) software was used to examine the similarity between pCP13 and other members of this family of *C. perfringens* plasmids; specifically two plasmids, pCP-TS1 and pCP-OS1, that encode the recently identified binary enterotoxin BEC (19), a cryptic plasmid pJFP55H from a NetF$^+$ strain, JFP55 (43), and a bacteriocin encoding plasmid, pBCNF5603, from the enterotoxin-producing *C. perfringens* type F isolate F5603 (19,21,43). The Pcp locus was highly conserved in pCP-TS1 and pCP-OS1 (98% nt identity), including all the putative conjugation machinery homologues (*pcpB6*, *pcpB4*, *pcpD4, pcpB1* and *pcpD2*), suggesting that these plasmids may be conjugative (Figure 2.2, Table S2.2). pJFP55H also encoded these conjugation homologues (Figure 2.2), but with lower aa sequence identity (Table S2.2). By contrast, the pBCNF5603 sequence had only limited homology to pCP13, with similarity in the replication region, conserved hypothetical genes and an adjacent putative *pcpD2* relaxase gene, which suggests that this plasmid is non-conjugative, but may be able to be mobilised by pCP13-family plasmids.

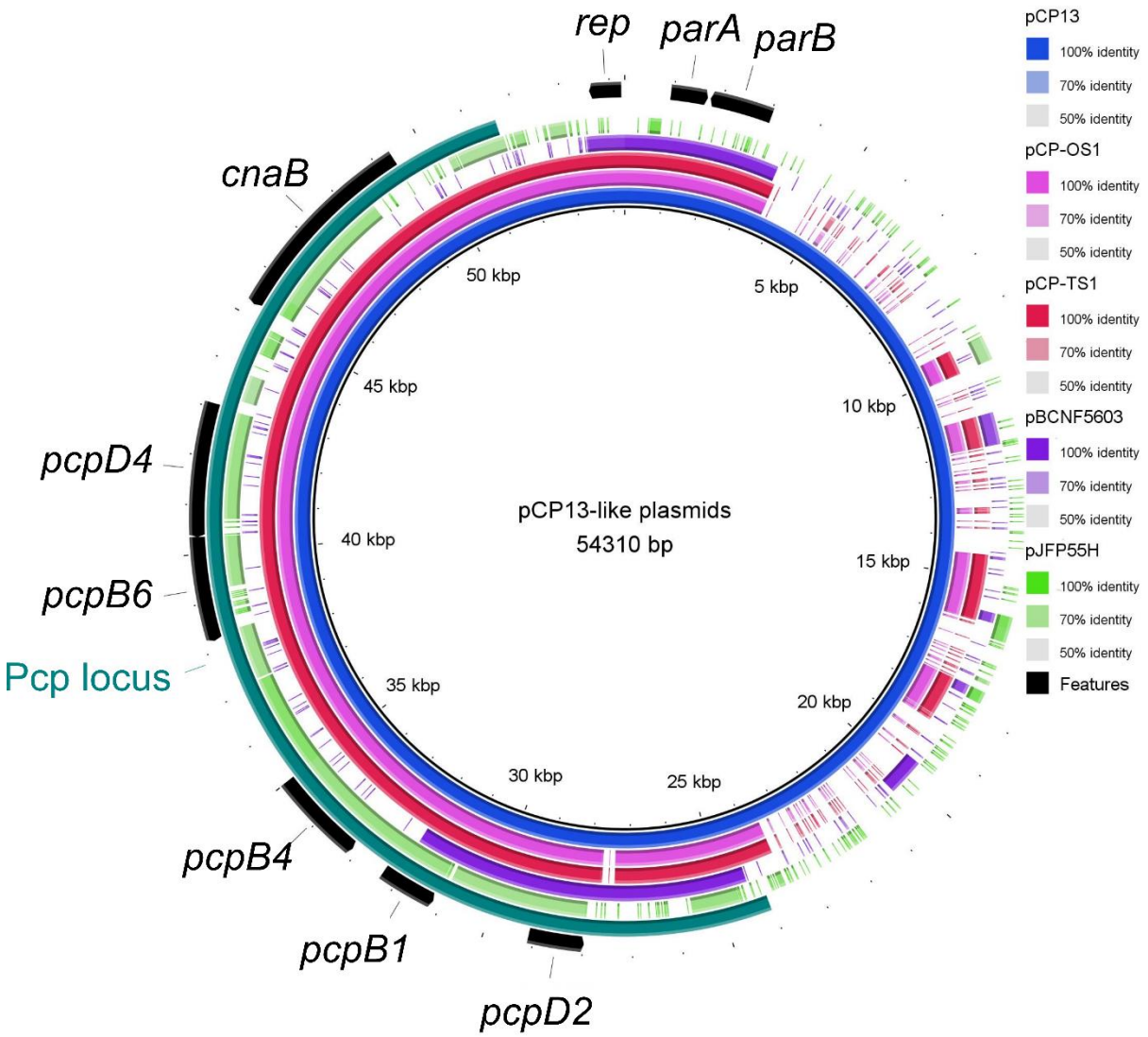

Figure 2.2. Nucleotide sequence alignment of pCP13-like plasmids shows the presence of conserved putative conjugation loci: The sequences of pCP13 (blue), the *becAB*-encoding plasmids pCP-OS1 (pink) and pCP-TS1 (red), the bacteriocin plasmid pBCNF5603 (purple), and the cryptic plasmid pJFP55H (green), were aligned using BRIG (38). Solid colour reflects 100% nt identity, fainter colour indicates between 50% and 70% nt identity, grey features indicate less than 50% nt identity and absence of a solid colour reflects a region lower than the similarity threshold. The Pcp locus is indicated by the teal arc. Conserved genes of interest *rep*, *parA*, *parB* and putative conjugation homologues (*virB4*, *virB6*, *virD4*, hydrolase, relaxase and *cna*) are indicated in black.

Previously in pCS1-1, pCLL and pCP13 we identified a putative conserved *oriT* sequence that had a similar genetic structure to *oriT* from the Mob_{MG} relaxase-encoding plasmid pWBG749 from *Staphylococcus aureus* (23,44). Using this pCP13 *oriT* sequence as a reference point, we identified a comparable relaxase region, complete with a conserved 67 bp *oriT* sequence, in pCP-OS1, pCP-TS1, pBCNF5603 and pJFP55H (Figure 2.3). This *oriT* sequence was structurally conserved and contained all the elements previously described for pCS1-1 and the conjugative *S. aureus* plasmids pWBG749 including three inverted repeats (IRs) and a conserved core region, which contains the site that is nicked by the relaxase (23,44). The *oriT* sequences of pCP-OS1 and pCP-TS1 were closely related to *oriT* from pCP13 (98% nt identity), whereas the pJFP55H and pBCNF5603 *oriT* sequences (79-80% nt identity) were more divergent, but more related to each other (92% nt identity). The major difference between the pBCNF5603/pJFP55H and pCP13 *oriT* sites was in the sequence of IR2 (Figure 2.3). IR2 is a specificity factor that is associated with distinct *oriT* families of different mobilisable staphylococcal plasmids (44), suggesting that pCP13-like and pBCNF5603 plasmids may represent distinct *oriT* families.

pCP13 is conjugative:

To assess the conjugative potential of pCP13, a genetically marked derivative was constructed using TargeTron mutagenesis. The *cpb2* toxin gene of pCP13 was insertionally inactivated with a group II intron containing an *ermB* resistance determinant to yield the strain JIR13270. *cpb2* was chosen for inactivation as it is located outside of the putative conjugation locus and has no known function in plasmid replication, regulation, stability or transfer. Therefore, its inactivation was unlikely to confound the results of the conjugation assays.

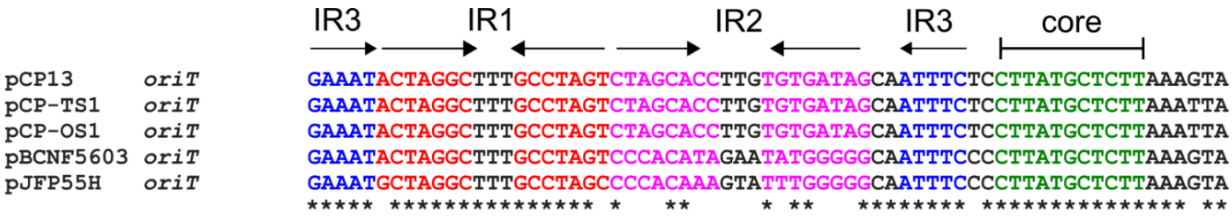

Figure 2.3. pCP13-like *oriT* sites are conserved. The *oriT* sequences of the *C. perfringens* pCP13-like plasmids were aligned using Clustal Omega. Inverted repeat (IR) 1 shown in red, IR2 shown in pink, IR3 is shown in blue and the core region is shown in green. Asterisks indicate identical sequences.

A suitable isogenic plasmid-free recipient strain was constructed by insertionally inactivating the *parB* gene of pCP13 in JIR325 and screening for a derivatve that no longer carried the resultant unstable plasmid. To produce a suitable conjugation recipient, a spontaneous chromosomal Sm^RChl^R mutant of this plasmid-free strain JIR13211 [or JIR325(pCP13)$^-$] was selected by passage on medium containing streptomycin and potassium chlorate, as before (25). The resultant mutant, JIR13647, was used as a recipient in subsequent mating assays. JIR13270 (JIR325pCP13*cpb2*ΩTT*ermB*) was used as a donor in conjugation assays with the recipient strain, JIR13467, selecting for $Em^RSm^RChl^R$ transconjugants. The results showed that Em resistance was transferable on solid media at a transfer frequency of 2.1×10^{-1} transconjugants/donor (Figure 2.4). As expected, no colonies were observed with the donor or recipient strains alone on the selective media. Transfer of pCP13*cpb2*ΩTT*ermB* was confirmed by PFGE and subsequent Southern hybridisation (Figure S2.1). When these blots were probed with *ermB*-specific (insertion specific) or *pcpB6*-specific (pCP13 specific) probes a 54 kb band corresponding to pCP13 was observed in the donor cells and transconjugants, but not the recipient cells. Larger molecular weight bands present on the gel most likely corresponded to the open circular or supercoiled forms of the plasmid as the plasmid was not linearized before electrophoresis.

The transconjugants were able to act as donors in subsequent matings as shown by the transfer of Em resistance from the JIR13467-derived pCP13*cpb2*Ω*ermB* transconjugants to the Cm^R JIR13211 derivative, JIR13677 (Figure S2.2). Subsequent experiments showed that pCP13 transfer was DNase I independent (Figure S2.3) and required cell to cell contact, as a 0.45 µm filter placed between donor and recipient abrogated transfer (data not shown). These results provided evidence that plasmid transfer was mediated by conjugation. In addition, matings conducted in BHI broth yielded no transconjugants, suggesting that contact on a solid surface was required for conjugative pCP13 transfer, as it is for transfer of pCW3 (45) (Figure S2.3).

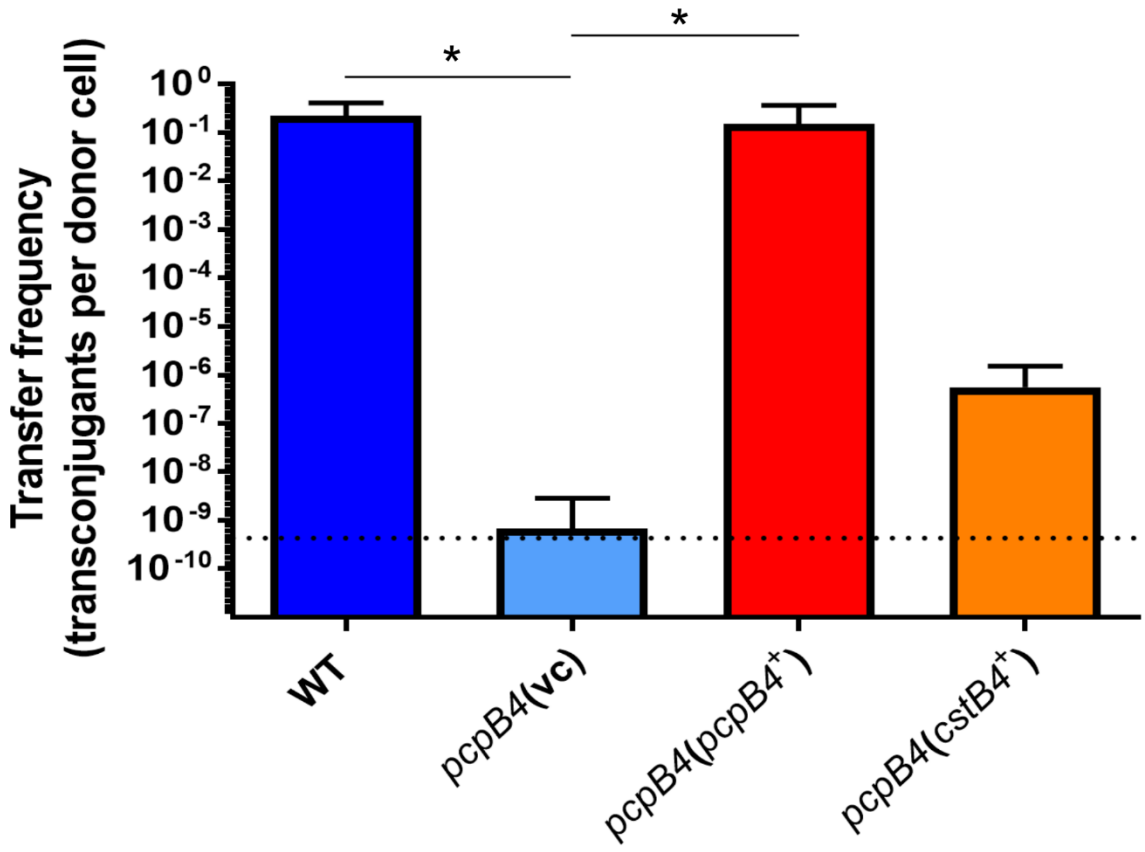

Figure 2.4. Conjugative transfer of pCP13 was abrogated upon mutation of *pcpB4* and restored upon complementation *in trans*. Transfer of pCP13 derivatives was assessed using a series of mixed plate matings with the plasmid-free recipient JIR13467. The transfer frequency was calculated as transconjugants per donor cell. Each donor is labelled on the X-axis, WT is the pCP13*cpb2*Ω*ermB* mutant, *pcpB4*(vc) is the *pcpB4* mutant with the vector control (vc) pRPF185, *pcpB4*(*pcpB4*$^{+}$) is the *pcpB4* mutant complemented with the wild-type *pcpB4* gene and *pcpB4*(*cstB4*$^{+}$) is the *pcpB4* mutant complemented with the *cstB4* gene. The recipient in all cases was JIR13467. Mann-Whitney U test n= 10, Mean ± SD, *p<0.05, average limit of detection (4.27 ×10^{-10} transconjugants/donor) indicated by the dotted line.

Mutation of *pcpB4* abrogates transfer

To examine whether the Pcp conjugation locus was responsible for the transfer of pCP13, the *virB4* homologue, *pcpB4*, was insertionally inactivated with an Em resistance determinant, as before. The resultant plasmid, pCP13*pcpB4*Ω*ermB*, could no longer encode its own transfer (6.9×10^{-9} transconjugants/donor cell) into the JIR13467 recipient (Figure 2.4). To complement the *pcpB4* mutation, the wild-type *pcpB4* gene was cloned into pRPF185 (30,46), so that its expression was induced by the addition of AnTc to the mating media, which did not affect the transfer frequency of the wild-type pCP13 plasmid (Figure S2.3). The results showed that complementation *in trans* with the wild-type *pcpB4* gene, restored the conjugation frequency of the mutant *pcpB4* plasmid to wild-type levels (Figure 2.4).

Cross-complementation of conjugation mutants with *P. sordellii* conjugation machinery partially restores transfer

The *C. perfringens* PcpB4 protein and the *P. sodellii* CstB4 protein have 53% aa sequence identity. Previously, we (23) constructed a *cstB4* mutant in the plasmid pCS1-1, which eliminated conjugative transfer in *P. sordellii*. This mutation could be complemented *in trans* with a wild-type *cstB4* gene, restoring the conjugation frequency to wild-type levels.

Here we have attempted to cross-complement the *pcpB4* and *cstB4* mutants with both the *P. sordellii* and *C. perfringens* homologues. The *pcpB4* and *cstB4* complementation vectors were introduced into the equivalent *C. perfringens* and *P. sordellii* mutants *via* transformation or RP4-mediated conjugation, respectively. Cross-complementation of the *C. perfringens pcpB4* mutant with *cstB4 in trans* appeared to partially restore conjugative transfer (Figure 2.4), however, this result was not statistically significant. In ten independent matings, the plasmid was observed to transfer at low levels in only four biological replicates. Cross-complementation of the *P. sordellii cstB4* mutant with *pcpB4 in trans* did not restore conjugative transfer of the *P. sordellii* plasmid. The transfer frequency of pCS1-1 is much lower

than pCP13 (10^{-1} transconjugants/donor compared to 10^{-5} transconjugants/donor)(23), therefore any cross-complementation of *cstB4* mutants with *pcpB4* may have been below the limit of detection.

Discussion

Conjugative transfer is a key driver of the dissemination of toxin genes and resistance determinants in the clostridia (11,47,48). In *C. perfringens*, many of the toxins that are intimately involved in the production of disease are encoded on large pCW3-like plasmids, many of which have been experimentally shown to be conjugative (9,10,45,49,50). The Tcp conjugation locus harboured by these plasmids has been well characterised both genetically and biochemically, leading to a greater understanding of the mechanism of conjugative transfer in *C. perfringens* (11).

In this study, we have expanded the *C. perfringens* conjugative plasmid lexis. We have shown that the beta2 toxin-encoding plasmid, pCP13, is a representative of a novel family of conjugative toxin plasmids in *C. perfringens*. Genetically marked pCP13 derivatives were readily transferable at high frequency similar to that of the pCW3 family (ca. 10^{-1} transconjugants/donor cell). By contrast, related plasmids in other clostridia, pCS1-1 and pCLL, transfer at much lower frequencies (ca. 10^{-5}-10^{-7} transconjugants/donor cell) (22,23). Transfer of pCP13 was DNase I resistant and required cell to cell contact, indicating that transfer of pCP13 occurred *via* conjugation.

Reannotation of the pCP13 nucleotide sequence revealed several putative conjugation related genes arranged into a Cst-like locus that we have designated the Pcp locus. The results presented here have provided evidence that the Pcp locus was responsible for the ability of pCP13 to encode its own conjugative transfer since mutation of the conjugation-related ATPase encoding gene, *pcpB4,* abrogated plasmid transfer (Figure 2.4). This phenotype was

rescued upon reintroduction of the *pcpB4* gene *in trans*. PcpB4 had only 18% aa sequence identity to the pCW3 accessory ATPase TcpF, however, it is more closely related to CstB4 from pCS1-1 (52% aa identity), which is required for the conjugative transfer of pCS1-1 (23). Cross-complementation of *pcpB4* and *cstB4* mutants with their respective homologues did not restore conjugative transfer to a significant level. Therefore, it appears that these conjugation loci represent an ancestral, evolutionarily conserved clostridial conjugation system compared with the Tcp conjugation locus of pCW3, which is only found in *C. perfringens* (4).

The Pcp locus appears to encode all of the components necessary for a Gram-positive conjugation apparatus, except for a VirB8 homologue. VirB8 proteins are integral membrane proteins that act as a scaffold for the formation of the mating-pore (51,52). These proteins generally have an N-terminal transmembrane domain (53). The only putative gene products with an N-terminal transmembrane domain large enough to constitute a VirB8 homologue in pCP13 and pCS1-1 are PcpL and CstL, respectively (23). Examination of their aa sequences did not reveal conserved VirB8 domains. However, these proteins may still have structural similarity to VirB8 proteins, as was observed for TcpC from pCW3 and TraM from the *Enterococcus* plasmid pIP501. These proteins were only identified as VirB8 homologues once their crystal structure was determined (13,52).

In conclusion, we have identified a new family of conjugative toxin plasmids in *C. perfringens*, changing the previously accepted paradigm that the pCW3 Tcp system is the only functional conjugation system in this important pathogen. Examination of the carriage and composition of the Pcp locus in other members of the pCP13-like family revealed that the BEC toxin-encoding plasmids pCP-OS1 and pCP-TS1 encoded an almost identical conjugation locus to pCP13 (98% nt sequence identity with pCP13, Figure 2.2), with the key conjugation proteins also similar to those of pCP13 (Table S2.2). The findings of this study have significant implications for the dissemination of virulence factors and toxin genes in *C. perfringens*,

especially the BEC toxin, which has been linked with cases of severe *C. perfringens* food-poisoning in Japan (19,20).

Acknowledgements

This research was supported by grants GNT1104502 from the National Health and Medical Research Council and DP160102680 from the Australian Research Council. TDW was supported by the Australian Government Research Training Program.

References

1. Uzal, F.A., Freedman, J.C., Shrestha, A., Theoret, J.R., Garcia, J., Awad, M.M., Adams, V., Moore, R.J., Rood, J.I. and McClane, B.A. (2014) Towards an understanding of the role of *Clostridium perfringens* toxins in human and animal disease. *Future Microbiology*, **9**, 361-377.
2. Wade, B., Keyburn, A.L., Haring, V., Ford, M., Rood, J.I. and Moore, R.J. (2016) The adherent abilities of *Clostridium perfringens* strains are critical for the pathogenesis of avian necrotic enteritis. *Vet. Microbiol.*, **197**, 53-61.
3. Timbermont, L., Haesebrouck, F., Ducatelle, R. and Van Immerseel, F. (2011) Necrotic enteritis in broilers: an updated review on the pathogenesis. *Avian Pathol.*, **40**, 341-347.
4. Li, J., Adams, V., Bannam, T.L., Miyamoto, K., Garcia, J.P., Uzal, F.A., Rood, J.I. and McClane, B.A. (2013) Toxin plasmids of *Clostridium perfringens*. *Microbiol. Mol. Biol. Rev.*, **77**, 208-233.
5. Garnier, T. and Cole, S.T. (1988) Studies of UV-inducible promoters from *Clostridium perfringens* in vivo and in vitro. *Mol. Microbiol.*, **2**, 607-614.
6. Shimizu, T., Ohtani, K., Hirakawa, H., Ohshima, K., Yamashita, A., Shiba, T., Ogasawara, N., Hattori, M., Kuhara, S. and Hayashi, H. (2002) Complete genome

sequence of *Clostridium perfringens*, an anaerobic flesh-eater. *Proc Natl Acad Sci U S A*, **99**, 996-1001.

7. Bannam, T.L., Teng, W.L., Bulach, D., Lyras, D. and Rood, J.I. (2006) Functional identification of conjugation and replication regions of the tetracycline resistance plasmid pCW3 from *Clostridium perfringens*. *J. Bacteriol.*, **188**, 4942-4951.
8. Adams, V., Han, X., Lyras, D. and Rood, J.I. (2018) Antibiotic resistance plasmids and mobile genetic elements of *Clostridium perfringens*. *Plasmid*.
9. Bannam, T.L., Yan, X.X., Harrison, P.F., Seemann, T., Keyburn, A.L., Stubenrauch, C., Weeramantri, L.H., Cheung, J.K., McClane, B.A., Boyce, J.D. *et al.* (2011) Necrotic enteritis-derived *Clostridium perfringens* strain with three closely related independently conjugative toxin and antibiotic resistance plasmids. *MBio*, **2**, e00190-00111.
10. Parreira, V.R., Costa, M., Eikmeyer, F., Blom, J. and Prescott, J.F. (2012) Sequence of two plasmids from *Clostridium perfringens* chicken necrotic enteritis isolates and comparison with *C. perfringens* conjugative plasmids. *PLOS One*, **7**, e49753.
11. Wisniewski, J.A. and Rood, J.I. (2017) The Tcp conjugation system of *Clostridium perfringens*. *Plasmid*, **91**, 28-36.
12. Traore, D.A.K., Wisniewski, J.A., Flanigan, S.F., Conroy, P.J., Panjikar, S., Mok, Y.F., Lao, C., Griffin, M.D.W., Adams, V., Rood, J.I. *et al.* (2018) Crystal structure of TcpK in complex with *oriT* DNA of the antibiotic resistance plasmid pCW3. *Nature Communications*, **9**, 3732.
13. Porter, C.J., Bantwal, R., Bannam, T.L., Rosado, C.J., Pearce, M.C., Adams, V., Lyras, D., Whisstock, J.C. and Rood, J.I. (2012) The conjugation protein TcpC from *Clostridium perfringens* is structurally related to the type IV secretion system protein VirB8 from Gram-negative bacteria. *Mol. Microbiol.*, **83**, 275-288.
14. Parsons, J.A., Bannam, T.L., Devenish, R.J. and Rood, J.I. (2007) TcpA, an FtsK/SpoIIIE homolog, is essential for transfer of the conjugative plasmid pCW3 in *Clostridium perfringens*. *J. Bacteriol.*, **189**, 7782-7790.

15. Steen, J.A., Bannam, T.L., Teng, W.L., Devenish, R.J. and Rood, J.I. (2009) The putative coupling protein TcpA interacts with other pCW3-encoded proteins to form an essential part of the conjugation complex. *J. Bacteriol.*, **191**, 2926-2933.

16. Bantwal, R., Bannam, T.L., Porter, C.J., Quinsey, N.S., Lyras, D., Adams, V. and Rood, J.I. (2012) The peptidoglycan hydrolase TcpG is required for efficient conjugative transfer of pCW3 in *Clostridium perfringens*. *Plasmid*, **67**, 139-147.

17. Wisniewski, J.A., Teng, W.L., Bannam, T.L. and Rood, J.I. (2015) Two novel membrane proteins, TcpD and TcpE, are essential for conjugative transfer of pCW3 in *Clostridium perfringens*. *J. Bacteriol.*, **197**, 774-781.

18. Wisniewski, J.A., Traore, D.A., Bannam, T.L., Lyras, D., Whisstock, J.C. and Rood, J.I. (2016) TcpM: a novel relaxase that mediates transfer of large conjugative plasmids from *Clostridium perfringens*. *Mol. Microbiol.*, **99**, 884-896.

19. Yonogi, S., Matsuda, S., Kawai, T., Yoda, T., Harada, T., Kumeda, Y., Gotoh, K., Hiyoshi, H., Nakamura, S., Kodama, T. *et al.* (2014) BEC, a novel enterotoxin of *Clostridium perfringens* found in human clinical isolates from acute gastroenteritis outbreaks. *Infect. Immun.*, **82**, 2390-2399.

20. Irikura, D., Monma, C., Suzuki, Y., Nakama, A., Kai, A., Fukui-Miyazaki, A., Horiguchi, Y., Yoshinari, T., Sugita-Konishi, Y. and Kamata, Y. (2015) Identification and characterization of a new enterotoxin produced by *Clostridium perfringens* isolated from food poisoning outbreaks. *PLOS One*, **10**, e0138183.

21. Miyamoto, K., Seike, S., Takagishi, T., Okui, K., Oda, M., Takehara, M. and Nagahama, M. (2015) Identification of the replication region in pBCNF5603, a bacteriocin-encoding plasmid, in the enterotoxigenic *Clostridium perfringens* strain F5603. *BMC Microbiol.*, **15**, 118.

22. Marshall, K.M., Bradshaw, M. and Johnson, E.A. (2010) Conjugative botulinum neurotoxin-encoding plasmids in *Clostridium botulinum*. *PLOS One*, **5**, e11087-e11087.

23. Vidor, C.J., Watts, T.D., Adams, V., Bulach, D., Couchman, E., Rood, J.I., Fairweather, N.F., Awad, M. and Lyras, D. (2018) *Clostridium sordellii* pathogenicity locus plasmid pCS1-1 encodes a novel clostridial conjugation locus. *MBio*, **9**.

24. Rood, J.I., Maher, E.A., Somers, E.B., Campos, E. and Duncan, C.L. (1978) Isolation and characterization of multiply antibiotic-resistant *Clostridum perfringens* strains from porcine feces. *Antimicrob. Agents Chemother.*, **13**, 871-880.

25. Rood, J.I. (1983) Transferable tetracycline resistance in *Clostridium perfringens* strains of porcine origin. *Canadian Journal of Microbiology*, **29**, 1241-1246.

26. Lyristis, M., Bryant, A.E., Sloan, J., Awad, M.M., Nisbet, I.T., Stevens, D.L. and Rood, J.I. (1994) Identification and molecular analysis of a locus that regulates extracellular toxin production in *Clostridium perfringens*. *Mol. Microbiol.*, **12**, 761-777.

27. Carter, G.P., Awad, M.M., Hao, Y., Thelen, T., Bergin, I.L., Howarth, P.M., Seemann, T., Rood, J.I., Aronoff, D.M. and Lyras, D. (2011) TcsL is an essential virulence factor in *Clostridium sordellii* ATCC 9714. *Infect. Immun.*, **79**, 1025-1032.

28. Couchman, E.C., Browne, H.P., Dunn, M., Lawley, T.D., Songer, J.G., Hall, V., Petrovska, L., Vidor, C., Awad, M., Lyras, D. *et al.* (2015) *Clostridium sordellii* genome analysis reveals plasmid localized toxin genes encoded within pathogenicity loci. *BMC Genomics*, **16**, 392.

29. Cheung, J.K., Keyburn, A.L., Carter, G.P., Lanckriet, A.L., Van Immerseel, F., Moore, R.J. and Rood, J.I. (2010) The VirSR two-component signal transduction system regulates NetB toxin production in *Clostridium perfringens*. *Infect. Immun.*, **78**, 3064-3072.

30. Fagan, R.P. and Fairweather, N.F. (2011) *Clostridium difficile* has two parallel and essential Sec secretion systems. *J. Biol. Chem.*, **286**, 27483-27493.

31. O'Connor, J.R., Lyras, D., Farrow, K.A., Adams, V., Powell, D.R., Hinds, J., Cheung, J.K. and Rood, J.I. (2006) Construction and analysis of chromosomal *Clostridium difficile* mutants. *Mol. Microbiol.*, **61**, 1335-1351.

32. Scott, P.T. and Rood, J.I. (1989) Electroporation-mediated transformation of lysostaphin-treated *Clostridium perfringens*. *Gene*, **82**, 327-333.

33. Gurjar, A., Li, J. and McClane, B.A. (2010) Characterization of toxin plasmids in *Clostridium perfringens* type C isolates. *Infect. Immun.*, **78**, 4860-4869.

34. McWilliam, H., Li, W., Uludag, M., Squizzato, S., Park, YM, Buso, N, Cowley, AP., Lopez, R.,. (2013) Analysis Tool Web Services from the EMBL-EBI. *Nucleic Acids Res.*, **41**,

35. Altschul, S.F., Gish, W., Miller, W., Myers, E.W. and Lipman, D.J. (1990) Basic local alignment search tool. *J. Mol. Biol.*, **215**, 403-410.

36. Gish, W. and States, D.J. (1993) Identification of protein coding regions by database similarity search. *Nat. Genet.*, **3**, 266-272.

37. Sullivan, M.J., Petty, N.K. and Beatson, S.A. (2011) Easyfig: a genome comparison visualizer. *Bioinformatics*, **27**, 1009-1010.

38. Alikhan, N.-F., Petty, N.K., Ben Zakour, N.L. and Beatson, S.A. (2011) BLAST Ring Image Generator (BRIG): simple prokaryote genome comparisons. *BMC Genomics*, **12**, 402.

39. Chen, Y., McClane, B.A., Fisher, D.J., Rood, J.I. and Gupta, P. (2005) Construction of an alpha toxin gene knockout mutant of *Clostridium perfringens* type A by use of a mobile group II intron. *Appl. Environ. Microbiol.*, **71**, 7542-7547.

40. Perutka, J., Wang, W., Goerlitz, D. and Lambowitz, A.M. (2004) Use of computer-designed group II introns to disrupt *Escherichia coli* DExH/D-box protein and DNA helicase genes. *J. Mol. Biol.*, **336**, 421-439.

41. Govind, R. and Dupuy, B. (2012) Secretion of *Clostridium difficile* toxins A and B requires the holin-like protein TcdE. *PLoS Path.*, **8**, e1002727-e1002727.

42. Thomas, C.M., Thomson, N.R., Cerdeno-Tarraga, A.M., Brown, C.J., Top, E.M. and Frost, L.S. (2017) Annotation of plasmid genes. *Plasmid*, **91**, 61-67.

43. Gohari, M.I., Parreira, V.R., Nowell, V.J., Nicholson, V.M., Oliphant, K. and Prescott, J.F. (2015) A novel pore-forming toxin in type A *Clostridium perfringens* is associated

with both fatal canine hemorrhagic gastroenteritis and fatal foal necrotizing enterocolitis. *PLOS One*, **10**, e0122684.

44. O'Brien, F.G., Yui Eto, K., Murphy, R.J.T., Fairhurst, H.M., Coombs, G.W., Grubb, W.B. and Ramsay, J.P. (2015) Origin-of-transfer sequences facilitate mobilisation of non-conjugative antimicrobial-resistance plasmids in *Staphylococcus aureus*. *Nucleic Acids Res.*, **43**, 7971-7983.

45. Rood, J.I., Scott, V.N. and Duncan, C.L. (1978) Identification of a transferable tetracycline resistance plasmid (pCW3) from *Clostridium perfringens*. *Plasmid*, **1**, 563-570.

46. Corrigan, R.M. and Foster, T.J. (2009) An improved tetracycline-inducible expression vector for *Staphylococcus aureus*. *Plasmid*, **61**, 126-129.

47. Li, J., Adams, V., Bannam, T.L., Miyamoto, K., Garcia, J.P., Uzal, F.A., Rood, J.I. and McClane, B.A. (2013) Toxin plasmids of *Clostridium perfringens*. *Microbiol. Mol. Biol. Rev.*, **77**, 208-233.

48. Adams, V., Li, J., Wisniewski, J.A., Uzal, F.A., Moore, R.J., McClane, B.A. and Rood, J.I. (2014) Virulence plasmids of spore-forming bacteria. *Microbiology Spectrum*, **2**, 10.1128/microbiolspec.PLAS-0024-2014.

49. Brynestad, S., Sarker, M.R., McClane, B.A., Granum, P.E. and Rood, J.I. (2001) Enterotoxin plasmid from *Clostridium perfringens* is conjugative. *Infect. Immun.*, **69**, 3483-3487.

50. Hughes, M.L., Poon, R., Adams, V., Sayeed, S., Saputo, J., Uzal, F.A., McClane, B.A. and Rood, J.I. (2007) Epsilon-toxin plasmids of *Clostridium perfringens* type D are conjugative. *J. Bacteriol.*, **189**, 7531-7538.

51. Goessweiner-Mohr, N., Arends, K., Keller, W. and Grohmann, E. (2013) Conjugative type IV secretion systems in Gram-positive bacteria. *Plasmid*, **70**, 289-302.

52. Goessweiner-Mohr, N., Grumet, L., Arends, K., Pavkov-Keller, T., Gruber, C.C., Gruber, K., Birner-Gruenberger, R., Kropec-Huebner, A., Huebner, J., Grohmann, E.

et al. (2013) The 2.5 Å structure of the enterococcus conjugation protein TraM resembles VirB8 type IV secretion proteins. *J Biol Chem*, **288**, 2018-2028.

53. Thorstenson, Y.R. and Zambryski, P.C. (1994) The essential virulence protein VirB8 localizes to the inner membrane of *Agrobacterium tumefaciens*. *J. Bacteriol.*, **176**, 1711-1717.

Supplementary material

Table S2.1: Oligonucleotide primers

Name	Sequence (5’ to 3’)	Purpose
JRP3867	CGAAATTAGAAACTTGCGTTCAGTAAAC	IBS universal for retargeting TargeTron plasmids.
JRP6261	AAAAAAGCTTATAATTATCCTTAATTTACGATATGGTGCGCCCAG ATAGGGTG	*cpb2* TT IBS2 for retargeting pJIR3566 Targetron vector to *cpb2*
JRP6262	CAGATTGTACAAATGTGGTGATAACAGATAAGTCGATATGAATA ACTTACCTTTCTTTGT	*cpb2* TT EBS1d for retargeting pJIR3566 Targetron vector to *cpb2*
JRP6263	TGAACGCAAGTTTCTAATTTCGGTTTAAATCCGATAGAGGAAAG TGTCT	*cpb2* TT EBS2 for retargeting pJIR3566 Targetron vector to *cpb2*
JRP6432	AAAAAAGCTTATAATTATCCTTATTTAACTCATTTGTGCGCCCAG ATAGGGTG	*parB* TT IBS2- for retargeting pJIR3566 Targetron vector to *parB*
JRP6433	CAGATTGTACAAATGTGGTGATAACAGATAAGTCTCATTTGCTAA CTTACCTTTCTTTGT	*parB* TT EBS1d for retargeting pJIR3566 Targetron vector to *parB*
JRP6434	TGAACGCAAGTTTCTAATTTCGATTTTAAATCGATAGAGGAAAGT GTCT	*parB* TT EBS2 for retargeting pJIR3566 Targetron vector to *parB*

JRP7162	AAAAAAGCTTATAATTATCCTTATGGTTCGGTAAGGTGCGCCCAGATAGGGTG	*pcpB4* TT IBS2 for retargeting pJIR3566 Targetron vector to *pcpB4*
JRP7163	CAGATTGTACAAATGTGGTGATAACAGATAAGTCGGTAAGTTTAACTTACCTTTCTTTGT	*pcpB4* TT EBS1d for retargeting pJIR3566 Targetron vector to *pcpB4*
JRP7164	TGAACGCAAGTTTCTAATTTCGATTAACCATCGATAGAGGAAAGTGTCT	*pcpB4* EBS2 for retargeting pJIR3566 Targetron vector to *pcpB4*
DLP798	AAAGAGCTCAGTAAGTAGAAAGTGAGGAATTTAATATG	*pcpB4* comp
DLP799	AAAGGATCCCGCTAATGAACTAATGAAAAGTACC	*pcpB4 comp*
JRP4632	AATAAGTAAACAGGTAACGTCT	*ermB* DIG labelled probe forward primer
JRP4633	GCTCCTTGGAAGCTGTCAGTAG	*ermB* DIG labelled probe reverse primer
JRP5658	GTGGATATTGAATCTCTTGCAGAAGATA	*parB* forward primer for construction of DIG-labelled probe
JRP5659	CTCTCATATCTACCAACCTGTGTAGCTG	*parB* reverse primer for construction of DIG-labelled probe
JRP5502	ATGATCCTAACCAACAACTAAAATC	*cpb2 probe* Fwd
JRP5503	CACCAAATACTCTAATTGATGC	*cpb2 probe* Rev
JRP4201	CCCCATAGTAAAAATAGGAATCAAATAATCATATC	*catP probe* Fwd

JRP4202	TATCACACAAATAAAGGAAAAGGGAATGAAAC	*catP probe* Rev
JRP6685	GAGGAATTTAATATGGGTATATTTAAAAGGG	*pcpB4 probe* Fwd
JRP6693	CTTTGTAAAGCCTTACTTCTATCTTCAGTTTC	*pcpB4 probe* Rev
JRP6683	GCAGAGCTCCTAAAAGCTAAAAAAGTTACAGGAGGTGAAG	*pcpB6* probe Fwd
JRP6684	GCGGATCCGCTACTAAGAGCATTGCAAAATCAAACAG	*pcpB6* probe Rev

Table S2.2 Comparison of key conjugation locus homologues from pCP13-like plasmids and pCW3

	Conserved conjugation homologues and percentage aa identity to pCP13 homologues*							
pCP13	**pCS1-1**	**pCLL**	**pCP-OS1**	**pCP-TS1**	**pBCNF5603**	**pJFP55H**	**pCW3**	**Putative function**
PcpD2	CstD2 43%	CLL_RS 34985 53%	PCPOS1_30 97%	PCPTS1_30 97%	PBCN11 97%	JFP55_pH0010 67%	TcpM 16%	Putative relaxase
PcpB1	CstB1 57%	CLL_RS 34965 59%	PCPOS1_35 99%	PCPTS1_35 99%	-	JFP55_pH0014 72%	TcpG 48%	Putative hydrolase
PcpB4	CstB4 52%	CLL_RS 34955 63%	PCPOS1_37 99%	PCPTS1_3 7 99%	-	JFP55_pH0016 71%	TcpF 18%	VirB4 homologue, putative conjugation ATPase

PcpB6	CstB6 34%	CLL_RS 34940 36%	PCPOS1_41 97%	PCPTS1_41 97%	-	JFP55_pH0028 54%	TcpH 20%	VirB6 homologue, putative mating pore scaffold protein
PcpD4	CstD4 49%	CLL_RS 34935 55%	PCPOS1_42 98%	PCPTS1_42 98%	-	JFP55_pH0029 61%	TcpA 21%	VirD4 homologue, putative coupling protein
CnaB	CnaB 44%	CLL_RS 35165 20%	Cna 98%	Cna 98%	-	Cna 54%	Cna 69%	Putative collagen adhesion protein

*aa sequence comparisons prepared using ClustalΩ

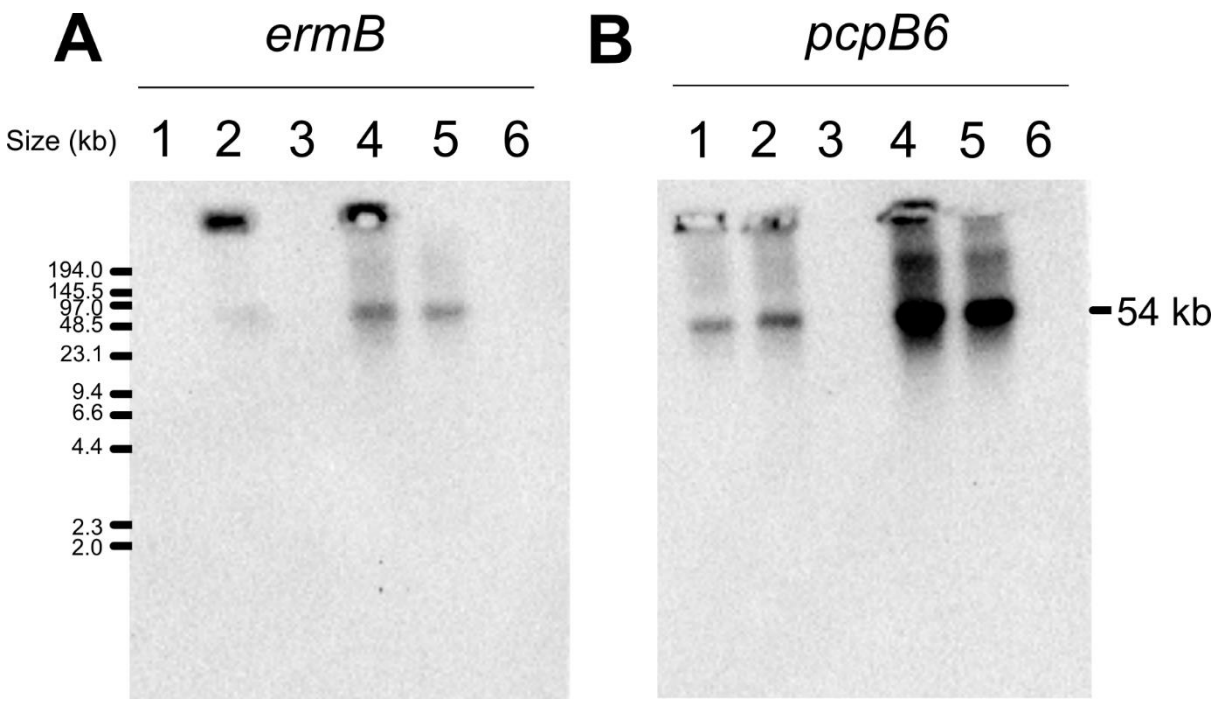

Figure S2.1. Southern hybridisation of PFGE of donor, recipient and transconjugants: 1 pCP13 positive control (JIR325), **2** JIR13270 donor, **3** JIR13467 recipient, **4** & **5** Transconjugants, and **6** pCP13 negative control (JIR13211). **A** Southern blot conducted with *ermB*-specific probe, **B** Southern blot conducted with *pcpB6*-specific probe (to indicate the presence of pCP13), both probes are indicated above the blots.

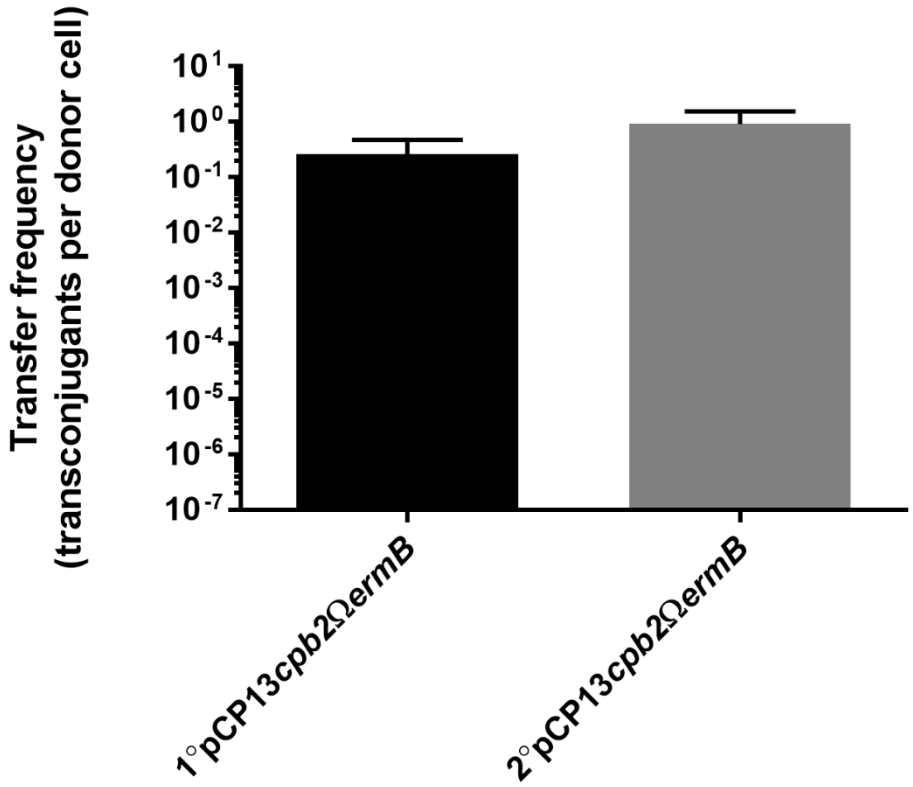

Figure S2.2. pCP13 secondary transfer. 1° denotes primary mating of 'WT' pCP13*cpb2ΩermB* between JIR13270 donor and JIR13467 recipient. 2° denotes secondary mating between JIR13467(pCP13cpb2ΩermB) transconjugants and JIR13677. Mean±SD, n=4.

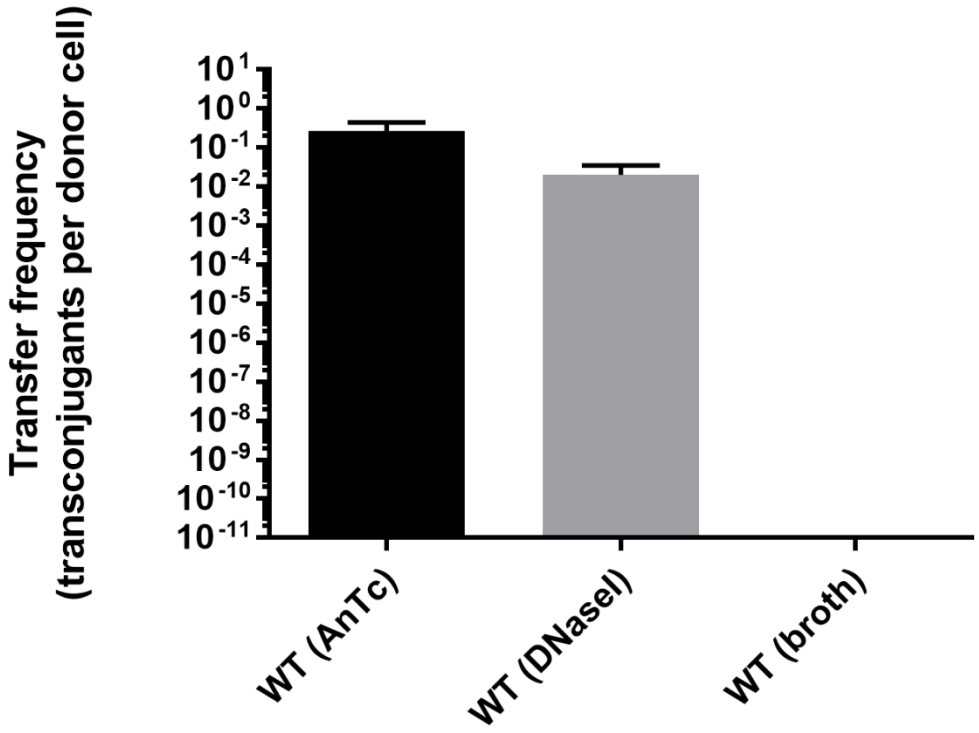

Figure S2.3. pCP13 transfer frequency in various conditions. 'Wild-type' (WT) pCP13*cpb2*Ω*ermB* transfer frequency in the presence of AnTc (n=4), 1 mg/ml DNase I (n=2) and in broth (n=4), Mean±SD.

Chapter 3

Plasmid partitioning systems of conjugative plasmids from *Clostridium perfringens*

Plasmid Partitioning Systems of Conjugative Plasmids from *Clostridium perfringens*

Vicki Adams[1], Thomas D. Watts[1], Dieter M. Bulach[1,2,3], Dena Lyras[1] and Julian I. Rood[1]*

[1]Department of Microbiology, Monash University, Clayton, Victoria, 3800, Australia

[2]Victorian Bioinformatics Consortium, Monash University, Clayton, Victoria, 3800, Australia

[3]Life Sciences Computation Centre, Victorian Life Sciences Computation Initiative, Carlton, Victoria, 3053, Australia

*Corresponding author: Julian I. Rood, Department of Microbiology, Monash University, Clayton, 3800, Australia

Tel: [redacted]

Fax: [redacted]

Email: [redacted]

Keywords: *Clostridium perfringens*, Plasmid, Conjugative, Plasmid partitioning, ParR, ParM, toxin plasmids

Abstract

Many pathogenic strains of *Clostridium perfringens* carry several highly similar toxin or antibiotic resistance plasmids that have 35 to 40 kb of very closely related syntenous sequences, including regions that carry the genes encoding conjugative transfer, plasmid replication and plasmid maintenance functions. Key questions are how are these closely related plasmids stably maintained in the same cell and what is the basis for plasmid incompatibility in *C. perfringens*? Comparative analysis of the Rep proteins encoded by these plasmids suggested that this protein was not the basis for plasmid incompatibility since plasmids carried in a single strain often encoded an almost identical Rep protein. These plasmids all carried a similar, but not identical, *parMRC* plasmid partitioning locus. Phylogenetic analysis of the deduced ParM proteins revealed that these proteins could be divided into ten separate groups. Importantly, in every strain that carried more than one of these plasmids the respective ParM proteins were from different phylogenetic groups. Similar observations were made from the analysis of phylogenetic trees of the ParR proteins and the *parC* loci. These findings provide evidence that the basis for plasmid incompatibility in the conjugative toxin and resistance plasmid family from *C. perfringens* resides in subtle differences in the *parMRC* plasmid partitioning loci carried by these plasmids.

Introduction

Clostridium perfringens is a ubiquitous Gram positive, rod-shaped, anaerobe that produces heat-resistant endospores (1,2). In addition to its prevalence in the environment *C. perfringens* is often found as a commensal organism within the gastrointestinal tract of both humans and animals; however, it can also act as a pathogen causing an array of diseases. These diseases range from enterotoxaemias and enteritis in humans and animals to potentially fatal wound infections in humans (1,3,4). Disease can be attributed to the ability of *C. perfringens* to produce an arsenal of at least 17 distinct extracellular toxins and enzymes (5-8). These toxins are intimately involved in the determination of disease and four of these toxins (α, β, ε and ι toxins) are used as the basis for typing *C. perfringens* isolates into toxinotypes A to E (1,5).

Many of these toxins, including three of the four typing toxins, are encoded by genes localised on large plasmids that have either been shown to be conjugative or are highly likely to be conjugative. Conjugative plasmids in *C. perfringens* are able to transfer at high frequencies and are not limited to carrying toxin genes, but may carry antibiotic resistance genes and catabolic functions (2). These plasmids include a series of plasmids that are either identical or highly related to the archetypal *C. perfringens* tetracycline resistance plasmid pCW3 (9-11)**.** The presence of these plasmids has significant implications for the dissemination of virulence and antimicrobial resistance determinants throughout *C. perfringens* populations (2,11).

Conjugative transfer in *C. perfringens* is mediated by plasmid-determined genes located within the *tcp* conjugation locus (11-15). Five toxin plasmids and several resistance plasmids have been shown experimentally to transfer and many more toxin plasmids have been shown to have an intact *tcp* locus, suggesting that these plasmids are also highly likely to be conjugative (2,16-20).

Southern hybridisation analyses of pulsed-field gels has revealed that strains of *C. perfringens* often possess several large plasmids that are closely related, but carry different toxin genes (21,22). This characteristic of *C. perfringens* strains is exemplified by the type A avian necrotic enteritis isolate EHE-NE18, where detailed sequence analysis has demonstrated that this strain carries three closely related conjugative plasmids, pJIR3535, pJIR3537 and pJIR3844, each of which encodes a different toxin gene (*netB* or *cpb2*) or antimicrobial resistance determinant (*tet*(P) operon) (Figure 3.1) (16). These findings raise the question as to how these large, closely related conjugative plasmids, which share near identical replication functions, are able to coexist within a single strain of *C. perfringens*. What is the mechanism of plasmid incompatibility in conjugative *C. perfringens* plasmids?

At present, eleven plasmids carrying the *tcp* locus have been fully sequenced (2,11,16,19,23-25), and several more plasmids have been partially sequenced (V. Adams, L. Weeramantri, J. Cheung, T. Stent, X. Han & J. Rood, unpublished results). Comparative sequence analysis has revealed that each of these conjugative plasmids is very closely related to pCW3 and shares a conserved ~35 kb backbone (2,11,16,19,20,23-25). Within the conserved region there are several loci of note, in particular the *tcp* locus and the central control region (CCR) (11,16,19) (Figure 3.1). The latter encodes genes involved in plasmid replication, regulation and maintenance (11,16,19). It includes the *rep* gene (11) and a *parMRC*-like partitioning locus (11,16,19,20).

Plasmid incompatibility is often determined by both plasmid replication mechanisms as well as partitioning systems that control plasmid segregation, and therefore the stable inheritance, of low-copy number plasmids in the cell division process. Partitioning systems are generally tripartite systems, are plasmid encoded and typically rely on the action of two *trans*-acting proteins, an NTPase and a DNA binding adaptor protein, and a *cis*-acting centromere site (26,27) (Figure 3.2). There are three types of partitioning systems in bacteria, each is categorised by the type of NTPase it encodes (26).

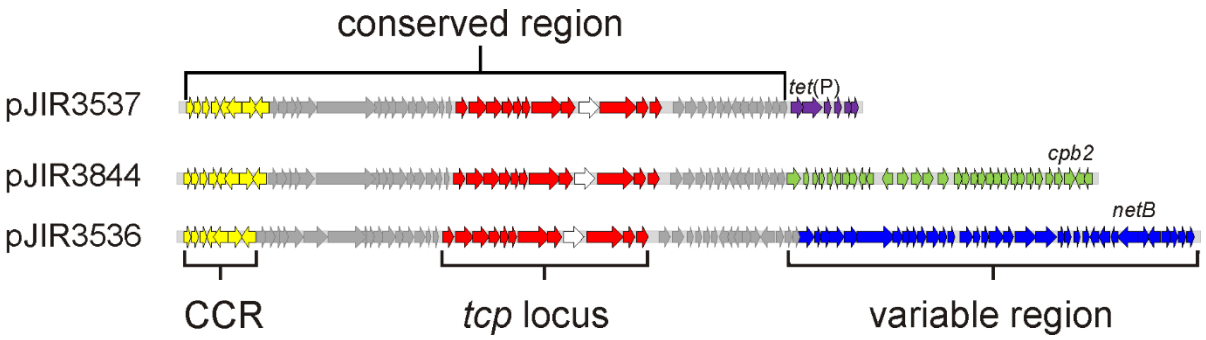

Figure 3.1. Genetic organisation of conjugative plasmids from strain EHE-NE18. Linear maps of pJIR3537 (49 kb), pJIR3844 (70 kb) and pJIR3535 (82 kb), the three large plasmids present in strain EHE-NE18, are shown. ORFs are indicated by the arrows. Related functional regions are indicated as follows – the central control region (CCR; yellow arrows), the conjugation locus (*tcp*; red arrows) and unique regions that are shown in purple, green and blue. Relevant toxin and antibiotic resistance genes are indicated. Grey arrows indicate conserved ORFs and the white arrow indicates a group II intron.

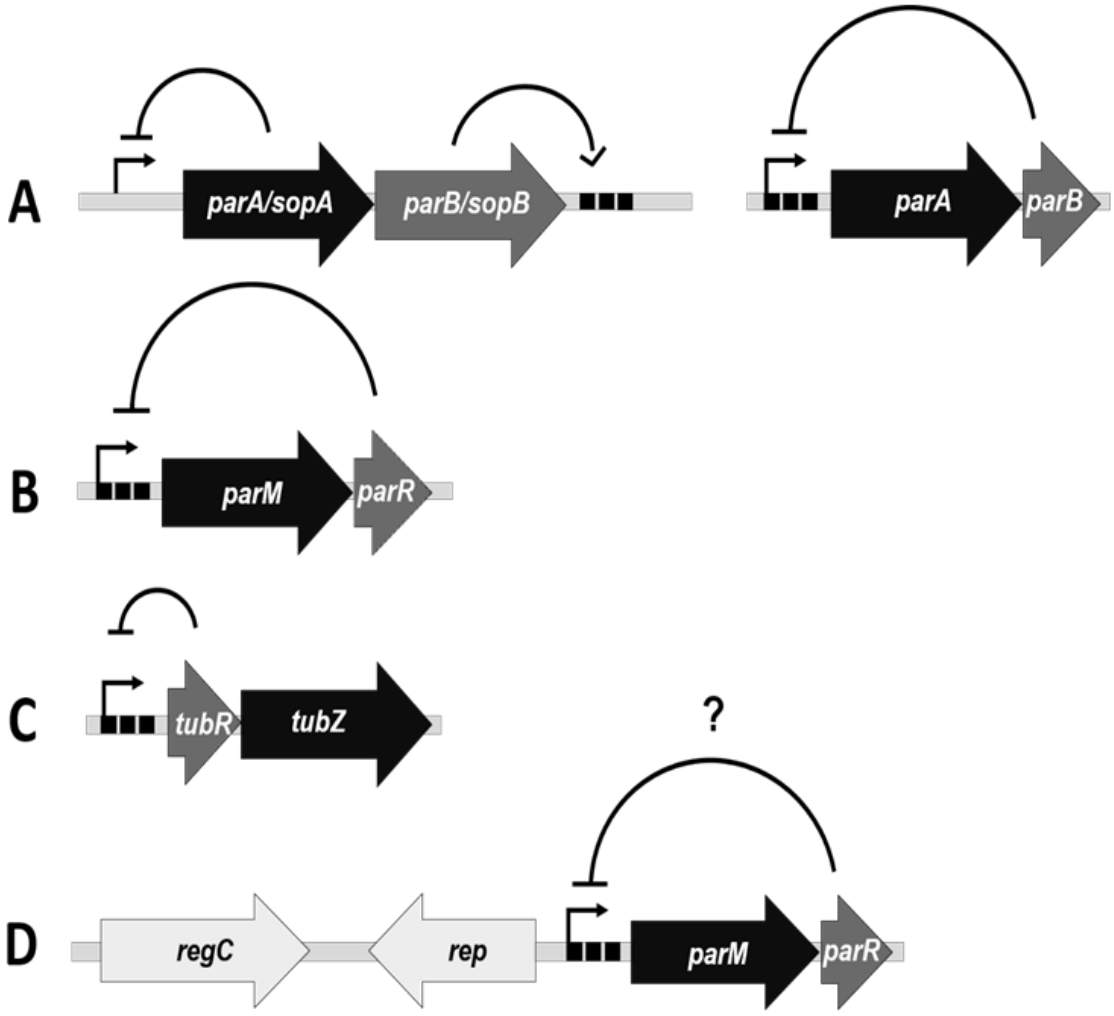

Figure 3.2. Genetic arrangement of partitioning loci. NTPase proteins are indicated by black arrows, DNA binding/adaptor proteins are indicated by grey arrows, white arrows indicate other ORFs not directly involved in partitioning, promoters are indicated by bent arrows. The curved lines ending with the straight line are used to indicate the operator/binding sites of the specified gene products. (A) Type I partitioning loci, with two variations, (B) type II partitioning system and (C) type III partitioning system. Adapted from (26). (D). The arrangement of ORFs in the pCW3-like plasmid partitioning regions are indicated.

Type I partitioning systems are characterised by a variant Walker A type ATPase known as ParA (28) (Figure 3.2A). These systems generally consist of three components, (i) a ParA/SopA ATPase, (ii) ParB/SopB, a DNA binding adaptor protein, and (iii) the plasmid-encoded centromere, *parS*/*sopC* (26,27,29). Type II or ParMRC partitioning systems (Figure 3.2B) comprise (i) a filament-forming actin/Hsp70 family ATPase, ParM, (ii) a DNA binding adaptor protein ParR, which binds to (iii) a centromeric site, *parC,* situated immediately upstream in the promoter region of *parM* (26,30-34) . In contrast to type I systems, ParMRC partitioning systems mediate plasmid segregation *via* a pushing mechanism, which has predominantly been characterised by study of the *parMRC*-like partitioning systems of the *Escherichia coli* plasmid R1 and the *Staphylococcus aureus* plasmid pSK41 (26,30,35,36). Capping of the ParM filaments by the ParR-*parC* complex works to stabilise ParM polymerisation, thus allowing sister plasmids that have been 'captured' by interacting bundles of anti-parallel ParM filaments to be segregated to either cell pole (34,37,38). Type III partitioning systems, or TubZRC systems, are analogous to ParMRC partitioning systems, however, the NTPase is a homologue of eukaryotic tubulin (Reviewed in (26)) (Figure 3.2C). In addition to these three partitioning types, there is a unique partitioning system encoded by the *S. aureus* multi-resistance plasmid pSK1 (39,40). This system is comprised of a single partitioning protein and has been shown to stabilise *S. aureus* mini-replicons (39).

These partitioning systems are widespread in bacteria and *C. perfringens* is no exception (16,19,20). Here we demonstrate that there are at least ten different clades of plasmid encoded *parMRC*-like homologues in *C. perfringens* and that all *C. perfringens* conjugative plasmids fall into one of ten distinct phylogenetic groups based upon their partitioning group. We propose that these different partitioning families form the basis for plasmid incompatibility in *C. perfringens*.

Materials and methods

Data acquisition and analysis.

ParM sequences were obtained by searching the NCBI databases using BlastP (blast.ncbi.nlm.nih.gov/Blast.cgi) and limiting the search to *C. perfringens* sequences. The pCW3 ParM amino acid sequence was used to interrogate the database initially. Additional ParM sequences were identified by searching with the ParM sequence obtained from sequencing of the epsilon toxin-encoding plasmid from strain CN3718. Finally, a DELTA-BLAST (blast.ncbi.nlm.nih.gov/Blast.cgi) search was performed to determine if any ParM sequences from *C. perfringens* had been overlooked. Rep protein analysis was carried out in a similar fashion except that PSI-BLAST (Blast blast.ncbi.nlm.nih.gov/Blast.cgi) was used instead of DELTA-BLAST since the pCW3-like Rep proteins contain no conserved domains. ParR protein sequences were identified by searching the DNA sequences encoding the ParM proteins identified previously and determining if a small ORF was located directly downstream of the *parM* gene. In most sequences, this ORF was annotated, in a few entries the ORF was not annotated, but was present. In some of the sequences the upstream or downstream data were missing. A similar approach was used to identify the *parC* regions, designated as the DNA sequence upstream of the *parM* gene. In pCW3-like plasmids, the *parC* region was further delineated by comparison to the conserved *oriV* region located between the *parM* and *rep* genes and the *parC* region was deemed to begin at the site of divergence between the *oriV* site and the *parM* gene.

Phylogenetic analysis.

The similarity of each of the ParM sequences initially was analysed using Clustal Omega (41). Amino acid identity matrices were examined and the ParM sequences were used to construct a phylogenetic tree using MEGA 6 (42). Tree construction involved Clustal W analysis followed by tree inference using the maximum likelihood method (43). Similar trees were constructed by inputting ParR sequences, *parC* sequences and Rep protein sequences.

Results and discussion

Plasmids can be allocated to phylogenetic groups based on their *parMRC* regions.

Examination of *C. perfringens* plasmid sequences that were located in the databases yielded several fully assembled plasmid sequences, whilst other sequences constituted either partially assembled sequences or data from whole genome sequencing projects (WGS) (Table 3.1) (44). Note that many of these strains carry multiple toxin plasmids that are closely related, as already described, in other strains the plasmid content was not specified. The tetracycline resistance plasmid pCW3 (11) is the smallest and best characterised conjugative plasmid from *C. perfringens* and therefore was used as the reference plasmid for these studies.

The two genes adjacent to, but divergently transcribed, from *rep* in the CCR of pCW3 were found to encode a putative ParM homologue and what was subsequently designated as a ParR homologue, with a potential centromere site immediately preceding the *parM* gene (11,16,19) (Figure 3.2D). It was previously observed that the conjugative plasmids carried by any one strain of *C. perfringens* all had different *parMR* alleles; the ParMRC system therefore was postulated to form the basis of a plasmid incompatibility locus (16,19) (Four alleles (A-D) were identified at that time; however, additional sequence data obtained from our studies suggested that there were further *parMR* alleles to be identified.

In the current study comparative analysis conducted using the NCBI BLAST server allowed the identification of ten ParM variants (Figure 3.3A). These proteins were identified with considerable confidence as their deduced amino acid sequences all showed a hit to conserved domain CD10227, namely the ParM_like domain.

Table 3.1. *C. perfringens* genome sequences

Strain	Plasmid/s	Characteristics/sequence type	GenBank Accession Number
CPF5603	pCPF5603	Enterotoxin (CPE)/fully assembled	AB236337
CPF4969	pCPF4969	Enterotoxin (CPE)/fully assembled	AB236336
CPF4013	pCPF4013	Enterotoxin(CPE)/partial sequence	AB236338
CW92	pCW3	Tet(P) tetracycline resistance determinant /fully assembled	DQ366035
CP8533	pCP8533etx	Type B; epsilon toxin/fully assembled	AB444205
PB-1	pCPPB-1	Type E; iota toxin/fully assembled	AB604032
EHE-NE18	pJIR3536 pJIR3537 pJIR3844	NetB toxin/fully assembled Tet(P) tetracycline resistance determinant/fully assembled Beta2 toxin/fully assembled	JN689219 JN689220 JN689217
NE10	pNetB-NE10	NetB/fully assembled	JQ655731
CP-1	pCpb2-CP-1	Beta2 toxin/fully assembled	JQ655732
F262	pF262A	Beta2 toxin/assembled	CM001478
CN4003	pJIR4163 pJIR4164	Beta2 toxin/partial assembly Epsilon toxin/partial assembly	Unpublished data Unpublished data
CN3718	pJIR3119	Epsilon/partial assembly	Unpublished data
ATCC3626	Not specified	Type B; beta and epsilon toxins/WGS	ABDV00000000
JGS1495	Not specified	Type C; beta toxin/WGS	ABDU00000000
JGS1721	Not specified	Type D; epsilon toxin/WGS	ABOO00000000
JGS1987	Not specified	Type E iota toxin/WGS	ABDW00000000
WAL-14572	Not specified	Tet(P) tetracycline resistance determinant /WGS	ADLP00000000

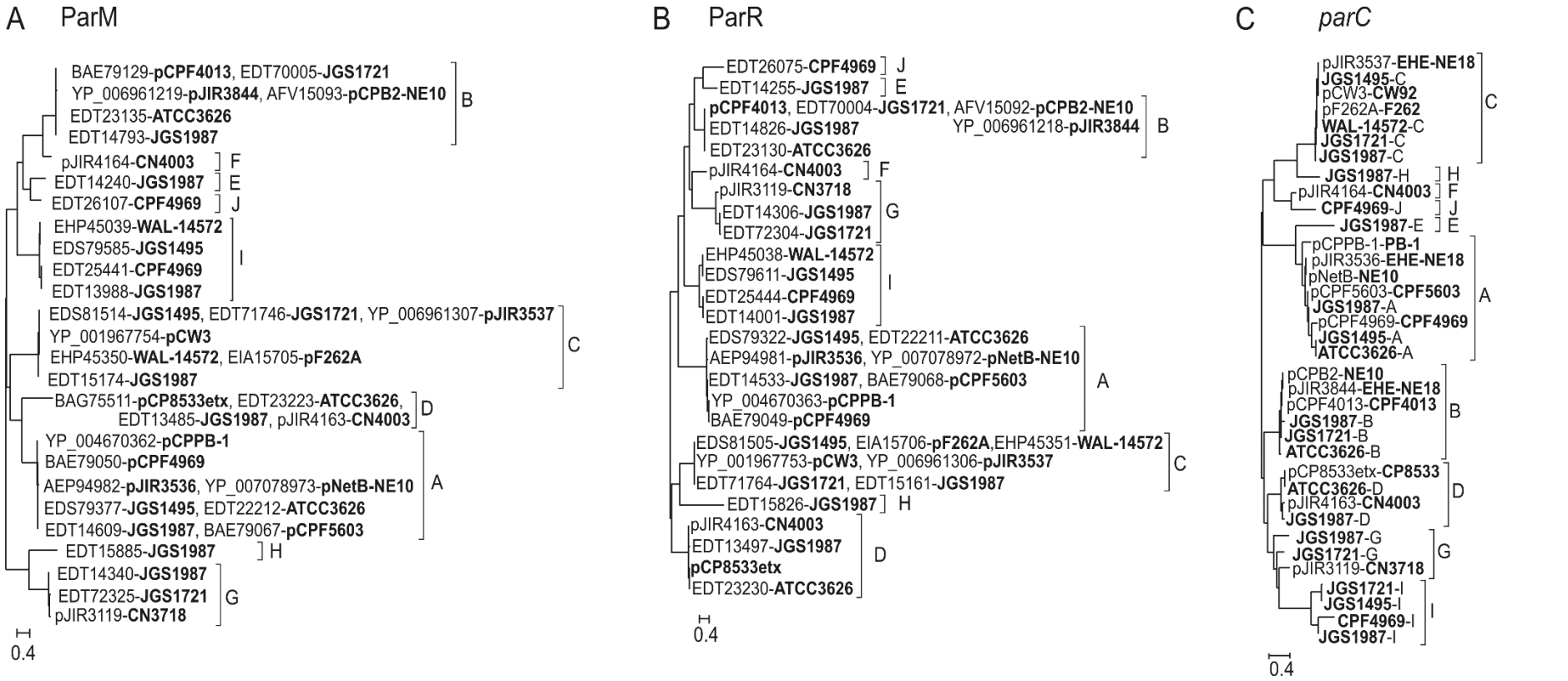

Figure 3.3. Phylogenetic analysis of the *parMRC* locus. The maximum likelihood method was used to confer evolutionary history using a JTT matrix-based model (43). The tree is drawn to scale (indicated below the figures); branch lengths were measured as the number of substitutions per site. Analyses were conducted using the software package MEGA 6 (42). (A) ParM analysis, protein accession numbers are followed by the strain or plasmid designations (bold type) separated by a hyphen. Identical sequences appear on the same line (or just below and aligned to the right), separated by a space. Par groups are indicated by a square bracket on the right of the figure with a letter (A to J). (B) ParR analysis, labelled as per the ParM data. (C) The tree generated from *parC* DNA sequences is labelled with the plasmid name followed by the strain (bold type) designation, or the strain (bold type) and the Par group letter after the hyphen.

Phylogenetic analysis indicated that there was more conservation within some of these ten groups than within others; for example, the group D ParM proteins all had identical amino acid sequences, whilst the group G and I ParM proteins showed 90% and 92% amino acid sequence identity, respectively. The highest level of identity between ParM groups was observed between groups B and F at 54% amino acid sequence identity and the lowest was 15% (between groups H-J and A-J). Most importantly, it was noted that no ParM proteins belonging to the same phylogenetic group were encoded on plasmids from the same strain (Figure 3.3A), providing evidence to support the hypothesis that the *parMRC* locus identified on these plasmids was responsible for plasmid incompatibility.

Identification of the cognate ParR proteins for each of these ParM sequences generally was accomplished by identifying the downstream open reading frame (ORF) from the *parM* gene. Sometimes this ORF had not been annotated. The conservation of ParR proteins is lower since this adapter protein binds to a specific DNA sequence and to a specific ParM protein. Therefore, the ParR proteins we identified were analysed firstly by Clustal W alignment and phylogenetic analysis (Figure 3.3B) and secondly by analysis of their primary sequence characteristics. Phylogenetic analysis resulted in the clustering of these ParR proteins into the same groups as their cognate ParM proteins (Figure 3.3A and B), which was consistent with their proposed role in functioning with their ParM counterpart to mediate specific plasmid partitioning. Identity within the ParR groups, ranged from 97% (group B) to 68% (group G), which was generally lower than for the equivalent ParM groups. The reason for this disparity is unclear, but it may suggest that although the functional regions of the ParR proteins are conserved, namely the DNA binding residues and ParR-ParM interaction sites, sequence variation is better tolerated within the ParR proteins than the equivalent ParM proteins. Analysis of the primary sequence data of the ParR proteins indicated that they were generally small proteins with an acidic pI (range 4.5 to 5.7), except for the group D proteins, which had a basic pI of 8.9.

The centromere-like *parC* site in well characterised ParMRC systems, is located upstream of *parM* (34). Consequently, the sequences upstream of the *C. perfringens parM* genes were analysed. In some plasmids the identification of the potential *parC* sequences was simplified due to the location of a pCW3-like *rep* gene upstream of the *parM* gene. Since the upstream DNA sequence of the pCW3-like *rep* genes also is well conserved (data not shown), the *parC* site was designated as the point of sequence divergence between the *rep* and *parM* genes. In some sequences, no pCW3-like *rep* gene was present on the contig and the *parC* sequence was designated as the intergenic region upstream of *parM*. These *parC* regions ranged in size between 127-300 bp in length. Phylogenetic analysis resulted in the same clustering of *parC* sites as their cognate ParM and ParR proteins (Figure 3.3C), although the sequence conservation between groups was lower, ranging from 66 to 92%. The %G+C content of these regions was very low, varying from 9 to 21% depending on the group. The average %G+C content for the *C. perfringens* chromosome is 28% and the average %G+C content for *C. perfringens* plasmids is approximately 25% (44). Therefore, even by *C. perfringens* standards the putative *parC* regions were very AT-rich and consequently identity between the *parC* groups also was relatively high (up to 65%).

Rep sequences do not correlate with plasmid incompatibility

Another mechanism that may contribute to plasmid incompatibility involves the sharing of plasmid replication processes (45). The replication protein, Rep, encoded by pCW3 has no sequence similarity to plasmid replication proteins from other bacterial species and was only identified by a series of deletion and transposon mutagenesis studies (11). This protein is highly conserved in conjugative plasmids from *C. perfringens*. Initial sequencing studies showed that the enterotoxin plasmids pCPF5603 and pCPF4969 encoded replication proteins that were nearly identical to Rep from pCW3 (11,23). Subsequent sequencing has demonstrated that the vast majority of *C. perfringens* conjugative plasmids encode a Rep protein that is either identical, or closely related, to Rep from pCW3 (2,11,16,19,23-25).

To determine if the Rep protein may contribute to plasmid incompatibility, comparative bioinformatics and phylogenetic analysis was carried out. The Rep proteins were identified either by sequence similarity to Rep from pCW3 or by manually examining contigs containing *parMR* genes. Presumptive Rep proteins were subjected to Clustal omega analysis and a phylogenetic tree was developed using MEGA6 software. This analysis indicated that although not all of these putative conjugative plasmids encoded a pCW3-like Rep protein, it was very common (Figure 3.4). Critically, there was no correlation between the Rep protein and the ParMRC group and multiple, closely related Rep proteins were encoded by different plasmids residing within the same strain (Figure 3.4). The best characterised example was again strain EHE-NE18. The Rep proteins of the three conjugative plasmids carried by EHE-NE18 were 98% identical at the amino acid level with only six amino acid substitutions between the three protein sequences. These data suggest that, in strains with multiple plasmids encoding highly related pCW3-like Rep proteins, this protein is not likely to play a significant role in plasmid incompatibility, although an involvement of Rep cannot be formally excluded.

Concluding remarks

The analysis of all known sequences, or parts thereof, from conjugative *C. perfringens* plasmids has shown that in any *C. perfringens* strain carrying multiple pCW3-like plasmids, these plasmids encode only ParMR proteins belonging to different phylogenetic groups. The ParMRC system provides the only mechanism for plasmid incompatibility that is consistent with the observed data obtained from the analysis of native *C. perfringens* isolates from many different sources. For example, the presence of ParRMC groups A, B and C, within the same cell provides a clear explanation for the stable maintenance of three independently conjugative, plasmids in strain EHE-NE18 (16).

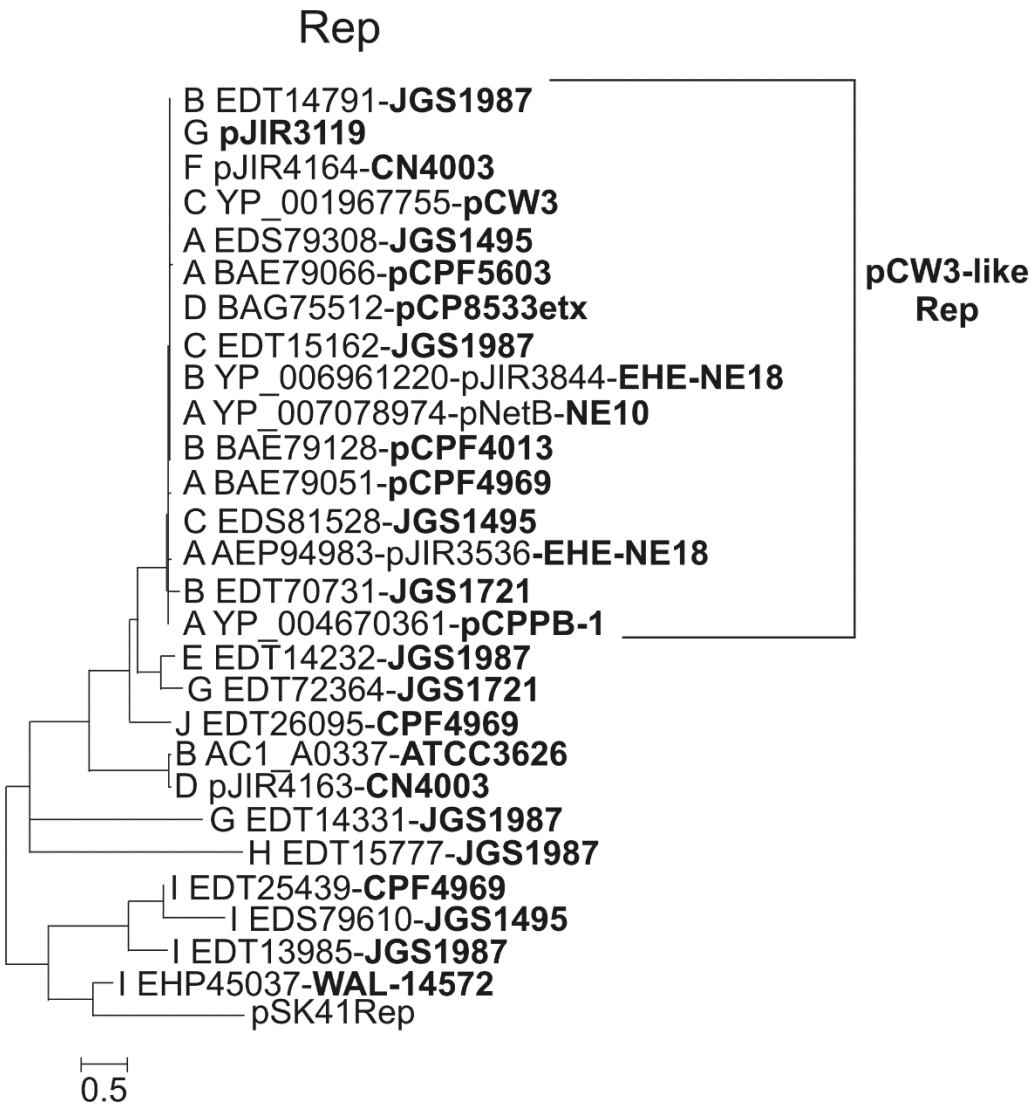

Figure 3.4. Phylogenetic analysis of Rep proteins. Tree construction was carried out as described for Fig. 3. Labels begin with the Par group designation of the neighbouring *parM* gene, followed by the accession number for the relevant Rep protein and then the strain or plasmid number (bold type).

These phylogenetic clades still need to be experimentally confirmed as incompatibility groups and the designation of Par proteins into functional groups based on sequence analysis alone must be interpreted with some caution, particularly as incompatibility has been demonstrated between *parMRC* systems demonstrating significant sequence divergence (46). Nevertheless, these data provide evidence that the *parMRC* locus may be the major factor that determines plasmid incompatibility in *C. perfringens* strains.

Acknowledgements

This research was supported by a grant from the Australian National Health and Medical Research Council (GNT1048676). TDW was the receipt of an Australian Postgraduate Award.

References

1. Rood, J.I. and Cole, S.T. (1991) Molecular genetics and pathogenesis of *Clostridium perfringens*. *Microbiol. Rev.*, **55**, 621-648.
2. Li, J., Adams, V., Bannam, T.L., Miyamoto, K., Garcia, J.P., Uzal, F.A., Rood, J.I. and McClane, B.A. (2013) Toxin plasmids of *Clostridium perfringens*. *Microbiol. Mol. Biol. Rev.*, **77**, 208-233.
3. Awad, M.M., Bryant, A.E., Stevens, D.L. and Rood, J.I. (1995) Virulence studies on chromosomal alpha-toxin and theta-toxin mutants constructed by allelic exchange provide genetic evidence for the essential role of alpha-toxin in *Clostridium perfringens*-mediated gas gangrene. *Molecular Microbiology*, **15**, 191-202.
4. Songer, J.G. (1996) Clostridial enteric diseases of domestic animals. *Clin. Microbiol. Rev.*, **9**, 216-234.
5. McDonel, J.L. (1980) *Clostridium perfringens* toxins (type A, B, C, D, E). *Pharmacol. Ther.*, **10**, 617-655.

6. Keyburn, A.L., Boyce, J.D., Vaz, P., Bannam, T.L., Ford, M.E., Parker, D., Di Rubbo, A., Rood, J.I. and Moore, R.J. (2008) NetB, a new toxin that is associated with avian necrotic enteritis caused by *Clostridium perfringens*. *PLOS Path.*, **4**, e26.

7. Yonogi, S., Matsuda, S., Kawai, T., Yoda, T., Harada, T., Kumeda, Y., Gotoh, K., Hiyoshi, H., Nakamura, S., Kodama, T. *et al.* (2014) BEC, a novel enterotoxin of *Clostridium perfringens* found in human clinical isolates from acute gastroenteritis outbreaks. *Infect. Immun.*, **82**, 2390-2399.

8. Uzal, F.A., Freedman, J.C., Shrestha, A., Theoret, J.R., Garcia, J., Awad, M.M., Adams, V., Moore, R.J., Rood, J.I. and McClane, B.A. (2014) Towards an understanding of the role of *Clostridium perfringens* toxins in human and animal disease. *Future Microbiology*, **9**, 361-377.

9. Abraham, L.J. and Rood, J.I. (1985) Molecular analysis of transferable tetracycline resistance plasmids from *Clostridium perfringens*. *J Bacteriol*, **161**, 636-640.

10. Rood, J.I., Maher, E.A., Somers, E.B., Campos, E. and Duncan, C.L. (1978) Isolation and characterization of multiply antibiotic-resistant *Clostridium perfringens* strains from porcine feces. *Antimicrob Agents and Chemother*, **13**, 871-880.

11. Bannam, T.L., Teng, W.L., Bulach, D., Lyras, D. and Rood, J.I. (2006) Functional identification of conjugation and replication regions of the tetracycline resistance plasmid pCW3 from *Clostridium perfringens*. *J Bacteriol* **188**, 4942-4951.

12. Bantwal, R., Bannam, T.L., Porter, C.J., Quinsey, N.S., Lyras, D., Adams, V. and Rood, J.I. (2012) The peptidoglycan hydrolase TcpG is required for efficient conjugative transfer of pCW3 in *Clostridium perfringens*. *Plasmid*, **67**, 139-147.

13. Parsons, J.A., Bannam, T.L., Devenish, R.J. and Rood, J.I. (2007) TcpA, an FtsK/SpoIIIE homolog, is essential for transfer of the conjugative plasmid pCW3 from *Clostridium perfringens*. *J Bacteriol*, **189**, 7782-7790.

14. Porter, C.J., Bantwal, R., Bannam, T.L., Rosado, C.J., Pearce, M.C., Adams, V., Lyras, D., Whisstock, J.C. and Rood, J.I. (2012) The conjugation protein TcpC from

Clostridium perfringens is structurally related to the type IV secretion system protein VirB8 from Gram-negative bacteria. *Mol Microbiol*, **83**, 275-288.

15. Wisniewski, J.A., Teng, W.L., Bannam, T.L. and Rood, J.I. (2014) Two novel membrane proteins TcpD and TcpE are essential for conjugative transfer of pCW3 in *Clostridium perfringens*. *J Bacteriol*.
16. Bannam, T.L., Yan, X.X., Harrison, P.F., Seemann, T., Keyburn, A.L., Stubenrauch, C., Weeramantri, L.H., Cheung, J.K., McClane, B.A., Boyce, J.D. *et al.* (2011) Necrotic enteritis-derived *Clostridium perfringens* strain with three closely related independently conjugative toxin and antibiotic resistance plasmids. *MBio*, **2**, e00190-00111.
17. Brynestad, S., Sarker, M.R., McClane, B.A., Granum, P.E. and Rood, J.I. (2001) Enterotoxin plasmid from *Clostridium perfringens* is conjugative. *Infect. Immun.*, **69**, 3483-3487.
18. Hughes, M.L., Poon., R., Adams, V., Sayeed, S., Saputo, S., Uzal, F.A., McClane, B.A. and Rood, J.I. (2007) Epsilon toxin plasmids of *Clostridium perfringens* type D are conjugative. *J Bacteriol*, **189**, 7531-7538.
19. Parreira, V.R., Costa, M., Eikmeyer, F., Blom, J. and Prescott, J.F. (2012) Sequence of two plasmids from *Clostridium perfringens* chicken necrotic enteritis isolates and comparison with *C. perfringens* conjugative plasmids. *PLOS One*, **7**, e49753.
20. Freedman, J.C., Theoret, J.R., Wisniewski, J.A., Uzal, F.A., Rood, J.I. and McClane, B.A. (2014) *Clostridium perfringens* type A-E toxin plasmids. *Res. Microbiol.*
21. Sayeed, S., Li, J. and McClane, B.A. (2010) Characterization of virulence plasmid diversity among *Clostridium perfringens* type B isolates. *Infect. Immun.*, **78**, 495-504.
22. Sayeed, S., Li, J. and McClane, B.A. (2007) Virulence plasmid diversity In *Clostridium perfringens* type D isolates. *Infect. Immun.*, **75**, 2391-2398.
23. Miyamoto, K., Fisher, D.J., Li, J., Sayeed, S., Akimoto, S. and McClane, B.A. (2006) Complete sequencing and diversity analysis of the enterotoxin-encoding plasmids in *Clostridium perfringens* type A non-food-borne human gastrointestinal disease isolates. *J. Bacteriol.*, **188**, 1585-1598.

24. Miyamoto, K., Li, J., Sayeed, S., Akimoto, S. and McClane, B.A. (2008) Sequencing and diversity analyses reveal extensive similarities between some epsilon-toxin-encoding plasmids and the pCPF5603 *Clostridium perfringens* enterotoxin plasmid. *J. Bacteriol.*, **190**, 7178-7188.

25. Miyamoto, K., Yumine, N., Mimura, K., Nagahama, M., Li, J., McClane, B.A. and Akimoto, S. (2011) Identification of novel *Clostridium perfringens* type E strains that carry an iota toxin plasmid with a functional enterotoxin gene. *PLOS One*, **6**, e20376.

26. Gerdes, K., Howard, M. and Szardenings, F. (2010) Pushing and pulling in prokaryotic DNA segregation. *Cell*, **141**, 927-942.

27. Gerdes, K., Moller-Jensen, J. and Bugge Jensen, R. (2000) Plasmid and chromosome partitioning: surprises from phylogeny. *Mol. Microbiol.*, **37**, 455-466.

28. Koonin, E.V. (1993) A superfamily of ATPases with diverse functions containing either classical or deviant ATP-binding motif. *J. Mol. Biol.*, **229**, 1165-1174.

29. Ogura, T. and Hiraga, S. (1983) Partition mechanism of F plasmid: two plasmid gene-encoded products and a cis-acting region are involved in partition. *Cell*, **32**, 351-360.

30. Gerdes, K. and Molin, S. (1986) Partitioning of plasmid R1. Structural and functional analysis of the *parA* locus. *J. Mol. Biol.*, **190**, 269-279.

31. Jensen, R.B. and Gerdes, K. (1997) Partitioning of plasmid R1. The ParM protein exhibits ATPase activity and interacts with the centromere-like ParR-parC complex. *J. Mol. Biol.*, **269**, 505-513.

32. Moller-Jensen, J., Jensen, R.B., Lowe, J. and Gerdes, K. (2002) Prokaryotic DNA segregation by an actin-like filament. *EMBO. J.*, **21**, 3119-3127.

33. van den Ent, F., Moller-Jensen, J., Amos, L.A., Gerdes, K. and Lowe, J. (2002) F-actin-like filaments formed by plasmid segregation protein ParM. *EMBO. J.*, **21**, 6935-6943.

34. Salje, J., Gayathri, P. and Lowe, J. (2010) The ParMRC system: molecular mechanisms of plasmid segregation by actin-like filaments. *Nat. Rev. Microbiol.*, **8**, 683-692.

35. Gerdes, K., Larsen, J.E. and Molin, S. (1985) Stable inheritance of plasmid R1 requires two different loci. *J. Bacteriol.*, **161**, 292-298.

36. Popp, D., Xu, W., Narita, A., Brzoska, A.J., Skurray, R.A., Firth, N., Ghoshdastider, U., Maeda, Y., Robinson, R.C. and Schumacher, M.A. (2010) Structure and filament dynamics of the pSK41 actin-like ParM protein: implications for plasmid DNA segregation. *J. Biol. Chem.*, **285**, 10130-10140.

37. Garner, E.C., Campbell, C.S., Weibel, D.B. and Mullins, R.D. (2007) Reconstitution of DNA segregation driven by assembly of a prokaryotic actin homolog. *Science*, **315**, 1270-1274.

38. Gayathri, P., Fujii, T., Moller-Jensen, J., van den Ent, F., Namba, K. and Lowe, J. (2012) A bipolar spindle of antiparallel ParM filaments drives bacterial plasmid segregation. *Science*, **338**, 1334-1337.

39. Firth, N., Apisiridej, S., Berg, T., O'Rourke, B.A., Curnock, S., Dyke, K.G. and Skurray, R.A. (2000) Replication of staphylococcal multiresistance plasmids. *J Bacteriol*, **182**, 2170-2178.

40. Simpson, A.E., Skurray, R.A. and Firth, N. (2003) A single gene on the staphylococcal multiresistance plasmid pSK1 encodes a novel partitioning system. *J. Bacteriol.*, **185**, 2143-2152.

41. Sievers, F., Wilm, A., Dineen, D., Gibson, T.J., Karplus, K., Li, W., Lopez, R., McWilliam, H., Remmert, M., Söding, J. *et al.* (2011) Fast, scalable generation of high-quality protein multiple sequence alignments using Clustal Omega. *Mol Syst Biol*, 10.1038/msb.2011.75.

42. Tamura, K., Stecher, G., Peterson, D., Filipski, A. and Kumar, S. (2013) MEGA6: Molecular Evolutionary Genetic Analysis version 6.0. *Molecular Biology and Evolution*, **30**, 2725-2729.

43. Jones, D.T., Taylor, W.R. and Thornton, J.M. (1992) The rapid generation of mutation data matrices from protein sequences. *Computer Applications in Biosciences*, **8**, 275-282.

44. Hassan, K.A., Elbourne, L.D.H., Tetu, S.G., Melville, S.B., Rood, J.I. and Paulsen, I.T. (2014) Genomic analyses of *Clostridium perfringens* isolates from five toxinotypes. *Res. Microbiol.*

45. Novick, R.P. (1987) Plasmid incompatibility. *Microbiol Rev*, **51**, 381-395.

46. Hyland, E.M., Wallace, E.W. and Murray, A.W. (2014) A model for the evolution of biological specificity: a cross-reacting DNA-binding protein causes plasmid incompatibility. *J. Bacteriol.*, **196**, 3002-3011.

Chapter 4

Evidence that compatibility of closely related replicons in *Clostridium perfringens* depends on linkage to *parMRC*-like partitioning systems of different subfamilies

Evidence that compatibility of closely related replicons in *Clostridium perfringens* depends on linkage to *parMRC*-like partitioning systems of different subfamilies

Thomas D. Watts[1], Priscilla A. Johanesen[1], Dena Lyras[1], Julian I., Rood[1*] and Vicki Adams[1*#]

[1]Infection and Immunity Program, Monash Biomedicine Discovery Institute and Department of Microbiology, Monash University, Victoria 3800, Australia

[*] Joint senior authors

[#]Corresponding author: Vicki Adams, Department of Microbiology, Monash University, Victoria, 3800, Australia.

Tel: [redacted]

Fax: [redacted]

Email: [redacted]

Keywords: Partitioning, incompatibility, *Clostridium perfringens*, ParR, ParM, toxin plasmids

Abstract

Clostridium perfringens produces an extensive repertoire of toxins and extracellular enzymes, many of which are intimately involved in the progression of disease and are encoded by genes on conjugative plasmids. In addition, many *C. perfringens* strains can carry up to five of these conjugative toxin or antimicrobial resistance plasmids, each of which has a similar 35 kb backbone. This conserved backbone includes the *tcp* conjugation locus and the central control region (CCR), which encodes genes involved in plasmid regulation, replication and partitioning, including a *parMRC* partitioning locus. Most conjugative plasmids in *C. perfringens* have a conserved replication protein, raising questions as to how multiple, closely related plasmids are maintained within a single strain. Bioinformatics analysis has highlighted the presence of at least 10 different *parMRC* partitioning system families (*parMRC*$_{A\text{-}J}$) in these plasmids, with differences in amino acid sequence identity between each ParM family ranging from 15% to 54%. No two plasmids that encode genes belonging to the same partitioning family have been observed in a single strain, suggesting that these families represent the basis for plasmid incompatibility. In an attempt to validate the proposed *parMRC* incompatibility groups, genetically marked *C. perfringens* plasmids encoding identical *parMRC*$_C$ or *parMRC*$_D$ homologues or different combinations of *parMRC*$_A$, *parMRC*$_C$ and *parMRC*$_D$ family homologues were introduced into a single strain *via* conjugation. The stability of each plasmid was determined using an incompatibility assay in which the plasmid profile of each strain was monitored over the course of two days in the absence of direct selection. The results showed that plasmids with identical *parMRC*$_C$ or *parMRC*$_D$ homologues were incompatible and could not coexist in the absence of external selection. By contrast, plasmids that encoded different *parMRC* homologues were compatible and could coexist in the same cell in the absence of selection, with the exception of strains housing *parMRC*$_C$ and *parMRC*$_D$ combinations, which showed a minor incompatibility phenotype. In conclusion, we have provided the first direct evidence of plasmid incompatibility in *Clostridium spp*. and have shown

experimentally that the compatibility of conjugative *C. perfringens* plasmids correlates with the presence of *parMRC*-like partitioning systems of different phylogenetic subfamilies.

Introduction

Plasmid incompatibility is defined as the inability of two plasmids to coexist in a single strain in the absence of selective pressure (1,2). Generally, plasmids that have common replication, replication control or maintenance elements are considered incompatible. The sharing of these mechanisms can result in an inability to correct copy number imbalances that occur as a consequence of random selection for replication or partitioning from an otherwise heterologous plasmid population (2), ultimately leading to destabilisation of plasmid inheritance.

The Gram-positive pathogen *Clostridium perfringens* produces an extensive repertoire of toxins and extracellular enzymes (3), many of which are encoded by genes that are carried on conjugative plasmids. *C. perfringens* strains can carry up to five conjugative toxin or antibiotic resistance plasmids, each of which shares an essentially conserved 35 kb backbone (4-9). The *tcp* conjugation locus is found within this conserved backbone as are the genes required for plasmid replication, regulation and maintenance, which are located within a locus called the Central Control Region (CCR) (5-7).

All known conjugative plasmids in *C. perfringens* are related to the archetypal, low copy number, tetracycline resistance plasmid pCW3 (4,7). Most of these plasmids have a very similar replication initiation or Rep protein, which raises questions as to how such plasmids can be stably maintained in the same cell. For example, the Australian necrotic enteritis strain EHE-NE18 carries three large conjugative plasmids pJIR3535, pJIR3537 and pJIR3844 that encode very similar Rep proteins (98% amino acid sequence identity) (5). These plasmids stably coexist despite the conventional relationship between shared replication mechanisms and plasmid incompatibility.

Previous studies have noted instances of apparent plasmid incompatibility in *C. perfringens,* where toxinotype B and C isolates seem to be restricted in regards to the β-toxin and ε-toxin plasmid combinations they can possess (10-13). A recent survey of available plasmid sequence data has started to provide some insight into the basis of plasmid compatibility in *C. perfringens* (14). The results highlighted the similarity observed between Rep proteins of this family of conjugative plasmids and identified the presence of ten families (*parMRC*$_{A-J}$) of *parMRC*-like plasmid partitioning systems, with differences in amino acid sequence identity between each ParM family ranging from 15% to 54% (5,6,14,15). Plasmids from the same *parMRC* phylogenetic group have not been found in a single *C. perfringens* isolate, suggesting that these partitioning families play a role in the determination of plasmid compatibility (14).

Plasmid partitioning is generally mediated by tripartite systems that can be classified into three families depending on the type of NTPase they encode: specifically, the type I (ParA Walker A-like), type II (ParM actin-like), and type III (TubZ Tubulin-like) families (16,17). Type II plasmid partitioning systems have been most well characterised in *Escherichia coli* and *Staphylococcus aureus* and generally consist of three components: ParM, an actin-like filament forming protein, ParR, a DNA-binding adapter protein that links the growing ParM filament to a plasmid centromere, called *parC* (17,18). Together these components act to mediate the correct positioning of plasmids on either side of the septum during cell division, thus ensuring that each daughter cell receives a copy of the plasmid. Although the role of *parMRC* systems has been well characterised in regards to their ability to stabilise plasmid inheritance, less is known about the way in which they contribute to plasmid incompatibility. Most research concerning partition-mediated incompatibility has focused on type I partition systems, where several models have been proposed (19-22).

The current study aimed to elucidate whether there was a direct relationship between the type II partitioning family designation and plasmid compatibility in *C. perfringens*. We postulated that plasmids encoding identical partitioning families would be incompatible when introduced

into a single *C. perfringens* strain, whereas plasmids that encoded different partitioning families will be compatible; that is, they would remain stable in the absence of direct selection. This hypothesis was tested by introducing native *C. perfringens* plasmids that encoded identical *parMRC*$_C$ or *parMRC*$_D$ homologues or different combinations of *parMRC*$_A$, *parMRC*$_C$ *and parMRC*$_D$ homologues into a single strain and determining the stability of each plasmid in the absence of direct selection. The results provide evidence that the *parMRC* systems are important for plasmid compatibility in *C. perfringens.*

Methods

Plasmids, bacterial strains and culture conditions. All *C. perfringens* strains and plasmids used in this study are listed in Table 4.1. Strains were grown in fluid thioglycolate medium (FTG) (Oxoid) or, tryptone-peptone-glucose (TPG) broth (23) and on nutrient agar (NA) (Rood, 1983) or brain heart infusion (BHI) agar (Difco) supplemented with glucose (0.375 % w/v). Where appropriate NA was supplemented with antibiotics at the following concentrations: chloramphenicol (Cm) 20 µg/ml, tetracycline (Tc) 10 µg/ml, erythromycin (Em) 50 µg/ml, rifampicin (Rif) 10 µg/ml, nalidixic acid (Nal) 10 µg/ml, streptomycin (Sm) 1 mg/ml and saturated potassium chlorate (Chl) 1% (v/v). All agar cultures were incubated overnight at 37°C in an anaerobic jar (Oxoid) containing 10% (v/v) CO_2, 10% (v/v) H_2 and 80% (v/v) N_2.

Table 4.1 Bacterial strains and plasmids

Strain	Description	Reference/origin
C. perfringens		
EHE-NE18	Australian necrotic enteritis isolate (pJIR3535, pJIR3537, pJIR3843, pJIR3844)	(24)
JIR39	CW362 Sm^RChl^R	(25)
JIR325	Strain 13 Rif^RNal^R	(26)
JIR4195	JIR325(pCW3) $Rif^RNal^R Tc^R$	(27)
JIR4323	JIR325(pJIR1584) $Rif^RNal^RCm^R$	JIR325-derived Cm^R transconjugant
JIR4394	Strain 13 Sm^RChl^R	(7)
JIR4984	JIR325(pJIR3120) $Rif^RNal^RCm^R$	(27)
JIR12012	JIR325(pJIR3118) Rif^RNal^R	(27)
JIR12293	JIR325(pJIR3536) $Rif^RNal^RCm^R$	(5)
JIR13003	EHE-NE18 (pJIR4709, pJIR3537, pJIR3843 pJIR3844) Em^RTc^R	(X. Han and J. I. Rood, unpublished)
JIR13172	JIR39(pCW3) $Sm^RChl^RTc^R$	Tc^R transconjugant (JIR4195 x JIR39)
JIR13264	JIR325(pJIR4533) $Rif^RNal^REm^R$	JIR325 derived Em^R transconjugant
JIR13265	JIR4394(pJIR4533) $Sm^RChl^REm^R$	Em^R transconjugant (JIR13264 x JIR4394)

JIR13492	JIR4394(pCW3) $Sm^RChl^RTc^R$	Tc^R transconjugant (JIR4195 x JIR4394)
JIR13493	JIR4394(pJIR4709) $Sm^RChl^REm^R$	Em^R transconjugant (JIR13003 x JIR4394)
JIR13405	JIR325(pCW3, pJIR1584) $Rif^RNal^RTc^RCm^R$ (C_{Tc}+C_{Cm})	Tc^R transconjugant (JIR13492 x JIR4323)
JIR13406	JIR325(pJIR3536, pCW3) $Rif^RNal^RTc^RCm^R$ (A_{Cm}+C_{Tc})	Cm^R transconjugant (JIR12293 x JIR4195)
JIR13407	JIR325(pJIR4709, pJIR3120) $Rif^RNal^REm^RCm^R$ (A_{Em}+D_{Cm})	Em^R transconjugant (JIR13493 x JIR4984)
JIR13408	JIR325(pCW3, pJIR3120) $Rif^RNal^RTc^RCm^R$ (C_{Tc}+D_{Cm})	Tc^RCm^R Transconjugant (JIR13492 x JIR4984)
JIR13409	JIR325(pJIR3120, pJIR4533) $Rif^RNal^REm^RCm^R$ (D_{Ern}+D_{Cm})	Em^RCm^R Transconjugant (JIR13265 x JIR4984)
JIR13410	JIR325(pCW3, pJIR4533) $Rif^RNal^RTc^REm^R$ (C_{Tc}+D_{Em})	Tc^REm^R Transconjugant (JIR13265 x JIR4195)

Plasmid	**Description**	**Reference**
pCW3	47 kb; Tc^R, *parMRC$_C$*	(28)
pJIR1584	pCW3 Δ*tet(P)*Ω*catQ*	(Johanesen, Lyras and Rood unpublished)
pJIR3118	48 kb; *etx$^+$, parMRC$_D$*	(27)

pJIR3120	pJIR3118 Δ*etx*Ω*catP*	(27)
pJIR3536	pJIR3535 Δ*netB*Ω*catP, parMRC$_A$*	(29)
pJIR4533	pJIR3118 *etx*::*ermB*	pJIR3118 *etx* TargeTron insertion mutant
pJIR4709	pJIR3535 Δ*netI*Ω*ermQ*	(X. Han and J. I. Rood, unpublished)

Cm^R, chloramphenicol resistance, Em^R, erythromycin resistance, Tc^R, tetracycline resistance, Nal^R, nalidixic acid resistance, Rif^R, rifampicin resistance, Sm^R, streptomycin resistance, Chl^R, potassium chlorate resistance.

Construction of genetically marked parMRCD family plasmids: All plasmids used in this study are listed in Table 4.1. The epsilon toxin gene, *etx*, in the *parMRC$_D$* family plasmid pJIR3118 was insertionally inactivated using TargeTron mutagenesis as previously described (5,30). Mutagenesis resulted in the insertion of a group II intron encoding the *ermB* erythromycin resistance determinant into the *etx* gene, resulting in the generation of pJIR4533. Mutants were confirmed as previously described by Southern hybridisation and PCR (Cheung (30).

Molecular methods: Genomic DNA (gDNA) was isolated after overnight growth in FTG broth, as previously described (31). PCR screening was conducted using *Taq* DNA polymerase (Roche) and a 0.5 µM of each specific oligonucleotide primer. Denaturation (94°C 30 seconds), annealing (50-55°C for 1 min) and extension (72 °C for 1 minute) steps were carried out for 35 cycles. All gDNA and PCR products were subjected to gel electrophoresis on either a 0.8% (w/v) or 1% (w/v) agarose gel for 40 minutes at 100 V, before being visualised using a Chemidoc XRS+ (Biorad). All oligonucleotide primers used are listed in Table S4.1. Alignment of the putative origin of replication sequences and Rep proteins for pJIR3118, pJIR3536 and pCW3 were prepared using CLUSTALΩ web tool (32).

Construction of incompatibility test strains: Conjugation was performed as previously described (25,28). All transconjugants were selected on nutrient agar supplemented with appropriate antibiotic selection. Incompatible plasmids were maintained by selection for the antibiotic resistance determinants carried by each plasmid.

Stability assay: *C. perfringens* strains carrying two conjugative plasmids with different resistance genes were subcultured from glycerol stocks stored at -20°C into pre-boiled FTG media before being incubated overnight at 37°C. Each strain was plated onto nutrient agar (NA) supplemented with the appropriate antibiotics and incubated anaerobically at 37°C for 24 hours. Single colonies were taken from these plates and subcultured onto NA supplemented with appropriate antibiotics and incubated anaerobically at 37°C overnight. To determine the relative stability of each plasmid, each strain was passaged on solid media, and sampled, before 100 colonies were patched onto appropriate selective media each day on three consecutive days. On day 0 an initial sample was taken from the primary streak of the overnight selection plates and resuspended in 500 µL of heart infusion (BHI) diluent (BHI (Oxoid) broth diluted 1:5). This cell suspension was serially diluted and plated onto appropriate selection plates for both plasmids, each strain was incubated anaerobically at 37°C overnight. One hundred colonies of each strain were patched onto selection plates for each plasmid. The relative stability of each plasmid was determined by comparing the growth of the patches on each selection plate. This process was repeated on days 1 and 2, however, dilutions of each strain were plated onto nutrient agar supplemented with antibiotics to select for each plasmid individually. Strains were patched as before and the relative stability of each plasmid was determined as before. gDNA was harvested from each strain on days 0 and 2 and PCRs specific for the relevant *parM* and antimicrobial resistance genes were used to determine plasmid profiles at these time points. A control experiment was also conducted to determine the baseline stability of each individual plasmid (pCW3, pJIR1584, pJIR3120, pJIR4533, pJIR4250 or pJIR3536). Separate strains each carrying one of these plasmids were passaged

on NA without selection for two days, and plasmid stabilities were determined by comparing the number of patches grown on medium with and without antibiotics.

Results

Plasmids that share identical *parMRC$_C$* or *parMRC$_D$* partitioning systems are incompatible in *C. perfringens*

Previous studies have identified ten families of *parMRC*-like partitioning systems in *C. perfringens* (*parMRC$_{A-J}$*) (5-7,14,15). It was suggested that these partitioning systems form the basis for plasmid incompatibility, since multiple plasmids encoding identical *parMRC*-like partitioning systems have not been observed in native *C. perfringens* isolates (12,14). To test this hypothesis conjugative transfer was used to construct a series of strains that each contained two genetically marked derivatives of the native conjugative *C. perfringens* plasmids, pJIR3535 (*parMRC$_A$*), pCW3 (*parMRC$_C$*) and pJIR3118 (*parMRC$_D$*) (Table 4.1) (Figure 4.1).

The stability of each plasmid alone was assessed prior to construction of these test strains. Separate strains that each harboured one conjugative plasmid (pCW3, pJIR1584, pJIR3120, pJIR4533, pJIR4709 or pJIR3536) were passaged for two days on non-selective media. Samples were taken at the start and conclusion of the experiment and the percentage of the population that had retained the plasmid was determined by comparing the number of patches grown on media supplemented with antibiotics to the number of patches grown on media without antibiotics. All plasmids remained stable over the course of the experiment (Figure S4.1).

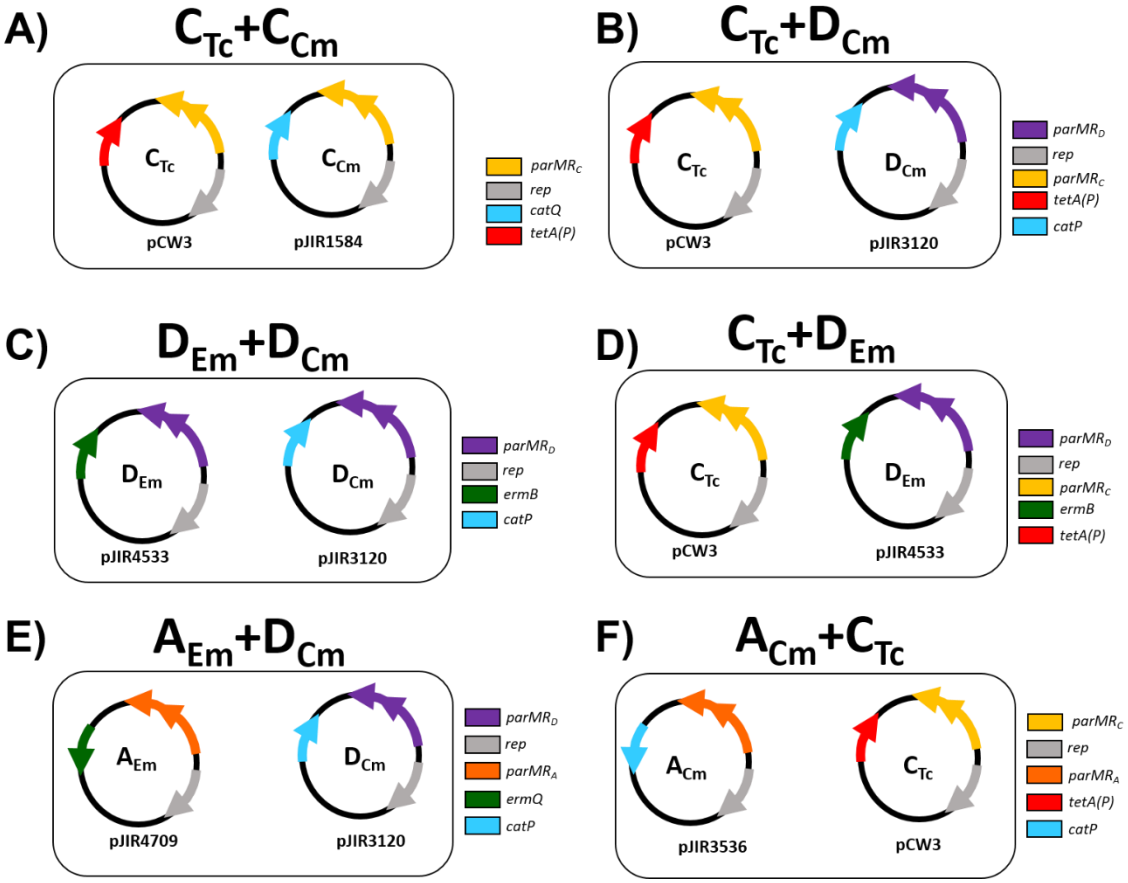

Figure 4.1. Diagrammatic representation of strains used in plasmid stability experiments. Strains were constructed by transferring each plasmid into a JIR325 background *via* conjugation. Each strain was given a designation (e.g. C_{Tc}+C_{Cm}) based on the *parMRC* family plasmids they carry and the selection markers present on those plasmids. Legend: A) JIR13405 (Shown as C_{Tc}+C_{Cm}) contains two *parMRC*$_C$ plasmids, pCW3 and pJIR1584. B) JIR13408 (C_{Tc}+D_{Cm}) contains a *parMRC*$_C$ encoding-plasmid pCW3 and a *parMR*$_D$ encoding-plasmid pJIR3120. C) JIR13409 (D_{Ern}+D_{Cm}) contains two *parMRC*$_D$ encoding-plasmid pJIR4533 and pJIR3120 D) JIR13410 (C_{Tc}+D_{Em}) contains a *parMRC*$_C$ encoding-plasmid pCW3 and a *parMRC*$_D$-encoding plasmid, pJIR4533 E) JIR13407 (A_{Em}+D_{Cm}) contains a *parMRC*$_A$ encoding-plasmid pJIR4250 and a *parMRC*$_D$ encoding-plasmid pJIR3120. F) JIR13406 (A_{Cm}+C_{Tc}) contains a *parMRC*$_A$ encoding plasmid pJIR3536 and a *parMRC*$_C$ encoding-plasmid pCW3. The *tetA(P)* gene is represented by the red arrow, *catQ* is shown in blue, the grey arrow indicates *rep*, *parMR*$_A$ is indicated by the orange arrows *parMR*$_C$ is indicated by the yellow arrows, *parMRC*$_D$ is denoted by the purple arrows.

To determine the relative stability of multiple plasmids encoding identical *parMRC* homologues, the *parMRC*$_C$ family plasmids pCW3 (Tc^R) and pJIR1584 (Cm^R) were introduced into a JIR325 background *via* conjugation to construct JIR13405. This derivative was designated as the C_{Tc}+C_{Cm} strain where C represents the *parMRC* family designation of each plasmid and the subscripts denote the resistance determinant present on each plasmid (Figure 4.1A).

The resultant C_{Tc}+C_{Cm} strain was passaged on media supplemented with tetracycline or chloramphenicol to select for each plasmid individually (pCW3 and pJIR1584, respectively). Viable counts were carried out each day (0, 1, 2) and 100 single colonies were cross-patched onto media selective for each plasmid to determine their relative stability. Near symmetric loss of the non-selected plasmid was observed. Selection on tetracycline for pCW3 led to loss of pJIR1584, with only 8% of the population retaining the plasmid after two days (Figure 4.2A), and selection on chloramphenicol for pJIR1584 led to the loss of pCW3, with only 18% of the population retaining pCW3 after two days (Figure 4.2A). To validate the incompatibility observed between plasmids carrying the same *parMRC* locus a similar experiment was carried out with a strain (D_{Em}+D_{Cm}) carrying two *parMRC*$_D$ family plasmids pJIR3120 (Cm^R) and pJIR4533 (Em^R) (Figure 4.1C). This strain was passaged on media supplemented with erythromycin or chloramphenicol to select for pJIR4533 or pJIR3120, respectively. Selection of pJIR4533 using erythromycin resulted in the loss of pJIR3120, with only 8% of the population retaining the plasmid after two days (Figure 4.2B). Similarly, when pJIR3120 was selected using chloramphenicol, pJIR4533 was lost, with only 41% retention at day 2. PCR screening of genomic DNA samples before and after passage for *par* (*parM*$_C$ and *parM*$_D$) and antibiotic resistance genes (*tetA*(P) *ermB* and *catP*) supported the designated plasmid profiles deduced from the observed resistance profiles (data not shown).

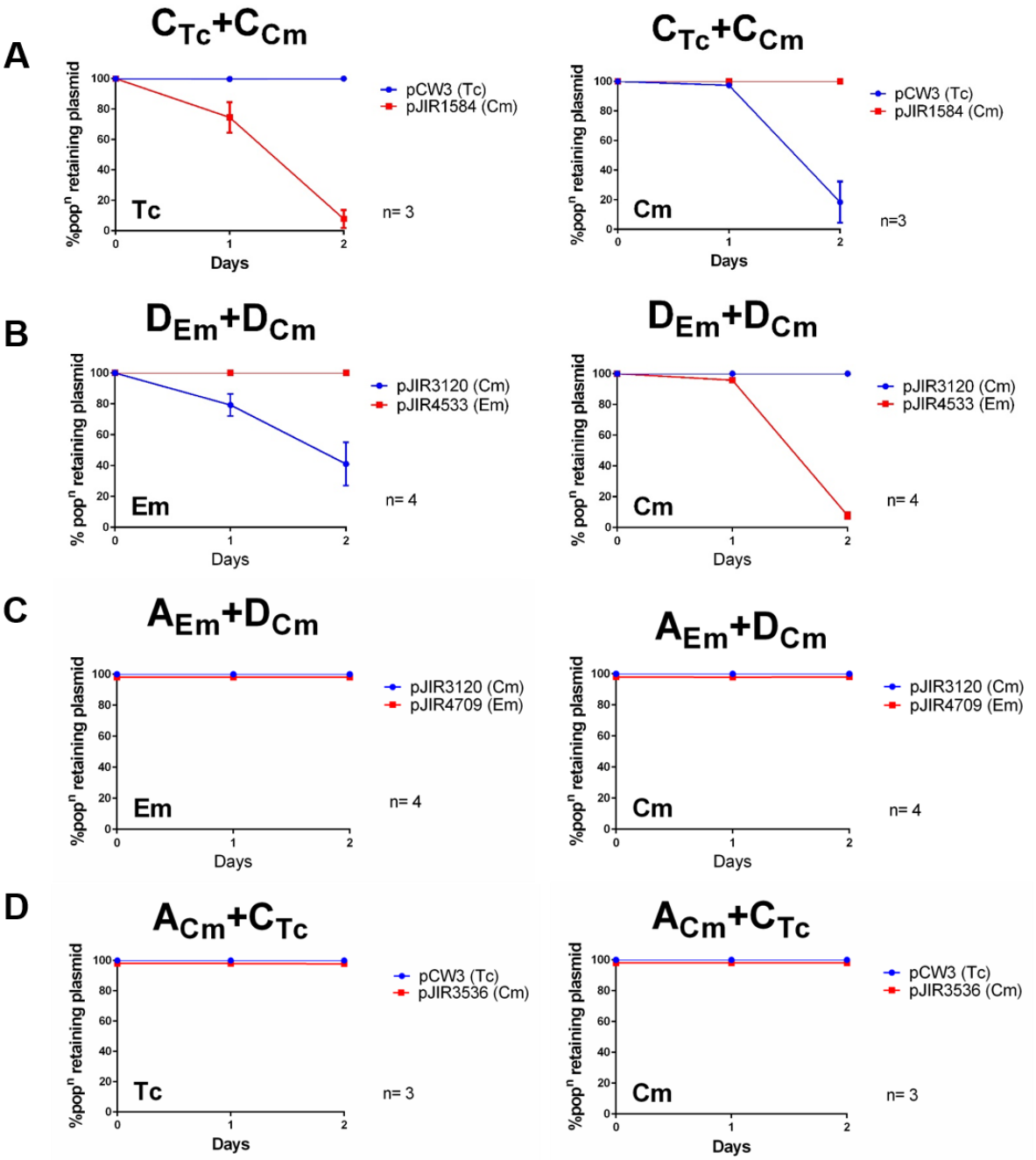

Figure 4.2. Plasmid stability assays: Each strain carried two plasmids as described earlier and as indicated by the strain designations. The strains $C_{Tc}+C_{Cm}$ (A) $D_{Em}+D_{Cm}$ (B), $A_{Em}+D_{Cm}$ (C) and $A_{Cm}+C_{Tc}$ (D) were passaged on medium selective for one plasmid only (indicated on each graph) for two days. The relative plasmid stability was determined at 0, 1 and 2 days by patching 100 colonies onto each medium. Error bars represent the mean±SEM.

C. perfringens **plasmids that encode different *parMRC*-like partitioning systems are compatible**

To determine if plasmids encoding distinct *parMRC* homologues could stably coexist when introduced into a single strain of *C. perfringens*, several strains containing co-resident plasmids encoding different partitioning system homologues were constructed. Pairs of these plasmids were introduced into a JIR325 background to construct the A_{Cm}+C_{Tc}, A_{Em}+D_{Cm} (Figure 4.1E & 4.1F) and C_{Tc}+D_{Cm} strains (Figure 4.1B), which then were passaged and the stability of the co-resident plasmids determined as before. The results showed that the A_{Cm}+C_{Tc} and A_{Em}+D_{Cm} plasmid combinations were 100% stable over the course of the experiments, even when selection was for the co-resident plasmid (Figure 4.2C & 4.2D). The C_{Tc}+D_{Cm} test strain, however, showed slight plasmid instability. When passaged in the presence of chloramphenicol selection (pJIR3120), tetracycline resistance (pCW3) was lost to some extent with 88% of the population continuing to carry the plasmid. By contrast, pJIR3120 remained stable even in the absence of selection for chloramphenicol resistance (Figure 4.3A). PCR analysis of the *par* and antibiotic resistance genes supported all of the plasmid profiles deduced by the resistance profiles, both before and after passage.

To determine if this minor plasmid incompatibility phenotype observed between the C_{Tc} and D_{Cm} plasmids was an artefact introduced by antibiotic selection, an alternative C_{Tc}+D_{Em} strain was constructed using the plasmids pCW3 (*parMRC*$_C$,Tc^R) and pJIR4533 (*parMRC*$_D$, Em^R). This strain was passaged and tested as before, the results revealed only a minimal loss of tetracycline resistance upon passage in the presence of erythromycin (98% stability) (Figure 4.3B). Both C+D strains were also passaged in the absence of any selection for six days. A similar trend was observed, with pCW3 slightly less stable than pJIR3120 (Figure 4.3C). To ensure that the trend observed for these plasmid combinations was due to interaction between the plasmids rather than an inherent instability of pCW3, parent strains carrying each individual plasmid (pCW3, pJIR4533 or pJIR3120) were passaged on non-selective media and their

stability was determined. Passage on non-selective media did not result in any significant instability (Figure S4.1) suggesting that the low-level C+D instability was a result of plasmid interactions.

The minor incompatibility phenotype observed for the C_{Tc}+D_{Cm} combination was not seen for the A_{Cm}+C_{Tc} or A_{Em}+D_{Cm} combinations. This result suggested that the partition systems of the C_{Tc} and D_{Cm} plasmids may be more similar than that of the A_{Cm}+C_{Tc} or A_{Em}+D_{Cm} combinations, potentially leading to the minor incompatibility phenotype. However, there was no apparent correlation between the amino acid or nucleotide sequence identity of the ParM, ParR or *parC* components and the minor incompatibility phenotype (Table 4.2), suggesting that these different partitioning systems were unlikely to be involved in this phenomenon.

Table 4.2 Sequence identity between *parMRC* components of the plasmids pJIR3536 (A), pCW3 (C) and pJIR3120 (D).

Component	% Identity		
ParM*			
	$ParM_A$	$ParM_C$	$ParM_D$
$ParM_A$	100%		
$ParM_C$	26.2%	100%	
$ParM_D$	32.3%	24.5%	100%
ParR*			
	$ParR_A$	$ParR_C$	$ParR_D$
$ParR_A$	100%		
$ParR_C$	15.4%	100%	
$ParR_D$	18.6%	27.3%	100%
***parC*#**			
	$parC_A$	*$parC_C$*	*$parC_D$*
$parC_A$	100%		
$parC_C$	46.6%	100%	
$parC_D$	46.7%	44.8%	100%

* Amino acid sequence identity.
# Nucleotide sequence identity.

Since another facet of plasmid incompatibility involves shared replication mechanisms, the putative origin of replication and replication initiator proteins of each plasmid were compared. The amino acid sequences of the Rep proteins from pCW3, pJIR3120 and pJIR3536 (a plasmid that was compatible with pCW3 and pJIR3120) were highly conserved (98% amino acid identity) with no obvious patterns of amino acid sequence changes (Figure S4.2).

The putative origin of replication (*oriV*) of pCW3-like plasmids consists of a series of conserved inverted repeat structures (IR1-IR5). Alignment of the *oriV* sites (from downstream of IR1 to the *rep* start codon) of pCW3 (C), pJIR3536 (A) and pJIR3120 (D) showed that when compared to the *oriV* of pCW3, the *oriV* site of pJIR3536 had five nucleotide differences within the IR2 loop, as well as two nucleotide differences in the left-hand repeat and eight other nucleotide substitutions downstream of IR2 (Figure 4.4). pCW3 and pJIR3536 were stable when introduced into JIR325, suggesting that differences in the partitioning family as well as differences in the *oriV* were enough to allow these plasmids to coexist. By contrast, pJIR3120 showed two single nucleotide differences within the loop of IR2, but was otherwise identical to the pCW3 origin. When pCW3 and pJIR3120 were introduced into JIR325, pCW3 was lost at low frequency from the population in the absence of selection. When JIR325 carrying pCW3 in isolation was passaged in the absence of selection, the plasmid was stable, indicating that the C_{Tc}+D_{Cm} result was due to the introduction of a pJIR3118 derivative. This result suggests that replication and partitioning mechanisms may play a cooperative role in plasmid incompatibility.

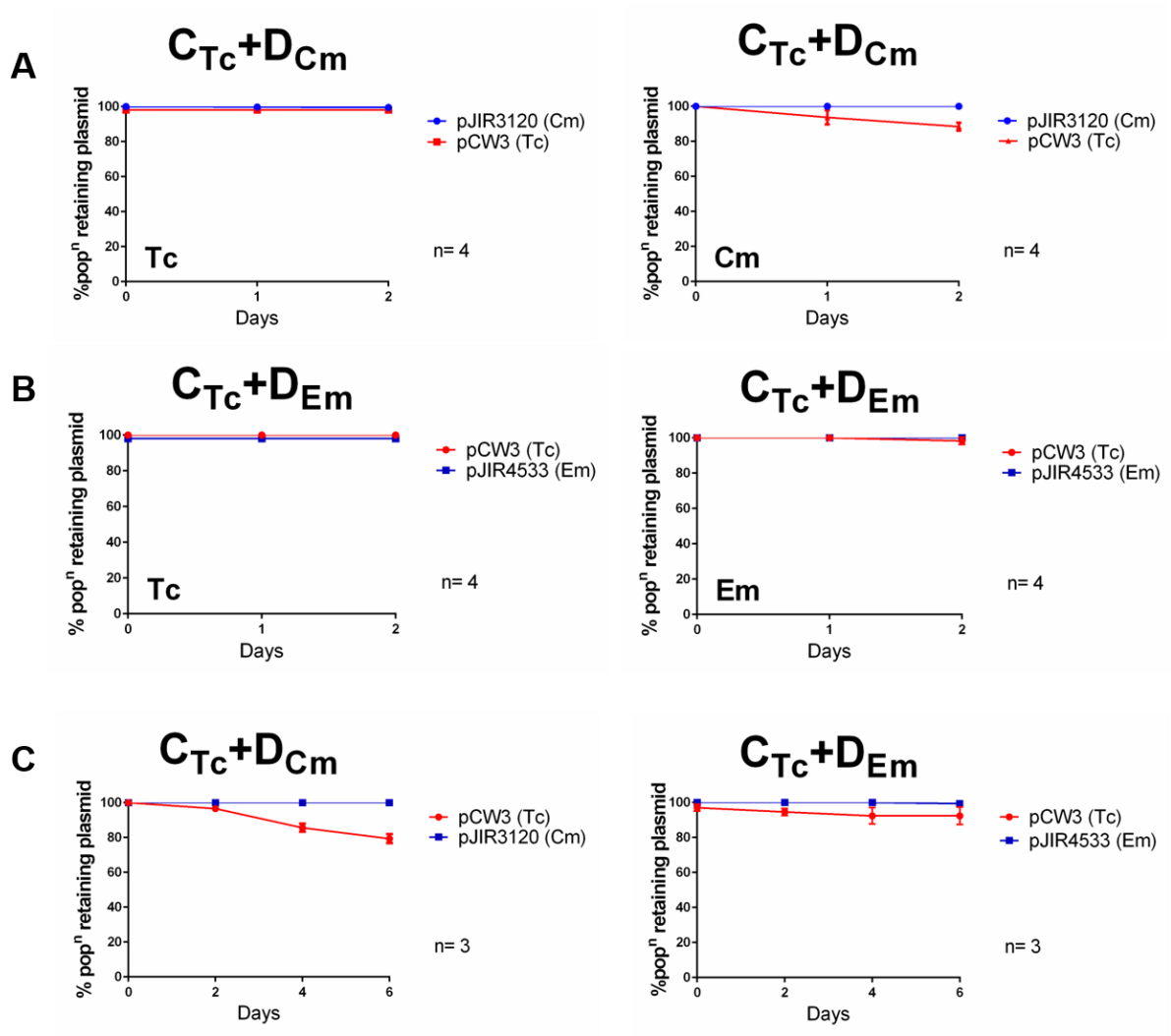

Figure 4.3. C+D plasmid stability assays: Each strain carried two plasmids as described earlier and as indicated by the strain designations. The strains $C_{Tc}+D_{Cm,}$ (A) and $C_{Tc}+D_{Em}$ (B) were passaged on medium selective for each plasmid (indicated on each graph) over the course of two days. The relative plasmid stability was determined at 0, 1 and 2 days by patching 100 colonies onto each medium. (C) Both incompatibility strains $C_{Tc}+D_{Cm}$ and $C_{Tc}+D_{Em}$ were passaged in the absence of selection for 6 days and plasmid stability was determined on 0, 2, 4 and 6 days as described above. Error bars represent the mean±SEM.

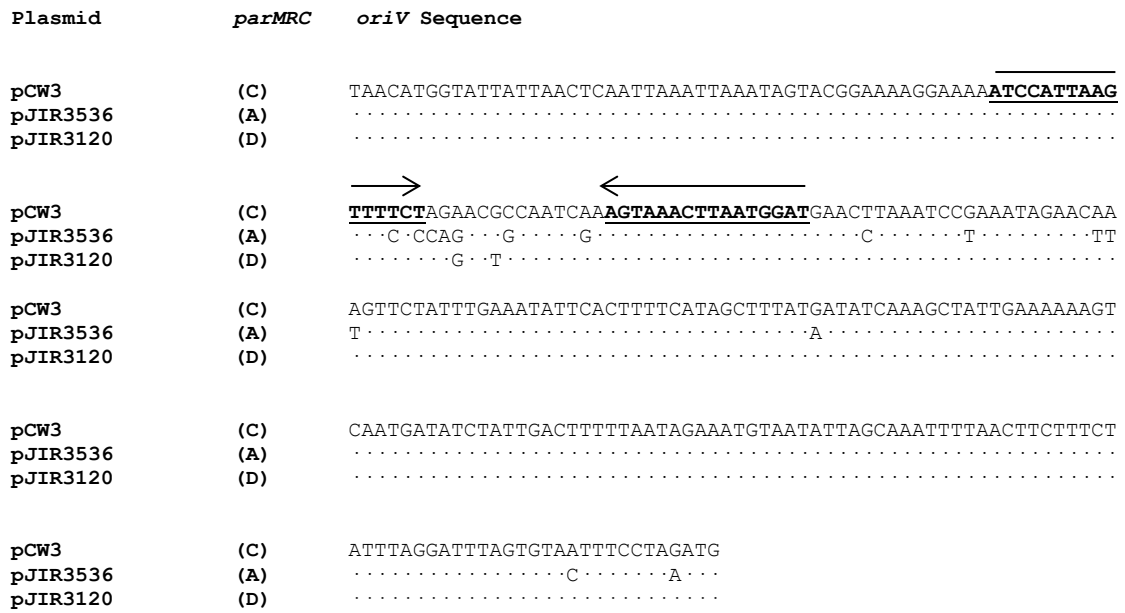

Figure 4.4. Sequence alignments of *oriV* from pJIR3536, pJIR3120 and pCW3. The *oriV* regions (downstream of IR-1 to the *rep* start codon) of pCW3, pJIR3120 and pJIR3536 were aligned using the EMBL-EBI Clustal Ω alignment tool (32). All sequences were aligned using pCW3 as a reference, conserved nucleotides are shown as dots and nucleotide changes are indicated. IR2 is indicated by the arrows and shown by the underlined and bolded text.

Discussion

The link between plasmid incompatibility and shared replication control and initiation mechanisms is well established (2,33,34). However, previous studies have shown that *C. perfringens* isolates can house multiple, highly similar, conjugative plasmids (4-6,8,9), despite sharing Rep proteins with ≥98% amino acid sequence identity (7,14). This observation suggests that plasmid encoded factors other than the replication region are contributing to plasmid incompatibility in *C. perfringens*.

In this study, we have provided evidence that, in this series of plasmids, incompatibility correlated with the *parMRC* system designation. When plasmids encoding identical *parMRC* systems were introduced into the same *C. perfringens* strain they were incompatible (C_{Tc}+C_{Cm} and D_{Em}+D_{Cm}). By contrast, when plasmids with different *parMRC* families were introduced into the same *C. perfringens* strain they were compatible (A_{Cm}+C_{Tc}, A_{Em}+D_{Cm}, C_{Tc}+D_{Cm} and C_{Tc}+D_{Em}). To our knowledge, this is the first definitive report of plasmid incompatibility in *Clostridium spp*.

Several models for partition based incompatibility have been proposed, however most research has focused on the Type I partition systems of the *E. coli* plasmids P1, pB171 and F, rather than the Type II *parMRC* partition systems that are encoded by the pCW3-like plasmids. A simple mismatched pairing model has been used to describe incompatibility mediated by *parMRC* partitioning systems in other bacteria (35-38). In this model two plasmids that share similar *parC* centromeres form heterologous pairs mediated by their similar ParR and ParM components, ultimately leading to incorrect segregation/positioning at cell division and the generation of daughter populations retaining only one plasmid type (20,35,36,38-40). Support for this model was provided by studies that showed that the promiscuous pB171 ParR protein could bind to both its cognate *parC* centromere as well as the centromere of an

unrelated pCP301 plasmid, leading to destabilisation of proper partitioning and incompatibility (41).

A similar scenario can be envisioned for partition-mediated incompatibility in *C. perfringens*, where ParR homologues are predicted to interact with their cognate *parC* centromere with higher affinity than a disparate *parC* centromere site. When a resident plasmid shares the same centromere as a newly introduced plasmid, the inheritance of one or both plasmids will be destabilised, thereby leading to incompatibility. Functional characterisation of the *C. perfringens* ParMRC components and their protein-protein and protein-DNA interactions is required to validate this hypothesis.

Although our results show that two plasmids encoding identical partitioning systems are incompatible, there are other plasmid-encoded factors that may contribute to incompatibility. Although the Rep proteins and *oriV* sites of pCW3-like conjugative plasmids do not resolve into clear phylogenetic groups, subtle differences either in the sequence of the Rep proteins, the Rep binding sites in *oriV* or the sequences of unidentified control elements also may contribute to incompatibility. Plasmids encoding different *parMRC* homologues were shown to be completely stable when introduced into the same strain (A_{Em}+D_{Cm} and A_{Cm}+C_{Tc}), with the exception of the pCW3 and pJIR3118-based plasmid combinations (C+D), which showed a slight plasmid incompatibility phenotype (Figure 4.3). This result supports the assertion that factors other than partition components may also contribute to plasmid incompatibility. In this context, although alignment of the Rep amino acid sequences showed no obvious conserved changes some sequence variation was observed in the IR2 loop region of the *oriV* sites. IR2 is essential for plasmid replication, as shown by previous transposon mutagenesis studies (7).

The role of IR2 in plasmid incompatibility is unclear, but it may constitute either an important regulatory element or the site of Rep binding and therefore replication initiation. Other studies have shown that it is possible to generate new incompatibility groups by introducing a single

base pair change in the negative control element RNA I of ColE1 (34), therefore we cannot rule out the possibility that even minor sequence changes may affect plasmid incompatibility in *C. perfringens*. Our results suggest that both the replication and *parMRC* partitioning systems are involved in plasmid incompatibility. The C_{Tc}+D_{Em} minor incompatibility phenotype suggests that when the replicon is very similar, but the partition systems are different, limited incompatibility is observed. This result may imply that otherwise identical replicons are rendered compatible by the possession of different *parMRC* partitioning homologues. Whether this compatibility is a result of spatial resolution or isolation of different plasmid populations by their partitioning system within the cell is unclear and requires further experimental interrogation. By contrast, when plasmids share both a similar replicon and *parMRC* partitioning system (C_{Tc}+C_{Cm} or D_{Em}+D_{Cm}), strong incompatibility is observed. The mechanism by which these two systems cooperate to influence plasmid incompatibility is not clear. Future experiments are required to test each of these factors in isolation on otherwise identical vectors.

In summary, we report an important increase in our understanding of plasmid incompatibility in *C. perfringens* by demonstrating experimentally that essentially native *C. perfringens* plasmids may be incompatible and that this incompatibility correlates with the *parMRC* phylogenetic groups of the plasmids. Further studies are required to address the more subtle contributions of variation of the Rep protein and the *oriV* site to plasmid incompatibility.

Acknowledgements

This research was supported by Discovery Project Grant DP160102680 from the Australian Research Council. TDW was the recipient of an Australian Postgraduate Award.

References

1. Novick, R.P., Clowes, R.C., Cohen, S.N., Curtiss, R., 3rd, Datta, N. and Falkow, S. (1976) Uniform nomenclature for bacterial plasmids: a proposal. *Bacteriological Reviews*, **40**, 168-189.
2. Novick, R.P. (1987) Plasmid incompatibility. *Microbiological Reviews*, **51**, 381-395.
3. Revitt-Mills, S.A., Rood, R.I. and V., A. (2015) *Clostridium perfringens* extracellular toxins and enzymes: 20 and counting. *Microbiology Australia*, **36**, 114-117.
4. Li, J., Adams, V., Bannam, T.L., Miyamoto, K., Garcia, J.P., Uzal, F.A., Rood, J.I. and McClane, B.A. (2013) Toxin plasmids of *Clostridium perfringens*. *MMBR* **77**, 208-233.
5. Bannam, T.L., Yan, X.X., Harrison, P.F., Seemann, T., Keyburn, A.L., Stubenrauch, C., Weeramantri, L.H., Cheung, J.K., McClane, B.A., Boyce, J.D. *et al.* (2011) Necrotic enteritis-derived *Clostridium perfringens* strain with three closely related independently conjugative toxin and antibiotic resistance plasmids. *MBio*, **2**, e00190-00111.
6. Parreira, V.R., Costa, M., Eikmeyer, F., Blom, J. and Prescott, J.F. (2012) Sequence of two plasmids from *Clostridium perfringens* chicken necrotic enteritis isolates and comparison with *C. perfringens* conjugative plasmids. *PLOS One*, **7**, e49753.
7. Bannam, T.L., Teng, W.L., Bulach, D., Lyras, D. and Rood, J.I. (2006) Functional identification of conjugation and replication regions of the tetracycline resistance plasmid pCW3 from *Clostridium perfringens*. *J Bacteriol* **188**, 4942-4951.
8. Miyamoto, K., Fisher, D.J., Li, J., Sayeed, S., Akimoto, S. and McClane, B.A. (2006) Complete sequencing and diversity analysis of the enterotoxin-encoding plasmids in *Clostridium perfringens* type A non-food-borne human gastrointestinal disease isolates. *J. Bacteriol.*, **188**, 1585-1598.
9. Miyamoto, K., Li, J., Sayeed, S., Akimoto, S. and McClane, B.A. (2008) Sequencing and diversity analyses reveal extensive similarities between some epsilon-toxin-encoding plasmids and the pCPF5603 *Clostridium perfringens* enterotoxin plasmid. *J. Bacteriol.*, **190**, 7178-7188.

10. Gurjar, A., Li, J. and McClane, B.A. (2010) Characterization of toxin plasmids in *Clostridium perfringens* type C isolates. *Infect. Immun.*, **78**, 4860-4869.

11. Sayeed, S., Li, J. and McClane, B.A. (2010) Characterization of virulence plasmid diversity among *Clostridium perfringens* type B isolates. *Infect. Immun.*, **78**, 495-504.

12. Freedman, J.C., Theoret, J.R., Wisniewski, J.A., Uzal, F.A., Rood, J.I. and McClane, B.A. (2014) *Clostridium perfringens* type A-E toxin plasmids. *Res. Microbiol.*, **166**, 264-279.

13. Lepp, D., Gong, J., Songer, J.G., Boerlin, P., Parreira, V.R. and Prescott, J.F. (2013) Identification of accessory genome regions in poultry *Clostridium perfringens* isolates carrying the *netB* plasmid. *J. Bacteriol.*, **195**, 1152-1166.

14. Adams, V., Watts, T.D., Bulach, D.M., Lyras, D. and Rood, J.I. (2015) Plasmid partitioning systems of conjugative plasmids from *Clostridium perfringens*. *Plasmid*, **80**, 90-96.

15. Adams, V., Li, J., Wisniewski, J.A., Uzal, F.A., Moore, R.J., McClane, B.A. and Rood, J.I. (2014) Virulence plasmids of spore-forming bacteria. *Microbiology Spectrum*, **2**, 10.1128/microbiolspec.PLAS-0024-2014.

16. Salje, J., Gayathri, P. and Lowe, J. (2010) The ParMRC system: molecular mechanisms of plasmid segregation by actin-like filaments. *Nat. Rev. Microbiol.*, **8**, 683-692.

17. Gerdes, K., Howard, M. and Szardenings, F. (2010) Pushing and pulling in prokaryotic DNA segregation. *Cell*, **141**, 927-942.

18. Baxter, J.C. and Funnell, B.E. (2014) Plasmid partition mechanisms. *Microbiology spectrum*, **2**, 10.1128/microbiolspec.PLAS-0023-2014.

19. Diaz, R., Rech, J. and Bouet, J.Y. (2015) Imaging centromere-based incompatibilities: Insights into the mechanism of incompatibility mediated by low-copy number plasmids. *Plasmid*, **80**, 54-62.

20. Bouet, J.Y., Nordstrom, K. and Lane, D. (2007) Plasmid partition and incompatibility--the focus shifts. *Mol. Microbiol.*, **65**, 1405-1414.

21. Bouet, J.Y., Rech, J., Egloff, S., Biek, D.P. and Lane, D. (2005) Probing plasmid partition with centromere-based incompatibility. *Mol. Microbiol.*, **55**, 511-525.

22. Ebersbach, G., Sherratt, D.J. and Gerdes, K. (2005) Partition-associated incompatibility caused by random assortment of pure plasmid clusters. *Mol. Microbiol.*, **56**, 1430-1440.

23. Rood, J.I., Maher, E.A., Somers, E.B., Campos, E. and Duncan, C.L. (1978) Isolation and characterization of multiply antibiotic-resistant *Clostridum perfringens* strains from porcine feces. *Antimicrob. Agents Chemother.*, **13**, 871-880.

24. Sheedy, S.A., Ingham, A.B., Rood, J.I. and Moore, R.J. (2004) Highly conserved alpha-toxin sequences of avian isolates of *Clostridium perfringens*. *J. Clin. Microbiol.*, **42**, 1345-1347.

25. Rood, J.I. (1983) Transferable tetracycline resistance in *Clostridium perfringens* strains of porcine origin. *Canadian Journal of Microbiology*, **29**, 1241-1246.

26. Lyristis, M., Bryant, A.E., Sloan, J., Awad, M.M., Nisbet, I.T., Stevens, D.L. and Rood, J.I. (1994) Identification and molecular analysis of a locus that regulates extracellular toxin production in *Clostridium perfringens*. *Mol. Microbiol.*, **12**, 761-777.

27. Hughes, M.L., Poon, R., Adams, V., Sayeed, S., Saputo, J., Uzal, F.A., McClane, B.A. and Rood, J.I. (2007) Epsilon-toxin plasmids of *Clostridium perfringens* type D are conjugative. *J. Bacteriol.*, **189**, 7531-7538.

28. Rood, J.I., Scott, V.N. and Duncan, C.L. (1978) Identification of a transferable tetracycline resistance plasmid (pCW3) from *Clostridium perfringens*. *Plasmid*, **1**, 563-570.

29. Keyburn, A.L., Boyce, J.D., Vaz, P., Bannam, T.L., Ford, M.E., Parker, D., Di Rubbo, A., Rood, J.I. and Moore, R.J. (2008) NetB, a new toxin that is associated with avian necrotic enteritis caused by *Clostridium perfringens*. *PLOS Path.*, **4**, e26.

30. Cheung, J.K., Keyburn, A.L., Carter, G.P., Lanckriet, A.L., Van Immerseel, F., Moore, R.J. and Rood, J.I. (2010) The VirSR two-component signal transduction system

regulates NetB toxin production in *Clostridium perfringens*. *Infect. Immun.*, **78**, 3064-3072.

31. O'Connor, J.R., Lyras, D., Farrow, K.A., Adams, V., Powell, D.R., Hinds, J., Cheung, J.K. and Rood, J.I. (2006) Construction and analysis of chromosomal *Clostridium difficile* mutants. *Mol. Microbiol.*, **61**, 1335-1351.
32. McWilliam, H., Li, W., Uludag, M., Squizzato, S., Park, YM, Buso, N, Cowley, AP., Lopez, R.,. (2013) Analysis Tool Web Services from the EMBL-EBI. *Nucleic Acids Res.*, **41**.
33. Molin, S. and Nordstrom, K. (1980) Control of plasmid R1 replication: functions involved in replication, copy number control, incompatibility, and switch-off of replication. *J. Bacteriol.*, **141**, 111-120.
34. Tomizawa, J. and Itoh, T. (1981) Plasmid ColE1 incompatibility determined by interaction of RNA I with primer transcript. *Proc Natl Acad Sci U S A* **78**, 6096-6100.
35. Jensen, R.B., Lurz, R. and Gerdes, K. (1998) Mechanism of DNA segregation in prokaryotes: replicon pairing by *parC* of plasmid R1. *Proc Natl Acad Sci U S A*, **95**, 8550-8555.
36. Breuner, A., Jensen, R.B., Dam, M., Pedersen, S. and Gerdes, K. (1996) The centromere-like *parC* locus of plasmid R1. *Mol. Microbiol.*, **20**, 581-592.
37. Gerdes, K. and Molin, S. (1986) Partitioning of plasmid R1. Structural and functional analysis of the *parA* locus. *J. Mol. Biol.*, **190**, 269-279.
38. Austin, S. and Nordstrom, K. (1990) Partition-mediated incompatibility of bacterial plasmids. *Cell*, **60**, 351-354.
39. Funnell, B.E. (2005) Partition-mediated plasmid pairing. *Plasmid*, **53**, 119-125.
40. Jensen, R.B., Dam, M. and Gerdes, K. (1994) Partitioning of plasmid R1. The *parA* operon is autoregulated by ParR and its transcription is highly stimulated by a downstream activating element. *J. Mol. Biol.*, **236**, 1299-1309.

41. Hyland, E.M., Wallace, E.W. and Murray, A.W. (2014) A model for the evolution of biological specificity: a cross-reacting DNA-binding protein causes plasmid incompatibility. *J. Bacteriol.*, **196**, 3002-3011.

Supplementary material

Table S4.1. Oligonucleotide primers.

Primer	Gene	Sequence (5'-3')
JRP5117	*parM*$_C$	TTTCCCTTGGTTTTGCCATT
JRP5118	*parM*$_C$	GGATGATTTTAGTGGGAATGAT
JRP5119	*parM*$_A$	TTAGGTAAAACTGATACTCCATCCC
JRP5120	*parM*$_A$	GGGAAGTATTCACTTCACCAGATAG
JRP5121	*parM*$_B$	TTTACCCCATTTAGCTTCAGC
JRP5122	*parM*$_B$	CCAGCTTCTAATTTAGGAATAAGTG
JRP5123	*parM*$_D$	AACACCCCACTTAGCAAGCA
JRP5124	*parM*$_D$	GGCGAAGGATTTGCAACATAT
JRP4201	*catP*	CCCCATAGTAAAAATAGGAATCAAATAATCATATC
JRP4202	*catP*	TATCACACAAATAAAGGAAAAGGGAATGAAAC
JRP6704	*catQ*	GATAACCGTCGCAAACCGC
JRP6705	*catQ*	CCTGAAACTGTACCCTACGC
JRP6598	*tetA(P)*	GTGGACCGATTATAGGAATCATAGCTAC
JRP6599	*tetA(P)*	CCTCTCTTACGCTCAAGCTCC
JRP4555	*ermB*	GTTTACTTTGGCGTGTTTCATTGC
JRP3590	*ermB*	AATAAGTAAACAGGTAACGTCT
JRP6001	*ermQ*	CCAGGAAAAGGTCATATAACAGAAGC
JRP6002	*ermQ*	CTAAGACGCAATCTACACTAGGC
JRP6600	*regA*	CGTGCTCCTTTGGAGGTG
JRP6601	*regA*	CAGATACTCCTGCAATCTTTGAAACC
JRP4230	*netB*	CACCATGAGTGAATTAAATGACATAAAC

JRP4231	*netB*	CAGATAATATTCTATTTTATGATCTTG
JRP5503	atyp*cpb2*	CACCAAATACTCTAATTGATGC
JRP5504	atyp*cpb2*	GGAGACGCTGTTAGTTTTACACG

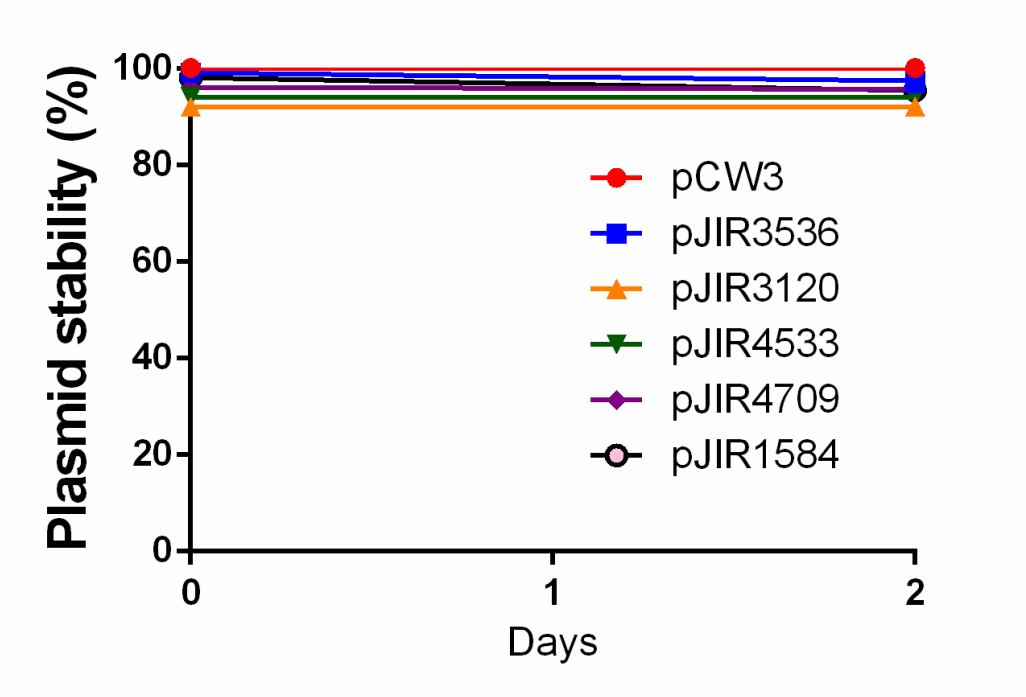

Figure S4.1. Plasmid stability assays for strains carrying individual plasmids. JIR325 derivatives containing pCW3, pJIR1584, pJIR3120, pJIR4533, pJIR4250 or pJIR3536 were passaged in the absence of selection for 2 days. Samples were taken on day 0 and day 2 and plasmid stability was determined by assessing the antibiotic resistance profile at each time point. pCW3 is shown in red, pJIR3536 is shown in blue, pJIR3120 is shown in yellow, pJIR4533 is shown in green, pJIR4709 is shown in purple and pJIR1584 is shown in pink. n=3**.** Note that the lines are offset vertically so that each graph can be readily seen.

```
Plasmid          parMRC   Rep sequence

pCW3             (C)      MKGVIFMAHIHLLTKEQLEQEKRFNLEERDFHVLNQIEYKESRRKAQSILRFIRKGILLN
pJIR3536         (A)      ------MAHIHLLTKEQLEQEKRFNLEERDFHVLNQIEYKESRRKAQSILRFIRKGILLN
pJIR3120         (D)      MKGVIFMAHIHLLTKEQLEQEKRFNLEERDFHVLNQIEYKESRRKAQSILRFIRKGILLN
                                ************************************************

pCW3             (C)     NGSWSISFSKIHKDYNDWVNKKKKKRPELKNISLKQIKNIVNKLKDLGLLIIENVKKRNC
pJIR3536         (A)     NGSWSISFSKIHKDYNDWVNKKKKKRPELKNISLKQIKNIVNKLKDLGLLIIENVKKRNC
pJIR3120         (D)     NGSWSISFSKIHKDYNDWVNKKKKKRPELKNISLKQIKNIVNKLKDLGLLIIENVKKRNC
                         ************************************************************

pCW3             (C)      YFLPLPNKLPNNENITIPDTTSIEGNQATPRYIRNNNIDIDSNSNSKEFNADMYEKCTSL
pJIR3536         (A)      YFLPLPNKLPNNENITIPDTTSIEGNQTTPRYIRNNNIDIDSNSNSKEFNADMYEKCTSL
pJIR3120         (D)      YFLPLPDKLPNNENITIPDTTSIEGNQATPRYIRNNNIDIDSNSNSKEFNADMYEKCTSL
                          ******:********************:*******************************

pCW3             (C)      VDVRNKVKELLKAARVKSSWIKNKVLTKLSENYRNITVKFLESYINTVIENTRNTYYSNY
pJIR3536         (A)      VDVRSKVKELLKAARVKSSWIKNKVLTKLSENYRNITVKFLESYINTVIENTRNTYYSNY
pJIR3120         (D)      VDVRNKVKELLKTARVKSSWIKNKVLTKLSENYRNITVKFLESYINTVIENTRNTYYSNY
                          ****.*******:************************************************

pCW3             (C)      RKYIKNNANNRALPNFTERNYSKDYWKYLEENLCFN
pJIR3536         (A)      RKYIKNNANNRVLPNFTERNYSKDYWKYLEENLCFN
pJIR3120         (D)      RKYIKNNANNRVLPNFTERNYSKDYWKYLEENLCFN
                          ***********.************************
```

Figure S4.2. Sequence alignments of Rep from pJIR3536, pJIR3120 and pCW3. The Rep amino acid sequences of pCW3, pJIR3536 and pJIR3120 were aligned using the EMBL-EBI Clustal Ω alignment tool (32). All sequences were aligned using pCW3 as a reference, conserved residues are denoted by asterisks, whereas non-conserved residues are denoted by dots beneath the alignment.

Chapter 5

The specificity of ParR binding is related to the compatibility of conjugative plasmids in *Clostridium perfringens*

The specificity of ParR binding determines the compatibility of conjugative plasmids in *Clostridium perfringens*

Thomas D. Watts[1], Daouda A.K. Traore[2,3], Sarah C. Atkinson[2], Carmen Lao[1], Natalie Caltabiano[1], Julian I. Rood[1*], and Vicki Adams[1*#].

Infection and Immunity Program, Monash Biomedicine Discovery Institute and Department of Microbiology[1] and Department of Biochemistry and Molecular Biology[2], Monash University, Victoria 3800, Australia

[3]Faculté des Sciences et Techniques, Université des Sciences, des Techniques et des Technologies de Bamako (USTTB), BP E3206 Bamako, Mali.

[*]Joint senior authors

[#]Corresponding author: Vicki Adams, Department of Microbiology, Monash University, Victoria, 3800, Australia.

Tel: +[redacted]

Fax: [redacted]

Email: [redacted]

Keywords: Plasmid partitioning, Plasmid maintenance, Plasmid incompatibility, *Clostridium perfringens*, ParR, *parC*, surface plasmon resonance, DNA-binding, analytical ultracentrifugation

Abstract

Plasmids that encode the same replication machinery are generally unable to coexist in the same bacterial cell. However, *Clostridium perfringens* strains often carry multiple conjugative toxin or antibiotic resistance plasmids that are closely related and encode similar Rep proteins. In many bacteria, plasmid partitioning upon cell division involves a ParMRC system and there are ~10 different ParMRC families in *C. perfringens*, with differences in amino acid sequences between each ParM family (15% - 54% identity). Since plasmids encoding genes belonging to the same ParMRC family are not observed in the same strain, these families appear to represent the basis for plasmid compatibility in *C. perfringens*. To understand this process, we examined the key recognition steps between ParR DNA-binding proteins and their *parC* binding sites. The ParR proteins bound to sequences within a *parC* site from the same ParMRC family, but could not interact with a *parC* site from a different ParMRC family. These data provide evidence that compatibility of the conjugative toxin plasmids of *C. perfringens* is mediated by their *parMRC*-like partitioning systems. This process provides a selective advantage by enabling the host bacterium to maintain separate plasmids that encode toxins that are specific for different host targets.

Introduction

Low-copy number plasmids usually require an active partitioning system to ensure that they are faithfully inherited by daughter cells upon cell division (1). Type II or ParMRC plasmid partitioning systems encode three components: *parC,* a plasmid-encoded centromere, ParM, an actin-like ATPase that forms filaments in the presence of ATP or GTP and ParR, a DNA-binding adaptor protein that binds to *parC* (2-6). ParMRC systems stabilise the inheritance of plasmids by positioning them on either side of the cell septum prior to cell division.

ParR proteins are typically ribbon-helix-helix proteins that bind direct repeats within *parC*, either as a dimer or a dimer of dimers (5,7-10). The *parC* centromere usually consists of a series of direct repeats upstream of the *parM* gene, however, its precise genetic structure differs between plasmids. Binding of ParR acts to seed the formation of a higher order solenoid-shaped structure, termed the segrosome, where the DNA wraps around ParR leaving a core of ParM interaction sites (9,10). Polymerising ParM filaments then link the ParR-*parC* complexes of two sister plasmids and push them to either cell pole (2,3,11-13). The initial step, in which ParR recognises and interacts with *parC*, is important in determining partition specificity between plasmids.

Plasmid incompatibility generally occurs when two co-resident plasmids encode the same essential replication or partitioning machinery (14). Most studies to date have focused on the partition specificity and incompatibility mediated by Type I or ParABS partitioning systems (15) (16-18), there is only limited evidence that partition-mediated incompatibility can also be facilitated by ParMRC-like partitioning systems (19).

In this study, we focused on partition-mediated incompatibility in *Clostridium perfringens,* a Gram-positive pathogen. In humans and animals *C. perfringens* produces an extensive range of toxins, which it uses to cause diseases that range from mild food poisoning to often fatal

infections such as clostridial myonecrosis, enteritis and enterotoxaemia (20). Most *C. perfringens* toxins are encoded on large, low-copy number, conjugative plasmids (21) that are similar to the tetracycline resistance plasmid, pCW3 (21-27). These plasmids have approximately 35 kb of sequence similarity that includes the *tcp* conjugation locus and genes involved in replication, regulation and stable plasmid maintenance (Figure 5.1) (22,23,27-29). Even though these plasmids have similar replication regions, including a highly conserved replication protein, *C. perfringens* strains frequently carry up to five discrete plasmids (23,30). This phenomenon is typified by the avian necrotic enteritis isolate EHE-NE18, which stably maintains three large, closely related conjugative plasmids with Rep proteins that have 98% amino acid (aa) sequence identity (23,30).

Bioinformatics analysis has revealed the presence of at least ten families of ParMRC partitioning systems ($ParMRC_{A-J}$) in these pCW3-like plasmids. The ParM components have >90% aa sequence identity within a family, and 15-54% aa sequence identity between families, and the ParR and *parC* components show a similar trend (30). A representative of the $ParMRC_B$ family was shown to be a true partitioning system, as addition of this partitioning system to an unstable mini-replicon was sufficient to stabilise its inheritance in *E. coli* (31). Strains of *C. perfringens* do not usually carry plasmids that encode the same ParMRC partitioning system (23,27,30), which suggests that these plasmids have evolved different partition specificities to ensure they are stably maintained within a single *C. perfringens* cell. We recently showed that pCW3-like plasmids with identical partitioning systems could not be maintained in a single cell without selection, whereas plasmids with ParMRC systems from different families were stably maintained in *C. perfringens* cells (32). This finding suggested that differences in ParMRC plasmid partitioning systems were responsible for determining plasmid incompatibility between similar replicons and dictated which plasmid combinations could co-exist in an isolate.

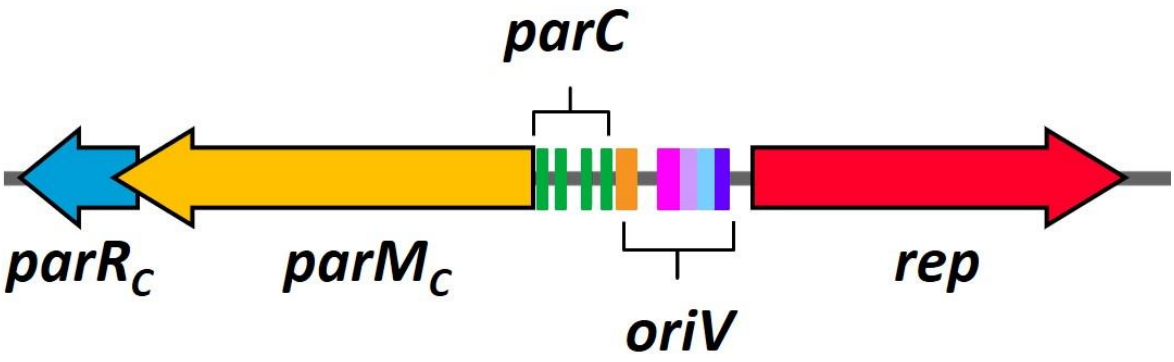

Figure 5.1. Replication and *parMRC* locus of pCW3: *parM*$_C$ is shown in yellow, *parR*$_C$ is shown in blue, the *parC*$_C$ site (four direct repeats shown in green) is upstream of *parM*$_C$, the five inverted repeats (IR) of *oriV* (IR1 in orange, IR2 in pink, IR3 in lavender, IR4 in blue, IR5 in purple) are shown upstream of *rep*, which is indicated by the red arrow.

In this study, we have utilised Surface Plasmon Resonance (SPR) and Analytical Ultracentrifugation (AUC) to demonstrate that differences in the ParR and *parC* components of these partitioning families are reflected in their binding specificity, providing the essential biochemical evidence for the critical role of the ParMRC system in determining plasmid compatibility in *C. perfringens*.

Results

Identification of the pCW3 ParR$_C$ binding site

The recognition steps between ParM, ParR and *parC* components both within and between different families of *parMRC* systems are likely to be key drivers in determining the specificity of the partition reaction and therefore plasmid incompatibility in *C. perfringens*. The ParR-*parC* interaction is of particular interest as this is the first recognition step in the partitioning reaction (8,10,11) and is responsible for the incompatibility phenotype in some other plasmids (19).

Surface plasmon resonance (SPR) was employed to interrogate ParR-*parC* interactions. We first chose to examine the interaction between ParR$_C$ and *parC*$_C$ from pCW3, as pCW3 is the most well characterised conjugative antimicrobial resistance plasmid in *C. perfringens* (28). To perform SPR, a recombinant His$_6$-tagged ParR$_C$(pCW3) protein was expressed in *E. coli* and purified (Figure S5.1). A series of overlapping oligonucleotide fragments were designed (33) based on the 192 bp *parC*$_C$ region of pCW3 (Figure 5.1). These oligonucleotides were annealed to produce a fragment array consisting of 18 double-stranded *parC*$_C$ fragments (denoted C1-C18) (Figure 5.2A).

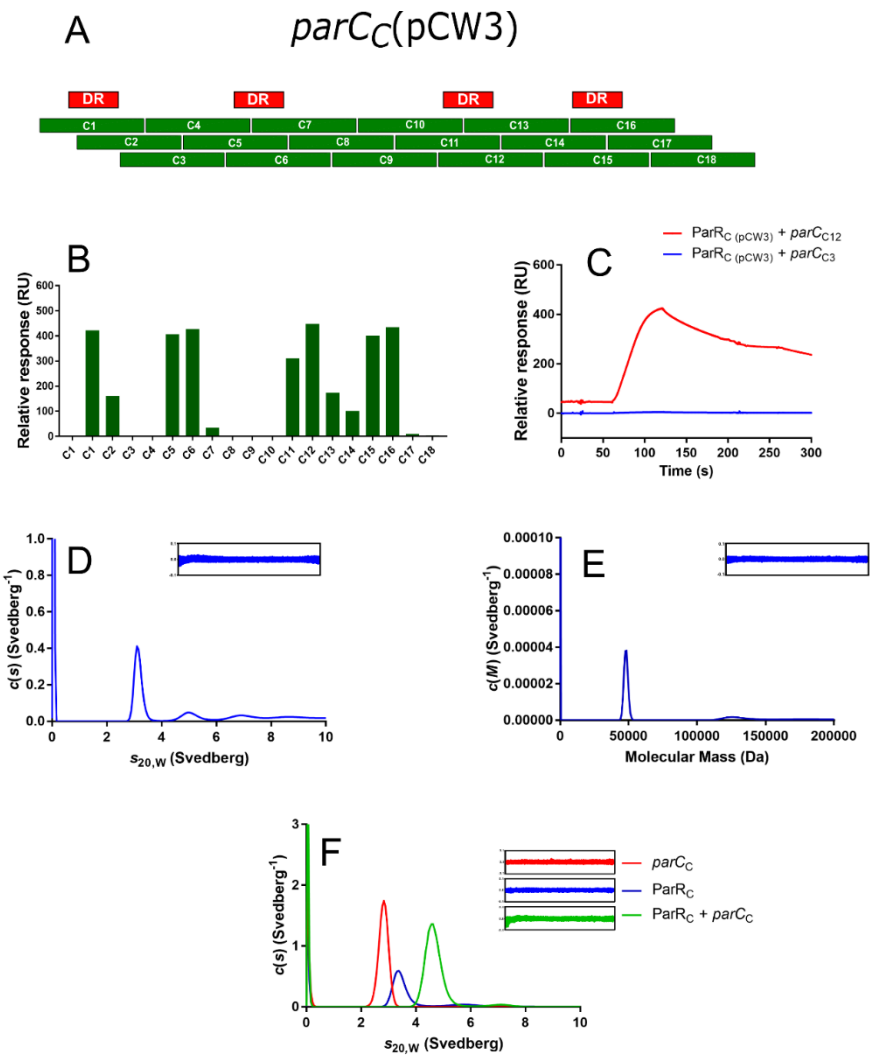

Figure 5.2. ParR$_C$(pCW3) binds to a cognate *parC$_C$*(pCW3) sequence. (A) Schematic of the *parC$_C$*(pCW3) fragment array that consists of 30 bp fragments that overlap by 20 bp, direct repeats are indicated above the fragment array in red. **(B)** Representative ParR$_C$(pCW3) binding to the *parC$_C$*(pCW3) fragment array as determined by SPR. **(C)** Representative SPR binding curves for ParR$_C$(pCW3) and *parC$_C$*(pCW3) fragments, ParR$_C$(pCW3) + C3 binding curve is shown in blue, and ParR$_C$(pCW3) + C12 binding curve is shown in red. AUC sedimentation velocity experiments were also conducted on ParR$_C$(pCW3), *parC$_C$*(pCW3) fragment C5 and ParR$_C$(pCW3) and *parC$_C$*(pCW3) fragment C5 in combination. **(D)** The continuous sedimentation coefficient distribution [*c*(*s*)] as a function of normalised sedimentation coefficient ($s_{20,W}$) for ParR$_C$(pCW3). **(E)** The continuous mass distribution *c*(*M*) distribution as a function of molecular mass (Da) for ParR$_C$(pCW3). **(F)** The continuous sedimentation coefficient distribution [*c*(*s*)] as a function of $s_{20,W}$ for *parC$_C$*(pCW3) C5 (red), ParR$_C$(pCW3) (blue) and, ParR$_C$(pCW3) and *parC$_C$*(pCW3) C5 in combination (green). Residuals for each fit are shown as insets, confirming the validity of the fit of the data.

The stability and specificity of the ParR-*parC* interaction was assessed by challenging each *parC*$_C$ fragment with ParR$_C$(pCW3) (Figures 5.2B & 5.2C). Strong interactions (a binding stability value >100 Response Units (RU)) between ParR$_C$(pCW3) and fragments C1 (256 RU), C5 (249 RU), C6 (282 RU), C11 (154 RU), C12 (348 RU), C15 (217 RU) and C16 (311 RU) were observed. Weaker interactions (a stability value between baseline and 100 RU) were also noted for fragments C2 (54 RU), C7 (9 RU), C13 (48 RU) and C14 (42 RU). The strong interactions that were observed between *parC*$_C$(pCW3) fragments and ParR$_C$ were mapped to the *parC*$_C$(pCW3) nucleotide sequence, which showed that binding corresponded with the presence of four conserved 17 bp direct repeats (5'-AAACATCACAATTTTAC). The SPR results also indicate that a single fragment with the conserved *parC*$_C$ repeat was sufficient for ParR$_C$ binding.

AUC sedimentation velocity experiments were used to support the results obtained by SPR and provide insight into the multimeric state of ParR$_C$ in solution. The interaction between ParR$_C$(pCW3) and the *parC*$_C$(pCW3) fragment C5 was chosen for interrogation as the C5 fragment encodes a centrally located direct repeat and showed strong binding to ParR$_C$(pCW3) by SPR. The results showed that ParR$_C$(pCW3) primarily sedimented as a single species with a sedimentation coefficient ($s_{20,w}$) of 3.1 S (Figure 5.2D), which corresponds to a molecular mass of 48 kDa (Figure 5.2E). The molecular mass of His$_6$-tagged ParR$_C$(pCW3) as predicted from the amino acid sequence is 10.9 kDa, suggesting that ParR$_C$(pCW3) exists as a tetramer in solution. The *parC*$_C$(pCW3) C5 fragment sedimented as a single species with a sedimentation coefficient of 2.7 S (Figure 5.2F). When ParR$_C$(pCW3) and *parC*$_C$(pCW3) C5 were combined prior to centrifugation, a distinct shift in sedimentation coefficient to 4.2 S was observed (Figure 5.2F), which was consistent with binding in a 1:1 ratio of ParR$_C$(pCW3) complex (four molecules) to each *parC*$_C$(pCW3) binding site. This result confirmed that ParR$_C$(pCW3) and *parC*$_C$(pCW3) (C5) could interact in solution, which was consistent with the results obtained *via* SPR.

ParR homologues cannot bind to non-cognate *parC* centromeres from a different phylogenetic ParMRC family

To determine if the interaction of ParR and *parC* components is ParMRC-family specific, two more ParR and *parC* families were included in the SPR analysis. $ParR_B$ from pJIR4165 and $ParR_D$ from pJIR3118 have 11% and 26% aa sequence identity to $ParR_C$(pCW3), respectively, and were expressed and purified (Figure S5.1). In addition, $parC_B$(pJIR4165) and $parC_D$(pJIR3118) fragment arrays were synthesised to yield fragments B1-B25 and D1-D21 (Figure 5.3A), these regions respectively have 45% and 47% nucleotide sequence identity to $parC_C$(pCW3) (Table S5.1). $ParR_B$(pJIR4165), $ParR_C$(pCW3) and $ParR_D$(pJIR3118) were tested against each *parC* fragment array ($parC_B$(pJIR4165), $parC_C$(pCW3) and $parC_D$(pJIR3118)) in separate SPR experiments (Figure 5.3).

The results showed that each ParR homologue bound only to its cognate *parC* fragment array. $ParR_C$(pCW3) bound to its cognate $parC_C$ fragment array as before (Figure 5.3C), but did not bind to the non-cognate $parC_B$(pJIR4165) or $parC_D$(pJIR3118) fragments. $ParR_B$(pJIR4165) bound to 12 $parC_B$(pJIR4165) fragments with strongest binding (binding stability value of >300 RU) to fragments B2 (383 RU), B17 (368 RU) and B21 (377 RU) (Figure 5.3B). Unlike the $parC_C$(pCW3) site, which had a clear correlation between binding and the direct repeat structures, the $parC_B$(pJIR4165) region was more complex.

The $parC_B$(pJIR4165) site consists of several different direct repeats and two inverted repeat structures, and many of these structures overlap. Therefore, mapping of $ParR_B$(pJIR4165) binding to the $parC_B$(pJIR4165) region did not indicate a clear $ParR_B$(pJIR4165) binding site. $ParR_C$(pCW3) was able to bind to its cognate $parC_C$(pCW3) as before. $ParR_C$(pCW3) was tested against $parC_B$(pJIR4165) and $parC_D$(pJIR3118) fragment arrays and showed no interaction with these non-cognate sequences (Figure 5.3C).

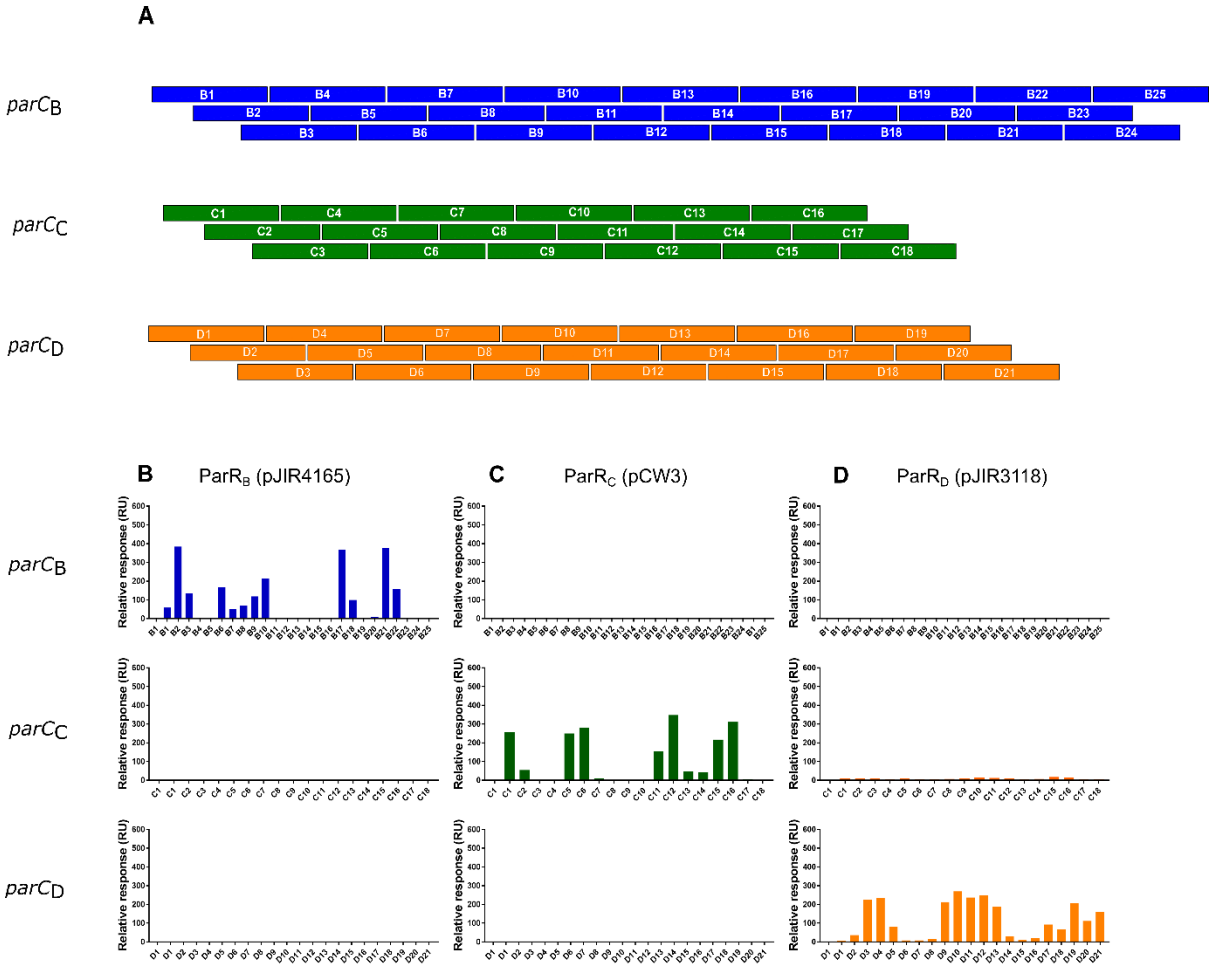

Figure 5.3. Surface plasmon resonance analysis demonstrated that ParR homologues bind to their cognate *parC* sites. A) Schematic of *parC* overlapping fragments. *parC*$_B$(pJIR4165), *parC*$_C$(pCW3) and *parC*$_D$(pJIR3118) fragment arrays were constructed to test binding of ParR homologues to each *parC* region. All fragment arrays consisted of 30 bp oligonucleotides with 20 bp of overlapping sequence and were designed using POOP. Antisense oligonucleotides were constructed with the ReDCaT linker sequence present at the 3' end of each fragment in the diagram above. Oligonucleotides were annealed before being captured onto the ReDCaT primed Streptavidin (SA) chip *via* the complementary base pairing between the ReDCaT linker and the complementary ReDCaT sequence on the Biacore T200 chip. B) SPR profiles obtained when ParR$_B$(pJIR4165) was tested against *parC*$_B$(pJIR4165) (blue), *parC*$_C$(pCW3) (Green) and *parC*$_D$(pJIR3118) (Orange) C) Shows ParR$_C$(pCW3) binding profiles, D) Shows ParR$_D$(pJIR3118) binding profiles. The first lane in every binding graph shows a no protein control with the fragments C1, B1 and D1.

SPR analysis of the *parC*$_D$(pJIR3118) fragment array with its cognate ParR$_D$(pJIR3118) protein showed strong binding stability values (>100 RU) with fragments D3 (225 RU), D4 (232 RU), D9 (213 RU), D10 (270 RU), D11 (236 RU), D12 (250 RU) and D13 (187 RU) and weaker interactions (below 100 RU) with eight other oligonucleotide fragments (Figure 5.3D). Inspection of the *parC*$_D$(pJIR3118) region revealed several different direct and inverted repeat structures, mostly consisting of variations of a conserved, AT-rich direct repeat (5'-TTATTTAAT).

However, mapping of the ParR$_D$(pJIR3118) interactions did not give a clear indication of the specific ParR$_D$ binding site. ParR$_D$(pJIR3118) did not interact with the *parC*$_B$(pJIR4165) fragment array and showed only very weak interactions with most of the fragments from the *parC*$_C$(pCW3) array (stability values between 5-15 RU above baseline). These interactions are likely to be non-specific as a low level of binding was observed for all fragments, including the ReDCaT control fragment. The non-specific interactions were minimised by the addition of dextran to the SPR sample buffer, which had no effect on binding to the *parC*$_D$(pJIR3118) fragments. Overall, these results highlight the specificity of the ParR-*parC* interactions, where ParR homologues only bind to their cognate *parC* component and have either no interaction or very weak inter-family interactions.

ParR homologues recognise and bind non-cognate *parC* fragment arrays from the same ParRMC family

Our earlier work suggested that ParMRC components from the same family would be able to interact with one another, thus leading to interference with the partition process and plasmid incompatibility (32). To provide biochemical evidence for this hypothesis three different ParR homologues (ParR$_B$, ParR$_C$ and ParR$_D$) from the *C. perfringens* strain JGS1987 were expressed, purified (Figure S5.1) and used to assess their capacity to facilitate intra-family interactions. There is an unpublished whole genome shotgun sequence available for strain

JGS1987 (GenBank accession number: ABDW00000000) and it was chosen for analysis as an earlier bioinformatic survey revealed that this strain was particularly rich in *parMRC* genes (30). The JGS1987 sequence contains seven different *parM* alleles, which suggests that there may be seven potential plasmids present in this strain. Since these plasmid sequences had not been closed or given plasmid names, each putative plasmid was designated based on the strain of origin and the *parMRC* genes associated with that contig, yielding pJGS1987B, pJGS1987C and pJGS1987D etc. The JGS1987 $ParR_B$, $ParR_C$ and $ParR_D$ homologues have 96%, 96% and 95% aa sequence identity to the equivalent $ParR_B$(pJIR4165), $ParR_C$(pCW3) and $ParR_D$(pJIR3118) proteins (Table S5.1) (34). The corresponding JGS1987 *parC* regions also show high levels (82% to 91%) of nucleotide sequence similarity to the equivalent homologues (Table S5.1). We postulated that the respective JGS1987-derived ParR proteins would cross-react with *parC* arrays from other members of the same ParMRC family. To examine this hypothesis, we tested the existing suite of *parC* fragment arrays with the purified ParR homologues from JGS1987.

The JGS1987 ParR homologues interacted with non-cognate *parC* fragment arrays from the same ParMRC family, but not with non-cognate *parC* fragments from different families (Figure 5.4). $ParR_B$(pJGS1987B) interacted with $parC_B$(pJIR4165) with a comparable binding pattern to $ParR_B$(pJIR4165) (Figure 5.4A). Strong binding stability (>200 RU) scores were recorded for interactions between $ParR_B$(pJGS1987B) and $parC_B$(pJIR4165) fragments B1, B2, B3, B6, B8, B9, B10, B17, B18, B20, B21, B22 and B25. Weaker binding stability scores were seen for fragments B4, B7, B11, B16 and B23. Similarly, $ParR_C$(pJGS1987C) interacted only with $parC_C$(pCW3), with the same binding pattern as observed for $ParR_C$(pCW3) (Figure 5.4B). High binding stability (>200 RU) scores were recorded for interactions between $ParR_C$(pJGS1987C) and $parC_C$(pCW3) fragments C1, C5, C6, C11, C12 and C15. Weaker binding stability scores were recorded for C2, C13 and C14.

$ParR_D$(pJGS1987D) only interacted with its non-cognate, but intrafamily array from *$parC_D$*(pJIR3118) (Figure 5.4C). Strong binding stability scores were recorded for interactions between $ParR_D$(pJGS1987D) and *$parC_D$*(pJIR3118) fragments D3, D4, D9, D10, D11, D12, D13 and D19. Weaker binding stability scores were recorded for fragments D2, D5, D14, D16, D17, D18 and D20. Representative binding curves for each ParR-*parC* interaction pair are presented in Figure S5.2. These data showed that ParR homologues interacted with non-cognate *parC* fragments from the same phylogenetic ParMRC family, thus confirming a subset of the bioinformatically derived phylogenetic groups of these homologues.

Discussion

In this study we have demonstrated that ParR homologues from the pCW3-family of conjugative *C. perfringens* plasmids specifically recognise and bind to their cognate *parC* sites, providing biochemical evidence for the biological relevance of the phylogenetic ParMRC families that were previously identified (30). DNA binding studies showed that ParR proteins interacted with sequences within a centromeric *parC* site from the same ParMRC family, but could not interact with a non-cognate *parC* site from a different ParMRC family. We also demonstrated that ParR proteins can bind to non-cognate *parC* sites from the same ParMRC family (Figure 5.4). These findings are consistent with our previous phenotypic analysis of ParMRC-encoding plasmids in *C. perfringens,* where plasmids from the same partitioning family were unable to be maintained in a single *C. perfringens* isolate in the absence of selection (32). These combined data provide clear experimental evidence that variation in the ParMRC partitioning systems represents a major molecular mechanism by which native *C. perfringens* isolates can maintain multiple closely related plasmids in the same cell.

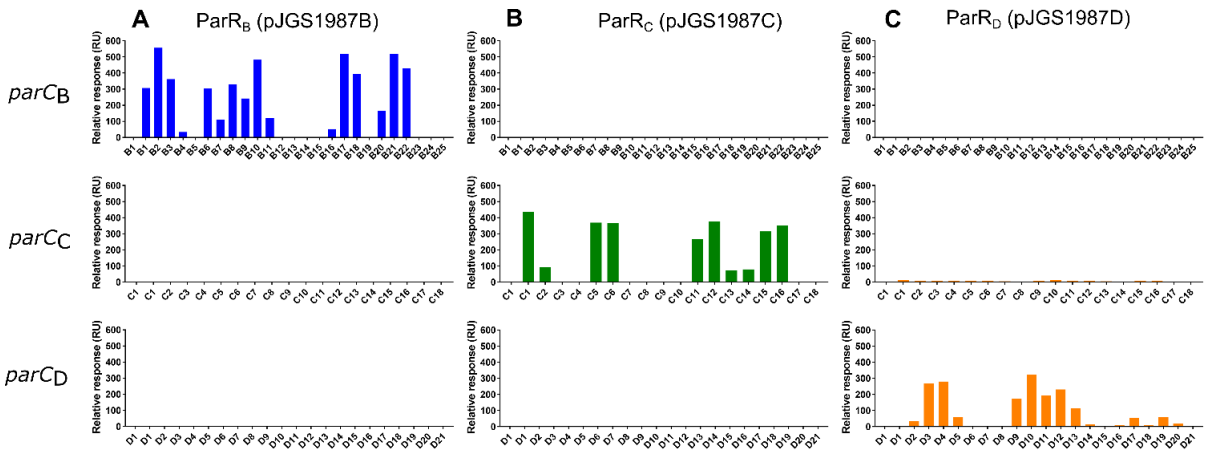

Figure 5.4. **JGS1987 ParR homologues bind to non-cognate *parC* from the same family**. ParR$_B$, ParR$_C$ and ParR$_D$ homologues from the *C. perfringens* isolate, JGS1987, were tested against *parC$_B$*(pJIR4165), *parC$_C$*(pCW3) and *parC$_D$*(pJIR3118) fragment arrays, and binding stability was measured using surface plasmon resonance. **A)** Shows ParR$_B$(pJGS1987B) binding profiles when used to challenge *parC$_B$*(pJIR4165) (blue), *parC$_C$*(pCW3) and *parC$_D$*(pJIR3118). **B)** Shows ParR$_C$(pJGS1987C) binding profiles (blue) **C)** Shows ParR$_D$(pJGS1987D) binding profiles (orange). The first fragment in every graph shows a no protein control

All ParR proteins characterised to date bind to directly repeated sequences, however, the repeats they interact with vary between plasmid systems. For example, ParR from the *E. coli* plasmid R1 requires a minimum of two 11 bp repeats for binding (11), ParR from pB171 (*E. coli*) binds two 10 bp direct repeats upstream of *parM* (35) and ParR from the *Staphylococcus aureus* plasmid pSK41 binds to 20 bp repeats (10).

The direct repeats in the *C. perfringens parC* sites differ substantially between families, with respect to both their nucleotide sequence and their spacing within the centromere. $ParR_C$ binding correlated with four 17 bp direct repeats within the $parC_C$ region. These repeat structures are conserved between $parC_C$ regions of different plasmids, supporting the assertion that ParR is able to recognise and bind to these sites. By contrast, the $ParR_B$ and $ParR_D$ binding sites were more difficult to delineate because there were multiple direct and inverted repeat structures within the $parC_B$ and $parC_D$ regions.

Our findings support the hypothesis that the inability of ParR proteins to discriminate between closely related *parC* sites is responsible for previously observed ParMRC-mediated plasmid incompatibility (32). The consequence would be the incorrect linkage of two heterologous plasmids, eventually leaving distinct populations of daughter cells each containing only one of these plasmids (14,17,18,36). Although the heterologous pairing model is not favoured for type I partitioning mediated incompatibility (16,18), there is evidence that suggests this model could explain ParMRC-based plasmid incompatibility. For example, ParR from R1 is capable of linking replicons before partitioning and promiscuous binding of ParR from pB171 is responsible for plasmid incompatibility (8,19).

Analysis of our sedimentation velocity data showed that $ParR_C$(pCW3) formed a tetrameric complex in solution. Upon the addition of a cognate $parC_C$ fragment containing the 17 bp direct repeat, a higher sedimentation coefficient was observed. This result provides additional evidence of the formation of specific complexes between ParR and *parC* recognition

sequences in solution. These data are consistent with previous structural studies of ParR proteins from pSK41 and pB171 (9,10), which form tight dimers in solution and bind cooperatively to the DNA major groove within the *parC* centromere (5,8-11). Once bound to *parC*, ParR forms a segrosome, where contacts between each ParR dimer are made, ultimately resulting in the formation of a dimer-of-dimers.

Replicon coevolution appears to be widespread in *C. perfringens*, where different isolates often carry closely related plasmids with different ParMRC partitioning systems (21,23,27). For example, the avian necrotic enteritis strain EHE-NE18 has three plasmids that have similar replication proteins, but different families of ParMRC system ($ParMRC_A$, $ParMRC_B$ and $ParMRC_C$) (23). Based on the $ParR_B$, $ParR_C$ and $ParR_D$ binding data reported here, and the previous genetic studies (32), it is concluded that to ensure that each plasmid is segregated independently these ParMRC systems have coevolved to carry different partition specificities.

The evolution of multiple ParMRC partition specificities in *C. perfringens* cells is reminiscent of the evolution of independent ParABS systems in *Burkholderia cenopacia*. The pathogenic *B. cenopacia* strain J2315 maintains three chromosomes and a large, low-copy number plasmid (37). The type I ParABS partitioning systems of these replicons have coevolved to become distinct so that each replicon is partitioned independently (37-40). Likewise, *Rhizobium leguminosarum bv. trifolii* RepB (ParB homologue) proteins discriminate between similar *parS* centromeres to independently segregate and maintain a chromosome in addition to four plasmids (41). Unlike *B. cenopacia* and *R. leguminosarum*, where the selection pressure to maintain multiple chromosomes and plasmids seems to have driven the coevolution of separate partition specificities, the selective pressure that has resulted in the generation of so many *parMRC* alleles in these conjugative *C. perfringens* plasmids remains unclear. One explanation may be that the ParMRC systems act as a means of competitive exclusion. It can be envisioned that upon entry into a new cell *via* conjugation, pCW3-like plasmids could displace resident plasmids that encode similar partitioning systems, thereby

excluding them from the population. In addition, the plasmid-encoded toxin and antibiotic resistance genes may result in the positive selection of these plasmids in certain environmental niches, providing a selective advantage for the host cell if it can maintain these closely related plasmids. There is most certainly more complexity involved in the incompatibility phenotype in *C. perfringens*, since other factors such as the timing of plasmid replication, the plasmid copy number and plasmid replication initiation and regulatory proteins may play at least some role in determining whether two replicons are incompatible or are maintained in the same cell, as in other bacteria (14,15,18,42).

In conclusion, we have shown that interaction between the ParMRC partitioning components ParR and *parC* only occurs between members of the same phylogenetic family. These results provide biochemical insight into the basis of *C. perfringens* plasmid incompatibility and explain how multiple plasmids with similar replicons can be maintained within a single *C. perfringens* isolate.

Materials and methods

Plasmids, bacterial strains, and culture conditions. All *C. perfringens* strains**,** *Escherichia coli* strains and plasmids used in this study are listed in Table 5.1. All *E*. *coli* strains were grown on 2 × yeast tryptone (2YT) agar supplemented with 100 µg/ml of ampicillin and incubated at 37 °C overnight. *E. coli* expression strains were grown in either 2YT broth or autoinduction media (AIM) (43,44).

Construction of ParR expression vectors. The $parR_C$ gene from pCW3 was codon optimised for expression in *E. coli*, synthesised by GenScript and cloned into the EcoRV site of pUC57-Kan. Codon optimised $parR_C$ then was subcloned into the NdeI/XhoI sites of pET22b(+). $parR_D$(pJIR3118) was PCR amplified from CN1020 gDNA isolated as before (O'Connor *et al*., 2006) and cloned into the NdeI/XhoI site of pET22b (+) for expression.

parR$_B$(pJIR4165), *parR*$_B$(pJGS1987B) *parR*$_C$(pJGS1987C) and *parR*$_D$(pJGS1987D) were codon optimised and synthesised before being cloned into pET22b(+) NdeI/XhoI sites by GenScript.

ParR expression and purification. ParR proteins with C-terminal His_6-tags were expressed using C43(DE3), C41(DE3) or BL21(DE3). *E. coli* cells were grown at either 28 °C in AIM for 24 hours before lowering the temperature to 22 °C for 6 hours, or were grown in 2YT broth at 37 °C to an OD_{600} of 0.6 and induced with the addition of 0.1 mM IPTG for 3 hours (Table S5.2). Cells were lysed using a cell disrupter (Avestin) (Lysis buffer: 20 mM TRIS (pH 7.9), 300 mM NaCl, 10% glycerol, 1 mg/ml DNase I and cOmplete protease inhibitors (Roche)) and proteins were purified (Figure S5.1) using TALON resin (Clontech) and eluted with the addition of increasing concentrations of imidazole (5 mM-200 mM) in purification buffer (20 mM TRIS (pH 7.9), 300 mM NaCl, 10% glycerol) and confirmed by Western blotting. All ParR proteins were buffer exchanged into buffer A (10 mM HEPES (pH 7.4), 300 mM NaCl, 3 mM EDTA, 0.05% $Tween_{20}$, 0.02% NaN_3) using a 3 kDa centrifugal filter (Amicon) before dilution to 0.1 µM. Independent preparations of each purified ParR protein were used as biological repeats for SPR.

Fragment array preparation for SPR experiments. *parC* fragment arrays were constructed as previously described (33) using the Re-usable DNA capture technique (ReDCaT) method. Briefly, the *parC* regions of pCW3 (192 bp), pJIR3118 (230 bp) and pJIR4165 (262 bp) were used as templates for the Perl overlapping oligo program (POOP). POOP produced a series of overlapping forward and reverse 30 bp oligonucleotides (20 bp overlap). Reverse strand oligonucleotides had a 20 bp 3' sequence (5'-CCTACCCTACGTCCTCCTGC-3') that was complementary to the ReDCaT sequence (the ligands used in SPR experiments are listed in Table S5.3). Oligonucleotides were synthesised (Integrated DNA technologies) at a concentration of 100 µM in IDTE buffer (10 mM Tris,

0.1 mM EDTA, pH 8.0). To construct fragments for SPR analysis, complimentary oligonucleotides were mixed in a ratio of 1.2:1 forward to reverse, annealed at 98 °C for 10 minutes and cooled for 30 minutes at room temperature. Fragments were then diluted to 0.5 nM in buffer A.

Surface plasmon resonance. SPR experiments were based upon the ReDCaT method as previously described (33) and conducted using the Biacore T200 system (GE Healthcare Life Sciences). All experiments were carried out on an S series Biacore sensor chip (GE Healthcare Life Sciences) with streptavidin (SA) pre-immobilised to a carboxymethylated dextran matrix for capture of biotinylated interaction partners.

Prior to SPR, all four flow cells of the SA chip were washed three times with buffer containing 1 M NaCl and 50 mM NaOH. After washing and priming with buffer A, biotinylated ReDCaT linker (100 nM) (5'-biotin-GCAGGAGGACGTAGGGTAGG-3') was immobilised to all four flow cells at 5 ul/min to a capture level of ~500 Response Units (RU). Subsequently**,** the chip was primed with buffer A and the ReDCaT complementary oligonucleotide (500 nM) was captured on flow cell 1, *parC* ligands diluted in buffer A to a concentration of 500 nM were captured to flow cells 2-4 (*parC*$_B$, *parC*$_C$, *parC*$_D$ fragments on flow cells 2, 3 and 4, respectively) to a density of approximately 200 RU under flow conditions (10 µl/min for 30 seconds). DNA capture levels are listed in Table S5.4. The first flow cell was used as a reference cell for subsequent measurements on flow cells 2 to 4. Each ParR protein (ParR$_B$(pJIR4165), ParR$_B$(pJGS1987B), ParR$_C$(pCW3), ParR$_C$(pJGS1987), ParR$_D$(pJGS1987)) was diluted to a concentration of 0.1 µM in buffer A and ParR$_D$(pJIR3118) was diluted in buffer A with 1 mg/ml dextran to reduce non-specific binding. Proteins were flowed through all four flow cells at 30 µl/min with 60 seconds association and 60 seconds dissociation. Binding stability measurements were recorded 10 seconds after the end of sample injection. All four flow cells of the chip were regenerated after each cycle using regeneration buffer (1 M NaCl and 50 mM NaOH) to leave

only the biotinylated ReDCaT oligonucleotide. All experiments were conducted at 20 °C. All SPR methods were programmed using the Biacore T200 control software and data were analysed using the Biacore evaluation software version 2.0.

Analytical Ultracentrifugation. Sedimentation velocity experiments were performed in an Optima Analytical Ultracentrifuge (Beckman Coulter) equipped with UV/Vis scanning optics. $ParR_C$(pCW3) was prepared at a concentration of 0.5 mg/mL with and without 0.1 mg/mL *parC*$_C$ DNA (fragment C5). Reference (400 µL of buffer A without $tween_{20}$) and sample (370 µL) solutions were loaded into double-sector cells with quartz windows. These cells were mounted in an An-50 Ti 8-hole rotor. Proteins and DNA were centrifuged at 40,000 rpm at 20°C, and radial absorbance data were collected at appropriate wavelengths (~280 nm) in continuous mode every 20 seconds. The partial specific volume ($\bar{\nu}$) of $ParR_C$ (0.7372), buffer density (1.0119 g/ml) and buffer viscosity (0.0104 P) was determined using the program SEDNTERP (45). The $\bar{\nu}$ of *parC*$_C$ C5 DNA (0.5500) was determined using UltraScan III (46). Data were fitted to continuous size-distribution [*c(s)*] and continuous mass distribution [*c*(*M*)] models using the program SEDFIT (47). All sedimentation coefficient data were normalised to standard conditions at 20°C in water ($s_{20,W}$), relevant hydrodynamic properties are listed in Table S5.5.

Acknowledgements

This research was supported by the Australian Research Council [grant DP160102680 to JIR, CL and VA]. The Australian Government Research Training Program (RTP) to TDW. National Health and Medical Research Council Fellowship [1072267 to SCA].

References

1. Gerdes, K., Howard, M. and Szardenings, F. (2010) Pushing and pulling in prokaryotic DNA segregation. *Cell*, **141**, 927-942.

2. Moller-Jensen, J., Jensen, R.B., Lowe, J. and Gerdes, K. (2002) Prokaryotic DNA segregation by an actin-like filament. *EMBO J.*, **21**, 3119-3127.

3. van den Ent, F., Moller-Jensen, J., Amos, L.A., Gerdes, K. and Lowe, J. (2002) F-actin-like filaments formed by plasmid segregation protein ParM. *EMBO J.*, **21**, 6935-6943.

4. Breuner, A., Jensen, R.B., Dam, M., Pedersen, S. and Gerdes, K. (1996) The centromere-like *parC* locus of plasmid R1. *Mol. Microbiol.*, **20**, 581-592.

5. Dam, M. and Gerdes, K. (1994) Partitioning of plasmid R1. Ten direct repeats flanking the parA promoter constitute a centromere-like partition site *parC*, that expresses incompatibility. *J. Mol. Biol.*, **236**, 1289-1298.

6. Gerdes, K., Rasmussen, P.B. and Molin, S. (1986) Unique type of plasmid maintenance function: postsegregational killing of plasmid-free cells. *Proc Natl Acad Sci U S A*, **83**, 3116-3120.

7. Jensen, R.B., Dam, M. and Gerdes, K. (1994) Partitioning of plasmid R1. The *parA* operon is autoregulated by ParR and its transcription is highly stimulated by a downstream activating element. *J. Mol. Biol.*, **236**, 1299-1309.

8. Jensen, R.B., Lurz, R. and Gerdes, K. (1998) Mechanism of DNA segregation in prokaryotes: replicon pairing by *parC* of plasmid R1. *Proc Natl Acad Sci U S A*, **95**, 8550-8555.

9. Moller-Jensen, J., Ringgaard, S., Mercogliano, C.P., Gerdes, K. and Lowe, J. (2007) Structural analysis of the ParR/*parC* plasmid partition complex. *EMBO J.*, **26**, 4413-4422.

10. Schumacher, M.A., Glover, T.C., Brzoska, A.J., Jensen, S.O., Dunham, T.D., Skurray, R.A. and Firth, N. (2007) Segrosome structure revealed by a complex of ParR with centromere DNA. *Nature*, **450**, 1268-1271.

11. Moller-Jensen, J., Borch, J., Dam, M., Jensen, R.B., Roepstorff, P. and Gerdes, K. (2003) Bacterial mitosis: ParM of plasmid R1 moves plasmid DNA by an actin-like insertional polymerization mechanism. *Mol. Cell*, **12**, 1477-1487.

12. Gayathri, P., Fujii, T., Moller-Jensen, J., van den Ent, F., Namba, K. and Lowe, J. (2012) A bipolar spindle of antiparallel ParM filaments drives bacterial plasmid segregation. *Science*, **338**, 1334-1337.

13. Bharat, T.A., Murshudov, G.N., Sachse, C. and Lowe, J. (2015) Structures of actin-like ParM filaments show architecture of plasmid-segregating spindles. *Nature*, **523**, 106-110.

14. Novick, R.P. (1987) Plasmid incompatibility. *Microbiological Reviews*, **51**, 381-395.

15. Ebersbach, G., Sherratt, D.J. and Gerdes, K. (2005) Partition-associated incompatibility caused by random assortment of pure plasmid clusters. *Mol. Microbiol.*, **56**, 1430-1440.

16. Bouet, J.Y., Rech, J., Egloff, S., Biek, D.P. and Lane, D. (2005) Probing plasmid partition with centromere-based incompatibility. *Mol. Microbiol.*, **55**, 511-525.

17. Funnell, B.E. (2005) Partition-mediated plasmid pairing. *Plasmid*, **53**, 119-125.

18. Bouet, J.Y., Nordstrom, K. and Lane, D. (2007) Plasmid partition and incompatibility--the focus shifts. *Mol. Microbiol.*, **65**, 1405-1414.

19. Hyland, E.M., Wallace, E.W. and Murray, A.W. (2014) A model for the evolution of biological specificity: a cross-reacting DNA-binding protein causes plasmid incompatibility. *J. Bacteriol.*, **196**, 3002-3011.

20. Uzal, F.A., Freedman, J.C., Shrestha, A., Theoret, J.R., Garcia, J., Awad, M.M., Adams, V., Moore, R.J., Rood, J.I. and McClane, B.A. (2014) Towards an understanding of the role of *Clostridium perfringens* toxins in human and animal disease. *Future Microbiology*, **9**, 361-377.

21. Li, J., Adams, V., Bannam, T.L., Miyamoto, K., Garcia, J.P., Uzal, F.A., Rood, J.I. and McClane, B.A. (2013) Toxin plasmids of *Clostridium perfringens*. *Microbiol. Mol. Biol. Rev.*, **77**, 208-233.

22. Bannam, T.L., Teng, W.L., Bulach, D., Lyras, D. and Rood, J.I. (2006) Functional identification of conjugation and replication regions of the tetracycline resistance plasmid pCW3 from *Clostridium perfringens*. *J. Bacteriol.*, **188**, 4942-4951.

23. Bannam, T.L., Yan, X.X., Harrison, P.F., Seemann, T., Keyburn, A.L., Stubenrauch, C., Weeramantri, L.H., Cheung, J.K., McClane, B.A., Boyce, J.D. *et al.* (2011) Necrotic enteritis-derived *Clostridium perfringens* strain with three closely related independently conjugative toxin and antibiotic resistance plasmids. *mBio*, **2**, e00190-00111.

24. Han, X., Du, X.D., Southey, L., Bulach, D.M., Seemann, T., Yan, X.X., Bannam, T.L. and Rood, J.I. (2015) Functional analysis of a bacitracin resistance determinant located on ICE*Cp1*, a novel Tn*916*-like element from a conjugative plasmid in *Clostridium perfringens*. *Antimicrob. Agents Chemother.*, **59**, 6855-6865.

25. Miyamoto, K., Fisher, D.J., Li, J., Sayeed, S., Akimoto, S. and McClane, B.A. (2006) Complete sequencing and diversity analysis of the enterotoxin-encoding plasmids in *Clostridium perfringens* type A non-food-borne human gastrointestinal disease isolates. *J. Bacteriol.*, **188**, 1585-1598.

26. Miyamoto, K., Li, J., Sayeed, S., Akimoto, S. and McClane, B.A. (2008) Sequencing and diversity analyses reveal extensive similarities between some epsilon-toxin-encoding plasmids and the pCPF5603 *Clostridium perfringens* enterotoxin plasmid. *J. Bacteriol.*, **190**, 7178-7188.

27. Parreira, V.R., Costa, M., Eikmeyer, F., Blom, J. and Prescott, J.F. (2012) Sequence of two plasmids from *Clostridium perfringens* chicken necrotic enteritis isolates and comparison with *C. perfringens* conjugative plasmids. *PLOS One*, **7**, e49753.

28. Wisniewski, J.A. and Rood, J.I. (2017) The Tcp conjugation system of *Clostridium perfringens*. *Plasmid*, **91**, 28-36.

29. Traore, D.A.K., Wisniewski, J.A., Flanigan, S.F., Conroy, P.J., Panjikar, S., Mok, Y.F., Lao, C., Griffin, M.D.W., Adams, V., Rood, J.I. *et al.* (2018) Crystal structure of TcpK in complex with *oriT* DNA of the antibiotic resistance plasmid pCW3. *Nature Communications*, **9**, 3732.

30. Adams, V., Watts, T.D., Bulach, D.M., Lyras, D. and Rood, J.I. (2015) Plasmid partitioning systems of conjugative plasmids from *Clostridium perfringens*. *Plasmid*, **80**, 90-96.

31. Chen, S., Larsson, M., Robinson, R.C. and Chen, S.L. (2017) Direct and convenient measurement of plasmid stability in lab and clinical isolates of *E. coli*. *Scientific Reports*, **7**, 4788.

32. Watts, T.D., Johanesen, P.A., Lyras, D., Rood, J.I. and Adams, V. (2017) Evidence that compatibility of closely related replicons in *Clostridium perfringens* depends on linkage to *parMRC*-like partitioning systems of different subfamilies. *Plasmid*, **91**, 68-75.

33. Stevenson, C.E., Assaad, A., Chandra, G., Le, T.B., Greive, S.J., Bibb, M.J. and Lawson, D.M. (2013) Investigation of DNA sequence recognition by a streptomycete MarR family transcriptional regulator through surface plasmon resonance and X-ray crystallography. *Nucleic Acids Res.*, **41**, 7009-7022.

34. McWilliam, H., Li, W., Uludag, M., Squizzato, S., Park, YM, Buso, N, Cowley, AP., Lopez, R.,. (2013) Analysis Tool Web Services from the EMBL-EBI. *Nucleic Acids Res.*, **41**, W597-600

35. Ringgaard, S., Ebersbach, G., Borch, J. and Gerdes, K. (2007) Regulatory cross-talk in the double par locus of plasmid pB171. *J. Biol. Chem.*, **282**, 3134-3145.

36. Austin, S. and Nordstrom, K. (1990) Partition-mediated incompatibility of bacterial plasmids. *Cell*, **60**, 351-354.

37. Dubarry, N., Pasta, F. and Lane, D. (2006) ParABS systems of the four replicons of *Burkholderia cenocepacia*: new chromosome centromeres confer partition specificity. *J. Bacteriol.*, **188**, 1489-1496.

38. Passot, F.M., Calderon, V., Fichant, G., Lane, D. and Pasta, F. (2012) Centromere binding and evolution of chromosomal partition systems in the Burkholderiales. *J. Bacteriol.*, **194**, 3426-3436.

39. Du, W.L., Dubarry, N., Passot, F.M., Kamgoue, A., Murray, H., Lane, D. and Pasta, F. (2016) Orderly replication and segregation of the four replicons of *Burkholderia cenocepacia* J2315. *PLOS Genet.*, **12**, e1006172.

40. Pillet, F., Passot, F.M., Pasta, F., Anton Leberre, V. and Bouet, J.Y. (2017) Analysis of ParB-centromere interactions by multiplex SPR imaging reveals specific patterns for binding ParB in six centromeres of Burkholderiales chromosomes and plasmids. *PLOS One*, **12**, e0177056.

41. Koper, P., Zebracki, K., Marczak, M., Skorupska, A. and Mazur, A. (2016) RepB proteins of the multipartite *Rhizobium leguminosarum* bv. *trifolii* genome discriminate between centromere-like *parS* sequences for plasmid segregational stability. *Mol. Microbiol.*, **102**, 446-466.

42. Diaz, R., Rech, J. and Bouet, J.Y. (2015) Imaging centromere-based incompatibilities: Insights into the mechanism of incompatibility mediated by low-copy number plasmids. *Plasmid*, **80**, 54-62.

43. Studier, F.W. (2005) Protein production by auto-induction in high density shaking cultures. *Protein Expr Purif*, **41**, 207-234.

44. Studier, F.W. (2014) Stable expression clones and auto-induction for protein production in *E. coli*. *Methods in Molecular Biology*, **1091**, 17-32.

45. Laue, T.M. (1992) Computer-aided interpretation of analytical sedimentation data for proteins. *Analytical Ultracentrifugation in Biochemistry and Polymer Science*, 90-125.

46. Demeler, B. (2005) In Scott, D. J., Harding, S. E. and Rowe, A. J. (eds.), *Analytical Ultracentrifugation: Techniques and Methods*. pp. 210-230.

47. Schuck, P. (2000) Size-distribution analysis of macromolecules by sedimentation velocity ultracentrifugation and lamm equation modeling. *Biophys. J.*, **78**, 1606-1619.

Supplementary material

Table S5.1. Amino acid sequence identity matrix of ParR homologues and nucleotide sequence identity matrix of *parC* regions

A. ParR amino acid sequence identity matrix						
	$ParR_C$ (pCW3)	$ParR_C$ (pJGS1987C)	$ParR_B$ (pJIR4165)	$ParR_B$ (pJGS1987B)	$ParR_D$ (pJIR3118)	$ParR_D$ (pJGS1987D)
$ParR_C$ (pCW3)	100%					
$ParR_C$ (pJGS1987C)	95%	100%				
$ParR_B$ (pJIR4165)	11%	13%	100%			
$ParR_B$ (pJGS1987B)	11%	13%	96%	100%		
$ParR_D$ (pJIR3118)	26%	26%	24%	24%	100%	
$ParR_D$ (pJGS1987D)	24%	24%	25%	24%	95%	100%
B. *parC* nucleotide sequence identity matrix						
	parC$_B$ (pJIR4165)[a]	*parC*$_B$ (pJGS1987B)	*parC*$_C$ (pCW3)[a]	*parC*$_C$ (pJGS1987C)	*parC*$_D$ (pJIR3118)[a]	*parC*$_D$ (pJGS1987D)
parC$_B$ (pJIR4165)[a]	100%					
parC$_B$ (pJGS1987B)	85%	100%				
parC$_C$ (pCW3)[a]	45%	43%	100%			
parC$_C$ (pJGS1987C)	48%	47%	91%	100%		
parC$_D$ (pJIR3118)[a]	48%	50%	47%	50%	100%	
parC$_D$ (pJGS1987D)	53%	55%	54%	54%	82%	100%

Percentage nt and aa similarity determined using Clustal Omega multiple sequence alignment (McWilliam et al., 2013) [a]*parC* regions were used to generate fragment arrays for surface plasmon resonance experiments

Table S5.2. ParR proteins properties and expression conditions

Analyte (C-terminal His6 tag)	Molecular weight (kDa)	Parent plasmid	*E. coli* Expression strain	Expression media	Expression conditions
$ParR_C$ (pCW3)	10.9	pCW3	C43(DE3)	Autoinduction media	28 °C 24 h/ 22°C 6 h
				2YT + 0.1 mM IPTG	37 °C 4 h
$ParR_C$ (pJGS1987C)	11	pJGS1987C	C43(DE3)	Autoinduction media	28 °C 24 h/ 22°C 6 h
$ParR_B$ (pJIR4165)	13.7	pJIR4165	C43(DE3)	Autoinduction media	28 °C 24 h/ 22°C 6 h
				2YT + 0.1 mM IPTG	37 °C 4 h
$ParR_B$ (pJGS1987B)	13.7	pJGS1987B	BL21(DE3)	Autoinduction media	28 °C 24 h/ 22°C 6 h
$ParR_D$ (pJIR3118)	12.6	pJIR3118	C41(DE3)	Autoinduction media	28 °C 24 h/ 22°C 6 hrs
				2YT + 0.1 mM IPTG	37 °C 4 h
$ParR_D$ (pJGS1987D)	12.2	pJGS1987D	C41(DE3)	Autoinduction media	28 °C 24 h/ 22°C 6 h

Table S5.3. *parC* oligos and ligand molecular weight and size

Oligos	Sequence 5'-3'	Size (nt)	Purpose
JRP7138	5'-biotinylation-GGATGGGATGCAGGAGGACG	20	ReDCaT oligonucleotide
JRP6712	CCTACCCTACGTCCTCCTGC	20	ReDCaT complementary (comp) oligonucleotide
JRP6917	TTTATTAATTTCACTATATGTATATACTGA	30	B1
JRP6918	TCAGTATATACATATAGTGAAATTAATAAA[a] cctaccctacgtcctcctgc[b]	50	B1 comp
JRP6919	TCACTATATGTATATACTGAATATATACAT	30	B2
JRP6920	ATGTATATATTCAGTATATACATATAGTGAcctaccctacgt cctcctgc	50	B2 comp
JRP6921	TATATACTGAATATATACATATAGTGTTAT	30	B3
JRP6922	ATAACACTATATGTATATATTCAGTATATAcctaccctacgt cctcctgc	50	B3 comp
JRP6923	ATATATACATATAGTGTTATATATAATAAT	30	B4
JRP6924	ATTATTATATATAACACTATATGTATATATcctaccctacgt cctcctgc	50	B4 comp
JRP6925	ATAGTGTTATATATAATAATCAATTATATA	30	B5
JRP6926	TATATAATTGATTATTATATATAACACTATcctaccctacgt cctcctgc	50	B5 comp
JRP6927	ATATAATAATCAATTATATATACTCAGTAT	30	B6

JRP6928	ATACTGAGTATATATAATTGATTATTATATcctaccctacgtcctcctgc	50	B6 comp
JRP6929	CAATTATATATACTCAGTATATATAATTAT	30	B7
JRP6930	ATAATTATATATACTGAGTATATATAATTGcctaccctacgtcctcctgc	50	B7 comp
JRP6931	TACTCAGTATATATAATTATATTTTGTATA	30	B8
JRP6932	TATACAAAATATAATTATATATACTGAGTAcctaccctacgtcctcctgc	50	B8 comp
JRP6933	ATATAATTATATTTTGTATATATTCAGTAT	30	B9
JRP6934	ATACTGAATATATACAAAATATAATTATATcctaccctacgtcctcctgc	50	B9 comp
JRP6935	ATTTTGTATATATTCAGTATATATAAAAAG	30	B10
JRP6936	CTTTTTATATATACTGAATATATACAAAATcctaccctacgtcctcctgc	50	B10 comp
JRP6937	TATTCAGTATATATAAAAAGTGAGGGATTT	30	B11
JRP6938	AAATCCCTCACTTTTTATATATACTGAATAcctaccctacgtcctcctgc	50	B11 comp
JRP6939	ATATAAAAAGTGAGGGATTTAAAGAGAATA	30	B12
JRP6940	TATTCTCTTTAAATCCCTCACTTTTTATATcctaccctacgtcctcctgc	50	B12 comp
JRP6941	TGAGGGATTTAAAGAGAATAATAGTATTTT	30	B13
JRP6942	AAAATACTATTATTCTCTTTAAATCCCTCAcctaccctacgtcctcctgc	50	B13 comp
JRP6943	AAAGAGAATAATAGTATTTTGAAGAAAAAT	30	B14
JRP6944	ATTTTTCTTCAAAATACTATTATTCTCTTTcctaccctacgtcctcctgc	50	B14 comp
JRP6945	ATAGTATTTTGAAGAAAAATAGGTATAAAC	30	B15

JRP6946	GTTTATACCTATTTTTCTTCAAAATACTATcctaccctacgtcctcctgc	50	B15 comp
JRP6947	GAAGAAAAATAGGTATAAACTCAGTATATA	30	B16
JRP6948	TATATACTGAGTTTATACCTATTTTTCTTCcctaccctacgtcctcctgc	50	B16 comp
JRP6949	AGGTATAAACTCAGTATATACATGATTGAA	30	B17
JRP6950	TTCAATCATGTATATACTGAGTTTATACCTcctaccctacgtcctcctgc	50	B17 comp
JRP6951	TCAGTATATACATGATTGAAAAGTTGTTTT	30	B18
JRP6952	AAAACAACTTTTCAATCATGTATATACTGAcctaccctacgtcctcctgc	50	B18 comp
JRP6953	CATGATTGAAAAGTTGTTTTTAGTATATAT	30	B19
JRP6954	ATATATACTAAAAACAACTTTTCAATCATGcctaccctacgtcctcctgc	50	B19 comp
JRP6955	AAGTTGTTTTTAGTATATATCTAGTATATA	30	B20
JRP6956	TATATACTAGATATATACTAAAAACAACTTcctaccctacgtcctcctgc	50	B20 comp
JRP6957	TAGTATATATCTAGTATATACTAAATTTAT	30	B21
JRP6958	ATAAATTTAGTATATACTAGATATATACTAcctaccctacgtcctcctgc	50	B21 comp
JRP6959	CTAGTATATACTAAATTTATAAAAGATAAT	30	B22
JRP6960	ATTATCTTTTATAAATTTAGTATATACTAGcctaccctacgtcctcctgc	50	B22 comp
JRP6961	CTAAATTTATAAAAGATAATTAATTTTGAA	30	B23
JRP6962	TTCAAAATTAATTATCTTTTATAAATTTAGcctaccctacgtcctcctgc	50	B23 comp
JRP6963	AAAAGATAATTAATTTTGAAAGGAGCATTA	30	B24

JRP6964	TAATGCTCCTTTCAAAATTAATTATCTTTTcctaccctacgtcctcctgc	50	B24 comp
JRP6965	AAGATAATTAATTTTGAAAGGAGCATTAAA	30	B25
JRP6966	TTTAATGCTCCTTTCAAAATTAATTATCTTcctaccctacgtcctcctgc	50	B25 comp
JRP6713	AATTAAAAACATCACAATTTTACGTAATGA	30	C1
JRP6714	TCATTACGTAAAATTGTGATGTTTTTAATTcctaccctacgtcctcctgc	50	C1 comp
JRP6715	ATCACAATTTTACGTAATGACAGTTTGTTG	30	C2
JRP6716	CAACAAACTGTCATTACGTAAAATTGTGATcctaccctacgtcctcctgc	50	C2 comp
JRP6717	TACGTAATGACAGTTTGTTGAAAATGAAAA	30	C3
JRP6718	TTTTCATTTTCAACAAACTGTCATTACGTAcctaccctacgtcctcctgc	50	C3 comp
JRP6719	CAGTTTGTTGAAAATGAAAAAAACATCACA	30	C4
JRP6720	TGTGATGTTTTTTTCATTTTCAACAAACTGcctaccctacgtcctcctgc	50	C4 comp
JRP6721	AAAATGAAAAAAACATCACAATTTTACGGA	30	C5
JRP6722	TCCGTAAAATTGTGATGTTTTTTTCATTTTcctaccctacgtcctcctgc	50	C5 comp
JRP6723	AAACATCACAATTTTACGGAAAATGCTTGA	30	C6
JRP6724	TCAAGCATTTTCCGTAAAATTGTGATGTTTcctaccctacgtcctcctgc	50	C6 comp
JRP6725	ATTTTACGGAAAATGCTTGATTTAGATTGA	30	C7
JRP6726	TCAATCTAAATCAAGCATTTTCCGTAAAATcctaccctacgtcctcctgc	50	C7 comp
JRP6727	AAATGCTTGATTTAGATTGAAAAAAATGAT	30	C8

JRP6728	ATCATTTTTTTCAATCTAAATCAAGCATTTcctaccctacgtcctcctgc	50	C8 comp
JRP6729	TTTAGATTGAAAAAAATGATAATATAAAAA	30	C9
JRP6730	TTTTTATATTATCATTTTTTTCAATCTAAAcctaccctacgtcctcctgc	50	C9 comp
JRP6731	AAAAAATGATAATATAAAAACATAAACATC	30	C10
JRP6732	GATGTTTATGTTTTTATATTATCATTTTTTcctaccctacgtcctcctgc	50	C10 comp
JRP6733	AATATAAAAACATAAACATCACAATTTTAC	30	C11
JRP6734	GTAAAATTGTGATGTTTATGTTTTTATATTcctaccctacgtcctcctgc	50	C11 comp
JRP6735	CATAAACATCACAATTTTACGTAATTTAGA	30	C12
JRP6736	TCTAAATTACGTAAAATTGTGATGTTTATGcctaccctacgtcctcctgc	50	C12 comp
JRP6737	ACAATTTTACGTAATTTAGATTTTGCAAGT	30	C13
JRP6738	ACTTGCAAAATCTAAATTACGTAAAATTGTcctaccctacgtcctcctgc	50	C13 comp
JRP6739	GTAATTTAGATTTTGCAAGTAAAAAACATC	30	C14
JRP6740	GATGTTTTTTACTTGCAAAATCTAAATTACcctaccctacgtcctcctgc	50	C14 comp
JRP6741	TTTTGCAAGTAAAAAACATCACAATTTTAC	30	C15
JRP6742	GTAAAATTGTGATGTTTTTTACTTGCAAAAcctaccctacgtcctcctgc	50	C15 comp
JRP6743	AAAAAACATCACAATTTTACATAATAGAAA	30	C16
JRP6744	TTTCTATTATGTAAAATTGTGATGTTTTTTcctaccctacgtcctcctgc	50	C16 comp
JRP6745	ACAATTTTACATAATAGAAAGGATTGATAA	30	C17

JRP6746	TTATCAATCCTTTCTATTATGTAAAATTGTcctaccctacgtcctcctgc	50	C17 comp
JRP6747	AATTTTACATAATAGAAAGGATTGATAAAA	30	C18
JRP6748	TTTTATCAATCCTTTCTATTATGTAAAATTcctaccctacgtcctcctgc	50	C18 comp
JRP6967	TTTATTTTGTTTTGAAAATCGAATAATATT	30	D1
JRP6968	AATATTATTCGATTTTCAAAACAAAATAAAcctaccctacgtcctcctgc	50	D1 comp
JRP6969	TTTGAAAATCGAATAATATTAAATAATATC	30	D2
JRP6970	GATATTATTTAATATTATTCGATTTTCAAAcctaccctacgtcctcctgc	50	D2 comp
JRP6971	GAATAATATTAAATAATATCAAATAATATT	30	D3
JRP6972	AATATTATTTGATATTATTTAATATTATTCcctaccctacgtcctcctgc	50	D3 comp
JRP6973	AAATAATATCAAATAATATTATTTAATGTC	30	D4
JRP6974	GACATTAAATAATATTATTTGATATTATTTcctaccctacgtcctcctgc	50	D4 comp
JRP6975	AAATAATATTATTTAATGTCGGTATTGTGG	30	D5
JRP6976	CCACAATACCGACATTAAATAATATTATTTcctaccctacgtcctcctgc	50	D5 comp
JRP6977	ATTTAATGTCGGTATTGTGGCTTTGAGGAA	30	D6
JRP6978	TTCCTCAAAGCCACAATACCGACATTAAATcctaccctacgtcctcctgc	50	D6 comp
JRP6979	GGTATTGTGGCTTTGAGGAAAGGTTATTTA	30	D7
JRP6980	TAAATAACCTTTCCTCAAAGCCACAATACCcctaccctacgtcctcctgc	50	D7 comp
JRP6981	CTTTGAGGAAAGGTTATTTAATGTTAAATG	30	D8

JRP6982	CATTTAACATTAAATAACCTTTCCTCAAAGcctaccctacg tcctcctgc	50	D8 comp
JRP6983	AGGTTATTTAATGTTAAATGATATTAAATA	30	D9
JRP6984	TATTTAATATCATTTAACATTAAATAACCTcctaccctacgt cctcctgc	50	D9 comp
JRP6985	ATGTTAAATGATATTAAATAACATTAAAAG	30	D10
JRP6986	CTTTTAATGTTATTTAATATCATTTAACATcctaccctacgtc ctcctgc	50	D10 comp
JRP6987	ATATTAAATAACATTAAAAGATACTAATTA	30	D11
JRP6988	TAATTAGTATCTTTTAATGTTATTTAATATcctaccctacgtc ctcctgc	50	D11 comp
JRP6989	ACATTAAAAGATACTAATTAATATTATTTA	30	D12
JRP6990	TAAATAATATTAATTAGTATCTTTTAATGTcctaccctacgt cctcctgc	50	D12 comp
JRP6991	ATACTAATTAATATTATTTAATTATTGACT	30	D13
JRP6992	AGTCAATAATTAAATAATATTAATTAGTATcctaccctacgt cctcctgc	50	D13 comp
JRP6993	ATATTATTTAATTATTGACTATGGGAGATT	30	D14
JRP6994	AATCTCCCATAGTCAATAATTAAATAATATcctaccctacgt cctcctgc	50	D14 comp
JRP6995	ATTATTGACTATGGGAGATTAGTGTGATAT	30	D15
JRP6996	ATATCACACTAATCTCCCATAGTCAATAATcctaccctacg tcctcctgc	50	D15 comp
JRP6997	ATGGGAGATTAGTGTGATATTATTTAATCA	30	D16
JRP6998	TGATTAAATAATATCACACTAATCTCCCATcctaccctacg tcctcctgc	50	D16 comp
JRP6999	AGTGTGATATTATTTAATCATAAAAGATAT	30	D17

JRP7000	ATATCTTTTATGATTAAATAATATCACACTcctaccctacgtcctcctgc	50	D17 comp
JRP7001	TATTTAATCATAAAAGATATTAAATAATAT	30	D18
JRP7002	ATATTATTTAATATCTTTTATGATTAAATAcctaccctacgtcctcctgc	50	D18 comp
JRP7003	TAAAAGATATTAAATAATATTAAATATTTT	30	D19
JRP7004	AAAATATTTAATATTATTTAATATCTTTTAcctaccctacgtcctcctgc	50	D19 comp
JRP7005	TAAATAATATTAAATATTTTCTTTGAAAAG	30	D20
JRP7006	CTTTTCAAAGAAAATATTTAATATTATTTAcctaccctacgtcctcctgc	50	D20 comp
JRP7007	TAAATATTTTCTTTGAAAAGGAGAGTTAAT	30	D21
JRP7008	ATTAACTCTCCTTTTCAAAGAAAATATTTAcctaccctacgtcctcctgc	50	D21 comp

[a]Uppercase sequence corresponds to the unique *parC* fragment

[b]Lowercase sequence corresponds to the 3’ ReDCaT complementary tail

Table S5.4. Binding of ParR homologues to *parC* using surface plasmon resonance

	$ParR_B$(pJIR4165)				**$ParR_C$(pCW3)**				**$ParR_D$(pJIR3118)**			
	Replicate 1		Replicate 2		Replicate 1		Replicate 2		Replicate 1		Replicate 2	
Oligo	DNA Captured (RU)	Response (RU)	DNA Captured (RU)	Response (RU)	DNA captured (RU)	Response (RU)	DNA captured (RU)	Response (RU) replicate 2	DNA captured (RU)	Response (RU)	DNA Captured (RU)	Response (RU)
B1	210.3	58	162.1	10.1	313.1	-2.8			251.5	1.1		
B2	266.2	383.7	169.3	88.7	345	-2.7			264.9	2.3		
B3	257.6	133.8	164.3	26.3	366.2	-3			256.8	1.3		
B4	258	2.1	171.1	-1.8	352.9	-3.4			258.8	1.6		
B5	261.5	1.1	174.6	-2.4	348.1	-2.9			251.4	0.6		
B6	239.1	166.9	173.9	61.5	355.8	-3.3			258.4	1.5		
B7	199.6	52.2	132.5	12.3	300.4	-3.1			206.1	0.3		
B8	266.7	69.6	182.2	11.1	351	-3			270.5	0.1		
B9	264.1	118.9	184.9	33.1	360.4	-3.1			263	2.1		
B10	163	216.4	190.4	61.1	379.3	-3			268.4	0		
B11	242.5	4.2	168.7	-1.9	370.8	-3.3			246.6	-0.7		
B12	264.4	0.7	182.6	-2.5	371.2	-3.6			261.3	-0.9		
B13	239	0.7	201.2	-2.8	313.9	-2.8			203.9	-0.6		
B14	291.1	0.3	206.9	-2.5	364.6	-3			287.3	1.8		
B15	275.5	0.4	191.2	-2.4	398.3	-3.3			272.1	0.2		
B16	279.3	2.3	204.4	-3	378.8	-3.6			273.9	-2		
B17	274.9	368.6	202.3	77.1	366.8	-2.8			275.8	-1.2		
B18	265.2	99.8	204.5	21.2	369	-2.9			267.9	-0.6		
B19	288.4	2.4	213.8	-2.6	391.7	-3.4			284.8	5.5		
B20	205.8	10.1	217.6	-1.6	381.7	-3.4			277	1.5		
B21	235.6	377.2	195.3	83.2	318.8	-3.4			248.4	2.4		
B22	248.3	156.5	210	38.6	394.8	-2.8			273.1	2.6		
B23	149.9	3.2	220.8	-2.8	387.4	-4.1			279.4	1.2		
B24	287.3	2	216.9	-2.9	393.8	-3.4			283.2	0.7		
B25	256	2.2	224.6	-2.9	404.1	-3.6			308.1	0.1		
C1	237.5	-1.7	191.6	-3	119.5	256.3	205.1	422.1	250.9	9.7		

C2	216.8	-0.6	189.6	-2.6	141.2	54.7	207.5	161.2	284.9	10.2		
C3	209.4	-1.4	192.9	-3	142	0.8	245.4	-1.8	242.6	8.5		
C4	224.6	-2.2	188.9	-2.9	140.7	0.9	223.9	-1.8	282	5.6		
C5	88.9	-0.4	201.8	-3.1	123.7	249.5	245.7	405.9	277.1	8.4		
C6	206.2	-1.6	207.1	-3.2	149.1	282.2	244.7	427	241	6.4		
C7	253.6	-1.6	219.2	-3.2	141.1	9.2	246.2	34.4	306.8	6.4		
C8	109.1	-0.5	211.9	-3.3	160.3	1.5	259.6	1.7	314.5	7		
C9	155.1	-0.9	206.4	-3.3	166.2	0.4	232.3	-1.5	272.6	8.1		
C10	232.9	-1.4	220.9	-3.3	162.6	1.5	262.6	-1	271.3	14.8		
C11	223	-1.7	220.6	-3.7	148.7	154.7	266.8	311.3	300.2	12.4		
C12	241.9	-1.7	220.5	-3.6	187.8	348.4	267.7	448.4	286.2	8.5		
C13	264.3	-2.1	230.5	-3.8	159	48.4	279.4	173.7	280.8	6.6		
C14	254.3	-3.1	222.4	-3.6	161.8	42.6	371.1	101.9	339.8	7.1		
C15	266.1	-2	233.2	-3.3	169	217	437.9	401.3	516.4	17.4		
C16	267.1	-2.6	236	-3.4	157.1	311.2	302.2	435	419.1	13.5		
C17	230.6	-0.9	223.5	-3.1	168.9	4.3	408.2	9.3	329.8	5.7		
C18	259.8	-2.1	232.9	-3.5	182.8	3.1	288	4	334.2	5.9		
D1	218.2	-3.8	158.9	-6	225.8	-5.1			111.8	7	236.8	5.4
D2	223.9	-2.6	167.6	-5.7	228	-4.6			114.7	36.4	243	37.9
D3	217.7	-3.8	160.3	-6.2	233.3	-4.9			111.8	225	235.6	155.1
D4	185	-2.9	164.6	-5.7	232.2	-4.8			109.7	232.7	240.8	157.8
D5	214.3	-3.9	168.2	-6.2	229.9	-4			113.4	80.5	251.1	75.5
D6	215.5	-2.9	169.7	-5.4	239.2	-3.4			116.1	8.9	260	4.3
D7	200.3	-3.2	168.9	-5.7	255.6	-4.6			114.3	8.4	256.4	3.9
D8	191.1	-2.4	181.4	-5.8	249	-4.8			121.7	15.5	276	10.3
D9	85.4	-0.4	178.3	-6.1	273.5	-4.6			111.3	213.4	254.3	149.7
D10	103.6	-0.7	188.4	-6	246.3	-4.7			111.8	270.1	261.6	169.8
D11	166.1	-3.7	191.3	-6.8	258	-4.4			115.1	236.5	273.3	157.6
D12	226.1	-3.2	189.4	-6.1	270.5	-4.2			115.9	250	277	158.8
D13	242.3	-3.9	197.7	-6.7	273.4	-4.3			110.2	187.9	272.3	138.2
D14	238.5	-4.1	196.7	-7	266.5	-4.8			112.3	28.9	279.9	27.7
D15	204.1	-2.6	207.7	-6.1	273.4	-4.2			113.8	9.6	289.3	3.5
D16	140.5	-1.4	212	-6.2	282.4	-4.1			114.9	21.5	289.7	25.8
D17	219.8	-3.4	198.7	-6.6	287.6	-4			112.2	92.2	279.7	91.4

D18	228.3	-3.8	194.9	-6.3	278.4	-4.3			109.5	68	283.1	60.5
D19	235.7	-3.7	190.3	-5.6	280.3	-4.2			113.6	207.1	291.9	145
D20	245.5	-4.1	211	-6.6	298.8	-4.4			114.3	111.4	297.1	97.7
D21	217.3	-3.6	215.5	-7.9	295	-4.3			140.1	158.9	300.9	5.4
	$ParR_B$(pJGS1987B)				**$ParR_C$(pJGS1987C)**				**$ParR_D$(pJGS1987D)**			
	Replicate 1		Replicate 2		Replicate 1		Replicate 2		Replicate 1		Replicate 2	
Oligo	DNAcaptured (RU)	Response (RU) replicate 1	DNAcaptured (RU)	Response (RU) replicate 2	DNAcaptured (RU)	Response (RU) replicate 1	DNAcaptured (RU)	Response (RU) replicate 2	DNAcaptured (RU)	Response (RU) replicate 1	DNAcaptured (RU)	Response (RU) replicate 2
B1	211.7	260.3	107.7	25	217.6	-3.1			200.3	-11.9		
B2	233.1	557.1	128.1	158.7	72.5	-5.9			229.5	-5.1		
B3	206.9	323.6	118.3	51.7	241.2	-5.9			223.5	-6.7		
B4	224.5	25.3	125	-55.1	234.1	-5.7			223.9	-3.3		
B5	229.5	-1.3	121.9	-62.2	236	-5.8			227.6	-6.5		
B6	227	278	121.3	45.8	241.2	-5.3			222.3	-4.3		
B7	175.1	96	92.8	-47.6	237.7	-5.3			169.3	-9.3		
B8	230.4	289	144.8	37.2	187.6	-6			227	-5		
B9	231.1	212.8	140.9	15.1	246.1	-5			224	0.4		
B10	233.1	483.7	106.1	100.2	243.5	-5.2			226.6	-3.9		
B11	207	102.4	113.7	-26.5	244.4	-5.4			201.2	-8.5		
B12	229.5	-9	106.5	-61.6	223.3	-5.4			219.8	-8.6		
B13	212.4	-10	144.2	-61.4	237.6	-5.9			214.3	-9.3		
B14	245.6	-9	88.3	-58.5	237.9	-5			237.1	3.1		
B15	225.2	-8.9	110.1	-58.3	262.5	-5.4			223.7	-1.2		
B16	231.6	42.5	129.1	-41.4	247.2	-5.5			228.6	-7.2		
B17	229.7	523.7	155.9	115.6	251	-5.3			225	-4.9		
B18	228.2	358.9	113.2	61.5	252.8	-5.1			227.2	-4.8		
B19	238.2	-8.1	126.1	-55.3	248.2	-3.1			192.2	1.3		
B20	211.7	260.3	127.4	-3.1	274.6	-4			238.6	-1		
B21	233.1	557.1	116.5	141.7	255.2	-3.8			217.1	-1.1		
B22	206.9	323.6	126.4	86	236.1	-3.3			232.1	-0.3		
B23	224.5	25.3	101	-52.9	249.6	-4.3			241.8	-3.1		

B24	229.5	-1.3	110.1	-53.8	260.2	-3.7			240.3	-4		
B25	227	278	102.9	-52.1	231.1	-5			250.1	-3.6		
C1	346.2	-1.7			333.7	511.4	148.9	64.9	339.4	-1.5		
C2	348.2	0.1			336.6	110.7	138.9	-15.5	343	14.7		
C3	344.1	0.3			323.5	-6.2	146.6	-6.8	344.7	12.8		
C4	323.1	-0.8			342.2	-7	147.3	186.1	335	10.8		
C5	365.1	0.3			351.7	456.5	141.5	183.2	354.3	8.6		
C6	322.7	4.5			349.8	452.6	149.7	3	362.9	12.7		
C7	1	-0.2			357.6	5.1	148.4	-13.4	366.1	10.5		
C8	367.6	-2.3			351.6	-3.5	154.6	-15.6	372.7	8.2		
C9	319.2	1.7			360.9	-5.8	147.5	-14.8	369.5	6.9		
C10	373.4	1.9			376	-5.7	148.2	96.4	381	10.5		
C11	360.4	1.4			364.1	343.5	150.5	195.7	397.3	20.3		
C12	384.2	1.1			380.3	505.6	152.2	58.9	384	12.9		
C13	387	0.2			379	96.6	150.5	118.4	395.7	11		
C14	395.3	-1.3			375.5	105.4	149.9	198.8	400.5	8.6		
C15	392.3	-0.6			386.7	428.5	152.3	-8.4	400.9	7.1		
C16	403.8	2.6			383.4	473.2	146	-11.6	409.8	11.1		
C17	381.5	-0.4			388.9	-0.5	148.9	64.9	408.6	10.2		
C18	389.9	-0.7			400.6	-3.8	138.9	-15.5	416.6	6.9		
D1	200.8	-3.4			326.2	-11.5			331.6	-1.3	160.5	-47
D2	203.5	-2.6			322.3	-11.5			335.2	42.8	159.8	101.1
D3	195.1	-2.3			316.6	-11.6			332.1	341.5	152.1	111.1
D4	200.3	-1.3			317.9	-12.6			326.7	356.4	171.8	-37
D5	211.1	-1.8			329.3	-10.1			326.7	80.6	163.8	-46.9
D6	221.4	-3.1			339.9	-13.1			342.2	-0.7	158.6	-51.4
D7	212.6	-4.3			345.4	-13			352	-1.9	160.9	-50.5
D8	238.1	-3.4			348.9	-10.8			360.5	4.8	154	49.4
D9	212.7	-2.8			336.8	-11.2			368	235.5	173.7	164.8
D10	213.9	-1.8			351.7	-11.8			348.2	459.8	163	80.8
D11	231.9	-1.9			354.2	-11.4			366.6	279.6	161.7	122.4
D12	246.6	-2			365.5	-11.5			369.4	346.7	150.9	10.3
D13	229.4	-1.8			374.9	-13			384.6	175.4	161.6	-51.6
D14	236.5	-2.9			360.1	-11.9			395.1	21.1	164.2	-45.3

D15	241.4	-3.6			373.8	-11.4			387	-2.7	163.5	-31.3
D16	241.7	-3.1			382.2	-11.1			396.6	14.1	157.7	-41.4
D17	230.2	-2.1			376.6	-11.1			404.2	87	155.3	51.6
D18	219.2	-2.7			385.3	-11.7			400.3	43.8	171.2	-36.7
D19	243	-3			394.1	-11.6			408.6	239.8	158.2	-56.6
D20	262.2	-2.3			396.3	-11.2			422.4	84.8	160.5	-47
D21	246.8	-3.7			399.8	-11.8			420.5	-1.3	159.8	101.1

Table S5.5. Hydrodynamic properties of $ParR_C$(pCW3) and *$parC_C$*(pCW3) C5 DNA determined by AUC experiments

Components	Mr[a] kDa	MW[b] (Da)	Sedimentation coefficient (*s*)[c]	Standardised sedimentation coefficient ($s_{20,w}$)	Oligomeric state	Partial specific volume
$ParR_C$(pCW3)	10.9	48439	2.86	3.1	Tetramer	0.7372
***$parC_C$* (pCW3) C5**	18.6	18426	2.6	2.8	Double stranded DNA	0.55

[a] Relative molecular weight calculated from amino acid sequence.
[b] Apparent molecular weight derived from c(M) analysis
[c] Sedimentation coefficient taken from the ordinate maximum of c(s) distribution

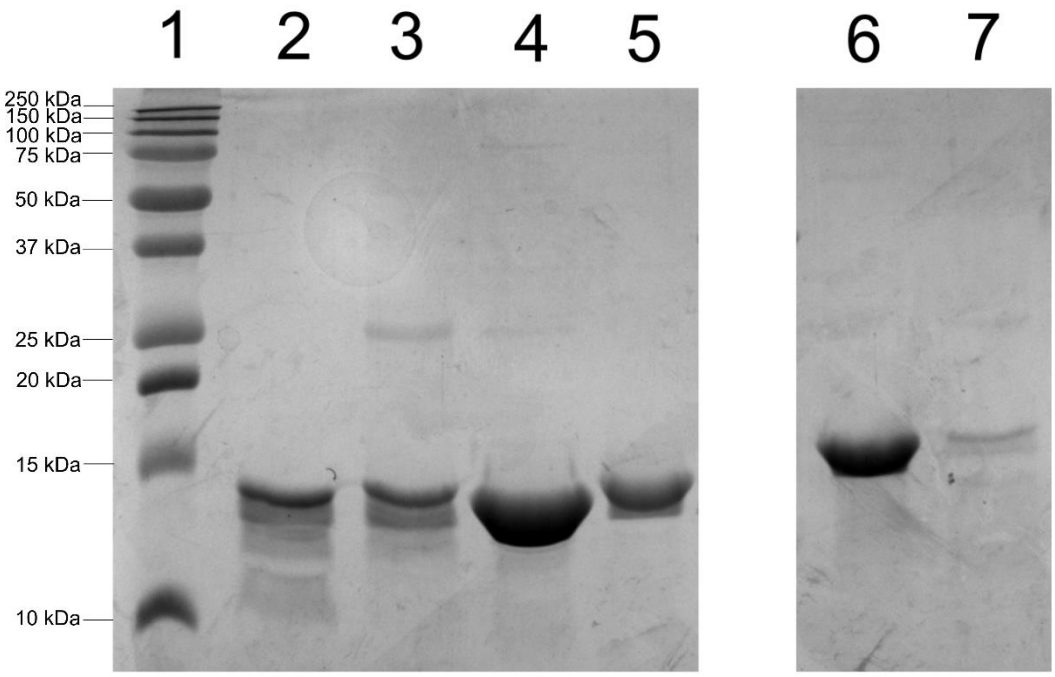

Figure S5.1. Purified recombinant ParR proteins. ParR proteins were purified and analysed using a 15% polyacrylamide gel stained with Coomassie brilliant blue. Legend: 1 BioRad protein standards, 2 $ParR_B$(pJIR4165), 3 $ParR_B$(pJGS1987B), 4 $ParR_C$(pCW3), 5 $ParR_C$(pJGS1987C), 6 $ParR_D$(pJGS1987D), 7 $ParR_D$(pJIR3118).

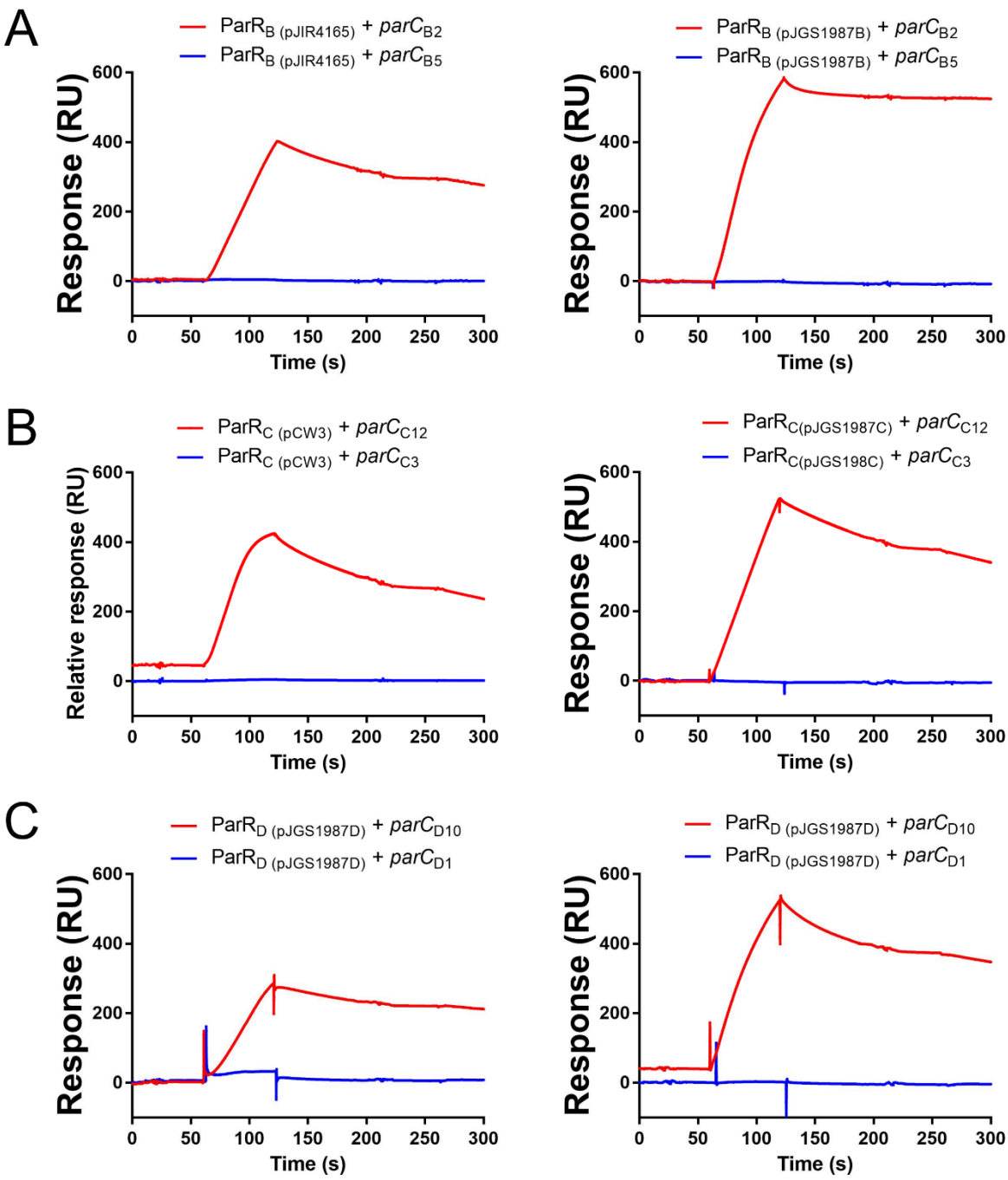

Figure S5.2. Representative SPR binding curves for each ParR homologue and cognate *parC* fragment interactions. Representative binding curves for each ParR-*parC* pair are shown. **A** shows representative binding curves for ParR$_B$ homologues, **B** shows representative binding curves for ParR$_C$ homologues, **C** Shows representative binding curves for ParR$_D$ homologues. The red curves represent a binding interaction, blue curves represent a non-binding interaction. The origins of the ParR and *parC* fragments are indicated above each graph.

Chapter 6

Discussion

In this thesis several key aspects of *C. perfringens* plasmid biology have been examined, specifically: plasmid conjugation, maintenance and incompatibility. The majority of toxin genes are carried by conjugative plasmids that are readily transferable between *C. perfringens* cells, allowing dissemination of key virulence factors throughout a bacterial population (1,2). In this thesis, the *C.perfringens* plasmid pCP13 was demonstrated to be conjugative. A novel conjugation locus was identified and appears to represent an evolutionarily conserved clostridial conjugation region. The *pcpB4* gene (encoding a VirB4 homologue) within this locus was inactivated and found to be essential for conjugative transfer of pCP13, thus supporting the hypothesis that pCP13 is a *bona fide* conjugative plasmid.

C. perfringens cells also have the ability to harbour multiple highly related toxin plasmids (3), thus maximising their toxin arsenal and enhancing their disease-causing potential. The mechanism by which *C. perfringens* can maintain multiple similar plasmids has not been characterised. The central aim of this thesis was to dissect the mechanism of genome maintenance in *C. perfringens* and to determine which plasmid-encoded factors play a role in this phenotype. The results showed that plasmid incompatibility corresponded with differences in the ParMRC partitioning systems of these plasmids. A combination of *in vivo* incompatibility assays and DNA binding studies showed that plasmids with the same partitioning system were incompatible, likely due to promiscuous binding of ParR adaptor proteins to *parC* sites from the same family. The results also showed that plasmids with different ParMRC systems had the ability to stably coexist in the same strain. It therefore appears that *C. perfringens* has evolved different partitioning specificities to ensure that similar replicons are independently partitioned and thus stably maintained within a single cell. The focus of this chapter will be to discuss how *C. perfringens* has evolved two different mechanisms that have the same net effect; that is, to increase the number of separate toxin plasmids that a *C. perfringens* cell can stably maintain.

The mechanism of conjugative transfer in *C. perfringens* has exclusively been studied in the context of pCW3 and related plasmids (2,4). The Tcp locus carried by these plasmids has been well

characterised genetically and biochemical analyses are ongoing (2,5). The capacity for other plasmid families in *C. perfringens* to undergo conjugative transfer has not been investigated. Therefore, the ability of pCP13 to transfer *via* conjugation was examined after it was shown to contain a potential conjugation locus (6).

To investigate whether the newly named Pcp locus was responsible for the conjugative transfer of pCP13, a *pcpB4* mutant was constructed and analysed. Mutation of *pcpB4* resulted in the abolition of pCP13 transfer, which was restored *via* complementation with the wild-type *pcpB4* gene *in trans*. These results showed that PcpB4 was essential for the conjugation process. To determine if PcpB4 shares a common mechanism with other VirB4 homologues, the protein structure could be determined using X-ray crystallography. Future experiments could also focus on determining the function of other genes in the Pcp locus, by inactivating each gene and examining the effect on conjugation frequency.

PcpB4 is related to CstB4 from pCS1-1 (52% aa identity), which is required for the conjugative transfer of pCS1-1 (6). Cross complementation of *pcpB4* and *cstB4* mutants with their respective homologues did not restore the transfer frequencies to wild-type levels. The *pcpB4* mutation complemented with the *cstB4* gene *in trans* showed an increase in conjugation transfer frequency (10^{-6}-10^{-7} transconjugants/donor), however, this result was not statistically significant, even though this experiment was repeated ten times. These results presumably reflected variability in transfer levels that were close to the limit of detectability. The inability of these genes to complement each other intimates that these systems have most likely become species locked due to differences in their replication proteins and their necessary adaptation to the host protein environment. However, the nt sequence similarity between pCS1-1, pCLL and pCP13 suggest that these conjugation loci represent an ancestral clostridial conjugation system that has evolutionarily diverged. In comparison, the Tcp conjugation locus of pCW3 is only found in *C. perfringens* and represents a different acquisition event; indeed several of the Tcp components show low level aa sequence identity to conjugation proteins from the conjugative transposon Tn*916* (7). These findings suggest that a

conjugative transposon integrated into an ancestral *C. perfringens* plasmid that was subsequently propagated throughout the species (1). Future experiments could explore the ability of the *virB4* orthologue *tcpF* from pCW3 to complement the pCP13 *pcpB4* mutant and *vice-versa*. These experiments would confirm that these two *C. perfringens* conjugation loci are functionally distinct. There is evidence that there is an operational difference between these conjugation systems since a *tcpF* mutant of pCW3 is non-conjugative in a JIR325 background that carries pCP13 (7).

Mating experiments showed that pCP13 was able to undergo transfer at high frequency (10^{-1} transconjugants/donor cell), similar to that of pCW3 (8). Although the conjugation loci of pCP13, pCLL and pCS1-1 are similar, the transfer frequency of pCP13 is much higher than the transfer frequencies of pCS1-1 and pCLL (10^{-5}-10^{-7} transconjugants/donor cell) (6,9). This difference in conugation frequencies may be species specific (8) and may depend differences in cell wall or cell surface structures, variability in the adhesins on the bacterial cell surface or differences in the cell wall thickness, or the presence or absence of a capsule. *C. perfringens* surface adhesins may be more efficient at binding to recipient cells, or the cell wall may be more readily hydrolysed by peptidoglycan hydrolases.

In the absence of any demonstration that a conjugation pilus is involved in Gram-positive conjugation, there is most likely still a mechanism for interaction between the donor and recipient cells (10). TraO from pIP501 has been suggested to act as a surface adhesin, assisting in binding to the recipient cell (11). Similarly, pCW3 encodes a putative collagen adhesin-like protein, CnaC, and a sortase that may play a role in surface adhesion (7). Genes encoding a related collagen-binding protein (CnaB) and sortase also were identified within the Pcp locus of pCP13 and homologous loci on pCLL and pCS1-1. Cna proteins are surface adhesins that have been implicated in binding collagen and host epithelial cells, as well as virulence, in bacteria such as *S. aureus* (12,13). The chromosomally-encoded collagen adhesin locus (including *cnaA*) in *C. perfringens* avian necrotic enteritis isolates was shown to correlate with binding to collagen and the ability to colonise the chicken intestine (14,15). Sortases facilitate attachment of proteins with LPxTG motifs,

such as the Cna proteins, to the Gram-positive cell wall and are often required for pilus biogenesis (16). The Cna and sortase proteins encoded by pCP13 may facilitate binding of *C perfringens* donor cells to recipient cells; however, this hypothesis remains to be explored.

There are only a few pCP13-like plasmid sequences available in the NCBI database (17-20). Comparison of the available pCP13 nucleotide sequence to the other members of the pCP13-like plasmid family showed different degrees of conservation. The BEC carrying plasmids, pCP-OS1 and pCP-TS1 (19), encoded an almost identical 27.5 kb conjugation locus as well as very similar replication and maintenance regions. The conserved conjugation locus encoded all the key conjugation homologues that were identified in the Pcp locus, with each homologue having between 97-99% aa sequence identity to their pCP13 counterparts. The level of similarity between these plasmids suggests that the BEC-carrying plasmids are also likely to be conjugative. To test this hypothesis, a mutant derivative of the pCP-OS1 plasmid could be constructed by insertionally-inactivating the *becA or becB* genes with an erythromycin resistance gene. This resultant plasmid could be used in subsequent mixed plate matings with a suitable recipient to determine its ability to undergo conjugative transfer.

By contrast, the 58 kb cryptic plasmid pJFP55H, from the NetF positive *C. perfringens* strain JFP55, carries a Pcp locus that encodes proteins with lower aa sequence similarity (Chapter 2, Figure 2.2) (20). Finally, the bacteriocin plasmid from the *C. perfringens* food poisoning isolate, F5603, pBCNF5603 (18), carries a conserved PcpD2 relaxase and *oriT* region, but lacks most of the major conjugation homologues that are likely to be required for independent transfer, which suggest that pBCNF5603 may be mobilisable by the pCP13 conjugation machinery. However, PcpD2 may be unable to recognise the putative *oriT* from pBCNF5603 due to differences in the IR2 region (Chapter 2) in which case, pBCNF5603 would not be mobilised by pCP13.

Studies in *S. aureus* have shown that differences in the IR2 sequence correspond with different *oriT* sequence families (21). Whether the sequence differences are enough to mechanistically separate

the *oriT* sites in pCP13 and pBCNF5603 remains to be determined. To test this hypothesis and probe the importance of *oriT* IR2 differences in relaxase recognition, *in vivo* mobilisation experiments could be conducted. The putative *oriT* region from each pCP13 plasmid could be cloned into a non-conjugative vector and the ability of pCP13 to mobilise these plasmids into a suitable recipient could be assessed (22). Further characterisation of the relaxase-*oriT* interaction could also be performed using SPR to investigate interactions between the purified putative pCP13 relaxase (PcpD2) and different *oriT* site derivatives to identify the nucleotide sequences that are important for binding and cleavage.

The transfer of pCP13-like plasmids has broader implications for the spread of virulence factors in *C. perfringens* populations. A scenario can be imagined in which a BEC toxin-plasmid is transferred from an invading *C. perfringens* isolate to a commensal *C. perfringens* isolate in the gastrointestinal tract. This transfer event would convert the commensal cell to a toxin-producing *C. perfringens* cell, thereby negating the need for the invading cells to properly colonise the host to cause disease (23) (24). Transfer of pCW3-like plasmids has indeed been reported in several animal models, including broiler chickens and mice (24-26), suggesting that *in vivo* plasmid transfer may also be possible for pCP13-like plasmids.

One mechanism by which a *C. perfringens* cell may carry more than one toxin plasmid is to carry both a pCW3-toxin plasmid and a pCP13-toxin plasmid. Alternatively, previous work showed that *C. perfringens* strains often harbour multiple highly similar pCW3-like plasmids, several of which may encode different toxins (3,27). Each of these plasmids carry an almost identical replication region, however, they are stably maintained within the same strain (3,28). Plasmid incompatibility generally arises when two plasmids that have the same replication and maintenance machinery are introduced into the same bacterial cell (29), however, *C. perfringens* appears to be an exception to this rule (3). Closer examination of the pCW3 nucleotide sequence identified two genes adjacent to, but divergently transcribed from the *rep* gene, as well as an upstream repeat region that together resembled a ParMRC partitioning locus (3,7,27,28).

To investigate the contribution of the *C. perfringens* ParMRC partitioning systems to plasmid incompatibility, combinations of either identical or different ParMRC family plasmids were introduced into the same strain and their ability to coexist was determined (30). The results (Chapter 4) showed that plasmid incompatibility corresponded with the ParMRC family designation; that is, plasmids with the same partitioning system were unable to coexist within the same strain and plasmids with different partitioning systems were able to stably coexist. To further dissect the mechanism that governs this ParMRC-mediated incompatibility, SPR and AUC were employed to interrogate the specificity of the interaction between ParMRC components from different ParMRC families. The results of these DNA-binding studies showed that ParR proteins interacted with sequences within a centromeric *parC* site from the same ParMRC family, but could not interact with a non-cognate *parC* site from a different ParMRC family. The results also demonstrated that ParR proteins can bind to non-cognate *parC* sites from the same ParMRC family. These findings supported the phylogenetic groupings that were postulated previously (28) and correlated with the *in vivo* plasmid incompatibility data (30).

A bioinformatic survey of available pCW3-like plasmid sequences (outlined in Chapter 3) revealed that there are at least ten distinct ParMRC families ($ParMRC_{A-J}$) within *C. perfringens* (28,31). Importantly, the results showed that plasmids encoding the same partitioning system were generally not found within the same *C. perfringens* isolate (28). This observation suggested that these ParMRC systems may dictate which plasmid combinations can be co-maintained within a single isolate. Since that paper was published several more homologues have been identified, suggesting that future sequencing projects may result in the identification of additional *parMRC* variants in *C. perfringens* (V. Adams & J. Rood, unpublished). Finally, the scope of the ParMRC bioinformatics surveys should be broadened to include other members of the clostridia. Indeed, a putative ParMRC system was recently identified from the cryptic *C. difficile* plasmid, pDLL3026 (32).

Genetically marked derivatives of pCW3-like plasmids were used in the incompatibility study (Chapter 4). Whilst using native pCW3-like plasmids to test incompatibility is likely to reflect a more accurate representation of how incompatibility occurs in nature, it does not provide a clear indication of which factors are directly responsible for the incompatibility phenotype. There are multiple elements carried by these plasmids that may contribute to incompatibility, including the replication initiator and replication control genes.

To provide further genetic evidence that the plasmid incompatibility observed between native pCW3-like plasmids is ParMRC-mediated, a mini-replicon system could be developed, as previously described (33). The analysis of these otherwise isogenic vectors would allow the examination of the *parMRC* genes in isolation from any other potential stability or incompatibility determinants that are encoded by the native pCW3-like plasmids. There are two attributes that these mini-replicons would require in order to be of use in plasmid incompatibility and stability experiments: (i) compatible native pCW3-like replication regions to imitate the native copy number and (ii) different selectable markers so that each replicon may be selected independently when introduced into the same strain. Care would need to be taken when selecting suitable replication regions for these mini-replicons, a balance must be struck between imitating the native pCW3 plasmid (low copy number etc) and constructing base vectors that are already incompatible because their replication system is too similar.

Once these mini-replicon derivatives are constructed and shown to be compatible representatives of each *parMRC* gene family could be cloned into these vectors. Different combinations of mini-replicons carrying either similar or different ParMRC families could be introduced into the same strain and their relative stability determined. These experiments would confirm that the ParMRC systems directly contribute to pCW3-like plasmid incompatibility.

Since plasmid replication mechanisms are often responsible for incompatibility in other plasmids, it would also be worthwhile to further examine the *rep* and *oriV* regions in the pCW3-like plasmids and

determine their contribution to incompatibility. The results of the genetic incompatibility assays have already hinted that replication mechanisms may be involved, at least to some extent, in plasmid incompatibility in *C. perfringens*. An intermediate incompatibility phenotype was observed between $ParMRC_C$ and $ParMRC_D$ plasmids even though they had different partitioning systems (Chapter 4). Comparison of the Rep proteins from these plasmids showed that they were highly conserved (98% aa sequence identity) with no clear patterns or conserved changes in the aa sequences, however, alignment of the *oriV* sites revealed some sequence variation concentrated in the loop of IR2. This inverted repeat was previously shown to be essential for plasmid replication and most likely has an important replication control function in these plasmids (7). The *oriV* sequences of pCW3(*$parMRC_C$*) and pJIR3120 (*$parMRC_D$*) were almost identical, with only two nt sequence differences in the loop of IR2 (30). Indeed, small changes in replication associated RNA molecules contribute to the formation of different incompatibility groups in some *E. coli* plasmids, such as ColE1 (34). Therefore, the contribution of the IR2 region to plasmid incompatibility in *C. perfringens* cannot be ignored and will require further study. The results of this work suggest that the replication machinery and ParMRC systems may act in concert to influence plasmid incompatibility in *C. perfringens.*

There are two key recognition steps that determine the specificity of any ParMRC partition reaction (35,36). First, the ParR adaptor protein must recognise and bind to repeated sequences within the centromeric *parC* site. Next, the ParR/*parC* complex must interact with, and stabilise, the growing ParM filaments (36). The specificity of these interactions is important to ensure that different plasmids are partitioned independently within the cell and therefore are likely to play a role in partition-mediated plasmid incompatibility. This study focused on the interaction between ParR and *parC*, as it is the first recognition step in the partitioning reaction (37,38) and non-specific interaction between these components is responsible for the incompatibility phenotype reported for other plasmids (39).

ParR proteins in other bacteria have been found to bind to direct repeats in a centromeric *parC* region upstream of ParM. ParR from pSK41 recognises and binds to multiple 20 bp tandem repeats,

whereas ParR from R1 binds to ten 11 bp direct repeats (37,38). Similarly, ParR binding in pCW3-like plasmids appears to correlate with the presence of a series of direct repeats within the *parC* site. Binding of the $ParR_C$ proteins clearly corresponded with the presence of four 17 bp direct repeats in the $parC_C$ site (Chapter 5). By contrast, binding of $ParR_B$ and $ParR_D$ homologues was not as clearly delineated due to the presence of multiple overlapping direct and inverted repeat structures (Figure 6.1). Future studies might involve the more precise determination of the binding sites for these ParR proteins using SPR and a series of smaller dsDNA *parC* fragments. For example, $ParR_B$ homologues interacted with the $parC_B$ fragment B2 (Chapter 5). A series of sequential deletion derivatives of this fragment could be constructed and the ability of $ParR_B$ to interact with each of these fragments could be examined. The use of this "SPR footprinting" approach would assist in elucidating the minimal binding site for each of these ParR homologues.

To probe the ParR-*parC* interaction further, X-ray crystallography of ParR proteins from different families in complex with their cognate *parC* fragments could be carried out. Comparison of the structure of ParR-*parC* from different families would provide further insight into the structural basis of the specificity of ParR for its cognate *parC* site and give an indication of which residues are important for interaction. Preliminary attempts were made to obtain crystals of the $ParR_C$ protein, but these studies were unsuccessful.

In contrast to other ParR proteins, which form a tight dimer in solution (37,38), the sedimentation velocity data indicated that $ParR_C$ from pCW3 exists as a tetrameric complex. When a *parC* fragment containing the 17 bp direct repeat was added, a larger sedimentation coefficient was observed, suggesting that an interaction had occurred between the DNA and the $ParR_C$ tetramer. Other studies have shown that ParR proteins exist as a dimer-of-dimers when in complex with their cognate *parC* DNA (37,38). X-ray crystallographic structural data for $ParR_C$ in complex with $parC_C$ DNA could also provide support for the ParR-*parC* stoichiometry that was suggested by the AUC data (Chapter 5).
ParM proteins from other bacteria form filaments in the presence of ATP or GTP and these filaments interact with their cognate ParR-*parC* complex (40). This interaction represents the second

recognition step in the partition reaction. To test these interactions, similar SPR experiments to those previously undertaken (Chapter 5) could be conducted in which purified ParM is added to a ParR-*parC* complex that has been captured on a Streptavidin SPR chip.

To ensure that the purified ParM can form filaments, the buffer used for the experiment would have to be supplemented with adequate levels of Mg^{2+}, ATP or a non-hydrolysable ATP homologue. ATPγS and AMP-PNP have been used previously in other systems to lock ParM in the filament conformation and prevent depolymerisation (41). This locked ParM filament may be necessary to observe interaction between ParR-*parC* and ParM, otherwise the interactions may be transient or unstable. Once this method has been optimised for one set of ParMRC components, $ParM_B$, $ParM_C$ and $ParM_D$ homologues could be expressed and purified and inter-family interactions could be tested to determine if this interaction is specific as was observed for ParR-*parC*.

Questions remain about the precise mechanism and conceptual basis of partition-mediated incompatibility in *C. perfringens*. The results presented in this thesis suggest several scenarios that could be used to explain plasmid incompatibility and the ability of *C. perfringens* strains to maintain multiple closely related plasmids. The results showed that when two plasmids that have the same ParMRC family are introduced into the same strain they are incompatible and that ParR proteins from the same family bind to non-cognate *parC* sites from that family. These findings provide good evidence that the inability of promiscuous ParR proteins to discriminate between closely related *parC* sites from the same family is responsible for ParMRC-mediated incompatibility. The consequence of ParR binding promiscuity would be the formation of heterologous plasmid pairs. The inability to partition independently would lead to defects in plasmid segregation, which would result in the production of distinct bacterial sub-populations that only harbour one type of plasmid. Although the heterologous plasmid pairing model is not favoured for type I partitioning-mediated incompatibility (42-45), there is evidence to suggest that this model could explain ParMRC mediated incompatibility. For example, ParR from R1 can pair replicons before partitioning and promiscuous binding of ParR from pB171 is responsible for plasmid incompatibility (39,46).

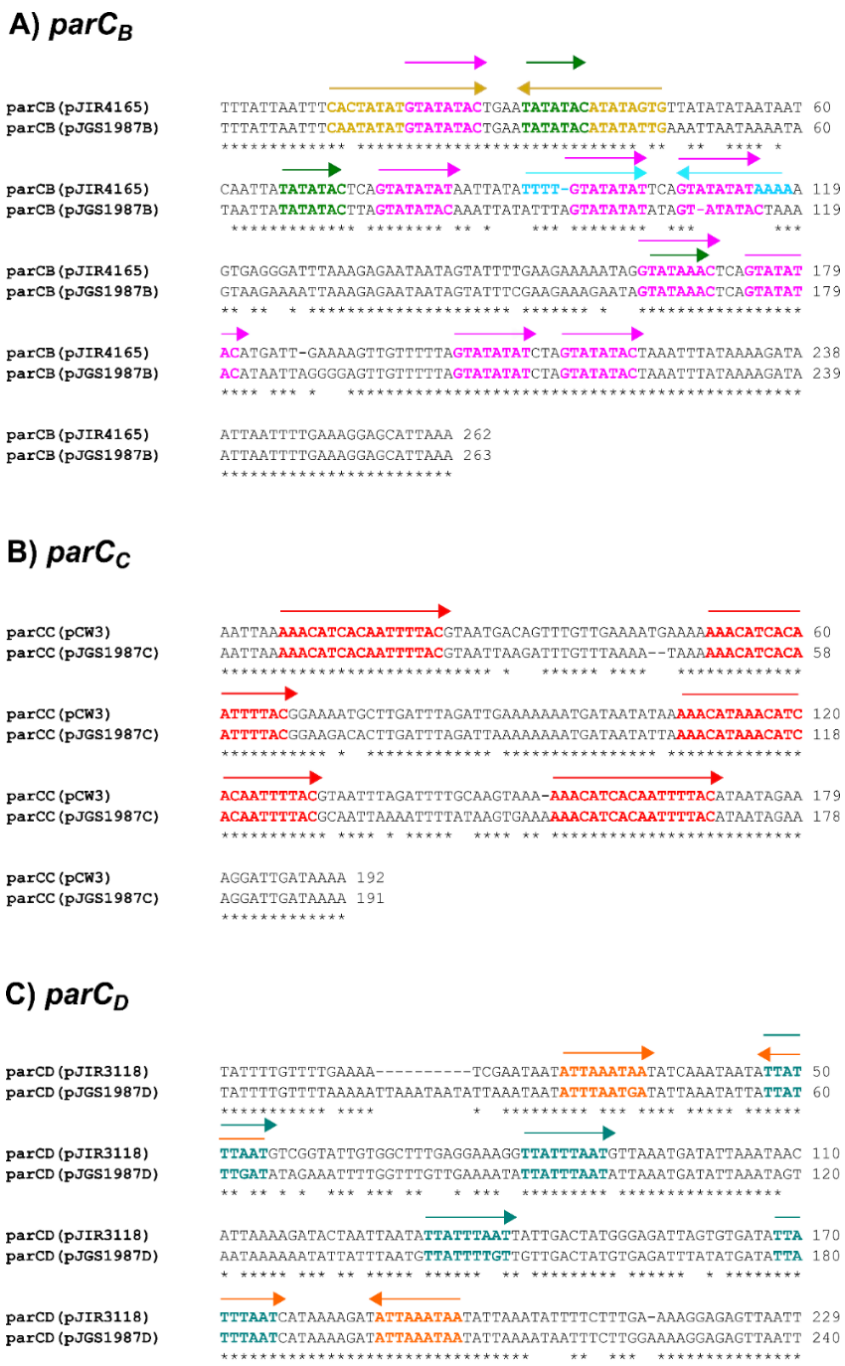

Figure 6.1. Conserved repeats in *parC* regions. Intra-family alignments of each *parC* region. **A)** shows a nucleotide sequence alignment between *parC*$_B$(pJIR4165) and *parC*$_B$(pJGS1987B), direct repeat type 1 (DR1) - pink, direct repeat type 2 - green (DR2), inverted repeat 1 - yellow (IR1) and inverted repeat 2 - blue. **B)** nucleotide sequence alignment between *parC*$_C$(pCW3) and *parC*$_C$(pJGS1987C), conserved direct repeats - red. **C)** nucleotide sequence alignment of *parC*$_D$(pJIR3118) and *parC*$_D$(pJGS1987D), direct repeats - blue, inverted repeats - orange.

The ParMRC partition process requires both plasmids to be linked *via* interaction between the ParR-*parC* complex and ParM filaments, before each plasmid is pushed to either cell pole (36,47,48) (Figure 6.2A). The heterologous pairing model is a conceptually simple model that explains the experimental data (Figure 6.2B). Whilst this model of incompatibility is attractive, whether it can be reconciled with the fact that after replication sister plasmids will be in closer proximity than other heterologous plasmids, and therefore are more likely to pair, remains to be determined. The heterologous plasmid pairing model is only robust if replication and partition are uncoupled, that is, if plasmids are chosen from a pool for partitioning and partition does not occur immediately after replication. If partition occurs directly after replication, sister plasmids will be partitioned before heterologous plasmid pairs can be formed. Conversely, sister plasmids may be initially partitioned, but then return to the plasmid pool through stochastic diffusion for subsequent rounds of partition during the cell cycle.

Plasmid partitioning systems at their core are a mechanism for plasmid positioning within the cell. A second scenario therefore presents itself, wherein these partitioning systems segregate similar pCW3-like plasmids into different plasmid clusters within the cell (Figure 6.2C). Plasmids such as R1 (low-copy number) and RK2 (high-copy number) have been observed to cluster into discrete foci within the cell (49,50), but whether this phenomenon is actively facilitated by ParMRC partitioning systems is unclear. The ParMRC partitioning systems may keep discrete plasmid clusters spatially isolated to ensure that the similar replication regions do not interfere, or to ensure that similar plasmids do not recombine with one another. ParMRC-mediated spatial isolation, or plasmid clustering, could therefore be a novel method of multipartite genome maintenance. In this scenario, if two plasmids have the same partitioning system, they will be relegated to the same plasmid cluster. These mixed clusters would present an opportunity for similar replication elements (such as diffusible RNA or Rep protein molecules) to interact and interfere, which would lead to copy number imbalances and plasmid incompatibility. Alternatively, the positioning of discrete plasmid clusters

may become perturbed once two plasmid species with the same partitioning system are introduced, as has been reported for type I partitioning systems from the dual partition locus plasmid pB171 from *E. coli* (45).

To examine these hypotheses, future experiments could be utilise either confocal or super-resolution fluorescent microscopy to observe the ability of partitioning proteins to pair heterologous plasmids, or to observe the localisation of different ParMRC family plasmids within a single cell. To carry out these experiments, partition proteins would need to be fluorescently labelled. Previous studies have labelled ParM proteins either by expressing ParM fusion proteins coupled to green fluorescent protein (GFP) or yellow fluorescent protein (YFP) or *via* immunofluorescence with primary antibodies raised to ParM (51-53). Folding of GFP and YFP is oxygen-dependent (54) and *C. perfringens* is an anaerobic organism. Consequently, there are inherent problems in constructing fusion proteins in *C. perfringens*. Several oxygen-independent fluorescent proteins are currently available (55-57), however, *C. perfringens* remains a relatively difficult genetic system to work with. A simpler approach may be to codon optimise each ParMRC system and reconstitute the system using a model organism such as *E. coli*. Previous studies have used *E. coli* as an ectopic host for the expression and imaging of other fluorescently labelled Gram-positive ParMRC systems (53).

In addition to fluorescently labelled partitioning components, the plasmids would need to be labelled to examine their cellular localisation. Previous studies have utilised a GFP-LacI repressor and a *lacO* operator array to specifically label plasmid DNA in the cell (51,52,58,59). The *lacO* array and *lacI* genes are inserted into the backbone of the plasmid of interest and introduced into a cell. The GFP-LacI then binds to the operator array, thereby labelling the plasmid of interest.

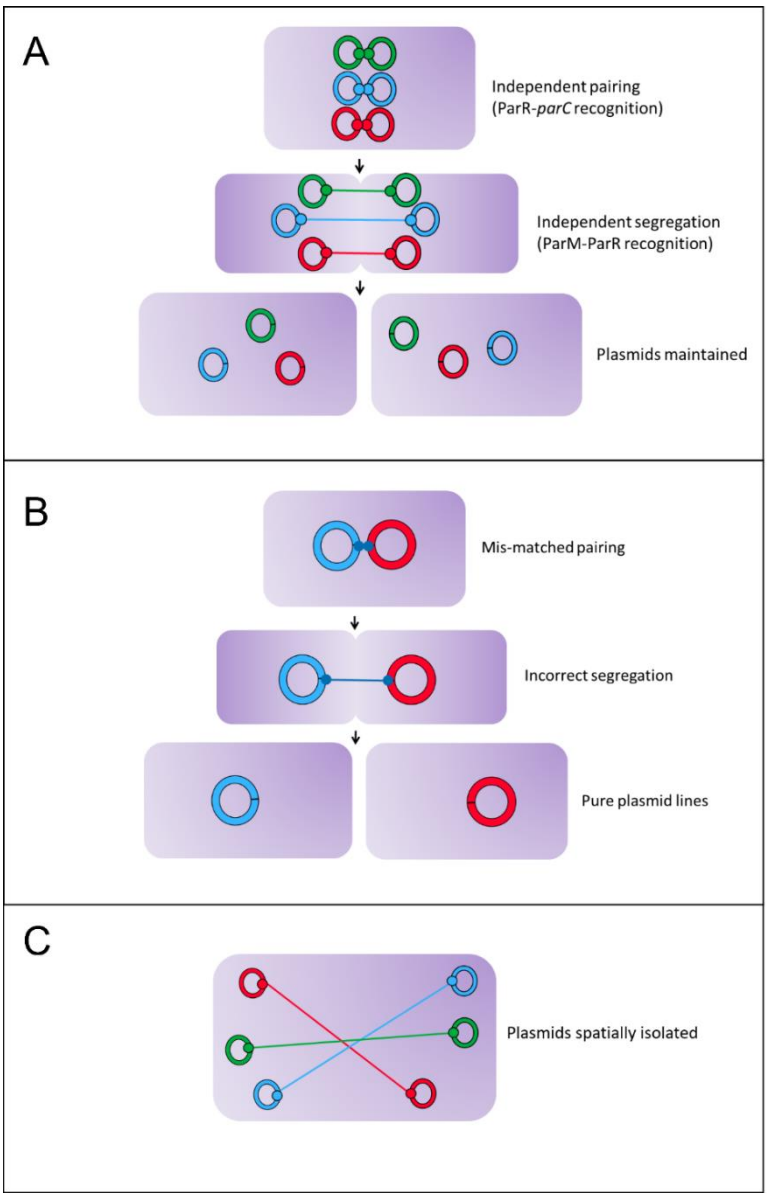

Figure 6.2. Models of multiple plasmid maintenance and incompatibility in *C. perfringens*: A) Three plasmids within a *C. perfringens* isolate (purple) are shown as green, blue and red open circles. Corresponding ParR adaptor proteins are shown as closed circles of the same colours. Each of these plasmids encodes a different ParMRC family, the sister plasmids are partitioned independently and ensure that each daughter cell receives a copy of each plasmid. B) shows a scenario in which each plasmid (red and blue open circles) is from the same ParMRC family (ParR blue closed circle). These heterologous plasmids are linked at their *parC* centromere site *via* the ParR protein. The ParM protein (blue line) acts to separate these plasmids to either cell pole, leading to partition of different plasmids into each daughter cell. This scenario ultimately leads to the production of two distinct subpopulations each housing only one plasmid type. C) This scenario shows plasmids segregated into separate clusters at different locations within the cell, so that similar replicons cannot interact with one another.

To further examine the mechanism of *C. perfringens* ParMR-mediated incompatibility, fluorescently labelled ParM derivatives from the various partitioning families could be constructed, e.g. YFP-$ParM_C$, RFP-$ParM_C$, YFP-$ParM_B$ and RFP-$ParM_B$. Next, a series of plasmids labelled with different fluorescent protein-LacI constructs could be constructed, e.g. GFP-LacI and BFP-LacI. Different combinations of ParMRC family vectors expressing fluorescently labelled ParM and LacI could be introduced together, and separately, into *E. coli*. These cells could then be imaged using confocal or super-resolution fluorescent microscopy to examine the dynamics of the partitioning reaction. These experiments could help answer several questions including: (a) do plasmids with similar centromeres form ParM-mediated heterologous pairs? (b) do different ParMRC plasmids cluster at different cellular locations? and (c) is this clustering mediated by ParM filaments?

In conclusion, the results of these studies show that the pCW3-like plasmids experience incompatibility and that this incompatibility correlates with ParMRC designation. These results have implications for the maintenance of large toxin and antimicrobial resistance plasmids in *C. perfringens*, but can also be applied to a broad range of important antimicrobial resistance plasmids that rely upon ParMRC systems for their faithful inheritance.

The results presented in this thesis show that *C. perfringens* can utilise at least two different strategies to maintain more than one toxin plasmid within a bacterial cell and spread these plasmids to other cells, thereby maximising its disease-causing potential and its ability to adapt to different ecological niches. *C. perfringens* cells can either (i) carry different toxins on compatible plasmids from different families, that is, a pCW3-like plasmid and a pCP13-like plasmid, and/or (ii) harbour multiple pCW3-like plasmids with different ParMRC partitioning systems. These plasmids are also independently conjugative and therefore capable of disseminating a large range of virulence factors. In the future, these maintenance and conjugation mechanisms could be an attractive target for therapeutic agents. The disruption of plasmid maintenance or conjugation could be exploited to drive

these important vehicles for the dissemination of antibiotic resistance determinants out of bacterial populations.

References

1. Li, J., Adams, V., Bannam, T.L., Miyamoto, K., Garcia, J.P., Uzal, F.A., Rood, J.I. and McClane, B.A. (2013) Toxin plasmids of *Clostridium perfringens*. *Microbiol. Mol. Biol. Rev.*, **77**, 208-233.
2. Wisniewski, J.A. and Rood, J.I. (2017) The Tcp conjugation system of *Clostridium perfringens*. *Plasmid*, **91**, 28-36.
3. Bannam, T.L., Yan, X.X., Harrison, P.F., Seemann, T., Keyburn, A.L., Stubenrauch, C., Weeramantri, L.H., Cheung, J.K., McClane, B.A., Boyce, J.D. *et al.* (2011) Necrotic enteritis-derived *Clostridium perfringens* strain with three closely related independently conjugative toxin and antibiotic resistance plasmids. *mBio*, **2**, e00190-00111.
4. Li, J., Adams, V., Bannam, T.L., Miyamoto, K., Garcia, J.P., Uzal, F.A., Rood, J.I. and McClane, B.A. (2013) Toxin plasmids of *Clostridium perfringens*. *Microbiol. Mol. Biol. Rev.*, **77**, 208-233.
5. Traore, D.A.K., Wisniewski, J.A., Flanigan, S.F., Conroy, P.J., Panjikar, S., Mok, Y.F., Lao, C., Griffin, M.D.W., Adams, V., Rood, J.I. *et al.* (2018) Crystal structure of TcpK in complex with oriT DNA of the antibiotic resistance plasmid pCW3. *Nature Communications*, **9**, 3732.
6. Vidor, C.J., Watts, T.D., Adams, V., Bulach, D., Couchman, E., Rood, J.I., Fairweather, N.F., Awad, M. and Lyras, D. (2018) Clostridium sordellii Pathogenicity Locus Plasmid pCS1-1 Encodes a Novel Clostridial Conjugation Locus. *MBio*, **9**.
7. Bannam, T.L., Teng, W.L., Bulach, D., Lyras, D. and Rood, J.I. (2006) Functional identification of conjugation and replication regions of the tetracycline resistance plasmid pCW3 from *Clostridium perfringens*. *J. Bacteriol.*, **188**, 4942-4951.
8. Rood, J.I., Scott, V.N. and Duncan, C.L. (1978) Identification of a transferable tetracycline resistance plasmid (pCW3) from *Clostridium perfringens*. *Plasmid*, **1**, 563-570.

9. Marshall, K.M., Bradshaw, M. and Johnson, E.A. (2010) Conjugative botulinum neurotoxin-encoding plasmids in *Clostridium botulinum*. *PLOS One*, **5**, e11087-e11087.

10. Grohmann, E., Christie, P.J., Waksman, G. and Backert, S. (2018) Type IV secretion in Gram-negative and Gram-positive bacteria. *Mol. Microbiol.*, **107**, 455-471.

11. Goessweiner-Mohr, N., Arends, K., Keller, W. and Grohmann, E. (2013) Conjugative type IV secretion systems in Gram-positive bacteria. *Plasmid*, **70**, 289-302.

12. Madani, A., Garakani, K. and Mofrad, M.R.K. (2017) Molecular mechanics of *Staphylococcus aureus* adhesin, CNA, and the inhibition of bacterial adhesion by stretching collagen. *PLOS One*, **12**, e0179601-e0179601.

13. Rhem, M.N., Lech, E.M., Patti, J.M., McDevitt, D., Höök, M., Jones, D.B. and Wilhelmus, K.R. (2000) The collagen-binding adhesin is a virulence factor in *Staphylococcus aureus* keratitis. *Infect. Immun.*, **68**, 3776-3779.

14. Wade, B., Keyburn, A.L., Haring, V., Ford, M., Rood, J.I. and Moore, R.J. (2016) The adherent abilities of *Clostridium perfringens* strains are critical for the pathogenesis of avian necrotic enteritis. *Vet. Microbiol.*, **197**, 53-61.

15. Wade, B., Keyburn, A.L., Seemann, T., Rood, J.I. and Moore, R.J. (2015) Binding of *Clostridium perfringens* to collagen correlates with the ability to cause necrotic enteritis in chickens. *Vet. Microbiol.*, **180**, 299-303.

16. Khare, B. and S, V.L.N. (2017) Pilus biogenesis of Gram-positive bacteria: Roles of sortases and implications for assembly. *Protein Sci.*, **26**, 1458-1473.

17. Shimizu, T., Ohtani, K., Hirakawa, H., Ohshima, K., Yamashita, A., Shiba, T., Ogasawara, N., Hattori, M., Kuhara, S. and Hayashi, H. (2002) Complete genome sequence of Clostridium perfringens, an anaerobic flesh-eater. *Proc Natl Acad Sci U S A*, **99**, 996-1001.

18. Miyamoto, K., Seike, S., Takagishi, T., Okui, K., Oda, M., Takehara, M. and Nagahama, M. (2015) Identification of the replication region in pBCNF5603, a bacteriocin-encoding plasmid, in the enterotoxigenic Clostridium perfringens strain F5603. *BMC Microbiol.*, **15**, 118.

19. Yonogi, S., Matsuda, S., Kawai, T., Yoda, T., Harada, T., Kumeda, Y., Gotoh, K., Hiyoshi, H., Nakamura, S., Kodama, T. *et al.* (2014) BEC, a novel enterotoxin of *Clostridium perfringens*

found in human clinical isolates from acute gastroenteritis outbreaks. *Infect. Immun.*, **82**, 2390-2399.

20. Gohari, M.I., Parreira, V.R., Nowell, V.J., Nicholson, V.M., Oliphant, K. and Prescott, J.F. (2015) A novel pore-forming toxin in type A *Clostridium perfringens* is associated with both fatal canine hemorrhagic gastroenteritis and fatal foal necrotizing enterocolitis. *PloS One*, **10**, e0122684.
21. O'Brien, F.G., Yui Eto, K., Murphy, R.J.T., Fairhurst, H.M., Coombs, G.W., Grubb, W.B. and Ramsay, J.P. (2015) Origin-of-transfer sequences facilitate mobilisation of non-conjugative antimicrobial-resistance plasmids in *Staphylococcus aureus*. *Nucleic Acids Res.*, **43**, 7971-7983.
22. Wisniewski, J.A., Traore, D.A., Bannam, T.L., Lyras, D., Whisstock, J.C. and Rood, J.I. (2016) TcpM: a novel relaxase that mediates transfer of large conjugative plasmids from *Clostridium perfringens*. *Mol. Microbiol.*, **99**, 884-896.
23. Brynestad, S., Sarker, M.R., McClane, B.A., Granum, P.E. and Rood, J.I. (2001) Enterotoxin plasmid from *Clostridium perfringens* is conjugative. *Infect. Immun.*, **69**, 3483-3487.
24. Hughes, M.L., Poon, R., Adams, V., Sayeed, S., Saputo, J., Uzal, F.A., McClane, B.A. and Rood, J.I. (2007) Epsilon-toxin plasmids of *Clostridium perfringens* type D are conjugative. *J. Bacteriol.*, **189**, 7531-7538.
25. Brefort, G., Magot, M., Ionesco, H. and Sebald, M. (1977) Characterization and transferability of *Clostridium perfringens* plasmids. *Plasmid*, **1**, 52-66.
26. Lacey, J.A., Keyburn, A.L., Ford, M.E., Portela, R.W., Johanesen, P.A., Lyras, D. and Moore, R.J. (2017) Conjugation-mediated horizontal gene transfer of *Clostridium perfringens* plasmids in the chicken gastrointestinal tract results in the formation of new virulent strains. *Appl. Environ. Microbiol.*
27. Parreira, V.R., Costa, M., Eikmeyer, F., Blom, J. and Prescott, J.F. (2012) Sequence of two plasmids from *Clostridium perfringens* chicken necrotic enteritis isolates and comparison with *C. perfringens* conjugative plasmids. *PLOS One*, **7**, e49753.

28. Adams, V., Watts, T.D., Bulach, D.M., Lyras, D. and Rood, J.I. (2015) Plasmid partitioning systems of conjugative plasmids from *Clostridium perfringens*. *Plasmid*, **80**, 90-96.

29. Novick, R.P. (1987) Plasmid incompatibility. *Microbiol Rev*, **51**, 381-395.

30. Watts, T.D., Johanesen, P.A., Lyras, D., Rood, J.I. and Adams, V. (2017) Evidence that compatibility of closely related replicons in *Clostridium perfringens* depends on linkage to parMRC-like partitioning systems of different subfamilies. *Plasmid*, **91**, 68-75.

31. Derman, A.I., Becker, E.C., Truong, B.D., Fujioka, A., Tucey, T.M., Erb, M.L., Patterson, P.C. and Pogliano, J. (2009) Phylogenetic analysis identifies many uncharacterized actin-like proteins (Alps) in bacteria: regulated polymerization, dynamic instability and treadmilling in Alp7A. *Mol. Microbiol.*, **73**, 534-552.

32. Amy, J., Bulach, D., Knight, D., Riley, T., Johanesen, P. and Lyras, D. (2018) Identification of large cryptic plasmids in *Clostridioides* (*Clostridium*) *difficile*. *Plasmid*, **96-97**, 25-38.

33. Gerdes, K. and Molin, S. (1986) Partitioning of plasmid R1. Structural and functional analysis of the parA locus. *J. Mol. Biol.*, **190**, 269-279.

34. Tomizawa, J. and Itoh, T. (1981) Plasmid ColE1 incompatibility determined by interaction of RNA I with primer transcript. *Proc Natl Acad Sci U S A*, **78**, 6096-6100.

35. Gerdes, K., Howard, M. and Szardenings, F. (2010) Pushing and pulling in prokaryotic DNA segregation. *Cell*, **141**, 927-942.

36. Salje, J., Gayathri, P. and Lowe, J. (2010) The ParMRC system: molecular mechanisms of plasmid segregation by actin-like filaments. *Nat. Rev. Microbiol.*, **8**, 683-692.

37. Moller-Jensen, J., Ringgaard, S., Mercogliano, C.P., Gerdes, K. and Lowe, J. (2007) Structural analysis of the ParR/parC plasmid partition complex. *EMBO J.*, **26**, 4413-4422.

38. Schumacher, M.A., Glover, T.C., Brzoska, A.J., Jensen, S.O., Dunham, T.D., Skurray, R.A. and Firth, N. (2007) Segrosome structure revealed by a complex of ParR with centromere DNA. *Nature*, **450**, 1268-1271.

39. Hyland, E.M., Wallace, E.W. and Murray, A.W. (2014) A model for the evolution of biological specificity: a cross-reacting DNA-binding protein causes plasmid incompatibility. *J. Bacteriol.*, **196**, 3002-3011.

40. Jensen, R.B. and Gerdes, K. (1997) Partitioning of plasmid R1. The ParM protein exhibits ATPase activity and interacts with the centromere-like ParR-*parC* complex. *J. Mol. Biol.*, **269**, 505-513.

41. Moller-Jensen, J., Jensen, R.B., Lowe, J. and Gerdes, K. (2002) Prokaryotic DNA segregation by an actin-like filament. *EMBO J.*, **21**, 3119-3127.

42. Bouet, J.Y., Rech, J., Egloff, S., Biek, D.P. and Lane, D. (2005) Probing plasmid partition with centromere-based incompatibility. *Mol. Microbiol.*, **55**, 511-525.

43. Bouet, J.Y., Nordstrom, K. and Lane, D. (2007) Plasmid partition and incompatibility--the focus shifts. *Mol. Microbiol.*, **65**, 1405-1414.

44. Diaz, R., Rech, J. and Bouet, J.Y. (2015) Imaging centromere-based incompatibilities: Insights into the mechanism of incompatibility mediated by low-copy number plasmids. *Plasmid*, **80**, 54-62.

45. Ebersbach, G., Sherratt, D.J. and Gerdes, K. (2005) Partition-associated incompatibility caused by random assortment of pure plasmid clusters. *Mol. Microbiol.*, **56**, 1430-1440.

46. Jensen, R.B., Lurz, R. and Gerdes, K. (1998) Mechanism of DNA segregation in prokaryotes: replicon pairing by *parC* of plasmid R1. *Proc Natl Acad Sci U S A*, **95**, 8550-8555.

47. Bharat, T.A., Murshudov, G.N., Sachse, C. and Lowe, J. (2015) Structures of actin-like ParM filaments show architecture of plasmid-segregating spindles. *Nature*, **523**, 106-110.

48. Gayathri, P., Fujii, T., Moller-Jensen, J., van den Ent, F., Namba, K. and Lowe, J. (2012) A bipolar spindle of antiparallel ParM filaments drives bacterial plasmid segregation. *Science*, **338**, 1334-1337.

49. Pogliano, J., Ho, T.Q., Zhong, Z. and Helinski, D.R. (2001) Multicopy plasmids are clustered and localized in *Escherichia coli*. *Proc Natl Acad Sci U S A*, **98**, 4486-4491.

50. Weitao, T., Dasgupta, S. and Nordstrom, K. (2000) Plasmid R1 is present as clusters in the cells of *Escherichia coli*. *Plasmid*, **43**, 200-204.

51. Jensen, R.B. and Gerdes, K. (1999) Mechanism of DNA segregation in prokaryotes: ParM partitioning protein of plasmid R1 co-localizes with its replicon during the cell cycle. *EMBO J.*, **18**, 4076-4084.

52. Moller-Jensen, J., Borch, J., Dam, M., Jensen, R.B., Roepstorff, P. and Gerdes, K. (2003) Bacterial mitosis: ParM of plasmid R1 moves plasmid DNA by an actin-like insertional polymerization mechanism. *Mol. Cell*, **12**, 1477-1487.

53. Brzoska, A.J., Jensen, S.O., Barton, D.A., Davies, D.S., Overall, R.L., Skurray, R.A. and Firth, N. (2016) Dynamic filament formation by a divergent bacterial actin-like ParM protein. *PLOS One*, **11**, e0156944.

54. Heim, R., Prasher, D.C. and Tsien, R.Y. (1994) Wavelength mutations and posttranslational autoxidation of green fluorescent protein. *Proc Natl Acad Sci U S A*, **91**, 12501-12504.

55. Drepper, T., Eggert, T., Circolone, F., Heck, A., Krauss, U., Guterl, J.K., Wendorff, M., Losi, A., Gartner, W. and Jaeger, K.E. (2007) Reporter proteins for *in vivo* fluorescence without oxygen. *Nat. Biotechnol.*, **25**, 443-445.

56. Mukherjee, A., Weyant, K.B., Agrawal, U., Walker, J., Cann, I.K.O. and Schroeder, C.M. (2015) Engineering and Characterization of New LOV-Based Fluorescent Proteins from *Chlamydomonas reinhardtii* and *Vaucheria frigida*. *ACS Synthetic Biology*, **4**, 371-377.

57. Mukherjee, A., Walker, J., Weyant, K.B. and Schroeder, C.M. (2013) Characterization of flavin-based fluorescent proteins: an emerging class of fluorescent reporters. *PLOS One*, **8**, e64753.

58. Straight, A.F., Belmont, A.S., Robinett, C.C. and Murray, A.W. (1996) GFP tagging of budding yeast chromosomes reveals that protein-protein interactions can mediate sister chromatid cohesion. *Curr. Biol.*, **6**, 1599-1608.

59. Robinett, C.C., Straight, A., Li, G., Willhelm, C., Sudlow, G., Murray, A. and Belmont, A.S. (1996) *in vivo* localization of DNA sequences and visualization of large-scale chromatin organization using lac operator/repressor recognition. *J. Cell Biol.*, **135**, 1685-1700.

Appendix A. *Clostridium sordellii* Pathogenicity Locus plasmid pCS1-1 encodes a novel clostridial conjugation locus

AMERICAN SOCIETY FOR MICROBIOLOGY | mBio®

RESEARCH ARTICLE

Clostridium sordellii Pathogenicity Locus Plasmid pCS1-1 Encodes a Novel Clostridial Conjugation Locus

Callum J. Vidor,[a] Thomas D. Watts,[a] Vicki Adams,[a] Dieter Bulach,[b]* Edward Couchman,[c] Julian I. Rood,[a] Neil F. Fairweather,[c] Milena Awad,[a] Dena Lyras[a]

[a]Infection and Immunity Program, Monash Biomedicine Discovery Institute and Department of Microbiology, Monash University, Clayton, Victoria, Australia

[b]Victorian Bioinformatics Consortium, Monash University, Clayton, Victoria, Australia

[c]Department of Life Sciences, Centre for Molecular Bacteriology and Infection, Imperial College London, London, United Kingdom

ABSTRACT A major virulence factor in *Clostridium sordellii*-mediated infection is the toxin TcsL, which is encoded within a region of the genome called the pathogenicity locus (PaLoc). *C. sordellii* isolates carry the PaLoc on the pCS1 family of plasmids, of which there are four characterized members. Here, we determined the potential mobility of pCS1 plasmids and characterized a fifth unique pCS1 member. Using a derivative of the pCS1-1 plasmid from strain ATCC 9714 which had been marked with the *ermB* erythromycin resistance gene, conjugative transfer into a recipient *C. sordellii* isolate, R28058, was demonstrated. Bioinformatic analysis of pCS1-1 identified a novel conjugation gene cluster defined as the *C. sordellii* transfer (*cst*) locus. Interruption of genes within the *cst* locus resulted in loss of pCS1-1 transfer, which was restored upon complementation in *trans*. These studies provided clear evidence that genes within the *cst* locus are essential for the conjugative transfer of pCS1-1. The *cst* locus is present on all pCS1 subtypes, and homologous loci were identified on toxin-encoding plasmids from *Clostridium perfringens* and *Clostridium botulinum* and also carried within genomes of *Clostridium difficile* isolates, indicating that it is a widespread clostridial conjugation locus. The results of this study have broad implications for the dissemination of toxin genes and, potentially, antibiotic resistance genes among members of a diverse range of clostridial pathogens, providing these microorganisms with a survival advantage within the infected host.

IMPORTANCE *C. sordellii* is a bacterial pathogen that causes severe infections in humans and animals, with high mortality rates. While the pathogenesis of *C. sordellii* infections is not well understood, it is known that the toxin TcsL is an important virulence factor. Here, we have shown the ability of a plasmid carrying the *tcsL* gene to undergo conjugative transfer between distantly related strains of *C. sordellii*, which has far-reaching implications for the ability of *C. sordellii* to acquire the capacity to cause disease. Plasmids that carry *tcsL* encode a previously uncharacterized conjugation locus, and individual genes within this locus were shown to be required for conjugative transfer. Furthermore, homologues on toxin plasmids from other clostridial species were identified, indicating that this region represents a novel clostridial conjugation locus. The results of this study have broad implications for the dissemination of virulence genes among members of a diverse range of clostridial pathogens.

KEYWORDS *Clostridium*, *Clostridium sordellii*, conjugation, PaLoc transfer, plasmid

Conjugation is a mechanism of lateral gene transfer by which mobile genetic elements undergo intra- and interspecies horizontal transfer via cell-to-cell contact. Such transfer events can lead to the dissemination of clinically relevant antibiotic

Received 22 September 2017 **Accepted** 15 November 2017 **Published** 16 January 2018

Citation Vidor CJ, Watts TD, Adams V, Bulach D, Couchman E, Rood JI, Fairweather NF, Awad M, Lyras D. 2018. *Clostridium sordellii* pathogenicity locus plasmid pCS1-1 encodes a novel clostridial conjugation locus. mBio 9: e01761-17. https://doi.org/10.1128/mBio.01761-17.

Editor Bruce A. McClane, University of Pittsburgh Sch. Med.

Address correspondence to Dena Lyras, dena.lyras@monash.edu.

* Present address: Dieter Bulach, Victorian Life Sciences Computation Initiative, The University of Melbourne, Victoria, Australia.

M.A. and D.L. contributed equally to this article and should be regarded as joint senior authors.

resistance- and virulence-related genes. Conjugative plasmids and integrative conjugative elements encode the machinery required for the transfer of a genetic element from a donor cell into a recipient cell (1). The conjugation machinery has two major components. The first is the relaxasome, a protein complex that binds to and processes the DNA for transfer (2). The major component of the relaxasome is the relaxase protein. The relaxase binds to the origin of transfer (*oriT*) of the target DNA, nicks it to produce single-stranded DNA, and facilitates its transfer between donor and recipient cells (1). The second major component is a type IV secretion system (T4SS) that actively pumps the relaxase-bound single-stranded target DNA from the donor cell through a mating channel into the recipient (1).

Conjugation is less well characterized in Gram-positive organisms, and several T4SS components from Gram-negative bacteria are not present (3). The processes occurring at the donor-recipient interface in Gram-positive conjugation systems are still poorly understood; however, cell-to-cell contact is known to be required for conjugative transfer (3, 4), and these systems do contain functional T4SS homologues (3).

In this work, we explored the conjugative transfer of virulence plasmids of the Gram-positive animal and human pathogen *Clostridium sordellii*. *C. sordellii*-mediated infections in animals usually manifest as severe enterotoxemia and can affect cattle (5), sheep (6, 7), and horses (8). Although rare, *C. sordellii*-mediated human infections are often severe, with overall mortality rates reaching 70% (9). The most common human *C. sordellii* diseases appear to be soft tissue infections, which can occur postsurgery or via trauma (9). *C. sordellii* intrauterine infections have also been recorded in women postpartum and postabortion (9–11). These intrauterine infections develop into a toxic shock-like syndrome, and, while such infections are also rare, the mortality rates in these cases are close to 100% (9–12).

Although the pathogenesis of *C. sordellii* infection is still poorly understood, the major virulence factors that lead to severe disease are thought to be two large clostridial toxins (LCTs), TcsH (hemorrhagic toxin) and TcsL (lethal toxin) (13). These toxins are homologues of the better-characterized toxins TcdA (toxin A) and TcdB (toxin B) from *Clostridium difficile*, respectively (14), and TcsL is also similar to Tcnα from *Clostridium novyi* (15) and TpeL from *Clostridium perfringens* (16). The LCTs function by inactivating small GTPases within mammalian cells, leading to an altered cytoskeleton, which results in cell rounding and death (17). The role of TcsL as a crucial virulence factor in *C. sordellii*-mediated disease has been validated by several studies (18–20).

Recent genomic analysis of *C. sordellii* isolates has revealed that TcsH and TcsL are encoded within a pathogenicity locus (PaLoc) related to the *tcdA*- and *tcdB*-encoding PaLoc of *C. difficile* (14). A homologous PaLoc encodes LCT TpeL in *C. perfringens* (21). The genomic context of the LCTs from clostridial species other than *C. sordellii* has largely been characterized, with each of these LCTs either associated with a mobile genetic element (22–25) or able to undergo horizontal gene transfer (26). The *C. difficile* PaLoc in almost all strains is found within a distinct region of the chromosome (27, 28), and while it is not associated with any identifiable mobile genetic elements, conjugative transfer into a nontoxigenic *C. difficile* strain, most likely as a result of random high-frequency recombination transfer of chromosomal DNA, has been demonstrated previously (26). The *tpeL*-associated PaLoc is carried on large conjugative plasmids containing a *tcp* locus from the paradigm *C. perfringens* pCW3 conjugative plasmid (24, 25), and it has been shown that at least one of these *tpeL* plasmids is conjugative (23). The *C. novyi* alpha toxin is carried on a phage genome that has been shown to infect and convert nontoxigenic isolates to a toxigenic phenotype (22, 29).

Until recently, the genomic context of the *C. sordellii* PaLoc was unknown; however, a recent study showed that toxigenic *C. sordellii* strains encoded their PaLoc on members of a related plasmid family, the pCS1 family (30). Four pCS1 family plasmids have been characterized to date (30). pCS1-1 is ~103 kb in size, contains a truncated *tcsH* gene, and is found in the *C. sordellii* type strain, ATCC 9714. pCS1-2 contains a PaLoc related to pCS1-1; however, it is larger (~117 kb) and contains a number of unique regions, while ~106-kb pCS1-3 is the only subtype to contain a full-length *tcsH*

gene. Finally, pCS1-4 is smaller (~99.9 kb) and does not contain the PaLoc. In place of this region, there are a number of open reading frames (ORFs) with unknown functions (30). Unlike the state of knowledge of the *C. difficile* PaLoc (26), the *tpeL*-containing plasmids (23), and the *tcn*α-containing phage (22, 29), the capacity of the members of the pCS1 family of plasmids or the *C. sordellii* PaLoc to undergo lateral gene transfer is unknown.

In this work, we sought to functionally characterize the members of the pCS1 family of plasmids and to determine whether they are able to undergo horizontal transfer in *C. sordellii*. Mating experiments showed that a marked version of pCS1-1 from the *C. sordellii* type strain, ATCC 9714, can undergo conjugative transfer into a nontoxigenic *C. sordellii* strain. Bioinformatic analysis of pCS1-1 allowed us to identify a putative novel conjugation locus present on this plasmid. Not only was this locus conserved among all pCS1 family plasmids, but homologous loci were present in other clostridial species, including *Clostridium botulinum*, *C. perfringens*, and *C. difficile*. Finally, insertional inactivation of specific genes within this putative conjugation locus confirmed the functional role that this region plays in the conjugation process.

RESULTS

Identification of toxigenic *C. sordellii* isolates and new pCS1 family plasmids. To expand on the characterization of the PaLoc located within toxigenic isolates of *C. sordellii*, eight previously uncharacterized *C. sordellii* isolates were screened by PCR for the presence of the *tcsH* and *tcsL* genes (data not shown). One isolate, S0804018, from a case of equine intestinal disease, was *tcsL* positive but *tcsH* negative. The genome of this isolate, along with the genomes of the previously characterized *tcsL*$^+$*tcsH*$^+$ isolates 7543-A and 7508-A, of unknown origin (31), was sequenced. The three isolates were confirmed to encode their LCTs within PaLoc regions identical to those previously characterized (14, 30, 31). With the use of PCR and Sanger sequencing, the contigs containing the PaLoc were closed, confirming that it was carried on a pCS1 family plasmid in each of the strains. The pCS1 plasmids from strains 7543-A (pCS1-6; MG205642) and 7508-A (pCS1-7; MG205641), in addition to being identical to one another, were identical in size (106,013 bp) and had 99% nucleotide identity to pCS1-3 from *C. sordellii* strain JGS6382. The pCS1 plasmid from strain S0804018 (pCS1-5; MG205643) was 92,347 bp in size and is the smallest characterized pCS1 family plasmid identified to date. While regions of pCS1-5 had a high level of nucleotide identity to the established pCS1 members (Fig. 1), a number of ORFs found on the other pCS1 plasmids were absent and two unique regions were present (Fig. 1). On pCS1-5, unique region 1 is predicted to encode hypothetical proteins along with two predicted adenylate/guanylate cyclases (pCS1-5_00054 and pCS1-5_00056). Unique region 2 comprises the majority of a single ORF (pCS1-5_00080), the product of which contains N-terminal DUF5011 domains and C-terminal leucine-rich repeat domains (pfam13306), potentially playing a role as a surface-exposed protein.

The *C. sordellii* pCS1-1 plasmid can undergo conjugative transfer. Bacterial matings were performed to determine if a member of the pCS1 plasmid family could undergo conjugative transfer. *C. sordellii* ATCC 9714 derivative DLL5002 was used as a donor as it contained pDLL230, an erythromycin resistance (Erm^r)-marked version of pCS1-1 (due to TargeTron insertional inactivation of *tcsL*), and was tetracycline sensitive (Tet^s). Tet^r *C. sordellii* isolate R28058 was used as the recipient strain. Erm^r Tet^r transconjugants were obtained from these matings; however, the level of transfer (55 $\pm$ 12.58 CFU/ml [mean $\pm$ standard error of the mean {SEM}]; $n = 3$) was low.

To confirm the transfer of pDLL230 from DLL5002 into R28058, six transconjugants from three independent matings were analyzed using phenotypic and PCR screening (data not shown). All transconjugants were deemed to have originated in R28058 and contained the *ermB* gene from the TargeTron procedure. To confirm that the entire pCS1-1 plasmid had transferred into the recipient strain, PCR analysis was performed on 6 transconjugants from two independent matings. ORFs present at various positions around pCS1-1, i.e., ATCC 9714 PCS11_00261 (*topA*), ATCC 9714 PCS11_00521, and

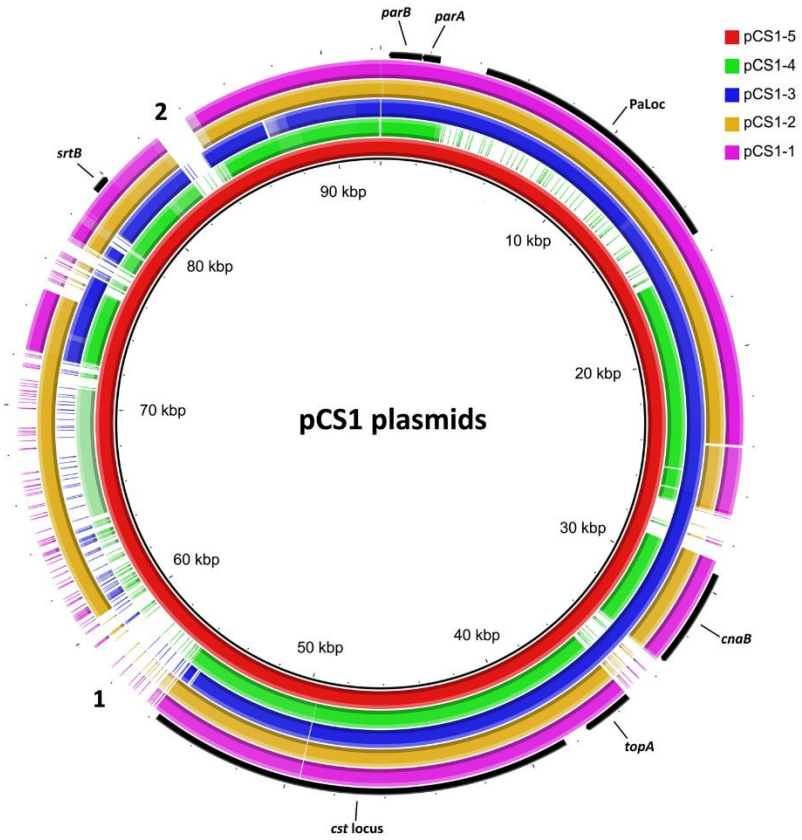

FIG 1 Comparison of pCS1-5 to other members of the pCS1 family. Shown is a visual representation of results of a blastn analysis comparing the pCS1-5 sequence and the other four unique pCS1 plasmid sequences. Each colored ring represents an individual pCS1 member. The innermost ring (colored red) and the coordinates (indicated in kilobases) represent pCS1-5. Plasmids displaying 70% to 100% identity to pCS1-5 at a particular location are represented with a solid block of color on the corresponding ring. Where the level of homology to a particular region is between 50% and 70%, it is represented as a pale block of color. Where identity to a particular region from pCS1-5 is less than 50%, it is represented by a gap on the corresponding ring. Regions present only on pCS1-5 are annotated with a number on the edge of the alignment. Genes and regions of interest from pCS1-1 are annotated on the outermost ring. The figure was produced using BRIG.

ATCC 9714 PCS11_00781, were detected in all transconjugants, suggesting that the whole plasmid had undergone transfer. To confirm this finding, the genome of one transconjugant, DLL5078, was sequenced. Analysis of this genome sequence showed that the chromosome of DLL5078 was indeed of an R28058 background and that it contained the entirety of pDLL230. On the basis of these findings, it was concluded that pCS1-1, and therefore the *C. sordellii* PaLoc, can undergo interstrain horizontal gene transfer.

The pCS1-1 plasmid is highly stable and contains a ParABS partitioning system. Since the initial matings into the R28058 recipient had a low frequency of pDLL230 transfer, the mating protocol was optimized (see Materials and Methods) and a derivative of ATCC 9714 that could be used as a recipient was constructed. To produce this recipient, it was necessary to cure pCS1-1 from ATCC 9714; however, stability studies performed using both ATCC 9714 and R28058 derivatives containing pDLL230 showed that the plasmid was 100% stable after multiple subcultures (data not shown). All members of the pCS1 family harbor *parA* and *parB* genes (Fig. 1), encoding putative

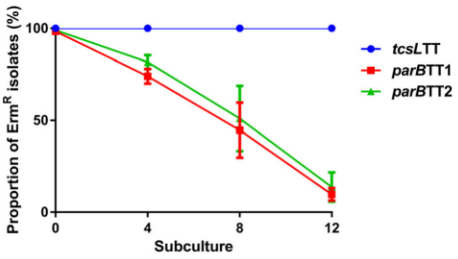

FIG 2 Stability assay demonstrating reduced pCS1-1 stability in the *C. sordellii parB* mutants. The stability of pCS1-1 in *tcsL* TargeTron mutant DLL5002 (*tcsL*TT) and independent pCS1-1 *parB* mutants DLL5138 and DLL5142 (*parB*TT1 and *parB*TT2, respectively) was assessed. Overnight 20-ml BHI broth cultures were inoculated with purified Erm^r colonies for all three strains. Each isolate was continuously subcultured 12 times (~120 generations) into fresh 20-ml BHI broth without selection in an attempt to cure the plasmid. Samples were taken from subcultures 0, 4, 8, and 12 and plated out for single colonies. One hundred colonies from each isolate were then patched onto Erm10 BHIS and BHIS plates without selection to determine the percentage of Erm^r plasmid-carrying isolates among the members of the population. Means ± standard errors are shown; $n = 3$.

components of an ABS plasmid partitioning system. To determine whether this system was involved in stabilizing the plasmid, the *parB* gene carried on pCS1-1 in ATCC 9714 was insertionally inactivated using a Targetron system (32). The insertional inactivation of *parB* was then confirmed using PCR (data not shown) and Southern hybridization (see Fig. S1 in the supplemental material). A plasmid stability assay was conducted on two independent *parB* mutants and on isogenic *tcsL* mutant derivative DLL5002 (*tcsL*TT), containing an intact *parB* gene. Both *parB* mutants displayed markedly reduced plasmid stability compared to the wild-type plasmid, with the majority (~80% to 95%) of the *parB* mutant populations losing the plasmid over ~120 generations (Fig. 2). This result indicates that the putative partitioning system present on these pCS1 plasmids is required for their stable inheritance.

A derivative of ATCC 9714 that had lost pCS1-1 was isolated from one of the colonies from these stability assays, and spontaneous streptomycin (Str; 1,000 μg/ml) and rifampin (Rif; 20 μg/ml) resistance mutants were isolated. One Str^r Rif^r pCS1-1-free isolate of ATCC 9714 was named DLL5153 and used as the recipient strain for future pCS1-1 matings. The combination of the newly constructed isogenic recipient and optimization of the mating protocol resulted in an ~10-fold to 50-fold increase in the transfer frequency of pCS1-1 to ~1,420 ± 420 CFU/ml (mean ± SEM; $n = 7$).

A novel conjugation locus present on pCS1 plasmids is related to loci on other clostridial plasmids. To elucidate the mechanism by which pCS1-1 undergoes horizontal gene transfer, bioinformatic analysis of the plasmid was performed. BLAST analysis (33) of several ORFs within an ~17.3-kb region of pCS1-1 identified homologues of the major components of a Gram-positive conjugation system, on the basis of hits in the Conserved Domain Database (34), as well as identifying motifs described in other studies (Table 1). Comparing this region with previously characterized conjugation loci, including the *tra* locus from multispecies Gram-positive plasmid pIP501 and the *tcp* locus from *C. perfringens* plasmid pCW3 (Fig. 3), little similarity was observed. Both the amino acid identities and arrangements of the ORFs differed, indicating that this ~17.3-kb region on pCS1-1 may represent part of a novel conjugation locus, which we have named the *C. sordellii* transfer (*cst*) locus (Fig. 3). ORFs encoding putative conjugation proteins were given a suffix related to their functional homologue within the paradigm Vir system of the *Agrobacterium tumefaciens* Ti plasmids (e.g., for the *virD4* functional homologue, *cstD4*). Any putative genes for which we could not identify a homologue from classical conjugation systems were given a suffix of a letter, from *A* to *R*, ascending in accordance with the order in which they appear 5′ to 3′ on the positive strand of the plasmid. The only well-characterized component of Gram-positive conjugation systems that could not be identified within this locus was a homologue of the

TABLE 1 ORFs within an ~17.3-kb region of pCS1-1 predicted to encode major components of a Gram-positive conjugation system[a]

Gene	Predicted function	Bioinformatic evidence
cstD4	Coupling protein	C terminus containing pfam12696 domain; mediation of interaction of coupling proteins with cognate relaxase (34); two predicted N-terminal transmembrane helices (3); Walker A and B motifs (61)
cstB6	Membrane pore component	Nonspecific/superfamily domain (TIGR02783) found in TrbL (mating pair formation pore-forming protein) of *trb* conjugation locus (34); 5–7 predicted transmembrane domains within the C-terminal half, 698 aa in length, and therefore most similar to class DELTA VirB6-like proteins (3)
cstB4	VirB4-like ATPase	Walker A and B motifs (62); multiple domains (pfam12846, TIGR02746, PRK13721) associated with conjugation-related ATPases (34)
cstB1	Peptidoglycan hydrolase	Short (22-aa) N-terminal sequence before single transmembrane domain; putative class ALPHA lytic transglycolylase (3); N-terminal nonspecific domains (pfam01464, cd00254) associated with lytic transglycolylases (34); C-terminal catalytic NlpC/P60 domain (34), also present in peptidoglycan hydrolase TcpG from pCW3 conjugation system (63, 64)
cstD2	Relaxase	Containing N-terminal catalytic tyrosine motifs and histidine triad motif of Mob_{MG} family of relaxases (clusters within Mob_P relaxase family) (35, 65)

[a]Gene names and predicted functions of their products are shown. The bioinformatic evidence for each ORF's predicted function is provided together with appropriate references. aa, amino acid.

VirB8 membrane structural component (3). A putative *oriT* gene was identified upstream of *cstM* comprising a core region (predicted to contain the relaxase nick site [35]) and three inverted repeats (Fig. 4A). This region displays both structural and sequence identity to *oriT* sequences from other Mob_{MG} relaxase-encoding plasmids, including members of the well-characterized pWBG749 family from *Staphylococcus aureus* (35) (Fig. 4A). To determine whether the newly defined *cst* locus is present on all pCS1 family plasmids, a nucleotide BLAST analysis was conducted using the BLAST ring image generator (BRIG) program (36). The alignment demonstrated that the entire *cst* locus is highly conserved among all unique pCS1 plasmids (Fig. 1).

Comparison of pCS1-1 to plasmids in other species identified a homologous putative conjugation locus present on conjugative botulinum neurotoxin-encoding plasmid pCLL from *C. botulinum* strain Eklund 17B (Fig. 3). Previous studies have shown that regions of pCLL share homology to a region of the *C. perfringens* pCP13 plasmid (37). Alignments of the predicted amino acid sequences from pCS1-1, pCLL, and pCP13 showed a significant degree of homology in both the arrangement of and amino acid sequence identity among both the conjugation-related proteins and hypothetical proteins encoded by these plasmids (Fig. 3; see also Table S1 in the supplemental material).

BLAST analysis performed using predicted proteins of the *cst* locus led to the identification of a *cst-like* locus in *C. difficile* (Fig. 3). This region was identified within contigs of draft genome sequences from *C. difficile* isolates P49 (GenBank accession no. AVMN01000016), 133 (NZ_MBGB01000023), and 20110869 (NZ_MTVT01000059). While not identical, all of the *C. difficile* contigs were of similar sizes, with a significant degree of nucleotide identity observed between them (Fig. S2). Along with the *cst*-like locus, all *C. difficile* contigs encoded plasmid-related genes, including those encoding a ParABS partitioning system and a toxin-antitoxin system. Note that there was a higher level of identity between *cst*-like loci from pCP13 and pCLL and those from pCS1-1 and *C. difficile* sequences, respectively (Table S1). The predicted *cst oriT* regions were also conserved among the clostridial species (Fig. 4); however, the predicted *oriT* of *C. difficile* strains P49 and 133 contains an insertion within IR2, which itself contains a fourth inverted repeat (Fig. 4B). Apart from the presence of homologous *parABS* partitioning genes on pCP13, pCS1, and the *C. difficile* sequences, and with the exception of the conjugation region, no significant identity was seen with any of the remaining plasmids (Fig. S3). This homologous *cst*-like region therefore appears to represent a novel clostridial conjugation locus.

Insertional inactivation of key genes within the *cst* locus abrogates conjugative transfer. To determine if genes within the *cst* region of pCS1-1 are responsible for conjugative transfer, mutagenesis of specific genes was performed. The *cstD4* gene (predicted to encode a coupling protein) and the *cstB4* gene (predicted to encode a

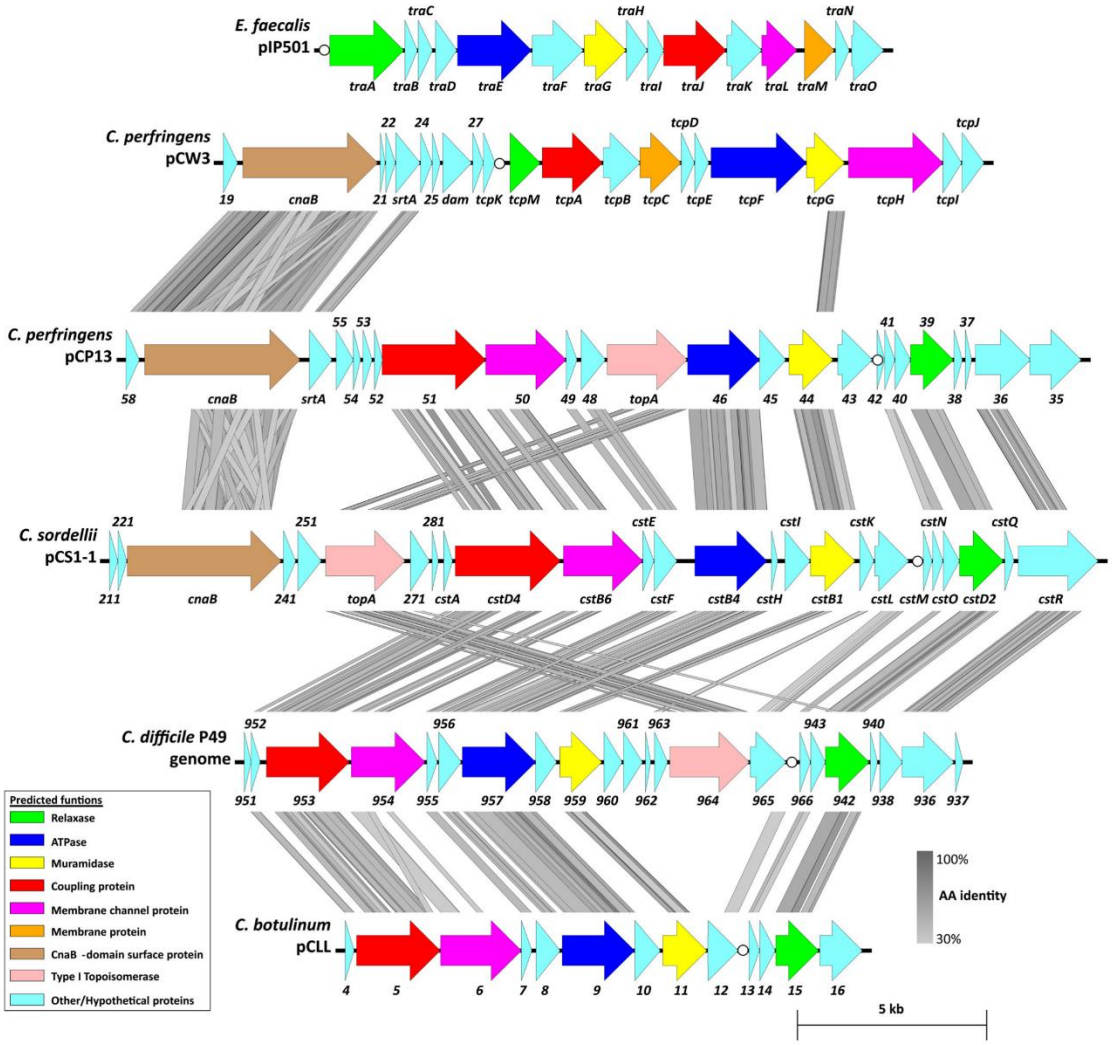

FIG 3 Comparison of the pCS1-1 *cst* locus and surrounding regions with both characterized and putative conjugation loci. Shown is a tblastX alignment of the characterized conjugation locus of broad-host-range plasmid pIP501 (AJ505823, L39769) and *C. perfringens* plasmid pCW3 (DQ366035), along with the putative conjugation locus from *C. perfringens* pCP13 (AP003515), *C. sordellii* pCS1-1 (LN679999), *C. botulinum* pCLL (CP001057), and the *C. difficile* strain P49 draft genome sequence (AVMN01000016). ORFs are colored according to known/predicted function (refer to key). Predicted *oriT* sequences are shown as a small white circle. Regions of amino acid identity between sequences are represented by gray bars. The cutoff value for amino acid identity is 30% across a region of 50 residues, with a maximum E value of 0.001. The higher the level of identity, the darker the gray, as illustrated by the legend. Previously named genes have been labeled as such. ORFs without classical gene names have been assigned a number designation. ORFs within the putative *C. sordellii cst* conjugation locus have been assigned a letter on the basis of the order in which they appear; however, those encoding putative components of a conjugation apparatus have been assigned a suffix based on the corresponding functional homologue from the Vir system of *A. tumefaciens* Ti plasmids (e.g., the VirD4 functional homologue is CstD4). *E. faecalis*, *Enterococcus faecalis*. The figure was produced using EasyFig.

conjugation-associated ATPase) were individually insertionally inactivated and the *cstD4* and *cstB4* mutants confirmed using PCR (data not shown) and Southern hybridization (Fig. S1). We also wished to examine the role of a putative sortase enzyme, encoded by the *srtB* gene carried on each member of the pCS1 family plasmids (Fig. 1), in conjugative transfer. Independent *srtB* insertional inactivation mutants were constructed and were confirmed by PCR (data not shown) and Southern hybridization (Fig. S1).

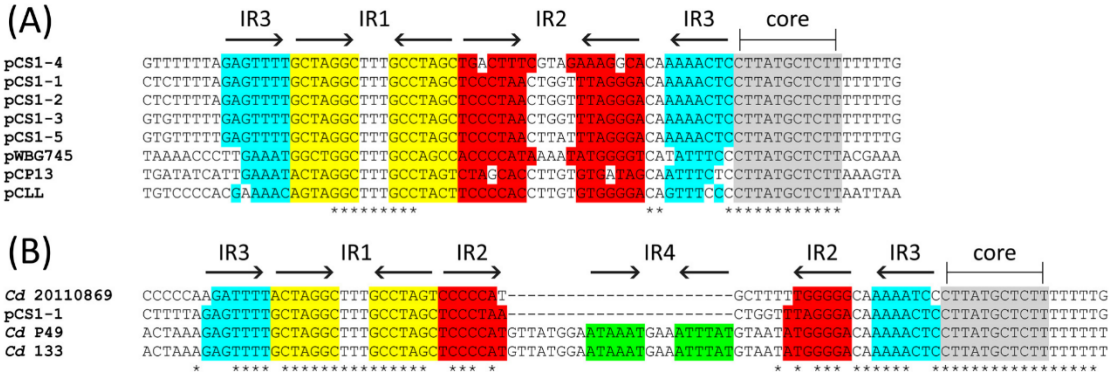

FIG 4 Nucleotide alignments of the predicted *oriT* regions from *cst*-like loci of the clostridia. Multiple-sequence alignments performed using Clustal Omega. The motifs associated with the *oriT* regions of Mob_{MG} relaxase-encoding plasmids are annotated on the alignment with lines/arrows above and highlighting of individual sequences with different colors as follows: gray, highly conserved core (predicted to contain the relaxase nick site [35]); yellow, inverted repeat 1 (IR1); red, IR2; blue, IR3. (A) The predicted *oriT* regions from unique pCS1 family plasmids, as well as those of pCLL and pCP13, were compared to the *oriT* of well-characterized Mob_{MG} relaxase-encoding plasmid pWBG745. (B) The predicted *oriT* regions of *cst*-like loci identified within the genome sequence of *C. difficile* (*Cd*) strains 20110869, P49, and 133 compared with that of pCS1-1. An additional IR, IR4, is annotated above the alignment with inverse arrows and highlighting of individual sequences in green.

Mating assays were conducted on the panel of mutants, and transfer frequencies were compared to those of conjugative pCS1-1 derivative pDLL230 from DLL5002 (*tcsL*TT). While the average plasmid transfer efficiencies of independent *srtB* mutants appeared slightly lower than that of the wild-type strain (Fig. S4), variations in transfer frequencies between replicates prevented confirmation of the role of SrtB in conjugation. However, as determined on the basis of these data, and under the conditions tested, SrtB is not essential to the conjugative transfer of pCS1-1. Both the *cstD4* and *cstB4* mutants (carrying the control vector pRPF185) were nonconjugative, with no Erm^r transconjugants detected for either mutant (see Materials and Methods for detection limits) (Fig. 5). To confirm the role of *cstD4* and *cstB4* in the conjugative transfer of pCS1-1, the mutants were complemented in *trans* with the wild-type genes, including

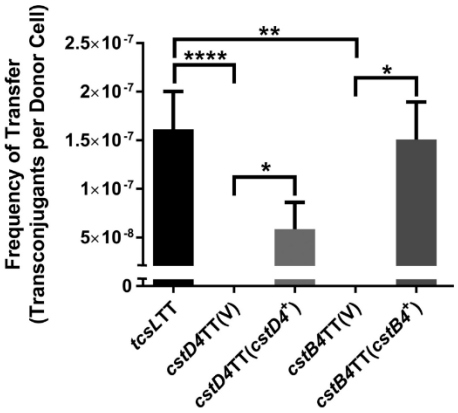

FIG 5 Analysis of pCS1-1 conjugative transfer of insertionally inactivated mutants of putative conjugation genes. Isogenic donor strains of each respective mutant are shown on the *x* axis. Wild-type transfer frequencies are illustrated for the *tcsL* TargeTron mutant "*tcsL*TT." Shown are conjugation frequencies of *cstD4* and *cstB4* mutants and the corresponding complemented strains. The transfer frequency is expressed as the number of transconjugants per donor cell obtained from each mating. Means ± standard errors are shown; $n \geq 4$. (V), strain containing vector plasmid pRPF185. Statistical analysis was carried out using a Mann-Whitney *U* test. *, $P \leq 0.05$; **, $P \leq 0.01$; ****, $P \leq 0.0001$.

their ribosome binding site (RBS) cloned into pRPF185. The transfer efficiency was restored in the complemented strains (Fig. 5), albeit not to wild-type levels for the complemented *cstD4* mutant. These results indicated that the products of *cstD4* and *cstB4* were required for pCS1-1 conjugative transfer and confirmed that the *cst* locus represents a novel clostridial conjugation region.

DISCUSSION

Toxin-encoding genes are regularly associated with mobile genetic elements in the clostridia, allowing their broader dissemination by horizontal gene transfer (28). *C. perfringens*, for example, carries the majority of its toxin genes on large conjugative plasmids (38), and the BoNT toxins from *C. botulinum* are often encoded on conjugative plasmids or transducing phage (28). The other members of the LCTs are also associated with mobile or likely mobile genetic elements (24, 25, 29). Here, we showed for the first time the ability of the *C. sordellii* TcsL-encoding PaLoc to undergo horizontal gene transfer via conjugation from type strain ATCC 9714 into a distantly related nontoxigenic *C. sordellii* strain (30). We identified a novel conjugation locus on pCS1-1, *cst*, which encodes the machinery required for plasmid transfer. The *cst* locus is highly conserved among all subtypes of the pCS1 family (Fig. 1), so it is likely that all members of this family can undergo conjugative transfer. Moreover, a previous phylogenetic analysis of *C. sordellii* strains indicated that different clades acquired the pCS1 plasmids in at least three separate events (30). The demonstration that pCS1-1 can undergo conjugative transfer, and the conservation of the *cst* locus among pCS1 plasmids, identified a mechanism by which members of the distinct clades may have acquired the PaLoc. These findings have important implications for *C. sordellii* disease pathogenesis since the gene encoding the major virulence factor TcsL (13) can be transferred between strains, potentially changing nontoxigenic strains to toxigenic ones through a conjugative transfer event.

The *cst* conjugation locus has homologues on other confirmed or predicted clostridial plasmids and represents a subtype of a novel clostridial conjugation locus of considerable importance, as well as suggesting a shared evolutionary history. These include botulinum neurotoxin-encoding plasmid pCLL from *C. botulinum*, *C. perfringens* plasmid pCP13, and putative plasmids of three *C. difficile* isolates (Fig. 3; see also Fig. S2). pCLL can undergo conjugative transfer between *C. botulinum* strains, and although sequence analysis was performed on pCLL, a conjugation locus was not identified (37). The transfer frequencies of pCLL ranged from 10^{-5} to 10^{-8} transconjugants per donor cell (37), which are similar to those that were seen for pCS1-1 here (10^{-5} to 10^{-7} transconjugants per donor cell). The difference in transfer frequencies observed between the donor and different recipient isolates in both species (37) may be due to factors affecting initial cell-to-cell contact, for example, the presence of agglutination factors or receptors; however, this hypothesis has not been examined experimentally. On the basis of sequence homology between the *C. sordellii cst* locus and the *C. botulinum cst*-like locus, we propose that the *cst*-like locus on pCLL is responsible for the conjugative transfer of this plasmid, although mutagenesis and phenotypic analyses of this region are required to confirm this role.

Previous studies noted that a number of ORFs on pCLL had homology to those on *C. perfringens* plasmid pCP13 (37); however, they were not identified as conjugation-related genes. pCP13 is thought to be nonconjugative (37), probably because a pCW3-like *tcp* locus is absent (39), since the only plasmid-encoded conjugation system identified in *C. perfringens* to date has been that encoded by the *tcp* locus. However, the presence of a *cst*-like locus on pCP13 suggests that this plasmid may be conjugative, which warrants further investigation. These experiments are particularly important in the context of the clinically important pCP13 derivatives that encode the novel enterotoxin BEC, which is involved in food-borne gastroenteritis (40).

Very few plasmids have been bioinformatically characterized in *C. difficile*, and their role in evolution and pathogenesis is unknown (41). Due to the presence of a *cst*-like locus and plasmid-related genes, it may be that the contigs described here represent

a novel family of conjugative plasmids in *C. difficile*. Differences were observed between the *cst*-like *oriT* in *C. difficile* and *cst* (Fig. 4A). Two *C. difficile* isolates contained a fourth inverted repeat within their predicted *oriT* genes which had inserted within inverted repeat 2 (IR2). Previous studies have shown the IR2 of Mob_{MG} relaxase-encoding plasmids to be a major factor in the specificity of relaxase-induced *oriT* nicking and plasmid mobilization (35). The major alteration in the structure of these *C. difficile oriT* sequences could mean an altered mechanism of *oriT* recognition and, if studied, could help elucidate the mechanism of Mob_{MG} relaxase *oriT* recognition. Further work will need to be conducted on these *C. difficile cst*-like loci to determine their role in conjugative transfer and, potentially, to confirm their presence on true extrachromosomal elements.

While differences were observed between the pCS1 family plasmids, including the newly characterized pCS1-5 plasmid, many putative genes were found to be conserved among the members. One example, the *srtB* gene, predicted to encode a sortase enzyme, was found upstream of the PaLoc region on all pCS1 plasmids (Fig. 1). A number of predicted surface-exposed proteins containing sortase recognition domains, including CnaB encoded directly upstream of the *cst* locus, are carried on pCS1-1 (30) (Fig. 1 and 3). We hypothesized that one or more of these cell wall-anchored proteins may behave as an adhesion factor to facilitate conjugative transfer, which has also been proposed for other Gram-positive conjugation systems, including that of pIP501 (3, 42). However, inactivation of *srtB* had little impact on the conjugative transfer of pCS1-1 (see Fig. S4 in the supplemental material), suggesting that the predicted sortase plays no role in conjugation.

Another feature that is common among the pCS1 plasmids is the presence of a putative partitioning locus containing the *parA* and *parB* genes (30) (Fig. 1). Here we showed that this region functions as a partitioning locus and that it is required for stable maintenance of pCS1-1 (Fig. 2). The conservation of this partitioning locus suggests that the other pCS1 subtypes are also likely to be highly stable; however, this idea is contrary to epidemiological findings. Although virulence studies indicate that TcsL is a major virulence factor of *C. sordellii*-mediated infection (18, 20), a low rate of *tcsL* or *tcsH* carriage of ~5% to 12% is reported for *C. sordellii* strains (30, 31, 43). Clinical reports and laboratory observations indicate that the majority of disease-causing *C. sordellii* isolates are likely to encode the LCTs but that they are quickly lost upon collection and subculture, suggesting that they may be encoded on unstable mobile genetic elements (30, 44). It has previously been hypothesized that the *C. sordellii* PaLoc may be present in different genomic locations, with the pCS1 plasmids representing stable variants of a highly unstable plasmid (30). On the basis of the data presented here, this stability may be due to the *parABS* partitioning locus. In future, multiple subcultures of clinical *C. sordellii* isolates should be avoided, and genomic DNA for sequencing should be extracted as soon as the organism is isolated from the host, which may allow potentially unstable PaLoc derivatives to be detected.

The results of this study provide a new perspective of the evolution of the LCTs among the clostridia. The clostridial LCTs are homologous between species, and the PaLoc regions flanking them are also conserved (14, 30, 45), indicating a common ancestry. The LCTs from *C. perfringens* and *C. novyi* are both associated with mobile genetic elements that are able to undergo horizontal transfer (24, 25, 29), and we have now shown that the *C. sordellii*-encoded LCT genes also have this ability. The documented transfer and integration of the *C. difficile* PaLoc appeared to result from a random high-frequency recombination (Hfr) mechanism (26), which may provide an explanation for the presence of PaLoc in previously nontoxigenic *C. difficile* clades (46). However, this hypothesis does not provide any insights into how PaLoc first arose in *C. difficile*. A recent PaLoc-focused phylogenetic analysis performed using genome sequences of diverse *C. difficile* isolates predicted that the ancestral population lacked the PaLoc and that the relationship of the PaLoc between clades is closer than for the remainder of the chromosome, suggesting a more recent acquisition of PaLoc instead of sequence variation inherited from a common ancestor (46). The sequence

conservation of PaLoc from *C. difficile* and *C. sordellii* has suggested they are evolutionarily related (27, 30), which is further supported by the finding that *C. difficile* is the closest relative to *C. sordellii* (30). We speculate that an ancestral version of the *C. sordellii* pCS1 plasmids may have undergone interspecies transfer into a *C. difficile* ancestor, allowing the integration of the PaLoc onto the *C. difficile* chromosome either through random integration or via an unknown site-specific mechanism. The presence of a *cst*-like locus within *C. difficile* isolates (Fig. 3; see also Fig. S2) could support this proposition. The results of this study have broad implications for the dissemination of toxins and, potentially, antibiotic resistance genes among a diverse range of clostridial species, providing these microorganisms with a survival advantage within the infected host.

MATERIALS AND METHODS

Strains, plasmids, and bacterial culture. For a full list of bacterial strains and plasmids used in this work, please refer to Table S2 and S3 in the supplemental material, respectively. Unless stated otherwise, *C. sordellii* isolates were grown in HIS broth (37 g/liter heart infusion broth [Oxoid], 5 g/liter yeast extract, 1 g/liter L-cysteine, 0.375% [wt/vol] glucose) or on HIS agar (HIS broth with 15 g/liter agar) at 37°C in an anaerobic chamber (Coy Laboratory Products, Inc.) in an atmosphere of 10% H_2, 10% CO_2, and 80% N_2. *Escherichia coli* strains were grown in 2YT broth (16 g/liter tryptone, 10 g/liter yeast extract, 5 g/liter NaCl) or on 2YT agar (2YT broth with 15 g/liter agar) at 37°C. When required after sterilization of media, the following antibiotics were included at the indicated concentrations (unless otherwise specified): erythromycin (Erm; 10 μg/ml), tetracycline (Tet; 10 μg/ml), chloramphenicol (Cm; 25 μg/ml), thiamphenicol (10 μg/ml), streptomycin (Str; 200 μg/ml), rifampin (Rif; 20 μg/ml), anhydrous tetracycline (AnTet; 20 ng/ml), and D-cycloserine (DCy; 250 μg/ml).

Molecular techniques. *C. sordellii* genomic DNA was extracted from 5 ml of overnight culture as previously described (47), with the omission of RNase upon DNA resuspension. Plasmid DNA from *E. coli* and *C. sordellii* was extracted using a QIAprep Spin Miniprep kit (Qiagen), with the addition of 10 mg/ml lysozyme in buffer P1 followed by incubation at 37°C for 15 min for *C. sordellii*. Chemically competent *E. coli* DH5α and HB101 cells were prepared and transformed with plasmid DNA as previously described (48). PCR was performed at a final concentration of 0.5 μM of each primer, using either *Taq* (Roche) or Phusion High Fidelity (NEB) DNA polymerases. For a list of primers used for PCR in this study, please refer to Table S4. PCR products were extracted using an Ultraclean 15 DNA purification kit (Mo Bio Laboratories, Inc.). All plasmids constructed as part of this study were confirmed by restriction digestion (Roche, NE) per the manufacturer's instructions and by agarose gel electrophoresis and Sanger sequencing analysis. Sequencing reactions were performed using Prism BigDye Terminator Mix (Applied Biosystems), and sequences were derived using an Applied Biosystems 3730S capillary sequencer. Sequences were analyzed using the Vector NTI suite (Invitrogen).

Genome sequencing, annotation, and analysis. *C. sordellii* genomic DNA was sequenced using either an Illumina Mi-Seq or Illumina Hi-Seq 1500 platform, with 150-bp reads produced using paired-end chemistry. Reads were quality trimmed using Nesoni clip (https://github.com/Victorian-Bioinformatics-Consortium/nesoni), followed by *de novo* assembly using SPAdes (49). For DLL5078, adapters were removed, and reads were assembled *de novo* using CLC genomics workbench version 7.0.3 (Qiagen). Plasmid sequences were closed using PCR. Autoannotation of sequences was performed using Prokka (50). Sequences not obtained as part of this study were obtained from GenBank (51), with primary accession numbers for each sequence listed in Table S2 and S3 (also see below). Sequences were further manually annotated using Artemis (Sanger) (52) on the basis of homology to entries in the Conserved Domain Database (34). Whole-plasmid comparisons and the resulting graphics were produced using the BLAST ring image generator (BRIG) tool (36). Sequence homology between conjugation loci was determined, and the resulting graphics were produced using Easyfig (53). Clustal Omega multiple-sequence alignments were conducted using EMBL-EBI tools (https://www.ebi.ac.uk/Tools/msa/clustalo/). Transmembrane helices were predicted using CBS TMHMM server 2.0 (http://www.cbs.dtu.dk/services/TMHMM).

Mating of *C. sordellii* to *C. sordellii* pCS1-1. Initial ATCC 9714 × R28058 matings were performed using a method for *C. perfringens* mixed-plate matings on solid media, as previously described (54, 55). Optimized matings of *C. sordellii* to *C. sordellii* were carried out using newly constructed recipient isolate DLL5153 as follows. Overnight 20-ml cultures of donor and recipient were used to inoculate fresh 20-ml broths to produce an optical density at 600 nm (OD_{600}) of 0.05. For isolates containing a pRPF185-based vector, trimethoprim (Tm) was included in overnight broths to ensure the stability of the plasmid. The cultures were grown until they reached an OD_{600} of 1.2 ± 0.2 (mid-to-late exponential phase). Cultures were mixed in a donor/recipient ratio of 1:4 (with a final volume of 1.4 ml) and were then pelleted at 17,000 × *g* for 1 min. The mating pellet was resuspended in 200 μl sterile HIS diluent (3.7 g/liter heart infusion broth [Oxoid], 0.5 g/liter yeast extract) and spread on a single thick HIS plate. For complementation matings with isolates carrying a pRPF185 derivative, the HIS plate contained AnTet to switch on transcription of the complementation product. The mating plate was incubated at 37°C in an anaerobic atmosphere (AnO_2) for ~18 h. Growth on the mating plate was removed into 3 ml of HIS diluent, followed by pipetting and brief vortex mixing to produce a homogenized culture. Serial 10-fold dilutions of the culture were carried out in HIS diluent, and duplicate 50-μl aliquots of 10^{-4}-to-10^{-7} dilutions were plated

onto separate halves of HIS plates containing Erm, Str, and Rif (Erm-Str-Rif) to obtain donor and recipient counts, respectively. Ten 100-μl aliquots of the undiluted reaction mixture and two aliquots of the 1-in-10 dilution were plated onto separate Erm-Str-Rif HIS plates to obtain transconjugant counts. The transfer frequencies of pCS1-1 are reported as either the number of Erm^r transconjugants per milliliter of mating mixture or the number of Erm^r transconjugants per donor cell. The detection limit for *cstD4* mutants was 1.61×10^{-10} to 5.56×10^{-10} transconjugants/donor cell, and the detection limit for *cstB4* mutants was 2.94×10^{-10} to 3.23×10^{-10} transconjugants/donor cell. Statistical analysis was performed using the Mann-Whitney *U* test.

pCS1-1 stability assays. Pure *C. sordellii* cultures from solid HIS media containing Erm were used to inoculate a 20-ml BHI broth (37 g/liter brain heart infusion broth [Difco], 1 g/liter sodium thioglycolate, 0.375% [wt/vol] glucose) containing Erm and grown overnight. The next morning, a 200-μl sample of this overnight culture was used to inoculate a 20-ml volume of fresh BHI broth with no selection, thereby producing a 1/100 dilution, and the fresh culture was grown throughout the day. This subculturing continued at intervals of 10 to 14 h until the original overnight culture had been subcultured a total of 12 times (~120 generations). Just prior to subculture of the original overnight culture and subcultures 4, 8, and 12, a sample was taken, serially diluted in BHI diluent (3.7 g/liter brain heart infusion broth [Difco], 0.1 g/liter sodium thioglycolate), and plated onto BHIS plates (37 g/liter brain heart infusion broth [Difco], 5 g/liter yeast extract, 15 g/liter agar, 1 g/liter L-cysteine, 0.375% [wt/vol] glucose) to obtain single colonies. For each time point and strain, 100 single colonies were patched onto BHIS plates containing Erm with no selection. The proportion of plasmid-carrying isolates was considered to be representative of the percentage of viable colonies resistant to Erm. To construct the new recipient (DLL5153), a plasmid-free isolate of *parB* mutant DLL5142 was plated onto HIS plates containing Str, and resistant isolates were selected. Str^r isolates were then plated onto HIS plates containing Rif, and resistant isolates were selected. The absence of pCS1-1 in DLL5153, a *C. sordellii* isolate of the ATCC 9714 background that was now Str^r Rif^r, was confirmed using PCR.

Mutagenesis. Insertional inactivation of *C. sordellii* genes was carried out using a TargeTron system. Potential intron insertion sites were identified using the Perutka Algorithm (56) and the ClosTron intron design tool (http://clostron.com/clostron2.php). The following sites (distances from the predicted start of the coding sequence) were chosen for insertion of the group II intron: *parB* (117/118-bp sense strand), *cstD4* (1,611/1,612-bp sense strand), *cstB4* (1,392/1,393-bp sense strand), and *srtB* (621/622-bp sense strand). Intron retargeting to these sites was performed with splicing by overhang extension PCR (SOE PCR) using retargeting primers as previously described (57). The retargeted 350-bp product was cloned into clostridial TargeTron vector pDLL46 between the HindIII and BsrGI sites. The retargeted plasmids were introduced into *C. sordellii* ATCC 9714 using RP4-mediated conjugation from an *E. coli* donor containing plasmid pVS520, as previously described (20). Isolated *C. sordellii* transconjugants were inoculated into 20-ml cultures containing Tm and AnTet and grown overnight to induce production of the intron. Putative insertional inactivation mutants were selected for by plating onto HIS Erm agar and then cross patching onto HIS Tm agar. Correct mutants were Erm^r but Tm^s due to the loss of the TargeTron vector. Correct insertions of the intron and the loss of the plasmid were confirmed using PCR and Southern hybridization. Southern hybridization was carried out as previously described (58) using gene-specific (gene of interest), intron-specific (*ermB*), and vector-specific (*catP*) digoxigenin (DIG)-labeled DNA probes. All probes were labeled using random labeling PCR according to the manufacturer's instructions (Roche). Hybridization was detected using the CDP-Star (Roche) detection system according to the manufacturer's instructions.

Complementation of *cstD4* and *cstB4* mutants. The complementation strategy was based on a previously described method (59, 60). In summary, the ORFs of *cstD4* and *cstB4* were PCR amplified from ATCC 9714 genomic DNA using primer DLP634 plus primer DLP574 for *cstD4* and primer DLP635 plus primer DLP636 for *cstB4*. DLP634 and DLP635 contained a SacI restriction site, and DLP574 and DLP635 contained a BamHI restriction site. The PCR products were digested with these two enzymes and cloned into pRPF185 vector, thereby placing the complementation products under the control of a tetracycline-inducible promoter. Complementation and vector control (pRPF185) plasmids were then introduced into the mutants using RP4-mediated conjugation from an *E. coli* donor containing the pVS520 plasmid, as previously described (20).

Data availability. Data referred to in this article have been submitted to Genbank under accession numbers MG205641, MG205642, and MG205643 (*C. sordellii*).

SUPPLEMENTAL MATERIAL

Supplemental material for this article may be found at https://doi.org/10.1128/mBio.01761-17.

FIG S1, JPG file, 0.4 MB.
FIG S2, JPG file, 2.8 MB.
FIG S3, JPG file, 2.8 MB.
FIG S4, JPG file, 1.1 MB.
TABLE S1, PDF file, 0.3 MB.
TABLE S2, PDF file, 0.5 MB.
TABLE S3, PDF file, 0.6 MB.
TABLE S4, PDF file, 0.2 MB.

ACKNOWLEDGMENTS

We thank David Powell and Kirill Tsyganov of the Monash Bioinformatics Platform for use of their prokaryotic genome sequence autoassembly and annotation pipeline. We thank Francisco A. Uzal of the University of California, Davis (UC Davis), for providing us with *C. sordellii* strain S0804018; Jacob Amy of the Monash Biomedical Discovery Institute (BDI) for helping in the assembly of the genome sequence of the R28058 transconjugant; Thomas Stent of the Monash BDI for helping us to reannotate the closed pCS1 plasmids; and Joshua Ramsay of Curtin University for his help in identifying the putative *oriT* regions.

D.L. was supported by Future Fellowship FT120100779 (Australian Research Council). C.J.V. was supported through an Australian Government Research Training Program Scholarship. E.C. was supported by a BBSRC studentship to N.F.F.

REFERENCES

1. Smillie C, Garcillán-Barcia MP, Francia MV, Rocha EPC, de la Cruz F. 2010. Mobility of plasmids. Microbiol Mol Biol Rev 74:434–452. https://doi.org/10.1128/MMBR.00020-10.
2. Ilangovan A, Connery S, Waksman G. 2015. Structural biology of the Gram-negative bacterial conjugation systems. Trends Microbiol 23:301–310. https://doi.org/10.1016/j.tim.2015.02.012.
3. Goessweiner-Mohr N, Arends K, Keller W, Grohmann E. 2015. Conjugation in Gram-positive bacteria. *In* Tolmasky MF, Alonso JC (ed), Plasmids—biology and impact in biotechnology and discovery. American Society of Microbiology, Washington, DC.
4. Grohmann E, Muth G, Espinosa M. 2003. Conjugative plasmid transfer in Gram-positive bacteria. Microbiol Mol Biol Rev 67:277–301. https://doi.org/10.1128/MMBR.67.2.277-301.2003.
5. Sasaki Y, Yamamoto K, Tamura Y, Takahashi T. 2001. Tetracycline-resistance genes of *Clostridium perfringens*, *Clostridium septicum* and *Clostridium sordellii* isolated from cattle affected with malignant edema. Vet Microbiol 83:61–69. https://doi.org/10.1016/S0378-1135(01)00402-3.
6. Al-Mashat RR, Taylor DJ. 1983. *Clostridium sordellii* in enteritis in an adult sheep. Vet Rec 112:19. https://doi.org/10.1136/vr.112.1.19.
7. Clark S. 2003. Sudden death in periparturient sheep associated with *Clostridium sordellii*. Vet Rec 153:340.
8. Ortega J, Daft B, Assis RA, Kinde H, Anthenill L, Odani J, Uzal FA. 2007. Infection of internal umbilical remnant in foals by *Clostridium sordellii*. Vet Pathol 44:269–275. https://doi.org/10.1354/vp.44-3-269.
9. Aldape MJ, Bryant AE, Stevens DL. 2006. *Clostridium sordellii* infection: epidemiology, clinical findings, and current perspectives on diagnosis and treatment. Clin Infect Dis 43:1436–1446. https://doi.org/10.1086/508866.
10. Cohen AL, Bhatnagar J, Reagan S, Zane SB, D'Angeli MA, Fischer M, Killgore G, Kwan-Gett TS, Blossom DB, Shieh WJ, Guarner J, Jernigan J, Duchin JS, Zaki SR, McDonald LC. 2007. Toxic shock associated with *Clostridium sordellii* and *Clostridium perfringens* after medical and spontaneous abortion. Obstet Gynecol 110:1027–1033. https://doi.org/10.1097/01.AOG.0000287291.19230.ba.
11. Agrawal P, Garg R. 2012. Fulminant leukemoid reaction due to postpartum *Clostridium sordellii* infection. J Glob Infect Dis 4:209–211. https://doi.org/10.4103/0974-777X.103899.
12. Fischer M, Bhatnagar J, Guarner J, Reagan S, Hacker JK, Van Meter SH, Poukens V, Whiteman DB, Iton A, Cheung M, Dassey DE, Shieh WJ, Zaki SR. 2005. Fatal toxic shock syndrome associated with *Clostridium sordellii* after medical abortion. N Engl J Med 353:2352–2360. https://doi.org/10.1056/NEJMoa051620.
13. Vidor C, Awad M, Lyras D. 2015. Antibiotic resistance, virulence factors and genetics of *Clostridium sordellii*. Res Microbiol 166:368–374. https://doi.org/10.1016/j.resmic.2014.09.003.
14. Sirigi Reddy AR, Girinathan BP, Zapotocny R, Govind R. 2013. Identification and characterization of *Clostridium sordellii* toxin gene regulator. J Bacteriol 195:4246–4254. https://doi.org/10.1128/JB.00711-13.
15. Busch C, Aktories K. 2000. Microbial toxins and the glycosylation of rho family GTPases. Curr Opin Struct Biol 10:528–535. https://doi.org/10.1016/S0959-440X(00)00126-3.
16. Amimoto K, Noro T, Oishi E, Shimizu M. 2007. A novel toxin homologous to large clostridial cytotoxins found in culture supernatant of *Clostridium perfringens* type C. Microbiology 153:1198–1206. https://doi.org/10.1099/mic.0.2006/002287-0.
17. Jank T, Aktories K. 2008. Structure and mode of action of clostridial glucosylating toxins: the ABCD model. Trends Microbiol 16:222–229. https://doi.org/10.1016/j.tim.2008.01.011.
18. Hao Y, Senn T, Opp JS, Young VB, Thiele T, Srinivas G, Huang SK, Aronoff DM. 2010. Lethal toxin is a critical determinant of rapid mortality in rodent models of *Clostridium sordellii* endometritis. Anaerobe 16:155–160. https://doi.org/10.1016/j.anaerobe.2009.06.002.
19. Geny B, Khun H, Fitting C, Zarantonelli L, Mazuet C, Cayet N, Szatanik M, Prevost MC, Cavaillon JM, Huerre M, Popoff MR. 2007. *Clostridium sordellii* lethal toxin kills mice by inducing a major increase in lung vascular permeability. Am J Pathol 170:1003–1017. https://doi.org/10.2353/ajpath.2007.060583.
20. Carter GP, Awad MM, Hao Y, Thelen T, Bergin IL, Howarth PM, Seemann T, Rood JI, Aronoff DM, Lyras D. 2011. TcsL is an essential virulence factor in *Clostridium sordellii* ATCC 9714. Infect Immun 79:1025–1032. https://doi.org/10.1128/IAI.00968-10.
21. Carter GP, Larcombe S, Li L, Jayawardena D, Awad MM, Songer JG, Lyras D. 2014. Expression of the large clostridial toxins is controlled by conserved regulatory mechanisms. Int J Med Microbiol 304:1147–1159. https://doi.org/10.1016/j.ijmm.2014.08.008.
22. Eklund MW, Poysky FT, Meyers JA, Pelroy GA. 1974. Interspecies conversion of *Clostridium botulinum* type C to *Clostridium novyi* type A by bacteriophage. Science 186:456–458. https://doi.org/10.1126/science.186.4162.456.
23. Han X, Du XD, Southey L, Bulach DM, Seemann T, Yan XX, Bannam TL, Rood JI. 2015. Functional analysis of a bacitracin resistance determinant located on ICECp1, a novel Tn916-like element from a conjugative plasmid in *Clostridium perfringens*. Antimicrob Agents Chemother 59:6855–6865. https://doi.org/10.1128/AAC.01643-15.
24. Gurjar A, Li J, McClane BA. 2010. Characterization of toxin plasmids in *Clostridium perfringens* type C isolates. Infect Immun 78:4860–4869. https://doi.org/10.1128/IAI.00715-10.
25. Sayeed S, Li J, McClane BA. 2010. Characterization of virulence plasmid diversity among *Clostridium perfringens* type B isolates. Infect Immun 78:495–504. https://doi.org/10.1128/IAI.00838-09.
26. Brouwer MS, Roberts AP, Hussain H, Williams RJ, Allan E, Mullany P. 2013. Horizontal gene transfer converts non-toxigenic *Clostridium difficile* strains into toxin producers. Nat Commun 4:2601. https://doi.org/10.1038/ncomms3601.
27. Monot M, Eckert C, Lemire A, Hamiot A, Dubois T, Tessier C, Dumoulard B, Hamel B, Petit A, Lalande V, Ma L, Bouchier C, Barbut F, Dupuy B. 2015. *Clostridium difficile*: new insights into the evolution of the pathogenicity locus. Sci Rep 5:15023. https://doi.org/10.1038/srep15023.
28. Popoff MR, Bouvet P. 2013. Genetic characteristics of toxigenic Clostridia and toxin gene evolution. Toxicon 75:63–89. https://doi.org/10.1016/j.toxicon.2013.05.003.
29. Eklund MW, Poysky FT, Peterson ME, Meyers JA. 1976. Relationship of bacteriophages to alpha toxin production in *Clostridium novyi* types A and B. Infect Immun 14:793–803.
30. Couchman EC, Browne HP, Dunn M, Lawley TD, Songer JG, Hall V, Petrovska L, Vidor C, Awad M, Lyras D, Fairweather NF. 2015. *Clostridium sordellii* genome analysis reveals plasmid localized toxin genes encoded

within pathogenicity loci. BMC Genomics 16:392. https://doi.org/10.1186/s12864-015-1613-2.
31. Thiele TL, Stuber TP, Hauer PJ. 2013. Detection of *Clostridium sordellii* strains expressing hemorrhagic toxin (TcsH) and implications for diagnostics and regulation of veterinary vaccines. Vaccine 31:5082–5087. https://doi.org/10.1016/j.vaccine.2013.08.065.
32. Heap JT, Pennington OJ, Cartman ST, Carter GP, Minton NP. 2007. The ClosTron: a universal gene knock-out system for the genus *Clostridium*. J Microbiol Methods 70:452–464. https://doi.org/10.1016/j.mimet.2007.05.021.
33. NCBI Resource Coordinators. 2016. Database resources of the National Center for Biotechnology Information. Nucleic Acids Res 44:D7–D19. https://doi.org/10.1093/nar/gkv1290.
34. Marchler-Bauer A, Derbyshire MK, Gonzales NR, Lu S, Chitsaz F, Geer LY, Geer RC, He J, Gwadz M, Hurwitz DI, Lanczycki CJ, Lu F, Marchler GH, Song JS, Thanki N, Wang Z, Yamashita RA, Zhang D, Zheng C, Bryant SH. 2015. CDD: NCBI's conserved domain database. Nucleic Acids Res 43:D222–D226. https://doi.org/10.1093/nar/gku1221.
35. O'Brien FG, Yui Eto K, Murphy RJ, Fairhurst HM, Coombs GW, Grubb WB, Ramsay JP. 2015. Origin-of-transfer sequences facilitate mobilisation of non-conjugative antimicrobial-resistance plasmids in *Staphylococcus aureus*. Nucleic Acids Res 43:7971–7983. https://doi.org/10.1093/nar/gkv755.
36. Alikhan NF, Petty NK, Ben Zakour NL, Beatson SA. 2011. BLAST Ring Image Generator (BRIG): simple prokaryote genome comparisons. BMC Genomics 12:402. https://doi.org/10.1186/1471-2164-12-402.
37. Marshall KM, Bradshaw M, Johnson EA. 2010. Conjugative botulinum neurotoxin-encoding plasmids in *Clostridium botulinum*. PLoS One 5:e11087. https://doi.org/10.1371/journal.pone.0011087.
38. Li J, Adams V, Bannam TL, Miyamoto K, Garcia JP, Uzal FA, Rood JI, McClane BA. 2013. Toxin plasmids of *Clostridium perfringens*. Microbiol Mol Biol Rev 77:208–233. https://doi.org/10.1128/MMBR.00062-12.
39. Bannam TL, Yan XX, Harrison PF, Seemann T, Keyburn AL, Stubenrauch C, Weeramantri LH, Cheung JK, McClane BA, Boyce JD, Moore RJ, Rood JI. 2011. Necrotic enteritis-derived *Clostridium perfringens* strain with three closely related independently conjugative toxin and antibiotic resistance plasmids. mBio 2:e00190-11. https://doi.org/10.1128/mBio.00190-11.
40. Yonogi S, Matsuda S, Kawai T, Yoda T, Harada T, Kumeda Y, Gotoh K, Hiyoshi H, Nakamura S, Kodama T, Iida T. 2014. BEC, a novel enterotoxin of *Clostridium perfringens* found in human clinical isolates from acute gastroenteritis outbreaks. Infect Immun 82:2390–2399. https://doi.org/10.1128/IAI.01759-14.
41. Mullany P, Allan E, Roberts AP. 2015. Mobile genetic elements in *Clostridium difficile* and their role in genome function. Res Microbiol 166:361–367. https://doi.org/10.1016/j.resmic.2014.12.005.
42. Bhatty M, Laverde Gomez JA, Christie PJ. 2013. The expanding bacterial type IV secretion lexicon. Res Microbiol 164:620–639. https://doi.org/10.1016/j.resmic.2013.03.012.
43. Walk ST, Jain R, Trivedi I, Grossman S, Newton DW, Thelen T, Hao Y, Songer JG, Carter GP, Lyras D, Young VB, Aronoff DM. 2011. Non-toxigenic *Clostridium sordellii*: clinical and microbiological features of a case of cholangitis-associated bacteremia. Anaerobe 17:252–256. https://doi.org/10.1016/j.anaerobe.2011.06.009.
44. Bouvet P, Sautereau J, Le Coustumier A, Mory F, Bouchier C, Popoff MR. 2015. Foot infection by *Clostridium sordellii*: case report and review of 15 cases in France. J Clin Microbiol 53:1423–1427. https://doi.org/10.1128/JCM.03414-14.
45. Carter GP, Cheung JK, Larcombe S, Lyras D. 2014. Regulation of toxin production in the pathogenic clostridia. Mol Microbiol 91:221–231. https://doi.org/10.1111/mmi.12469.
46. Dingle KE, Elliott B, Robinson E, Griffiths D, Eyre DW, Stoesser N, Vaughan A, Golubchik T, Fawley WN, Wilcox MH, Peto TE, Walker AS, Riley TV, Crook DW, Didelot X. 2014. Evolutionary history of the *Clostridium difficile* pathogenicity locus. Genome Biol Evol 6:36–52. https://doi.org/10.1093/gbe/evt204.
47. O'Connor JR, Lyras D, Farrow KA, Adams V, Powell DR, Hinds J, Cheung JK, Rood JI. 2006. Construction and analysis of chromosomal *Clostridium difficile* mutants. Mol Microbiol 61:1335–1351. https://doi.org/10.1111/j.1365-2958.2006.05315.x.
48. Inoue H, Nojima H, Okayama H. 1990. High efficiency transformation of *Escherichia coli* with plasmids. Gene 96:23–28. https://doi.org/10.1016/0378-1119(90)90336-P.
49. Bankevich A, Nurk S, Antipov D, Gurevich AA, Dvorkin M, Kulikov AS, Lesin VM, Nikolenko SI, Pham S, Prjibelski AD, Pyshkin AV, Sirotkin AV, Vyahhi N, Tesler G, Alekseyev MA, Pevzner PA. 2012. SPAdes: a new genome assembly algorithm and its applications to single-cell sequencing. J Comput Biol 19:455–477. https://doi.org/10.1089/cmb.2012.0021.
50. Seemann T. 2014. Prokka: rapid prokaryotic genome annotation. Bioinformatics 30:2068–2069. https://doi.org/10.1093/bioinformatics/btu153.
51. Clark K, Karsch-Mizrachi I, Lipman DJ, Ostell J, Sayers EW. 2016. GenBank. Nucleic Acids Res 44:D67–D72. https://doi.org/10.1093/nar/gkv1276.
52. Rutherford K, Parkhill J, Crook J, Horsnell T, Rice P, Rajandream MA, Barrell B. 2000. Artemis: sequence visualization and annotation. Bioinformatics 16:944–945. https://doi.org/10.1093/bioinformatics/16.10.944.
53. Sullivan MJ, Petty NK, Beatson SA. 2011. Easyfig: a genome comparison visualizer. Bioinformatics 27:1009–1010. https://doi.org/10.1093/bioinformatics/btr039.
54. Rood JI. 1983. Transferable tetracycline resistance in *Clostridium perfringens* strains of porcine origin. Can J Microbiol 29:1241–1246. https://doi.org/10.1139/m83-193.
55. Rood JI, Maher EA, Somers EB, Campos E, Duncan CL. 1978. Isolation and characterization of multiply antibiotic-resistant *Clostridium perfringens* strains from porcine feces. Antimicrob Agents Chemother 13:871–880. https://doi.org/10.1128/AAC.13.5.871.
56. Heap JT, Kuehne SA, Ehsaan M, Cartman ST, Cooksley CM, Scott JC, Minton NP. 2010. The ClosTron: mutagenesis in *Clostridium* refined and streamlined. J Microbiol Methods 80:49–55. https://doi.org/10.1016/j.mimet.2009.10.018.
57. Cheung JK, Keyburn AL, Carter GP, Lanckriet AL, Van Immerseel F, Moore RJ, Rood JI. 2010. The VirSR two-component signal transduction system regulates NetB toxin production in *Clostridium perfringens*. Infect Immun 78:3064–3072. https://doi.org/10.1128/IAI.00123-10.
58. Sambrook J, Fritsch EF, Maniatis T. 1989. Molecular cloning: a laboratory manual, 2nd ed, vol. 2. Cold Spring Harbor Laboratory Press, Cold Spring Harbor, NY.
59. Govind R, Dupuy B. 2012. Secretion of *Clostridium difficile* toxins A and B requires the holin-like protein TcdE. PLoS Pathog 8:e1002727. https://doi.org/10.1371/journal.ppat.1002727.
60. Fagan RP, Fairweather NF. 2011. *Clostridium difficile* has two parallel and essential Sec secretion systems. J Biol Chem 286:27483–27493. https://doi.org/10.1074/jbc.M111.263889.
61. Gunton JE, Gilmour MW, Alonso G, Taylor DE. 2005. Subcellular localization and functional domains of the coupling protein, TraG, from IncHI1 plasmid R27. Microbiology 151:3549–3561. https://doi.org/10.1099/mic.0.28255-0.
62. Guglielmini J, Néron B, Abby SS, Garcillán-Barcia MP, de la Cruz F, Rocha EP. 2014. Key components of the eight classes of type IV secretion systems involved in bacterial conjugation or protein secretion. Nucleic Acids Res 42:5715–5727. https://doi.org/10.1093/nar/gku194.
63. Bannam TL, Teng WL, Bulach D, Lyras D, Rood JI. 2006. Functional identification of conjugation and replication regions of the tetracycline resistance plasmid pCW3 from *Clostridium perfringens*. J Bacteriol 188:4942–4951. https://doi.org/10.1128/JB.00298-06.
64. Bantwal R, Bannam TL, Porter CJ, Quinsey NS, Lyras D, Adams V, Rood JI. 2012. The peptidoglycan hydrolase TcpG is required for efficient conjugative transfer of pCW3 in *Clostridium perfringens*. Plasmid 67:139–147. https://doi.org/10.1016/j.plasmid.2011.12.016.
65. Garcillán-Barcia MP, Francia MV, De La Cruz F. 2009. The diversity of conjugative relaxases and its application in plasmid classification. FEMS Microbiol Rev 33:657–687. https://doi.org/10.1111/j.1574-6976.2009.00168.x.

Appendix B. Plasmid partitioning systems of conjugative plasmids from *Clostridium perfringens*

Plasmid 80 (2015) 90–96

Contents lists available at ScienceDirect

Plasmid

journal homepage: www.elsevier.com/locate/yplas

Plasmid partitioning systems of conjugative plasmids from *Clostridium perfringens*

Vicki Adams [a], Thomas D. Watts [a], Dieter M. Bulach [a,b,c], Dena Lyras [a], Julian I. Rood [a,*]

[a] Department of Microbiology, Monash University, Clayton, Melbourne, Victoria, 3800, Australia
[b] Victorian Bioinformatics Consortium, Monash University, Clayton, Melbourne, Victoria, 3800, Australia
[c] Life Sciences Computation Centre, Victorian Life Sciences Computation Initiative, Carlton, Melbourne, Victoria, 3053, Australia

ARTICLE INFO

Article history:
Available online 27 April 2015
Communicated by Slade Jensen

Keywords:
Clostridium perfringens
Conjugative
Plasmid partitioning
ParR
ParM
Toxin plasmids

ABSTRACT

Many pathogenic strains of *Clostridium perfringens* carry several highly similar toxin or antibiotic resistance plasmids that have 35 to 40 kb of very closely related syntenous sequences, including regions that carry the genes encoding conjugative transfer, plasmid replication and plasmid maintenance functions. Key questions are how are these closely related plasmids stably maintained in the same cell and what is the basis for plasmid incompatibility in *C. perfringens*. Comparative analysis of the Rep proteins encoded by these plasmids suggested that this protein was not the basis for plasmid incompatibility since plasmids carried in a single strain often encoded an almost identical Rep protein. These plasmids all carried a similar, but not identical, *parMRC* plasmid partitioning locus. Phylogenetic analysis of the deduced ParM proteins revealed that these proteins could be divided into ten separate groups. Importantly, in every strain that carried more than one of these plasmids, the respective ParM proteins were from different phylogenetic groups. Similar observations were made from the analysis of phylogenetic trees of the ParR proteins and the *parC* loci. These findings provide evidence that the basis for plasmid incompatibility in the conjugative toxin and resistance plasmid family from *C. perfringens* resides in subtle differences in the *parMRC* plasmid partitioning loci carried by these plasmids.

1. Introduction

Clostridium perfringens is a ubiquitous Gram positive, rod-shaped, anaerobe that produces heat-resistant endospores (Li et al., 2013; Rood and Cole, 1991). In addition to its prevalence in the environment, *C. perfringens* is often found as a commensal organism within the gastrointestinal tract of both humans and animals; however, it can also act as a pathogen causing an array of diseases. These diseases range from enterotoxaemias and enteritis in humans and animals to potentially fatal wound infections in humans (Awad et al., 1995; Rood and Cole, 1991; Songer, 1996). Disease can be attributed to the ability of *C. perfringens* to produce an arsenal of at least 17 distinct extracellular toxins and enzymes (Keyburn et al., 2008; McDonel, 1980; Uzal et al., 2014; Yonogi et al., 2014). These toxins are intimately involved in the determination of disease and four of these toxins (α, β, ε and ι toxins) are used as the basis for typing *C. perfringens* isolates into toxinotypes A to E (McDonel, 1980; Rood and Cole, 1991).

Many of these toxins, including three of the four typing toxins, are encoded by genes localised on large plasmids that have either been shown to be conjugative or are highly likely to be conjugative. Conjugative plasmids in *C. perfringens* are able to transfer at high frequencies and are not limited to carrying toxin genes, but may carry antibiotic resistance genes and catabolic functions (Li et al., 2013). These

* Corresponding author. Department of Microbiology, Monash University, Clayton, Melbourne, Vic 3800, Australia. Fax: +61 3 9902 9222.
E-mail address: julian.rood@monash.edu (J.I. Rood).

http://dx.doi.org/10.1016/j.plasmid.2015.04.004
0147-619X/

plasmids include a series of plasmids that are either identical or highly related to the archetypal *C. perfringens* tetracycline resistance plasmid pCW3 (Abraham and Rood, 1985; Bannam et al., 2006; Rood et al., 1978). The presence of these plasmids has significant implications for the dissemination of virulence and antimicrobial resistance determinants throughout *C. perfringens* populations (Bannam et al., 2006; Li et al., 2013).

Conjugative transfer in *C. perfringens* is mediated by plasmid-determined genes located within the *tcp* conjugation locus (Bannam et al., 2006; Bantwal et al., 2012; Parsons et al., 2007; Porter et al., 2012; Wisniewski et al., 2015). Five toxin plasmids and several resistance plasmids have been shown experimentally to transfer and many more toxin plasmids have been shown to have an intact *tcp* locus, suggesting that these plasmids are also highly likely to be conjugative (Bannam et al., 2011; Brynestad et al., 2001; Freedman et al., 2014; Hughes et al., 2007; Li et al., 2013; Parreira et al., 2012).

Southern hybridisation analyses of pulsed-field gels have revealed that strains of *C. perfringens* often possess several large plasmids that are closely related, but carry different toxin genes (Sayeed et al., 2007, 2010). This characteristic of *C. perfringens* strains is exemplified by the type A avian necrotic enteritis isolate EHE-NE18, where detailed sequence analysis has demonstrated that this strain carries three closely related conjugative plasmids, pJIR3535, pJIR3537 and pJIR3844, each of which encodes a different toxin gene (*netB* or *cpb2*) or antimicrobial resistance determinant (*tet*(P) operon) (Fig. 1) (Bannam et al., 2011). These findings raise the question as to how these large, closely related conjugative plasmids, which share near identical replication functions, are able to coexist within a single strain of *C. perfringens*. What is the mechanism of plasmid incompatibility in conjugative *C. perfringens* plasmids?

At present, eleven plasmids carrying the *tcp* locus have been fully sequenced (Bannam et al., 2006, 2011; Li et al., 2013; Miyamoto et al., 2006, 2008, 2011; Parreira et al., 2012), and several more plasmids have been partially sequenced (V. Adams, L. Weeramantri, J. Cheung, T. Stent, X. Han & J. Rood, unpublished results). Comparative sequence analysis has revealed that each of these conjugative plasmids is very closely related to pCW3 and shares a conserved ~35 kb backbone (Bannam et al., 2006, 2011; Freedman et al., 2014; Li et al., 2013; Miyamoto et al., 2006, 2008, 2011; Parreira et al., 2012). Within the conserved region there are several loci of note, in particular the *tcp* locus and the central control region (CCR) (Bannam et al., 2006, 2011; Parreira et al., 2012) (Fig. 1). The latter encodes genes involved in plasmid replication, regulation and maintenance (Bannam et al., 2006, 2011; Parreira et al., 2012). It includes the *rep* gene (Bannam et al., 2006) and a *parMRC*-like partitioning locus (Bannam et al., 2006, 2011; Freedman et al., 2014; Parreira et al., 2012).

Plasmid incompatibility is often determined by both plasmid replication mechanisms as well as partitioning systems that control plasmid segregation, and therefore the stable inheritance, of low-copy number plasmids in the cell division process. Partitioning systems are generally tripartite systems, are plasmid encoded and typically rely on the action of two *trans*-acting proteins, an NTPase and a DNA binding adaptor protein, and a *cis*-acting centromere site (Gerdes et al., 2000, 2010) (Fig. 2). There are three types of partitioning systems in bacteria, and each is categorised by the type of NTPase it encodes (Gerdes et al., 2010).

Type I partitioning systems are characterised by a variant Walker A type ATPase known as ParA (Koonin, 1993) (Fig. 2A). These systems generally consist of three components: (i) a ParA/SopA ATPase; (ii) ParB/SopB, a DNA binding adaptor protein; and (iii) the plasmid-encoded centromere, *parS*/*sopC* (Gerdes et al., 2000, 2010; Ogura and Hiraga, 1983). Type II or ParMRC partitioning systems (Fig. 2B) comprise: (i) a filament-forming actin/Hsp70 family ATPase, ParM; and (ii) a DNA binding adaptor protein ParR, which binds to (iii) a centromeric site, *parC*, situated immediately upstream in the promoter region of *parM* (Gerdes and Molin, 1986; Gerdes et al., 2010; Jensen and Gerdes, 1997; Moller-Jensen et al., 2002; Salje et al., 2010; van den Ent et al., 2002) . In contrast to type I systems, ParMRC partitioning systems mediate plasmid segregation *via* a pushing mechanism, which has predominantly been characterised by studies on the *parMRC*-like partitioning systems of the *Escherichia coli* plasmid R1 and the *Staphylococcus aureus* plasmid pSK41 (Gerdes and Molin, 1986; Gerdes et al., 1985, 2010; Popp et al., 2010). Capping of the ParM filaments by the ParR-*parC* complex works to stabilise ParM polymerisation, thus allowing sister plasmids that have been 'captured' by interacting bundles of anti-parallel ParM filaments to be segregated to either cell pole (Garner et al., 2007; Gayathri et al., 2012; Salje et al., 2010). Type III partitioning systems, or TubZRC systems, are analogous to ParMRC partitioning systems; however, the NTPase is a

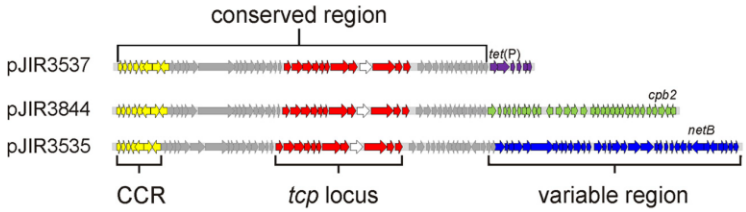

Fig. 1. Genetic organisation of conjugative plasmids from strain EHE-NE18. Linear maps of pJIR3537 (49 kb), pJIR3844 (70 kb) and pJIR3535 (82 kb), the three large plasmids present in strain EHE-NE18, are shown. ORFs are indicated by the arrows. Related functional regions are indicated as follows – the central control region (CCR; yellow arrows), the conjugation locus (*tcp*; red arrows) and unique regions that are shown in purple, green and blue. Relevant toxin and antibiotic resistance genes are indicated. Grey arrows indicate conserved ORFs and the white arrow indicates a group II intron.

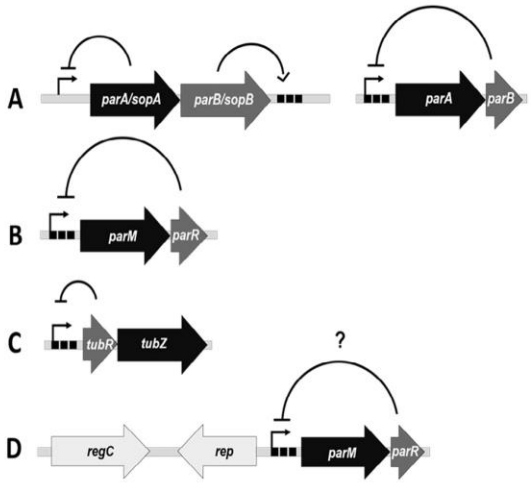

Fig. 2. Genetic arrangement of partitioning loci. NTPase proteins are indicated by black arrows, DNA binding/adaptor proteins are indicated by grey arrows, white arrows indicate other ORFs not directly involved in partitioning, promoters are indicated by bent arrows. The curved lines ending with the straight line are used to indicate the operator/binding sites of the specified gene products. (A) Type I partitioning loci, with two variations; (B) type II partitioning system; and (C) type III partitioning system. Adapted from Gerdes et al. (2010). (D). The arrangement of ORFs in the pCW3-like plasmid partitioning regions is indicated.

homologue of eukaryotic tubulin (reviewed in Gerdes et al., 2010) (Fig. 2C). In addition to these three partitioning types, there is a unique partitioning system encoded by the *S. aureus* multi-resistance plasmid pSK1 (Firth et al., 2000; Simpson et al., 2003). This system is comprised of a single partitioning protein and has been shown to stabilise *S. aureus* mini-replicons (Firth et al., 2000).

These partitioning systems are widespread in bacteria and *C. perfringens* is no exception (Bannam et al., 2011; Freedman et al., 2014; Parreira et al., 2012). Here we demonstrate that there are at least ten different clades of plasmid encoded *parMRC*-like homologues in *C. perfringens* and that all *C. perfringens* conjugative plasmids fall into one of ten distinct phylogenetic groups based upon their partitioning group. We propose that these different partitioning families form the basis for plasmid incompatibility in *C. perfringens*.

2. Materials and methods

2.1. Data acquisition and analysis

ParM sequences were obtained by searching the NCBI databases using BlastP (blast.ncbi.nlm.nih.gov/Blast.cgi) and limiting the search to *C. perfringens* sequences. The pCW3 ParM amino acid sequence was used to interrogate the database initially. Additional ParM sequences were identified by searching with the ParM sequence obtained from sequencing of the epsilon toxin-encoding plasmid from strain CN3718. Finally, a DELTA-BLAST (blast.ncbi.nlm.nih.gov/Blast.cgi) search was performed to determine if any ParM sequences from *C. perfringens* had been overlooked. Rep protein analysis was carried out in a similar fashion except that PSI-BLAST (Blast blast.ncbi.nlm.nih.gov/Blast.cgi) was used instead of DELTA-BLAST since the pCW3-like Rep proteins contain no conserved domains.

ParR protein sequences were identified by searching the DNA sequences encoding the ParM proteins identified previously and determining if a small ORF was located directly downstream of the *parM* gene. In most sequences, this ORF was annotated; in a few entries the ORF was not annotated, but was present. In some of the sequences, the upstream or downstream data were missing.

A similar approach was used to identify the *parC* regions, designated as the DNA sequence upstream of the *parM* gene. In pCW3-like plasmids, the *parC* region was further delineated by comparison to the conserved *oriV* region located between the *parM* and *rep* genes, and the *parC* region was deemed to begin at the site of divergence between the *oriV* site and the *parM* gene.

2.2. Phylogenetic analysis

The similarity of each of the ParM sequences initially was analysed using Clustal Omega (Sievers et al., 2011). Amino acid identity matrices were examined and the ParM sequences were used to construct a phylogenetic tree using MEGA 6 (Tamura et al., 2013). Tree construction involved Clustal W analysis followed by tree inference using the maximum likelihood method (Jones et al., 1992). Similar trees were constructed by inputting ParR sequences, *parC* sequences and Rep protein sequences.

3. Results and discussion

3.1. Plasmids can be allocated to phylogenetic groups based on their parMRC regions

Examination of *C. perfringens* plasmid sequences that were located in the databases yielded several fully assembled plasmid sequences, while other sequences constituted either partially assembled sequences or data from whole genome sequencing projects (WGS) (Table 1) (Hassan et al., 2015). Note that many of these strains carry multiple toxin plasmids that are closely related, as already described; in other strains, the plasmid content was not specified. The tetracycline resistance plasmid pCW3 (Bannam et al., 2006) is the smallest and best characterised conjugative plasmid from *C. perfringens* and therefore was used as the reference plasmid for these studies.

The two genes adjacent to, but divergently transcribed, from *rep* in the CCR of pCW3 were found to encode a putative ParM homologue and what was subsequently designated as a ParR homologue, with a potential centromere site immediately preceding the *parM* gene (Bannam et al., 2006, 2011; Parreira et al., 2012) (Fig. 2D). It was previously observed that the conjugative plasmids carried by any one strain of *C. perfringens* all had different *parMR* alleles; the ParMRC system therefore was postulated to form the basis of a plasmid incompatibility locus (Bannam et al., 2011; Freedman et al., 2014; Parreira et al., 2012). Four alleles (A–D) were identified at that time; however, additional

Table 1
C. perfringens genome sequences.

Strain	Plasmid/s	Characteristics/sequence type	GenBank accession number
CPF5603	pCPF5603	Enterotoxin (CPE)/fully assembled	AB236337
CPF4969	pCPF4969	Enterotoxin (CPE)/fully assembled	AB236336
CPF4013	pCPF4013	Enterotoxin(CPE)/partial sequence	AB236338
CW92	pCW3	Tet(P) tetracycline resistance determinant /fully assembled	DQ366035
NCTC 8533B4D	pCP8533etx	Type B; epsilon toxin/fully assembled	AB444205
PB-1	pCPPB-1	Type E; iota toxin/fully assembled	AB604032
EHE-NE18	pJIR3536	NetB toxin/fully assembled	JN689219
	pJIR3537	Tet(P) tetracycline resistance determinant/fully assembled	JN689220
	pJIR3844	Beta2 toxin/fully assembled	JN689217
NE10	pNetB-NE10	NetB/fully assembled	JQ655731
CP1	pCpb2-CP-1	Beta2 toxin/fully assembled	JQ655732
F262	pF262A	Beta2 toxin/assembled	CM001478
CN4003	pJIR4163	Beta2 toxin/partial assembly	Unpublished data
	pJIR4164	Epsilon toxin/partial assembly	Unpublished data
CN3718	pJIR3119	Epsilon/partial assembly	Unpublished data
ATCC3626	Not specified	Type B; beta and epsilon toxins/WGS	ABDV00000000
JGS1495	Not specified	Type C; beta toxin/WGS	ABDU00000000
JGS1721	Not specified	Type D; epsilon toxin/WGS	ABOO00000000
JGS1987	Not specified	Type E iota toxin/WGS	ABDW00000000
WAL-14572	Not specified	Tet(P) tetracycline resistance determinant /WGS	ADLP00000000

sequence data obtained from our studies suggested that there were further *parMR* alleles to be identified.

In the current study, comparative analysis conducted using the NCBI BLAST server allowed the identification of ten ParM variants (Fig. 3A). These proteins were identified with considerable confidence as their deduced amino acid sequences all showed a hit to conserved domain CD10227, namely the ParM_like domain. Phylogenetic analysis indicated that there was more conservation within some of these ten groups than within others; for example, the group D ParM proteins all had identical amino acid sequences, while the group G and I ParM proteins showed 90% and 92% amino acid sequence identity, respectively. The highest level of identity between ParM groups was observed between groups B and F at 54% amino acid sequence identity and the lowest was 15% (between groups H–J and A–J). Most importantly, it was noted that no ParM proteins belonging to the same phylogenetic group were encoded on plasmids from the

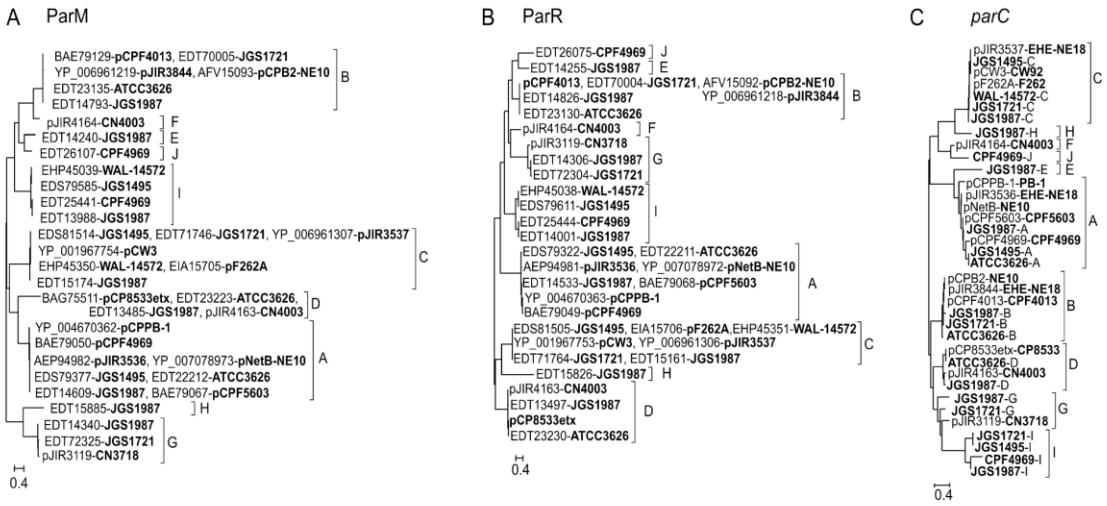

Fig. 3. Phylogenetic analysis of the *parMRC* locus. The maximum likelihood method was used to confer evolutionary history using a JTT matrix-based model (Jones et al., 1992). The tree is drawn to scale (indicated below the figures); branch lengths were measured as the number of substitutions per site. Analyses were conducted using the software package MEGA 6 (Tamura et al., 2013). (A) ParM analysis, protein accession numbers are followed by the strain or plasmid designations (bold type) separated by a hyphen. Identical sequences appear on the same line (or just below and aligned to the right), separated by a space. Par groups are indicated by a square bracket on the right of the figure with a letter (A to J). (B) ParR analysis, labelled as per the ParM data. (C) The tree generated from *parC* DNA sequences is labelled with the plasmid name followed by the strain (bold type) designation, or the strain (bold type) and the Par group letter after the hyphen.

same strain (Fig. 3A), providing evidence to support the hypothesis that the *parMRC* locus identified on these plasmids was responsible for plasmid incompatibility.

Identification of the cognate ParR proteins for each of these ParM sequences generally was accomplished by identifying the downstream open reading frame (ORF) from the *parM* gene. Sometimes this ORF had not been annotated. The conservation of ParR proteins is lower since this adapter protein binds to a specific DNA sequence and to a specific ParM protein. Therefore, the ParR proteins we identified were analysed firstly by Clustal W alignment and phylogenetic analysis (Fig. 3B) and secondly by analysis of their primary sequence characteristics. Phylogenetic analysis resulted in the clustering of these ParR proteins into the same groups as their cognate ParM proteins (Fig. 3A,B), which was consistent with their proposed role in functioning with their ParM counterpart to mediate specific plasmid partitioning. Identity within the ParR groups ranged from 97% (group B) to 68% (group G), which was generally lower than for the equivalent ParM groups. The reason for this disparity is unclear, but it may suggest that although the functional regions of the ParR proteins are conserved, namely the DNA binding residues and ParR-ParM interaction sites, sequence variation is better tolerated within the ParR proteins than the equivalent ParM proteins. Analysis of the primary sequence data of the ParR proteins indicated that they were generally small proteins with an acidic pI (range 4.5 to 5.7), except for the group D proteins which had a basic pI of 8.9.

The centromere-like *parC* site in well characterised ParMRC systems is located upstream of *parM* (Salje et al., 2010). Consequently, the sequences upstream of the *C. perfringens parM* genes were analysed. In some plasmids, the identification of the potential *parC* sequences was simplified due to the location of a pCW3-like *rep* gene upstream of the *parM* gene. Since the upstream DNA sequence of the pCW3-like *rep* genes also is well conserved (data not shown), the *parC* site was designated as the point of sequence divergence between the *rep* and *parM* genes. In some sequences, no pCW3-like *rep* gene was present on the contig and the *parC* sequence was designated as the intergenic region upstream of *parM*. These *parC* regions ranged in size between 127 and 300 bp in length. Phylogenetic analysis resulted in the same clustering of *parC* sites as their cognate ParM and ParR proteins (Fig. 3C), although the sequence conservation between groups was lower, ranging from 66 to 92%. The %G + C content of these regions was very low, varying from 9 to 21% depending on the group. The average %G + C content for the *C. perfringens* chromosome is 28% and the average %G + C content for *C. perfringens* plasmids is approximately 25% (Hassan et al., 2015). Therefore, even by *C. perfringens* standards the putative *parC* regions were very AT-rich and consequently identity between the *parC* groups also was relatively high (up to 65%).

3.2. Rep sequences do not correlate with plasmid incompatibility

Another mechanism that may contribute to plasmid incompatibility involves the sharing of plasmid replication processes (Novick, 1987). The replication protein, Rep,

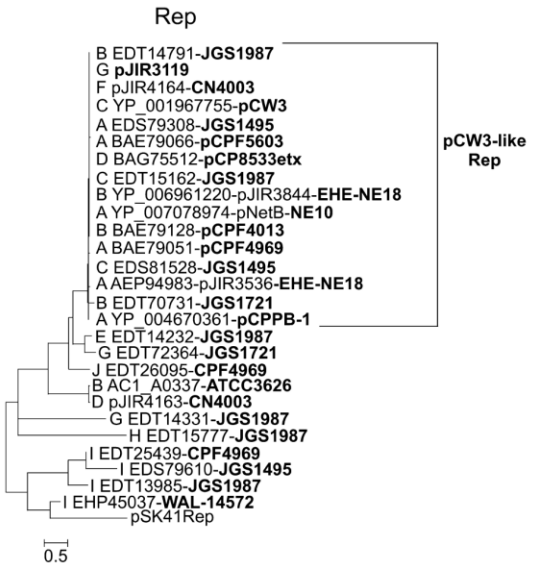

Fig. 4. Phylogenetic analysis of Rep proteins. Tree construction was carried out as described for Fig. 3. Labels begin with the Par group designation of the neighbouring *parM* gene, followed by the accession number for the relevant Rep protein and then the strain or plasmid number (bold type).

encoded by pCW3 has no sequence similarity to plasmid replication proteins from other bacterial species and was only identified by a series of deletion and transposon mutagenesis studies (Bannam et al., 2006). This protein is highly conserved in conjugative plasmids from *C. perfringens*. Initial sequencing studies showed that the enterotoxin plasmids pCPF5603 and pCPF4969 encoded replication proteins that were nearly identical to Rep from pCW3 (Bannam et al., 2006; Miyamoto et al., 2006). Subsequent sequencing has demonstrated that the vast majority of *C. perfringens* conjugative plasmids encode a Rep protein that is either identical, or closely related, to Rep from pCW3 (Bannam et al., 2006, 2011; Li et al., 2013; Miyamoto et al., 2006, 2008, 2011; Parreira et al., 2012).

To determine if the Rep protein may contribute to plasmid incompatibility, comparative bioinformatics and phylogenetic analysis was carried out. The Rep proteins were identified either by sequence similarity to Rep from pCW3 or by manually examining contigs containing *parMR* genes. Presumptive Rep proteins were subjected to Clustal omega analysis and a phylogenetic tree was developed using MEGA6 software. This analysis indicated that although not all of these putative conjugative plasmids encoded a pCW3-like Rep protein, it was very common (Fig. 4). Critically, there was no correlation between the Rep protein and the ParMRC group, and multiple, closely related Rep proteins were encoded by different plasmids residing within the same strain (Fig. 4). The best characterised example was again strain EHE-NE18. The Rep proteins of the three conjugative plasmids carried by EHE-NE18 were 98% identical at the amino acid level, with only six amino acid substitutions between the three protein sequences. These data

suggest that in strains with multiple plasmids encoding highly related pCW3-like Rep proteins, this protein is not likely to play a significant role in plasmid incompatibility, although its involvement cannot be formally excluded.

4. Concluding remarks

The analysis of all known sequences, or parts thereof, from conjugative *C. perfringens* plasmids has shown that in any *C. perfringens* strain carrying multiple pCW3-like plasmids, these plasmids encode only ParMR proteins belonging to different phylogenetic groups. The ParMRC system provides the only mechanism for plasmid incompatibility that is consistent with the observed data obtained from the analysis of native *C. perfringens* isolates from many different sources. For example, the presence of ParRMC groups A, B and C within the same cell provides a clear explanation for the stable maintenance of three independently conjugative plasmids in strain EHE-NE18 (Bannam et al., 2011). These phylogenetic clades still need to be experimentally confirmed as incompatibility groups and the designation of Par proteins into functional groups based on sequence analysis alone must be interpreted with some caution, particularly as incompatibility has been demonstrated between *parMRC* systems demonstrating significant sequence divergence (Hyland et al., 2014). Nevertheless, these data provide evidence that the *parMRC* locus may be the major factor that determines plasmid incompatibility in *C. perfringens* strains.

Acknowledgments

This research was supported by a grant from the Australian National Health and Medical Research Council (GNT1048676). TDW was the receipt of an Australian Postgraduate Award.

Conflict of interest

The authors declare that they have no known conflicts of interest.

References

Abraham, L.J., Rood, J.I., 1985. Molecular analysis of transferable tetracycline resistance plasmids from *Clostridium perfringens*. J. Bacteriol. 161, 636–640.
Awad, M.M., et al., 1995. Virulence studies on chromosomal alpha-toxin and theta-toxin mutants constructed by allelic exchange provide genetic evidence for the essential role of alpha-toxin in *Clostridium perfringens*-mediated gas gangrene. Mol. Microbiol. 15, 191–202.
Bannam, T.L., et al., 2006. Functional identification of conjugation and replication regions of the tetracycline resistance plasmid pCW3 from *Clostridium perfringens*. J. Bacteriol. 188, 4942–4951.
Bannam, T.L., et al., 2011. Necrotic enteritis-derived *Clostridium perfringens* strain with three closely related independently conjugative toxin and antibiotic resistance plasmids. mBio. 2, e00190-11.
Bantwal, R., et al., 2012. The peptidoglycan hydrolase TcpG is required for efficient conjugative transfer of pCW3 in *Clostridium perfringens*. Plasmid 67, 139–147.
Brynestad, S., et al., 2001. Enterotoxin plasmid from *Clostridium perfringens* is conjugative. Infect. Immun. 69, 3483–3487.
Firth, N., et al., 2000. Replication of staphylococcal multiresistance plasmids. J. Bacteriol. 182, 2170–2178.
Freedman, J.C., et al., 2014. *Clostridium perfringens* type A-E toxin plasmids. Res. Microbiol. 14, 00184-3. doi:10.1016/j.resmic.2014.09.004.
Garner, E.C., et al., 2007. Reconstitution of DNA segregation driven by assembly of a prokaryotic actin homolog. Science 315, 1270–1274.
Gayathri, P., et al., 2012. A bipolar spindle of antiparallel ParM filaments drives bacterial plasmid segregation. Science 338, 1334–1337.
Gerdes, K., Molin, S., 1986. Partitioning of plasmid R1. Structural and functional analysis of the parA locus. J. Mol. Biol. 190, 269–279.
Gerdes, K., et al., 1985. Stable inheritance of plasmid R1 requires two different loci. J. Bacteriol. 161, 292–298.
Gerdes, K., et al., 2000. Plasmid and chromosome partitioning: surprises from phylogeny. Mol. Microbiol. 37, 455–466.
Gerdes, K., et al., 2010. Pushing and pulling in prokaryotic DNA segregation. Cell 141, 927–942.
Hassan, K.A., et al., 2015. Genomic analyses of *Clostridium perfringens* isolates from five toxinotypes. Res. Microbiol. 166, 255–263. doi:10.1016/j.resmic.2014.10.003.
Hughes, M.L., et al., 2007. Epsilon toxin plasmids of *Clostridium perfringens* type D are conjugative. J. Bacteriol. 189, 7531–7538.
Hyland, E.M., et al., 2014. A model for the evolution of biological specificity: a cross-reacting DNA-binding protein causes bacterial plasmid incompatibility. J. Bacteriol. 196, 3002–3011.
Jensen, R.B., Gerdes, K., 1997. Partitioning of plasmid R1. The ParM protein exhibits ATPase activity and interacts with the centromere-like ParR-parC complex. J. Mol. Biol. 269, 505–513.
Jones, D.T., et al., 1992. The rapid generation of mutation data matrices from protein sequences. Comput. Appl. Biosci. 8, 275–282.
Keyburn, A.L., et al., 2008. NetB, a new toxin that is associated with avian necrotic enteritis caused by *Clostridium perfringens*. PLoS Pathog. 4, e26.
Koonin, E.V., 1993. A superfamily of ATPases with diverse functions containing either classical or deviant ATP-binding motif. J. Mol. Biol. 229, 1165–1174.
Li, J., et al., 2013. Toxin plasmids of *Clostridium perfringens*. Microbiol. Mol. Biol. Rev. 77, 208–233.
McDonel, J.L., 1980. *Clostridium perfringens* toxins (type A, B, C, D, E). Pharmacol. Ther. 10, 617–655.
Miyamoto, K., et al., 2006. Complete sequencing and diversity analysis of the enterotoxin-encoding plasmids in *Clostridium perfringens* type A non-food-borne human gastrointestinal disease isolates. J. Bacteriol. 188, 1585–1598.
Miyamoto, K., et al., 2008. Sequencing and diversity analyses reveal extensive similarities between some epsilon-toxin-encoding plasmids and the pCPF5603 *Clostridium perfringens* enterotoxin plasmid. J. Bacteriol. 190, 7178–7188.
Miyamoto, K., et al., 2011. Identification of novel *Clostridium perfringens* type E strains that carry an iota toxin plasmid with a functional enterotoxin gene. PLoS ONE 6, e20376.
Moller-Jensen, J., et al., 2002. Prokaryotic DNA segregation by an actin-like filament. EMBO J. 21, 3119–3127.
Novick, R.P., 1987. Plasmid incompatibility. Microbiol. Rev. 51, 381–395.
Ogura, T., Hiraga, S., 1983. Partition mechanism of F plasmid: two plasmid gene-encoded products and a cis-acting region are involved in partition. Cell 32, 351–360.
Parreira, V.R., et al., 2012. Sequence of two plasmids from *Clostridium perfringens* chicken necrotic enteritis isolates and comparison with *C. perfringens* conjugative plasmids. PLoS ONE 7, e49753.
Parsons, J.A., et al., 2007. TcpA, an FtsK/SpoIIIE homolog, is essential for transfer of the conjugative plasmid pCW3 from *Clostridium perfringens*. J. Bacteriol. 189, 7782–7790.
Popp, D., et al., 2010. Structure and filament dynamics of the pSK41 actin-like ParM protein: implications for plasmid DNA segregation. J. Biol. Chem. 285, 10130–10140.
Porter, C.J., et al., 2012. The conjugation protein TcpC from *Clostridium perfringens* is structurally related to the type IV secretion system protein VirB8 from Gram-negative bacteria. Mol. Microbiol. 83, 275–288.
Rood, J.I., Cole, S.T., 1991. Molecular genetics and pathogenesis of *Clostridium perfringens*. Microbiol. Rev. 55, 621–648.
Rood, J.I., et al., 1978. Isolation and characterization of multiply antibiotic-resistant *Clostridium perfringens* strains from porcine feces. Antimicrob. Agents Chemother. 13, 871–880.
Salje, J., et al., 2010. The ParMRC system: molecular mechanisms of plasmid segregation by actin-like filaments. Nat. Rev. Microbiol. 8, 683–692.
Sayeed, S., et al., 2007. Virulence plasmid diversity In *Clostridium perfringens* type D isolates. Infect. Immun. 75, 2391–2398.
Sayeed, S., et al., 2010. Characterization of virulence plasmid diversity among *Clostridium perfringens* type B isolates. Infect. Immun. 78, 495–504.
Sievers, F., et al., 2011. Fast, scalable generation of high-quality protein multiple sequence alignments using Clustal Omega. Mol. Syst. Biol. 7, 539.

Simpson, A.E., et al., 2003. A single gene on the staphylococcal multiresistance plasmid pSK1 encodes a novel partitioning system. J. Bacteriol. 185, 2143–2152.
Songer, J.G., 1996. Clostridial enteric diseases of domestic animals. Clin. Microbiol. Rev. 9, 216–234.
Tamura, K., et al., 2013. MEGA6: Molecular Evolutionary Genetic Analysis version 6.0. Mol. Biol. Evol. 30, 2725–2729.
Uzal, F.A., et al., 2014. Towards an understanding of the role of *Clostridium perfringens* toxins in human and animal disease. Future Microbiol. 9, 361–377.
van den Ent, F., et al., 2002. F-actin-like filaments formed by plasmid segregation protein ParM. EMBO J. 21, 6935–6943.
Wisniewski, J.A., et al., 2015. Two novel membrane proteins TcpD and TcpE are essential for conjugative transfer of pCW3 in *Clostridium perfringens*. J. Bacteriol. 197, 74–81.
Yonogi, S., et al., 2014. BEC, a novel enterotoxin of *Clostridium perfringens* found in human clinical isolates from acute gastroenteritis outbreaks. Infect. Immun. 82, 2390–2399.

Appendix C. Evidence that compatibility of closely related replicons in *Clostridium perfringens* depends on linkage to *parMRC*-like partitioning systems of different subfamilies

Plasmid 91 (2017) 68–75

Contents lists available at ScienceDirect

Plasmid

journal homepage: www.elsevier.com/locate/yplas

Evidence that compatibility of closely related replicons in *Clostridium perfringens* depends on linkage to *parMRC*-like partitioning systems of different subfamilies

Thomas D. Watts, Priscilla A. Johanesen, Dena Lyras, Julian I. Rood[1], Vicki Adams*,[1]

Infection and Immunity Program, Monash Biomedicine Discovery Institute, Department of Microbiology, Monash University, Victoria 3800, Australia

ARTICLE INFO

Keywords:
Partitioning
Incompatibility
Clostridium perfringens
ParR
ParM
Toxin plasmids

ABSTRACT

Clostridium perfringens produces an extensive repertoire of toxins and extracellular enzymes, many of which are intimately involved in the progression of disease and are encoded by genes on conjugative plasmids. In addition, many *C. perfringens* strains can carry up to five of these conjugative toxin or antimicrobial resistance plasmids, each of which has a similar 35 kb backbone. This conserved backbone includes the *tcp* conjugation locus and the central control region (CCR), which encodes genes involved in plasmid regulation, replication and partitioning, including a *parMRC* partitioning locus. Most conjugative plasmids in *C. perfringens* have a conserved replication protein, raising questions as to how multiple, closely related plasmids are maintained within a single strain. Bioinformatics analysis has highlighted the presence of at least 10 different *parMRC* partitioning system families ($parMRC_{A-J}$) in these plasmids, with differences in amino acid sequence identity between each ParM family ranging from 15% to 54%. No two plasmids that encode genes belonging to the same partitioning family have been observed in a single strain, suggesting that these families represent the basis for plasmid incompatibility. In an attempt to validate the proposed *parMRC* incompatibility groups, genetically marked *C. perfringens* plasmids encoding identical $parMRC_C$ or $parMRC_D$ homologues or different combinations of $parMRC_A$, $parMRC_C$ and $parMRC_D$ family homologues were introduced into a single strain *via* conjugation. The stability of each plasmid was determined using an incompatibility assay in which the plasmid profile of each strain was monitored over the course of two days in the absence of direct selection. The results showed that plasmids with identical $parMRC_C$ or $parMRC_D$ homologues were incompatible and could not coexist in the absence of external selection. By contrast, plasmids that encoded different *parMRC* homologues were compatible and could coexist in the same cell in the absence of selection, with the exception of strains housing $parMRC_C$ and $parMRC_D$ combinations, which showed a minor incompatibility phenotype. In conclusion, we have provided the first direct evidence of plasmid incompatibility in *Clostridium* spp. and have shown experimentally that the compatibility of conjugative *C. perfringens* plasmids correlates with the presence of *parMRC*-like partitioning systems of different phylogenetic subfamilies.

1. Introduction

Plasmid incompatibility is defined as the inability of two plasmids to coexist in a single strain in the absence of selective pressure (Novick, 1987; Novick et al., 1976). Generally, plasmids that have common replication, replication control or maintenance elements are considered incompatible. The sharing of these mechanisms can result in an inability to correct copy number imbalances that occur as a consequence of random selection for replication or partitioning from an otherwise heterologous plasmid population (Novick, 1987), ultimately leading to destabilisation of plasmid inheritance.

The Gram-positive pathogen *Clostridium perfringens* produces an extensive repertoire of toxins and extracellular enzymes (Revitt-Mills et al., 2015), many of which are encoded by genes that are carried on conjugative plasmids. *C. perfringens* strains can carry up to five conjugative toxin or antibiotic resistance plasmids, each of which shares an essentially conserved 35 kb backbone (Bannam et al., 2006; Bannam et al., 2011; Li et al., 2013; Miyamoto et al., 2006; Miyamoto et al., 2008; Parreira et al., 2012). The *tcp* conjugation locus is found within this conserved backbone as are the genes required for plasmid replication, regulation and maintenance, which are located within a locus called the Central Control Region (CCR) (Bannam et al., 2006;

* Corresponding author.
E-mail address: vicki.adams@monash.edu (V. Adams).
[1] Joint senior authors.

http://dx.doi.org/10.1016/j.plasmid.2017.03.008
Received 22 December 2016; Received in revised form 29 March 2017; Accepted 30 March 2017
Available online 06 April 2017
0147-619X/

Bannam et al., 2011; Parreira et al., 2012).

All known conjugative plasmids in *C. perfringens* are related to the archetypal, low copy number, tetracycline resistance plasmid pCW3 (Bannam et al., 2006; Li et al., 2013). Most of these plasmids have a very similar replication initiation or Rep protein, which raises questions as to how such plasmids can be stably maintained in the same cell. For example, the Australian necrotic enteritis strain EHE-NE18 carries three large conjugative plasmids pJIR3535, pJIR3537 and pJIR3844 that encode very similar Rep proteins (98% amino acid sequence identity) (Bannam et al., 2011). These plasmids stably coexist despite the conventional relationship between shared replication mechanisms and plasmid incompatibility.

Previous studies have noted instances of apparent plasmid incompatibility in *C. perfringens*, where toxinotype B and C isolates seem to be restricted in regards to the β-toxin and ε-toxin plasmid combinations they can possess (Freedman et al., 2014; Gurjar et al., 2010; Lepp et al., 2013; Sayeed et al., 2010). A recent survey of available plasmid sequence data has started to provide some insight into the basis of plasmid compatibility in *C. perfringens* (Adams et al., 2015). The results highlighted the similarity observed between Rep proteins of this family of conjugative plasmids and identified the presence of ten families (*parMRC*$_{A–J}$) of *parMRC*-like plasmid partitioning systems, with differences in amino acid sequence identity between each ParM family ranging from 15% to 54% (Adams et al., 2014; Adams et al., 2015; Bannam et al., 2011; Parreira et al., 2012). Plasmids from the same *parMRC* phylogenetic group have not been found in a single *C. perfringens* isolate, suggesting that these partitioning families play a role in the determination of plasmid compatibility (Adams et al., 2015).

Plasmid partitioning is generally mediated by tripartite systems that can be classified into three families depending on the type of NTPase they encode: specifically, the type I (ParA Walker A-like), type II (ParM actin-like), and type III (TubZ Tubulin-like) families (Gerdes et al., 2010; Salje et al., 2010). Type II plasmid partitioning systems have been most well characterised in *Escherichia coli* and *Staphylococcus aureus* and generally consist of three components: ParM, an actin-like filament forming protein, ParR, a DNA-binding adapter protein that links the growing ParM filament to a plasmid centromere, called *parC* (Baxter and Funnell, 2014; Gerdes et al., 2010). Together these components act to mediate the correct positioning of plasmids on either side of the septum during cell division, thus ensuring that each daughter cell receives a copy of the plasmid. Although the role of *parMRC* systems has been well characterised in regards to their ability to stabilise plasmid inheritance, less is known about the way in which they contribute to plasmid incompatibility. Most research concerning partition-mediated incompatibility has focused on type I partition systems, where several models have been proposed (Bouet et al., 2007; Bouet et al., 2005; Diaz et al., 2015; Ebersbach et al., 2005).

The current study aimed to elucidate whether there was a direct relationship between the type II partitioning family designation and plasmid compatibility in *C. perfringens*. We postulated that plasmids encoding identical partitioning families would be incompatible when introduced into a single *C. perfringens* strain, whereas plasmids that encoded different partitioning families will be compatible; that is, they would remain stable in the absence of direct selection. This hypothesis was tested by introducing native *C. perfringens* plasmids that encoded identical *parMRC*$_C$ or *parMRC*$_D$ homologues or different combinations of *parMRC*$_A$, *parMRC*$_C$ *and parMRC*$_D$ homologues into a single strain and determining the stability of each plasmid in the absence of direct selection. The results provide evidence that the *parMRC* systems are important for plasmid compatibility in *C. perfringens*.

2. Methods

2.1. Plasmids, bacterial strains and culture conditions

All *C. perfringens* strains and plasmids used in this study are listed in Table 1. Strains were grown in fluid thioglycolate medium (FTG) (Oxoid) or, tryptone-peptone-glucose (TPG) broth (Rood et al., 1978a) and on nutrient agar (NA) (Rood, 1983) or brain heart infusion (BHI) agar (Difco) supplemented with glucose (0.375% w/v). Where appropriate NA was supplemented with antibiotics at the following concentrations: chloramphenicol (Cm) 20 μg/ml, tetracycline (Tc) 10 μg/ml, erythromycin (Em) 50 μg/ml, rifampicin (Rif) 10 μg/ml, nalidixic acid (Nal) 10 μg/ml, streptomycin (Sm) 1 mg/ml and satu-

Table 1
Bacterial strains and plasmids.

Strain	Description	Reference/origin
C. perfringens		
EHE-NE18	Australian necrotic enteritis isolate (pJIR3535, pJIR3537, pJIR3843, pJIR3844)	(Sheedy et al., 2004)
JIR39	CW362 Sm^RChl^R	(Rood, 1983)
JIR325	Strain 13 Rif^RNal^R	(Lyristis et al., 1994)
JIR4195	JIR325(pCW3) Rif^RNal^R Tc^R	(Hughes et al., 2007)
JIR4323	JIR325(pJIR1584) $Rif^RNal^RCm^R$	JIR325-derived Cm^R transconjugant
JIR4394	Strain 13 Sm^RChl^R	(Bannam et al., 2006)
JIR4984	JIR325(pJIR3120) $Rif^RNal^RCm^R$	(Hughes et al., 2007)
JIR12012	JIR325(pJIR3118) Rif^RNal^R	(Hughes et al., 2007)
JIR12293	JIR325(pJIR3536) $Rif^RNal^RCm^R$	(Bannam et al., 2011)
JIR13003	EHE-NE18 (pJIR4709, pJIR3537, pJIR3843 pJIR3844) Em^RTc^R	(X. Han and J. I. Rood, unpublished)
JIR13172	JIR39(pCW3) $Sm^RChl^RTc^R$	Tc^R transconjugant (JIR4195 × JIR39)
JIR13264	JIR325(pJIR4533) $Rif^RNal^REm^R$	JIR325 derived Em^R transconjugant
JIR13265	JIR4394(pJIR4533) $Sm^RChl^REm^R$	Em^R transconjugant (JIR13264 × JIR4394)
JIR13492	JIR4394(pCW3) $Sm^RChl^RTc^R$	Tc^R transconjugant (JIR4195 × JIR4394)
JIR13493	JIR4394(pJIR4709) $Sm^RChl^REm^R$	Em^R transconjugant (JIR13003 × JIR4394)
JIR13405	JIR325(pCW3, pJIR1584) $Rif^RNal^RTc^RCm^R$ (C_{Tc} + C_{Cm})	Tc^R transconjugant (JIR13492 × JIR4323)
JIR13406	JIR325(pJIR3536, pCW3) $Rif^RNal^RTc^RCm^R$ (A_{Cm} + C_{Tc})	Cm^R transconjugant (JIR12293 × JIR4195)
JIR13407	JIR325(pJIR4709, pJIR3120) $Rif^RNal^REm^RCm^R$ (A_{Em} + D_{Cm})	Em^R transconjugant (JIR13493 × JIR4984)
JIR13408	JIR325(pCW3, pJIR3120) $Rif^RNal^RTc^RCm^R$ (C_{Tc} + D_{Cm})	Tc^RCm^R transconjugant (JIR13492 × JIR4984)
JIR13409	JIR325(pJIR3120, pJIR4533) $Rif^RNal^REm^RCm^R$ (D_{Ern} + D_{Cm})	Em^RCm^R transconjugant (JIR13265 × JIR4984)
JIR13410	JIR325(pCW3, pJIR4533) $Rif^RNal^RTc^REm^R$ (C_{Tc} + D_{Em})	Tc^REm^R transconjugant (JIR13265 × JIR4195)
Plasmid	Description	Reference
pCW3	47 kb; Tc^R, *parMRC*$_C$	(Rood et al., 1978b)
pJIR1584	pCW3 Δ*tet(P)*Ω*catQ*	(Johanesen, Lyras and Rood unpublished)
pJIR3118	48 kb; *etx*$^+$, *parMRC*$_D$	(Hughes et al., 2007)
pJIR3120	pJIR3118 Δ*etx*Ω*catP*	(Hughes et al., 2007)
pJIR3536	pJIR3535 Δ*netB*Ω*catP*, *parMRC*$_A$	(Keyburn et al., 2008)
pJIR4533	pJIR3118 *etx*::*ermB*	pJIR3118 *etx* TargeTron insertion mutant
pJIR4709	pJIR3535 Δ*netI*Ω*ermQ*	(X. Han and J. I. Rood, unpublished)

Cm^R, chloramphenicol resistance, Em^R, erythromycin resistance, Tc^R, tetracycline resistance, Nal^R, nalidixic acid resistance, Rif^R, rifampicin resistance, Sm^R, streptomycin resistance, Chl^R, potassium chlorate resistance.

rated potassium chlorate (Chl) 1% (v/v). All agar cultures were incubated overnight at 37 °C in an anaerobic jar (Oxoid) containing 10% (v/v) CO_2, 10% (v/v) H_2 and 80% (v/v) N_2.

2.2. Construction of genetically marked $parMRC_D$ family plasmids

All plasmids used in this study are listed in (Table 1). The epsilon toxin gene, *etx*, in the $parMRC_D$ family plasmid pJIR3118 was insertionally inactivated using TargeTron mutagenesis as previously described (Cheung et al., 2010; Bannam et al., 2011). Mutagenesis resulted in the insertion of a group II intron encoding the *ermB* erythromycin resistance determinant into the *etx* gene, resulting in the generation of pJIR4533. Mutants were confirmed as previously described by Southern hybridisation and PCR (Cheung et al., 2010).

2.3. Molecular methods

Genomic DNA (gDNA) was isolated after overnight growth in FTG broth, as previously described (O'Connor et al., 2006). PCR screening was conducted using *Taq* DNA polymerase (Roche) and a 0.5 μM of each specific oligonucleotide primer. Denaturation (94 °C 30 s), annealing (50–55 °C for 1 min) and extension (72 °C for 1 min) steps were carried out for 35 cycles. All gDNA and PCR products were subjected to gel electrophoresis on either a 0.8% (w/v) or 1% (w/v) agarose gel for 40 min at 100 V, before being visualised using a Chemidoc XRS + (Biorad). All oligonucleotide primers used are listed in Supplementary Table 1. Alignment of the putative origin of replication sequences and Rep proteins for pJIR3118, pJIR3536 and pCW3 were prepared using CLUSTALΩ web tool (McWilliam et al., 2013).

2.4. Construction of incompatibility test strains

Conjugation was performed as previously described (Rood, 1983; Rood et al., 1978a, 1978b). All transconjugants were selected on nutrient agar supplemented with appropriate antibiotic selection. Incompatible plasmids were maintained by selection for the antibiotic resistance determinants carried by each plasmid.

2.5. Stability assay

C. perfringens strains carrying two conjugative plasmids with different resistance genes were subcultured from glycerol stocks stored at − 20 °C into pre-boiled FTG media before being incubated overnight at 37 °C. Each strain was plated onto nutrient agar (NA) supplemented with the appropriate antibiotics and incubated anaerobically at 37 °C for 24 h. Single colonies were taken from these plates and subcultured onto NA supplemented with appropriate antibiotics and incubated anaerobically at 37 °C overnight. To determine the relative stability of each plasmid, each strain was passaged on solid media, and sampled, before 100 colonies were patched onto appropriate selective media each day on three consecutive days. On day 0 an initial sample was taken from the primary streak of the overnight selection plates and resuspended in 500 μL of heart infusion (BHI) diluent (BHI (Oxoid) broth diluted 1:5). This cell suspension was serially diluted and plated onto appropriate selection plates for both plasmids, each strain was incubated anaerobically at 37 °C overnight. One hundred colonies of each strain were patched onto selection plates for each plasmid. The relative stability of each plasmid was determined by comparing the growth of the patches on each selection plate. This process was repeated on days 1 and 2, however, dilutions of each strain were plated onto nutrient agar supplemented with antibiotics to select for each plasmid individually. Strains were patched as before and the relative stability of each plasmid was determined as before. gDNA was harvested from each strain on days 0 and 2 and PCRs specific for the relevant *parM* and antimicrobial resistance genes were used to determine plasmid profiles at these time points. A control experiment was also conducted to determine the baseline stability of each individual plasmid (pCW3, pJIR1584, pJIR3120, pJIR4533, pJIR4250 or pJIR3536). Separate strains each carrying one of these plasmids were passaged on NA without selection for two days, and plasmid stabilities were determined by comparing the number of patches grown on medium with and without antibiotics.

3. Results

3.1. Plasmids that share identical $parMRC_C$ or $parMRC_D$ partitioning systems are incompatible in C. perfringens

Previous studies have identified ten families of *parMRC*-like partitioning systems in *C. perfringens* ($parMRC_{A–J}$) (Bannam et al., 2006; Bannam et al., 2011; Parreira et al., 2012; Adams et al., 2014; Adams et al., 2015). It was suggested that these partitioning systems form the basis for plasmid incompatibility, since multiple plasmids encoding identical *parMRC*-like partitioning systems have not been observed in native *C. perfringens* isolates (Freedman et al., 2014; Adams et al., 2015). To test this hypothesis conjugative transfer was used to construct a series of strains that each contained two genetically marked derivatives of the native conjugative *C. perfringens* plasmids, pJIR3535 ($parMRC_A$), pCW3 ($parMRC_C$) and pJIR3118 ($parMRC_D$) (Table 1) (Fig. 1).

The stability of each plasmid alone was assessed prior to construction of these test strains. Separate strains that each harboured one conjugative plasmid (pCW3, pJIR1584, pJIR3120, pJIR4533, pJIR4709 or pJIR3536) were passaged for two days on non-selective media. Samples were taken at the start and conclusion of the experiment and the percentage of the population that had retained the plasmid was determined by comparing the number of patches grown on media supplemented with antibiotics to the number of patches grown on media without antibiotics. All plasmids remained stable over the course of the experiment (Supplementary Fig. 1).

To determine the relative stability of multiple plasmids encoding identical *parMRC* homologues, the $parMRC_C$ family plasmids pCW3 (Tc^R) and pJIR1584 (Cm^R) were introduced into a JIR325 background *via* conjugation to construct JIR13405. This derivative was designated as the C_{Tc} + C_{Cm} strain where C represents the *parMRC* family designation of each plasmid and the subscripts denote the resistance determinant present on each plasmid (Fig. 1A).

The resultant C_{Tc} + C_{Cm} strain was passaged on media supplemented with tetracycline or chloramphenicol to select for each plasmid individually (pCW3 and pJIR1584, respectively). Viable counts were carried out each day (0, 1, 2) and 100 single colonies were cross-patched onto media selective for each plasmid to determine their relative stability. Near symmetric loss of the non-selected plasmid was observed. Selection on tetracycline for pCW3 led to loss of pJIR1584, with only 8% of the population retaining the plasmid after two days (Fig. 2A), and selection on chloramphenicol for pJIR1584 led to the loss of pCW3, with only 18% of the population retaining pCW3 after two days (Fig. 2A). To validate the incompatibility observed between plasmids carrying the same *parMRC* locus a similar experiment was carried out with a strain (D_{Em} + D_{Cm}) carrying two $parMRC_D$ family plasmids pJIR3120 (Cm^R) and pJIR4533 (Em^R) (Fig. 1C). This strain was passaged on media supplemented with erythromycin or chloramphenicol to select for pJIR4533 or pJIR3120, respectively. Selection of pJIR4533 using erythromycin resulted in the loss of pJIR3120, with only 8% of the population retaining the plasmid after two days (Fig. 2B). Similarly, when pJIR3120 was selected using chloramphenicol, pJIR4533 was lost, with only 41% retention at day 2. PCR screening of genomic DNA samples before and after passage for *par* ($parM_C$ and $parM_D$) and antibiotic resistance genes (*tetA*(P) *ermB* and *catP*) supported the designated plasmid profiles deduced from the observed resistance profiles (data not shown).

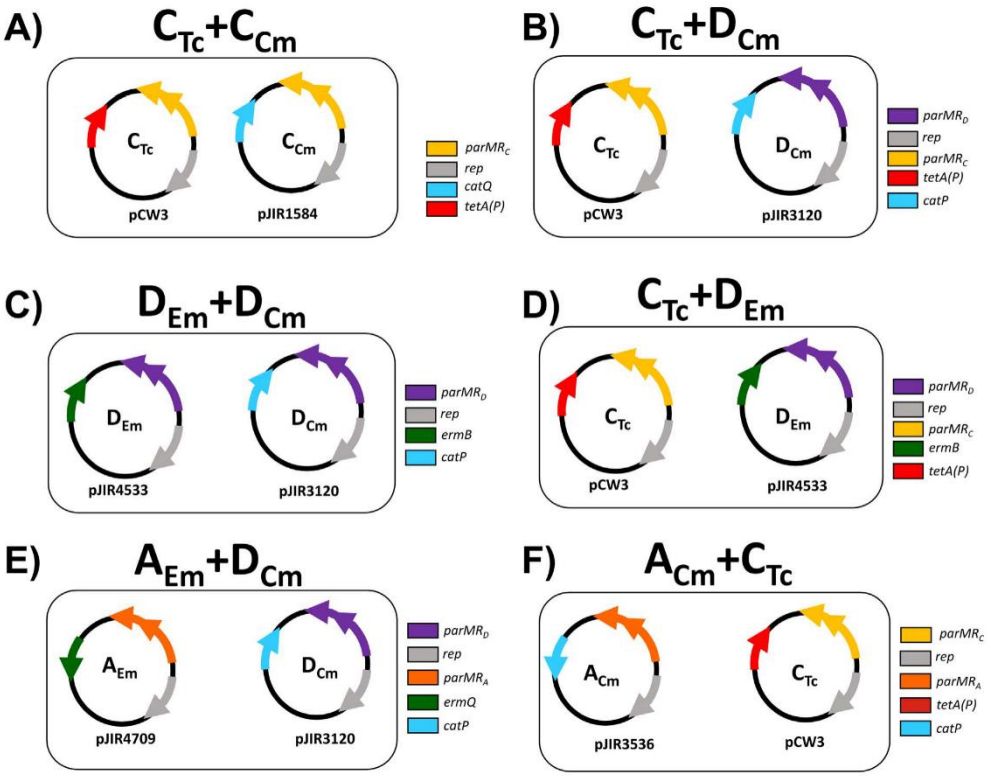

Fig. 1. Diagrammatic representation of strains used in plasmid stability experiments. Strains were constructed by transferring each plasmid into a JIR325 background *via* conjugation. Each strain was given a designation (*e.g.* C_{Tc} + C_{Cm}) based on the *parMRC* family plasmids they carry and the selection markers present on those plasmids. Legend: A) JIR13405 (shown as C_{Tc} + C_{Cm}) contains two $parMRC_C$ plasmids, pCW3 and pJIR1584. B) JIR13408 (C_{Tc} + D_{Cm}) contains a $parMRC_C$ encoding-plasmid pCW3 and a $parMR_D$ encoding-plasmid pJIR3120. C) JIR13409 (D_{Em} + D_{Cm}) contains two $parMRC_D$ encoding-plasmid pJIR4533 and pJIR3120. D) JIR13410 (C_{Tc} + D_{Em}) contains a $parMRC_C$ encoding-plasmid pCW3 and a $parMRC_D$-encoding plasmid, pJIR4533 E) JIR13407 (A_{Em} + D_{Cm}) contains a $parMRC_A$ encoding-plasmid pJIR4250 and a $parMRC_D$ encoding-plasmid pJIR3120. F) JIR13406 (A_{Cm} + C_{Tc}) contains a $parMRC_A$ encoding plasmid pJIR3536 and a $parMRC_C$ encoding-plasmid pCW3. The *tetA(P)* gene is represented by the red arrow, *catQ* is shown in blue, the grey arrow indicates *rep*, $parMR_A$ is indicated by the orange arrows $parMR_C$ is indicated by the yellow arrows, $parMRC_D$ is denoted by the purple arrows. (For interpretation of the references to colour in this figure legend, the reader is referred to the web version of this article.)

3.2. *C. perfringens plasmids that encode different parMRC-like partitioning systems are compatible*

To determine if plasmids encoding distinct *parMRC* homologues could stably coexist when introduced into a single strain of *C. perfringens*, several strains containing co-resident plasmids encoding different partitioning system homologues were constructed. Pairs of these plasmids were introduced into a JIR325 background to construct the A_{Cm} + C_{Tc}, A_{Em} + D_{Cm} (Fig. 1E & F) and C_{Tc} + D_{Cm} strains (Fig. 1B), which then were passaged and the stability of the co-resident plasmids determined as before. The results showed that the A_{Cm} + C_{Tc} and A_{Em} + D_{Cm} plasmid combinations were 100% stable over the course of the experiments, even when selection was for the co-resident plasmid (Fig. 2C & D). The C_{Tc} + D_{Cm} test strain, however, showed slight plasmid instability. When passaged in the presence of chloramphenicol selection (pJIR3120), tetracycline resistance (pCW3) was lost to some extent with 88% of the population continuing to carry the plasmid. By contrast, pJIR3120 remained stable even in the absence of selection for chloramphenicol resistance (Fig. 3A). PCR analysis of the *par* and antibiotic resistance genes supported all of the plasmid profiles deduced by the resistance profiles, both before and after passage.

To determine if this minor plasmid incompatibility phenotype observed between the C_{Tc} and D_{Cm} plasmids was an artefact introduced by antibiotic selection, an alternative C_{Tc} + D_{Em} strain was constructed using the plasmids pCW3 ($parMRC_C$, Tc^R) and pJIR4533 ($parMRC_D$, Em^R). This strain was passaged and tested as before, the results revealed only a minimal loss of tetracycline resistance upon passage in the presence of erythromycin (98% stability) (Fig. 3B). Both C + D strains were also passaged in the absence of any selection for six days. A similar trend was observed, with pCW3 slightly less stable than pJIR3120 (Fig. 3C). To ensure that the trend observed for these plasmid combinations was due to interaction between the plasmids rather than an inherent instability of pCW3, parent strains carrying each individual plasmid (pCW3, pJIR4533 or pJIR3120) were passaged on non-selective media and their stability was determined. Passage on non-selective media did not result in any significant instability (Supplementary Fig. 1) suggesting that the low-level C + D instability was a result of plasmid interactions.

The minor incompatibility phenotype observed for the C_{Tc} + D_{Cm} combination was not seen for the A_{Cm} + C_{Tc} or A_{Em} + D_{Cm} combinations. This result suggested that the partition systems of the C_{Tc} and D_{Cm} plasmids may be more similar than that of the A_{Cm} + C_{Tc} or A_{Em} + D_{Cm} combinations, potentially leading to the minor incompatibility phenotype. However, there was no apparent correlation between the amino acid or nucleotide sequence identity of the ParM, ParR or *parC* components and the minor incompatibility phenotype (Table 2), sug-

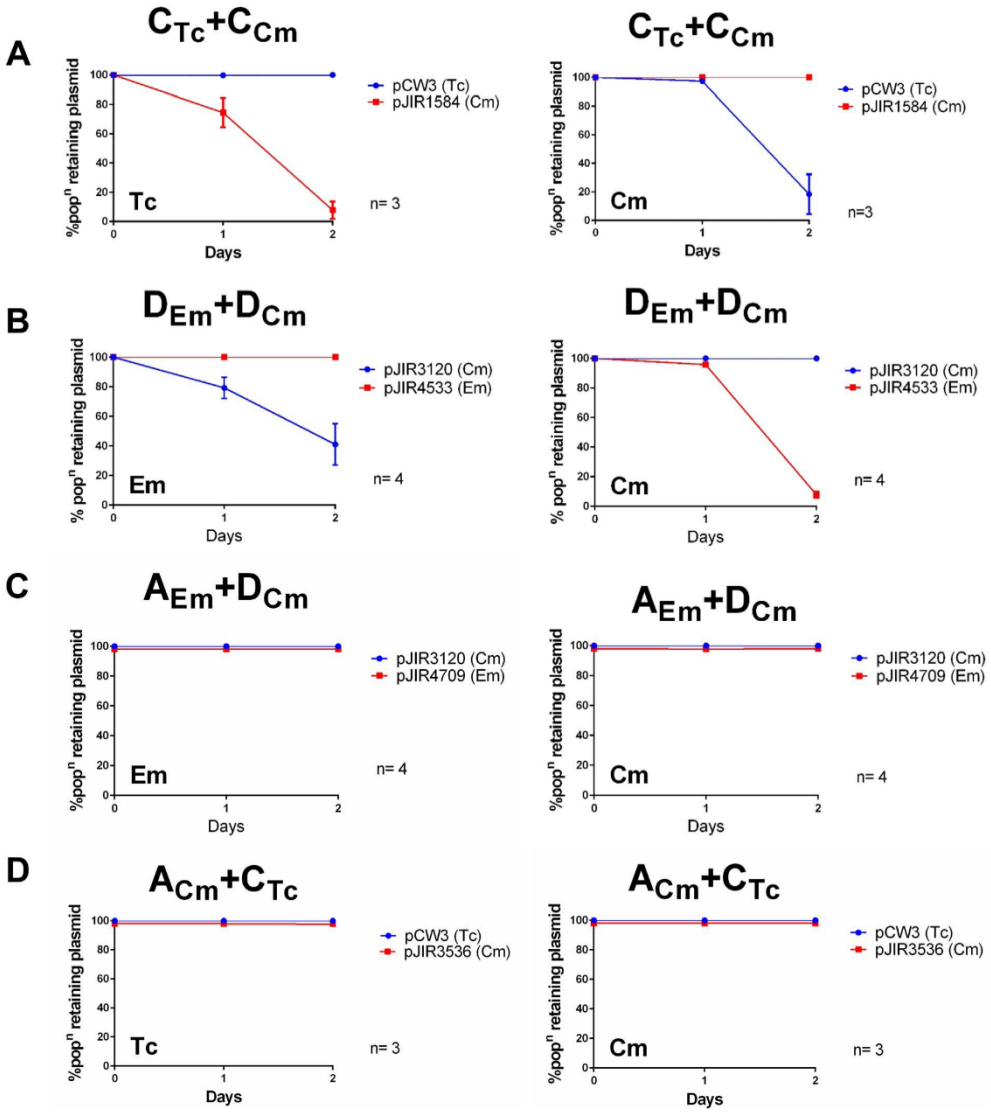

Fig. 2. Plasmid stability assays: Each strain carried two plasmids as described earlier and as indicated by the strain designations. The strains C_{Tc} + C_{Cm} (A) D_{Em} + D_{Cm} (B), A_{Em} + D_{Cm} (C) and A_{Cm} + C_{Tc} (D) were passaged on medium selective for one plasmid only (indicated on each graph) for two days. The relative plasmid stability was determined at 0, 1 and 2 days by patching 100 colonies onto each medium. Error bars represent the mean ± SEM.

gesting that these different partitioning systems were unlikely to be involved in this phenomenon.

Since another facet of plasmid incompatibility involves shared replication mechanisms, the putative origin of replication and replication initiator proteins of each plasmid were compared. The amino acid sequences of the Rep proteins from pCW3, pJIR3120 and pJIR3536 (a plasmid that was compatible with pCW3 and pJIR3120) were highly conserved (98% amino acid identity) with no obvious patterns of amino acid sequence changes (Supplementary Fig. 2).

The putative origin of replication (*oriV*) of pCW3-like plasmids consists of a series of conserved inverted repeat structures (IR1-IR5). Alignment of the *oriV* sites (from downstream of IR1 to the *rep* start codon) of pCW3 (C), pJIR3536 (A) and pJIR3120 (D) showed that when compared to the *oriV* of pCW3, the *oriV* site of pJIR3536 had five nucleotide differences within the IR2 loop, as well as two nucleotide differences in the left-hand repeat and eight other nucleotide substitutions downstream of IR2 (Fig. 4). pCW3 and pJIR3536 were stable when introduced into JIR325, suggesting that differences in the partitioning family as well as differences in the *oriV* were enough to allow these plasmids to coexist. By contrast, pJIR3120 showed two single nucleotide differences within the loop of IR2, but was otherwise identical to the pCW3 origin. When pCW3 and pJIR3120 were introduced into JIR325, pCW3 was lost at low frequency from the population in the absence of selection. When JIR325 carrying pCW3 in

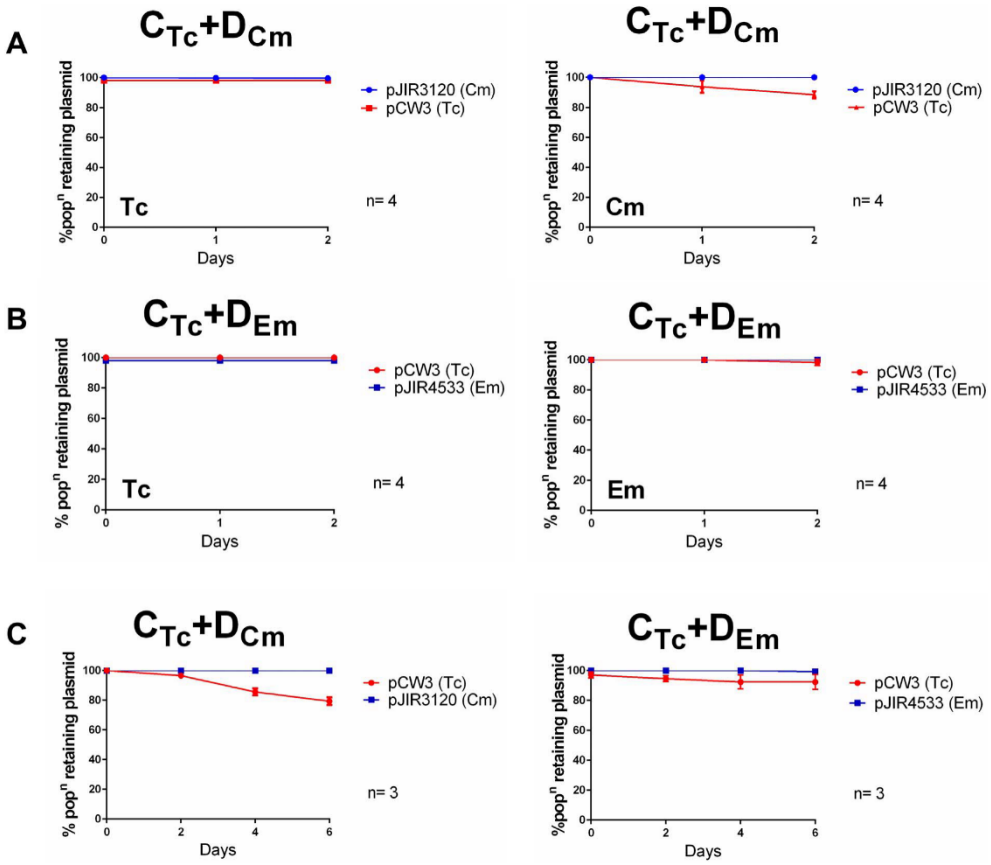

Fig. 3. C + D plasmid stability assays: Each strain carried two plasmids as described earlier and as indicated by the strain designations. The strains C_{Tc} + D_{Cm}, (A) and C_{Tc} + D_{Em} (B) were passaged on medium selective for each plasmid (indicated on each graph) over the course of two days. The relative plasmid stability was determined at 0, 1 and 2 days by patching 100 colonies onto each medium. (C) Both incompatibility strains C_{Tc} + D_{Cm} and C_{Tc} + D_{Em} were passaged in the absence of selection for 6 days and plasmid stability was determined on 0, 2, 4 and 6 days as described above. Error bars represent the mean ± SEM.

Table 2
Sequence identity between *parMRC* components of the plasmids pJIR3536 (A), pCW3 (C) and pJIR3120 (D).

Component	% Identity		
ParM[a]			
	$ParM_A$	$ParM_C$	$ParM_D$
$ParM_A$	100%		
$ParM_C$	26.2%	100%	
$ParM_D$	32.3%	24.5%	100%
ParR[a]			
	$ParR_A$	$ParR_C$	$ParR_D$
$ParR_A$	100%		
$ParR_C$	15.4%	100%	
$ParR_D$	18.6%	27.3%	100%
parC[b]			
	$parC_A$	$parC_C$	$parC_D$
$parC_A$	100%		
$parC_C$	46.6%	100%	
$parC_D$	46.7%	44.8%	100%

[a] Nucleotide sequence identity.
[b] Amino acid sequence identity.

isolation was passaged in the absence of selection, the plasmid was stable, indicating that the C_{Tc} + D_{Cm} result was due to the introduction of a pJIR3118 derivative. This result suggests that replication and partitioning mechanisms may play a cooperative role in plasmid incompatibility.

4. Discussion

The link between plasmid incompatibility and shared replication control and initiation mechanisms is well established (Molin and Nordstrom, 1980; Novick, 1987; Tomizawa and Itoh, 1981). However, previous studies have shown that *C. perfringens* isolates can house multiple, highly similar, conjugative plasmids (Bannam et al., 2011; Li et al., 2013; Miyamoto et al., 2006; Miyamoto et al., 2008; Parreira et al., 2012), despite sharing Rep proteins with ≥98% amino acid sequence identity (Adams et al., 2015; Bannam et al., 2006). This observation suggests that plasmid encoded factors other than the replication region are contributing to plasmid incompatibility in *C. perfringens*.

In this study, we have provided evidence that in this series of plasmids incompatibility correlated with the *parMRC* system designation. When plasmids encoding identical *parMRC* systems were introduced into the same *C. perfringens* strain they were incompatible

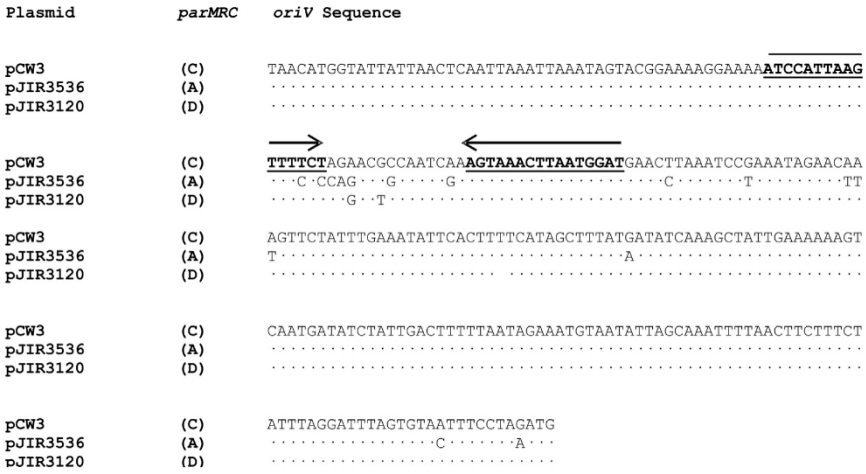

Fig. 4. Sequence alignments of *oriV* from pJIR3536, pJIR3120 and pCW3. The *oriV* regions (downstream of IR-1 to the *rep* start codon) of pCW3, pJIR3120 and pJIR3536 were aligned using the EMBL-EBI Clustal Ω alignment tool (McWilliam et al., 2013). All sequences were aligned using pCW3 as a reference, conserved nucleotides are shown as dots and nucleotide changes are indicated. IR2 is indicated by the arrows and shown by the underlined and bolded text.

(C_{Tc} + C_{Cm} and D_{Em} + D_{Cm}). By contrast, when plasmids with different *parMRC* families were introduced into the same *C. perfringens* strain they were compatible (A_{Cm} + C_{Tc}, A_{Em} + D_{Cm}, C_{Tc} + D_{Cm} and C_{Tc} + D_{Em}). To our knowledge, this is the first definitive report of plasmid incompatibility in *Clostridium spp*.

Several models for partition based incompatibility have been proposed, however most research has focused on the Type I partition systems of the *E. coli* plasmids P1, pB171 and F, rather than the Type II *parMRC* partition systems that are encoded by the pCW3-like plasmids. A simple mismatched pairing model has been used to describe incompatibility mediated by *parMRC* partitioning systems in other bacteria (Austin and Nordstrom, 1990; Breuner et al., 1996; Gerdes and Molin, 1986; Jensen et al., 1998). In this model two plasmids that share similar *parC* centromeres form heterologous pairs mediated by their similar ParR and ParM components, ultimately leading to incorrect segregation/positioning at cell division and the generation of daughter populations retaining only one plasmid type (Austin and Nordstrom, 1990; Bouet et al., 2007; Breuner et al., 1996; Funnell, 2005; Jensen et al., 1994; Jensen et al., 1998). Support for this model was provided by studies that showed that the promiscuous pB171 ParR protein could bind to both its cognate *parC* centromere as well as the centromere of an unrelated pCP301 plasmid, leading to destabilisation of proper partitioning and incompatibility (Hyland et al., 2014).

A similar scenario can be envisioned for partition-mediated incompatibility in *C. perfringens*, where ParR homologues are predicted to interact with their cognate *parC* centromere with higher affinity than a disparate *parC* centromere site. When a resident plasmid shares the same centromere as a newly introduced plasmid, the inheritance of one or both plasmids will be destabilised, thereby leading to incompatibility. Functional characterisation of the *C. perfringens* ParMRC components and their protein-protein and protein-DNA interactions is required to validate this hypothesis.

Although our results show that two plasmids encoding identical partitioning systems are incompatible, there are other plasmid-encoded factors that may contribute to incompatibility. Although the Rep proteins and *oriV* sites of pCW3-like conjugative plasmids do not resolve into clear phylogenetic groups, subtle differences either in the sequence of the Rep proteins, the Rep binding sites in *oriV* or the sequences of unidentified control elements also may contribute to incompatibility.

Plasmids encoding different *parMRC* homologues were shown to be completely stable when introduced into the same strain (A_{Em} + D_{Cm} and A_{Cm} + C_{Tc}), with the exception of the pCW3 and pJIR3118-based plasmid combinations (C + D), which showed a slight plasmid incompatibility phenotype (Fig. 3).

This result supports the assertion that factors other than partition components may also contribute to plasmid incompatibility. In this context, although alignment of the Rep amino acid sequences showed no obvious conserved changes some sequence variation was observed in the IR2 loop region of the *oriV* sites. IR2 is essential for plasmid replication, as shown by previous transposon mutagenesis studies (Bannam et al., 2006).

The role of IR2 in plasmid incompatibility is unclear, but it may constitute either an important regulatory element or the site of Rep binding and therefore replication initiation. Other studies have shown that it is possible to generate new incompatibility groups by introducing a single base pair change in the negative control element RNA I of ColE1 (Tomizawa and Itoh, 1981), therefore we cannot rule out the possibility that even minor sequence changes may affect plasmid incompatibility in *C. perfringens*. Our results suggest that both the replication and *parMRC* partitioning systems are involved in plasmid incompatibility. The C_{Tc} + D_{Em} minor incompatibility phenotype suggests that when the replicon is very similar, but the partition systems are different, limited incompatibility is observed. This result may imply that otherwise identical replicons are rendered compatible by the possession of different *parMRC* partitioning homologues. Whether this compatibility is a result of spatial resolution or isolation of different plasmid populations by their partitioning system within the cell is unclear and requires further experimental interrogation. By contrast, when plasmids share both similar replicon and *parMRC* partitioning system (C_{Tc} + C_{Cm} or D_{Em} + D_{Cm}), strong incompatibility is observed. The mechanism by which these two systems cooperate to influence plasmid incompatibility is not clear. Future experiments are required to test each of these factors in isolation on otherwise identical vectors.

In summary, we report an important increase in our understanding of plasmid incompatibility in *C. perfringens* by demonstrating experimentally that essentially native *C. perfringens* plasmids may be incompatible and that this incompatibility correlates with the *parMRC* phylogenetic groups of the plasmids. Further studies are required to address the more subtle contributions of variation of the Rep protein and the *oriV* site to plasmid incompatibility.

Acknowledgements

This research was supported by Discovery Project Grant DP160102680 from the Australian Research Council. TDW was the recipient of an Australian Postgraduate Award.

Appendix A. Supplementary data

Supplementary data to this article can be found online at http://dx.doi.org/10.1016/j.plasmid.2017.03.008.

References

Adams, V., Li, J., Wisniewski, J.A., Uzal, F.A., Moore, R.J., McClane, B.A., Rood, J.I., 2014. Virulence plasmids of spore-forming bacteria. Microbiol. Spectr. 2. http://dx.doi.org/10.1128/microbiolspec.PLAS-0024-2014.

Adams, V., Watts, T.D., Bulach, D.M., Lyras, D., Rood, J.I., 2015. Plasmid partitioning systems of conjugative plasmids from *Clostridium perfringens*. Plasmid 80, 90–96.

Austin, S., Nordstrom, K., 1990. Partition-mediated incompatibility of bacterial plasmids. Cell 60, 351–354.

Bannam, T.L., Teng, W.L., Bulach, D., Lyras, D., Rood, J.I., 2006. Functional identification of conjugation and replication regions of the tetracycline resistance plasmid pCW3 from *Clostridium perfringens*. J. Bacteriol. 188, 4942–4951.

Bannam, T.L., Yan, X.X., Harrison, P.F., Seemann, T., Keyburn, A.L., Stubenrauch, C., Weeramantri, L.H., Cheung, J.K., McClane, B.A., Boyce, J.D., Moore, R.J., Rood, J.I., 2011. Necrotic enteritis-derived *Clostridium perfringens* strain with three closely related independently conjugative toxin and antibiotic resistance plasmids. MBio 2, e00190-00111.

Baxter, J.C., Funnell, B.E., 2014. Plasmid partition mechanisms. Microbiol. Spectr. 2. http://dx.doi.org/10.1128/microbiolspec.PLAS-0023-2014.

Bouet, J.Y., Rech, J., Egloff, S., Biek, D.P., Lane, D., 2005. Probing plasmid partition with centromere-based incompatibility. Mol. Microbiol. 55, 511–525.

Bouet, J.Y., Nordstrom, K., Lane, D., 2007. Plasmid partition and incompatibility–the focus shifts. Mol. Microbiol. 65, 1405–1414.

Breuner, A., Jensen, R.B., Dam, M., Pedersen, S., Gerdes, K., 1996. The centromere-like *parC* locus of plasmid R1. Mol. Microbiol. 20, 581–592.

Cheung, J.K., Keyburn, A.L., Carter, G.P., Lanckriet, A.L., Van Immerseel, F., Moore, R.J., Rood, J.I., 2010. The VirSR two-component signal transduction system regulates NetB toxin production in Clostridium perfringens. Infect. Immun. 78, 3064–3072.

Diaz, R., Rech, J., Bouet, J.Y., 2015. Imaging centromere-based incompatibilities: insights into the mechanism of incompatibility mediated by low-copy number plasmids. Plasmid 80, 54–62.

Ebersbach, G., Sherratt, D.J., Gerdes, K., 2005. Partition-associated incompatibility caused by random assortment of pure plasmid clusters. Mol. Microbiol. 56, 1430–1440.

Freedman, J.C., Theoret, J.R., Wisniewski, J.A., Uzal, F.A., Rood, J.I., McClane, B.A., 2014. *Clostridium perfringens* type A–E toxin plasmids. Res. Microbiol. 166, 264–279.

Funnell, B.E., 2005. Partition-mediated plasmid pairing. Plasmid 53, 119–125.

Gerdes, K., Molin, S., 1986. Partitioning of plasmid R1. Structural and functional analysis of the parA locus. J. Mol. Biol. 190, 269–279.

Gerdes, K., Howard, M., Szardenings, F., 2010. Pushing and pulling in prokaryotic DNA segregation. Cell 141, 927–942.

Gurjar, A., Li, J., McClane, B.A., 2010. Characterization of toxin plasmids in *Clostridium perfringens* type C isolates. Infect. Immun. 78, 4860–4869.

Hughes, M.L., Poon, R., Adams, V., Sayeed, S., Saputo, J., Uzal, F.A., McClane, B.A., Rood, J.I., 2007. Epsilon-toxin plasmids of *Clostridium perfringens* type D are conjugative. J. Bacteriol. 189, 7531–7538.

Hyland, E.M., Wallace, E.W., Murray, A.W., 2014. A model for the evolution of biological specificity: a cross-reacting DNA-binding protein causes plasmid incompatibility. J. Bacteriol. 196, 3002–3011.

Jensen, R.B., Dam, M., Gerdes, K., 1994. Partitioning of plasmid R1. The parA operon is autoregulated by ParR and its transcription is highly stimulated by a downstream activating element. J. Mol. Biol. 236, 1299–1309.

Jensen, R.B., Lurz, R., Gerdes, K., 1998. Mechanism of DNA segregation in prokaryotes: replicon pairing by *parC* of plasmid R1. Proc. Natl. Acad. Sci. U. S. A. 95, 8550–8555.

Keyburn, A.L., Boyce, J.D., Vaz, P., Bannam, T.L., Ford, M.E., Parker, D., Di Rubbo, A., Rood, J.I., Moore, R.J., 2008. NetB, a new toxin that is associated with avian necrotic enteritis caused by *Clostridium perfringens*. PLoS Pathog. 4, e26.

Lepp, D., Gong, J., Songer, J.G., Boerlin, P., Parreira, V.R., Prescott, J.F., 2013. Identification of accessory genome regions in poultry *Clostridium perfringens* isolates carrying the *netB* plasmid. J. Bacteriol. 195, 1152–1166.

Li, J., Adams, V., Bannam, T.L., Miyamoto, K., Garcia, J.P., Uzal, F.A., Rood, J.I., McClane, B.A., 2013. Toxin plasmids of *Clostridium perfringens*. Microbiol. Mol. Biol. Rev. 77, 208–233.

Lyristis, M., Bryant, A.E., Sloan, J., Awad, M.M., Nisbet, I.T., Stevens, D.L., Rood, J.I., 1994. Identification and molecular analysis of a locus that regulates extracellular toxin production in *Clostridium perfringens*. Mol. Microbiol. 12, 761–777.

McWilliam, H., Li, W., Uludag, M., Squizzato, S., Park, Y.M., Buso, N., Cowley, A.P., Lopez, R., 2013. Analysis tool web services from the EMBL-EBI. Nucleic Acids Res. 41, W597–W600. http://dx.doi.org/10.1093/nar/gkt1376.

Miyamoto, K., Fisher, D.J., Li, J., Sayeed, S., Akimoto, S., McClane, B.A., 2006. Complete sequencing and diversity analysis of the enterotoxin-encoding plasmids in *Clostridium perfringens* type A non-food-borne human gastrointestinal disease isolates. J. Bacteriol. 188, 1585–1598.

Miyamoto, K., Li, J., Sayeed, S., Akimoto, S., McClane, B.A., 2008. Sequencing and diversity analyses reveal extensive similarities between some epsilon-toxin-encoding plasmids and the pCPF5603 *Clostridium perfringens* enterotoxin plasmid. J. Bacteriol. 190, 7178–7188.

Molin, S., Nordstrom, K., 1980. Control of plasmid R1 replication: functions involved in replication, copy number control, incompatibility, and switch-off of replication. J. Bacteriol. 141, 111–120.

Novick, R.P., 1987. Plasmid incompatibility. Microbiol. Rev. 51, 381–395.

Novick, R.P., Clowes, R.C., Cohen, S.N., Curtiss III, R., Datta, N., Falkow, S., 1976. Uniform nomenclature for bacterial plasmids: a proposal. Bacteriol. Rev. 40, 168–189.

O'Connor, J.R., Lyras, D., Farrow, K.A., Adams, V., Powell, D.R., Hinds, J., Cheung, J.K., Rood, J.I., 2006. Construction and analysis of chromosomal Clostridium difficile mutants. Mol. Microbiol. 61, 1335–1351.

Parreira, V.R., Costa, M., Eikmeyer, F., Blom, J., Prescott, J.F., 2012. Sequence of two plasmids from *Clostridium perfringens* chicken necrotic enteritis isolates and comparison with *C. perfringens* conjugative plasmids. PLoS One 7, e49753.

Revitt-Mills, S.A., Rood, R.I., V., A., 2015. *Clostridium perfringens* extracellular toxins and enzymes: 20 and counting. Microbiol. Aust. 36, 114–117.

Rood, J.I., 1983. Transferable tetracycline resistance in *Clostridium perfringens* strains of porcine origin. Can. J. Microbiol. 29, 1241–1246.

Rood, J.I., Maher, E.A., Somers, E.B., Campos, E., Duncan, C.L., 1978a. Isolation and characterization of multiply antibiotic-resistant *Clostridum perfringens* strains from porcine feces. Antimicrob. Agents Chemother. 13, 871–880.

Rood, J.I., Scott, V.N., Duncan, C.L., 1978b. Identification of a transferable tetracycline resistance plasmid (pCW3) from *Clostridium perfringens*. Plasmid 1, 563–570.

Salje, J., Gayathri, P., Lowe, J., 2010. The ParMRC system: molecular mechanisms of plasmid segregation by actin-like filaments. Nat. Rev. Microbiol. 8, 683–692.

Sayeed, S., Li, J., McClane, B.A., 2010. Characterization of virulence plasmid diversity among *Clostridium perfringens* type B isolates. Infect. Immun. 78, 495–504.

Sheedy, S.A., Ingham, A.B., Rood, J.I., Moore, R.J., 2004. Highly conserved alpha-toxin sequences of avian isolates of *Clostridium perfringens*. J. Clin. Microbiol. 42, 1345–1347.

Tomizawa, J., Itoh, T., 1981. Plasmid ColE1 incompatibility determined by interaction of RNA I with primer transcript. Proc. Natl. Acad. Sci. U. S. A. 78, 6096–6100.